UNIVERSIDADE DE BRASÍLIA

FACULDADE DE TECNOLOGIA

DEPARTAMENTO DE ENGENHARIA CIVIL E AMBIENTAL

MATHEMATICAL AND PROBABILISTIC MODELING APPROACH FOR ESTIMATION OF SURFACE SETTLEMENTS DUE TO TBM TUNNELING

VICTOR HUGO FRANCO RATTIA

ORIENTADOR: ANDRÉ PACHECO DE ASSIS

CO-ORIENTADOR: GILSON DE FARIAS NEVES GITIRANA JR.

TESE DE DOUTORADO EM GEOTECNIA

PUBLICAÇÃO: G.TD-151/2019

BRASÍLIA / DF: ABRIL de 2019

UNIVERSIDADE DE BRASÍLIA
FACULDADE DE TECNOLOGIA
DEPARTAMENTO DE ENGENHARIA CIVIL E AMBIENTAL

MATHEMATICAL AND PROBABILISTIC MODELING APPROACH FOR ESTIMATION OF SURFACE SETTLEMENTS DUE TO TBM TUNNELING

VICTOR HUGO FRANCO RATTIA

TESE DE DOUTORADO SUBMETIDA AO DEPARTAMENTO DE ENGENHARIA CIVIL E AMBIENTAL DA UNIVERSIDADE DE BRASÍLIA COMO PARTE DOS REQUISITOS NECESSÁRIOS PARA A OBTENÇÃO DO GRAU DE DOUTOR.

APROVADA POR :

_____

Prof. André Pacheco de Assis, PhD (UnB)
(ORIENTADOR)

_____

Prof. Gilson de Farias Neves Gitirana Jr., PhD (UFG)
(CO-ORIENTADOR)

_____

Prof. Juan Felix Rodriguez Rebolledo, DSc (UnB)
(EXAMINADOR EXTERNO)

_____

Prof. Tiago Gerheim Souza Dias, PhD (University of Southampton)
(EXAMINADOR EXTERNO)

_____

Prof. Marcos Noronha, DSc (UFSC)
(EXAMINADOR EXTERNO)

BRASÍLIA / DF: ABRIL de 2019

FICHA CATALOGRÁFICA

FRANCO, VICTOR HUGO

Mathematical and probabilistic modeling approach for estimation of surface settlements due to TBM tunneling. Distrito Federal, 2019.

xvi, 153 p., 210 x 297 mm (ENC/FT/UnB, Doutorado, Engenharia Civil e Ambiental, 2019).

Tese de Doutorado - Universidade de Brasília, Faculdade de Tecnologia.

Departamento de Engenharia Civil e Ambiental

1. Mathematical approach	2. Probabilistic approach
3. Surface settlement	4. TBM tunneling
I. ENC/FT/UnB	II. Título (série)

REFERÊNCIA BIBLIOGRÁFICA

FRANCO, V.H. (2019). Mathematical and probabilistic modeling approach for estimation of surface settlements due to TBM tunneling. Tese de Doutorado, Departamento de Engenharia Civil e Ambiental, Universidade de Brasília, Brasília, DF, 153 p.

CESSÃO DE DIREITOS

AUTOR: VICTOR HUGO FRANCO RATTIA

TÍTULO: Mathematical and probabilistic modeling approach for estimation of surface settlements due to TBM tunneling.

GRAU: Doutorado em Geotecnia   ANO: 2019

VICTOR HUGO FRANCO RATTIA

Depto. de Engenharia Civil e Ambiental (ENC) - FT

Universidade de Brasília (UnB)

Campus Darcy Ribeiro

CEP 70919-970 - Brasília - DF - Brasil

Agradecimentos

Neste momento, gostaria de agradecer a Deus por estar próximo a mim, neste tempo de transformações e aprendizado de minha vida.

À toda minha família, e de forma especial a minha mãe Nancy, minha irmã Vicfrancy, minha prima Zodalys, meu cunhado Jesus e meu primo Julio cesar pelo apoio oferecido para atingir este enorme desafio.

Aos professores André Pacheco de Assis e Gilson de Farias Neves Gitirana Jr. pela orientação, apoio e conhecimentos transmitidos no decorrer da minha pesquisa.

Aos meus queridos amigos da vida Elaine e Marco pela amizade oferecida desde minha chegada em Brasil e por ter me tratado como mais um da vossa família.

Aos colegas do Programa de Pós-Graduação em Geotecnia Leticia, Thiago e Andre agora grandes amigos pelos momentos compartidos durante todo esse periodo.

À Companhia do Metropolitano de São Paulo, especialmente ao Geólogo Hugo Cassio Rocha, pelo appoio oferecido em fornecer e autorizar o uso dos dados neste estudo.

MODELAGEM MATEMÁTICA E PROBABILÍSTICA PARA ESTIMATIVA DE RECALQUES SUPERFICIAIS DEVIDO A ESCAVAÇÃO COM TUNELADORAS

RESUMO

Tuneladoras ou TBMs em solos tornaram-se a opção preferida para a construção de túneis, em áreas urbanas. Rápido processo de escavação, ambiente de trabalho em segurança e relativo baixo impacto na indução de recalques superficiais são os principais fatores para o seu emprego. Durante a escavação, existem poucas ferramentas que possam fornecer estimativas dos recalques devido ao desempenho da TBM. Outro aspecto a ser considerado é a variabilidade dos parâmetros geotécnicos e a estratigrafia do perfil do solo, ja que constituem uma importante fonte de incerteza para a avaliação dos recalques. Essas incertezas são consideradas usando métodos probabilísticos que geralmente exigem um esforço de cálculo significativo. A presente tese tem como objetivo propor uma metodologia para estimativa dos recalques surperficiais durante escavação com tuneladoras. Primeiramente, é apresentado um procedimento probabilístico para lidar com as incertezas das propriedades geotécnicas e do perfil estratigráco na formação de recalques superficiais induzidos pela construcão de túneis. Finalmente, é apresentado um procedimento matemático com o escopo de propor um modelo para estimativa de recalques surperficiais durante a contrução de túneis com tuneladoras. Dito modelo considera a variabilidade dos parâmetros geotécnicos. A metodologia proposta é aplicada na recém construída extensão da Linha 5 do Metrô de São Paulo. A análise probabilística baseia-se na aplicação do método de estimativa pontuais híbrido o qual emprega um número reduzido de cálculos sem perder precisão. O procedimento também se baseia em análises de sensibilidade. Análises numéricas bidimensionais (2D) e tridimensionais (3D) são realizadas, utilizando um código comercial de elementos finitos. Três cenários probabilísticos baseados nos valores inferior, médio e superior do coeficiente de variação das variáveis de entrada foram considerados na análise da resposta do maciço para a Linha 5. Os resultados obtidos utilizando a metodologia proposta permite estimar o cenário probabilístico que melhor indique o coeficiente de variação ideal a ser adotado em cada variável de entrada. As propriedades elásticas do solo e a espessura da camada superior do solo tiveram a maior influência na geração de recalques superficiais. A abordagem matemática baseia-se no comportamento dos deslocamentos do maciço devido à pressão de suporte na face applicada pela TBM. O recalque superficial máximo e o volume perdido são considerados como as variáveis para descrever os recalques superficiais e a pressão de suporte na face da TBM como a variável para descrever a pressão de suporte interna do túnel. Um conjunto de modelos a partir da revisão de literatura são considerados e um critério de seleção é aplicado sobre esses modelos para escolher o modelo que melhor descreva a resposta desse sistema. Verificou-se que a curva não-linear de tensão-deformação proposta por Duncan & Chang (1970) fornece um bom ajuste dos dados tomados do estudo de caso. Os limites inferior e superior foram propostos neste modelo para consideração da variabilidade dos parâmetros geotécnicos e, finalmente, o significado físico dos parâmetros do modelo são proposto.

MATHEMATICAL AND PROBABILISTIC MODELING APPROACH FOR ESTIMATION OF SURFACE SETTLEMENTS DUE TO TBM TUNNELING

ABSTRACT

Tunnel Boring Machines (TBMs) for soils have become the preferred option for construction of tunnels, especially in urban areas. Rapid excavation process, safe working environment and relatively low impact on inducing ground movements at the surface have been the main factors for its employment. Even though, during tunneling, few tools exist that may provide an estimation of surface settlements due to the TBM performance. Another aspect to consider should be the variability of geotechnical parameters and ground profile stratigraphy because constitute a significant source of uncertainty for the assessment of ground movements. These uncertainties may be considered at the design during modeling by using probabilistic approaches that often require significant computation effort. The present research aims to propose methodological approach, where first a rational and efficient probabilistic framework to deal with the uncertainties of geotechnical properties and stratigraphic profile on tunneling-induced ground movement is presented to finally describe a mathematical procedure to propose a model, that considers variability of geotechnical parameters, for estimation of surface settlements during TBM tunneling. The proposed methodological approach was applied to the recently constructed extension of Line 5 of São Paulo Metro. The probabilistic approach based on the application of a hybrid point estimation method employs a reduced number of computations without losing accuracy. The framework also relies on sensitivity analyses. Two-dimensional (2D) and three-dimensional (3D) numerical analyses are carried out for Line 5 using a commercial finite element code. Three probabilistic scenarios based on the lower, mean, and upper bound values of the coefficient of variation of input variables are considered in the analysis of ground response for Line 5. The results obtained using the proposed framework allowed to estimate the probabilistic scenario that better provides an ideal coefficient of variation to adopt for input variables. The ground elastic properties and topsoil layer thickness had the most significant influence on ground movements. The mathematical approach is based on the behavior of ground movement due to applied TBM support pressure. Maximum surface settlement and Volume loss were considered as the variables to describe ground movement, and TBM face support pressure are considered as the variable for describing the tunnel internal support pressure. Set of candidate models are considered from the literature review, and a selection model criterion on these models are used in order to choose the model that better described the system response. It was found that the nonlinear stress-strain curve proposed by Duncan & Chang (1970) provide an excellent fitting to the data taken from the case study. Lower and upper bounds are proposed to this model for consideration of variability of geotechnical parameters and, finally, the physical meaning of the model parameters are proposed.

MODELAGE MATEMÁTICA Y PROBABILÍSTICA PARA ESTIMATIVA DE LOS ASENTAMIENTOS SUPERFICIALES DEBIDO A LA ESCAVACIÓN CON TUNELADORAS

RESUMEN

Máquinas tuneladoras o TBMs de suelos se han convertido en la opción preferida para la construcción de túneles, especialmente en áreas urbanas. El rápido proceso de excavación, un hambiente de trabajo seguro y un impacto relativamente bajo en la generación de asentamientos superficiales han sido los factores principales para su empleo. Durante la excavación, existen pocas herramientas que puedan proporcionar una estimación de los asentamientos en la superficie debido al desempeño de la TBM. Otro aspecto a ser considerado es la variabilidad de los parámetros geotécnicos y de la estratigrafía del perfil geologico, ya que constituyen una fuente importante de incertidumbre en la evaluación de los movimientos del suelo. Estas incertidumbres son consideradas en la fase de proyecto, durante la modelación, con el uso de métodos probabilísticos el cual a menudo requieren de un esfuerzo de cálculo significativo. La presente tesis busca proponer una metodología, para la análisis probabilística racional y eficiente de las incertidumbres de las propiedades geotécnicas y del perfil estratigráfico en el movimiento de suelo inducido por túneles; describir un procedimiento matemático y propuesta de un modelo, que considere la variabilidad de parámetros geotécnicos, en la estimación de asentamientos en la superficie. La metodología propuesta se aplicó a la recientemente construida extensión de la Línea 5 del Metro de São Paulo. La análisis probabilística se basa en la aplicación del método de puntos de estimativas híbrido el cual emplea un número reducido de cálculos sin perder precisión. Esta análisis también se basa en análisis de sensibilidad. Análisis numéricos bidimensionales (2D) y tridimensionales (3D) son realizados en la Línea 5 utilizando un código comercial de elementos finitos. Para la análisis de la respuesta del suelo de la Línea 5 son considerados tres escenarios probalilísticos baseados en los valores de límite inferior, medio y superior del coeficiente de variación de las variables de entrada. Los resultados obtenidos utilizando la análisis propuesta permitieron estimar el escenario probabilístico que mejor proporciona un coeficiente de variación ideal para adoptar en las variables de entrada. Las propiedades elásticas del suelo y la espesura de la camada superficial del suelo tuvieron la influencia más significativa en los movimientos del suelo. La análisis matemática se basa en el comportamiento del movimiento del suelo debido a la presión de soporte aplicada por la TBM. El asentamiento máximo de la superficie y la pérdida de suelo se consideraron como las variables para describir el movimiento del suelo, y la presión de soporte frontal de la TBM es considerada como variable para describir la presión de soporte interna del túnel. Un conjunto de modelos propuestos son considerados a partir de revisiones bibliográficas, y un criterio de selección de modelo es utilizado de manera de escoger el modelo que mejor describa la respuesta del sistema. fue encontrado que la curva de tensión-deformación propuesta por Duncan & Chang (1970) proporciona un excelente ajuste a los datos colectados del caso de estudio. Límites inferiores y superiores son propuesto al modelo para considerar la variabilidad de los parámetros geotécnicos y, finalmente, el significado físico de los parámetros del modelo es propuesto.

TABLE OF CONTENTS

LIST OF FIGURES

LIST OF TABLES

LIST OF SYMBOLS

Latin Symbols

a	- Length dimension parameter of the Yield density curve
b	- Dimensionless parameter of the Yield density curve
C	- Tunnel cover
C_c	- Compression index
C_v	- Coefficient of consolidation
C_u	- Undrained shear strength
c	- Cohesion
c'	- Effective cohesion
D	- Tunnel diameter
d	- Cohesion in the p-t plane
E_{ur}	- Unloading-reloading elastic modulus
$E(\cdot)$	- Expected value
e_0	- Initial void ration
G	- Shear modulus
G_p	- Tail void loss
H	- Tunnel axis depth
I_{max}	- Maximum inclination rate of building
i	- Trough width parameter
i'	- Trough width parameter of the Modified settlement curve
K	- Permeability; Bulk modulus
k	- Number of estimable parameters
k_0	- Coefficient of lateral earth pressure
k_{cr}	- Critical value of the coefficient of lateral earth pressure
$L(\cdot)$	- Likelihood function
L_f	- Load factor
MDL	- Minimum Description Length
n	- Number of observable data
OCR	- Overconsolidation ratio
P	- Applied TBM support pressure
P_0	- Estimated initial support pressure
P_f	- Probability of failure
P_{inj}	- TBM grout injection pressure
P_{min}	- Minimum value of applied TBM support pressure
P_S	- Internal support pressure
q_s	- Surface load

S_c	- Settlement at tunnel crown
S_{max}	- Maximum surface settlement
S_s	- Settlement at surface
u_{3d}^*	- Face loss
V_{loss}	- Volume loss
x_i	- Distance to the tunnel portal
x_f	- Distance to the tunnel face
Zi	- Depth of the bottom of the ith layer

Greek Symbols

α	- Parameter ensuring that i remains the distance to the inflection point of the Modified gaussian curve
β	- Angle of friction in the p-t plane; Reliability index
γ	- Specific unit weight; Skewness
γ_S	- Unit weight of the support medium
$\Delta\sigma$	- Increment stress
$\Delta\varepsilon$	- Increment strain
δ_v	- Correlation distance
η	- Shape function parameter of the Modified gaussian curve
θ	- Vector of probability density function parameters
κ	- Kurtosis
μ	- First order of statistical moment (mean)
ν	- Poisson's ratio
σ^2	- Second order of statistical moment (variance)
σ	- Standard deviation
σ_v	- Vertical stress
$\Phi(\cdot)$	- Standard normal cumulative distribution function
ϕ	- Angle of friction
ϕ'	- Effective angle of friction
ω	- Shield loss

Abbreviations

AIC	- Akaike Information Criterion
BEM	- Method of Bayesian Estimation
BIC	- Bayesian Information Criterion
CoV	- Coefficient of Variation
COB	- Dutch Centre Underground Bowen

CSRSM	- Collocation-Based Stochastic Response Surface Method
EPB	- Earth Pressure Balance
FEM	- Finite Element Method
FOSM	- First Order Second Moment
FORM	- First Order Reliability Method
FS	- Factor of Safety
HPEM	- Hybrid Point Estimate Method
LASM	- Limit Analysis Stress Method
LEM	- Limit Equilibrium Method
MC	- Monte Carlo
MLM	- Method of L-moments
MLS	- Method of Least Squares
MME	- Method of Maximum Entropy
MML	- Method of Maximum Likelihood
Mom	- Methods of moments
PDF	- Probability Density Function
PEM	- Point Estimate Method
PWM	- Method of probabilistic weighted moments
RBD	- Reliability-Based Design
SACI	- Instrumentation System for Interactive Monitoring and Control
SORM	- Second Order Reliability Method
SSE	- Sum of squared error
SS	- Slurry Shield
TBMs	- Tunnel Boring Machines
ULS	- Ultimate Limit State

1 INTRODUCTION

1.1 BACKGROUND

Nowadays the big cities around the world desperately require for new infrastructure and utility networks (water, electricity, gas, internet, etc.) to meet the needs for transportation and consumption of the people who live there. The perspective for the future is that this dynamic of expansion and concentration of people living in the cities increases in size and, therefore, the use for more infrastructure will be necessary.

Brazil, like other countries of the world, does not escape from this trend. The most important Brazilian cities are, today, in significant expansion and, consequently, they are demanding for new infrastructures to allow transportation of the inhabitants in a fast and efficient way as well as new utility networks to provide their basic needs.

Taking as an example the city of São Paulo and regarding, specifically, its metro system. Camargo & Almeida (1999) indicated that for 1999 the São Paulo Metro required a significant expansion of the current net. They arrived in that conclusion by considering the total extension of 44 km of the São Paulo Metro net (mostly underground) until 1999, and 18 million people as the potential number of users of the Metro system (population of Great São Paulo also for 1999). Then, by considering these two parameters, the ratio of the line extension to the number of users was of 2.5 km of line per millions of inhabitants. By 1999, several cities of the world had this ratio varying between 20 and 50 km of line per millions of inhabitants.

The Brazilian Institute of Geography and Statistic (IBGE), in its technical report on the estimation for the population of Brazil (IBGE., 2016), announced that the population of the Metropolitan Region of São Paulo was of 21 millions of inhabitants for the year of 2016. For this same year, the total extension of the São Paulo Metro system was of 78.4 km of track (9.3 km still on final preparation to operation). So, by making the same calculation made by Camargo & Almeida (1999), the new ratio of line extension and number of potential users is of 3.7 km of line per millions of inhabitants. This ratio is still low in comparison with the other cities of the world of 1999.

As demonstrated above with this specific case of the metro line for population, it is notorious the need for infrastructures. This need for infrastructures in cities where the area for construction is already urbanized has incited the use of the underground space as an alternative response to this requirement. In urban areas, the constructive methods most implemented for underground works have been the use of the sequential method and Tunnel Boring Machine (TBM) for soft ground.

The experience gained in many tunnel construction projects in urban areas, as well as recent studies in this topic, have confirmed that deformations on the ground due to tunneling propagates into the surface in the form of settlements. These deformations can cause damages to nearby buildings, infrastructures or utility networks.

According to Leca & New (2007), the magnitude of these deformations depends on the

geotechnical condition of the ground, geostatic stresses and surface loads, the hydro-geological condition as well as the type of tunnel and tunnel lining applied.

In general, the deformations that appear on the surface manifested in the form of settlement trough. When the ground is excavated, and there is not an immediate support action to avoid inward deformation of the tunnel (convergence), an increase of the quantity of extracted material respect to the theoretical section is produced. This difference between the theoretical with the real weight of extracted material is known as volume loss.

The settlement trough produced due to tunneling can be significantly reduced if TBMs are used. This, because these machines apply a continuous pressure against the tunnel face in order to balance the forces of weight ground and groundwater condition.

In practice, the design and subsequently the construction of tunnels in urban areas shown an incongruence in the way how volume loss and tunnel face stability are conceived. These two main factors are studied separately, without a possible correlation between them.

In the case of the volume loss, this parameter is established as an input parameter for calculating the tunnel-induced settlement on the surface. From this, classes of damages are defined for the buildings or infrastructure near the excavation.

For the case of tunnel face stability, the applied front pressure is estimated by considering the general stability of the tunnel (Ultimate Limit State - ULS) for the different geological conditions foresee along the tunnel section.

Lastly, another critical aspect not considered in a tunneling project, and it should be taking into account, is the inherent variability of the soil property, since influences the behavior of groundmass. This consideration, by part of geotechnical designers, involves the use of probabilistic analyses, which by now is not a familiar and widespread approach, thus given preferences to the use of deterministic approaches (Wedekin et al., 2012).

1.2 PROBLEM STATEMENT

Construction of tunnels in urban areas with Tunnel Boring Machines (TBMs) for soft ground has become a widely used alternative, in the last two decades, due to the advantages involved in time and long tunnel construction (> 1 km) as well as to provide a safe working environment for workers with respect to the use of sequential method.

Though, as any underground construction, the use of TBMs in soft ground also induces deformations on the ground that propagates into the surface in the form of settlements, which also can cause damage to buildings or infrastructure nearby the jobsite. In this context, it is necessary in the design stage to correlate the concepts of Volume Loss and Face Support Pressure to understand and provide an estimation of the ground movement due to tunneling.

Briefly speaking, the volume loss is implemented for the estimation of surface subsidence while the face pressure is calculated in terms of groundmass stability. These concepts manifest a

particular relationship, not so well documented, in which the face support pressure is expressed not only in terms of groundmass stability but also in such a way that excavation may induce negligible effects on ground displacements, by also considering the presence of adjacent structures.

Regarding the use of soft ground TBMs, Broere & Brinkgreve (2002) manifested, especially or Earth Pressure Balance (EPB) machines, that although the face stability of a tunnel is not generally a problem for EPB machines, an accurate indication of the minimum support pressure is needed to control surface settlements and thus prevent tunnel face collapse in case the excavation chamber of the EPB machine is partially filled. This statement also applies to Slurry Type TBMs.

Therefore, arises the interest for research in studying a possible correlation between the stability face pressure and the volume loss. In this manner. The excavation in urban areas might induce acceptable displacements in the groundmass that will produce negligible deformations on the nearby structures. Although the pressure applied at the tunnel face can be optimized by the application of a Safety Factor (SF), in order to consider uncertainty in the assumption of soil parameters, it is observed that in reality, such pressure is not enough to keep settlement within acceptable limits.

With the presumption of increment of vulnerability and serviceability of buildings, infrastructure and utility networks due to tunneling. It is highlighted the importance of this research in order to better optimize the induced surface settlements nearby excavation.

The groundmass has a reaction time, and so the deformations can manifest in a non-immediate way. Even though, during TBM advance, a grout injection is applied for the filling of the annular gap, which provides a contribution to the reduction of inward ground displacement but does not stop them. So, if the application of the face pressure is not correctly estimated and applied, displacement of groundmass will develop and will not be recoverable.

In the design stage, considering the enormous, consuming time for a 3D numerical analysis, the implementation of a correlation between the face support pressure and the volume loss could optimize the estimation of surface settlements. These types of analyses are mostly done by using deterministic approaches. So, it is necessary the integration of probabilistic technics in order to consider the geotechnical parameters as random input variables and then be able to provide a reliability assessment of the ground response due to tunneling.

Therefore, by considering the previous statements and the city of São Paulo as a real case scenario. Herein, the study of the extension works of Line 5 – Lilacs of São Paulo Metro is proposed. The study of the excavation process and monitoring results will be made in order to be able to reach a useful correlation tool for the next tunnel projects in the city of São Paulo and other cities of Brazil.

1.3 RESEARCH OBJECTIVES

The following research focuses on the study of a correlation between the tunnel face support pressure and the volume loss in order to optimize induced surface settlements due to TBM tunneling in soft ground and, in this way, to minimize the possible increase of damages to existing buildings, infrastructure or utility networks. For this purpose, the real case of extension of Line 5 – Lilacs of São Paulo metro is considered. Based on the data from this case study, the proposed prediction approach constitutes a Class-C prediction terminology as defined by Lambe (1973), in which the outcome of events is predicted after the event has occurred.

The specific objectives of this thesis are as follows:

– Identify the physical processes and soil variables that control the response of ground movements due to tunneling.

– Study the inherent variability of soil properties of the Metropolitan Region of São Paulo to define a representative range of variation of these geotechnical parameters.

– Establish a sensitivity analysis framework for the assessment of soil property variability on tunneling-induced surface settlements by performing probabilistic methods.

– Perform 3D numerical analysis for the estimation of the groundmass response (e.g., surface settlement, volume loss) due to the application of a tunnel support pressure (generated by soft ground TBMs), by considering the soil stratigraphy of the Line 5 extension.

– Analyze and compare the different analytical methods of tunnel face stability with the real pressure applied by soft ground TBMs.

– Collect and analyze the monitoring and soft ground TBMs performance data along Line 5 for comparison with the previous analyses.

– Study a relationship between the face support pressure and the volume loss by the implementation of a model selection criteria from a set of mathematical candidate models.

1.4 THESIS OUTLINE

This thesis consists of seven concise chapters; each one of them is briefly described below:

Chapter 1 is an introductory chapter and presents an overview of the research. The objectives and outline of the research will also be provided.

Chapter 2 presents a literature review described as follow: Section 2.1 covers the aspects regarding the current statistical and probabilistic approaches for the description of soil property uncertainty in solving tunneling problems. **Section 2.2** presents the type of tunnel construction methods and their respective impact in controlling the stability of the tunnel face. Description

of ground deformation around the tunnel will be provided as well as the different analytical and numerical approaches for evaluating tunnel face stability. **Section 2.3** presents a review for the description of ground movement, especially at the surface, induced by tunneling. The most typical methods for the estimation of ground movement are also described. Lastly, **Section 2.4** introduces the basic concepts for construction of a mathematical model that allows to describe in a simplified manner the behavior of the system. Types of models and model selection techniques will also be presented in order to choose the best model that provides a good representation of the system from a set of candidate models. Finally, a literature review that studied the relationship between the variables TBM support pressure and ground movement is presented as well as a series of candidate models is proposed to be used to study this relationship in this research.

Chapter 3 presents information about the case study of the extension of Line 5 – Lilacs of São Paulo metro will be presented from which input geotechnical variables as well as surface settlement and applied TBM support pressure are obtained in order to compare the real case with the proposed mathematical model.

Chapter 4 presents a methodological approach in which a series of sequential steps will be proposed in order to build the mathematical model for the estimation of ground movement due to TBM tunneling.

Chapter 5 presents the analysis and discussion of the geological and geotechnical data, monitoring data and TBM pressure values of the area of interest for the analysis of ground behavior due to TBM tunneling. Statistical analysis in terms of the first and second statistical order moment is presented for consideration of inherent variability of input parameters, and soil layer thickness is also presented based on the assumption of three probabilistic scenarios. Finally, a sensitivity analysis of soil properties for assessment of tunneling-induced ground movement is shown by performing a series of two-dimensional finite element analyses.

Chapter 6 presents analytical as well as two-dimensional and three-dimensional finite element analyses with the scope to evaluate the minimum support pressure for tunnel face stability. Tunnel construction is modeled by excavation steps, progressing in the longitudinal direction. Transverse and longitudinal settlement trough are assessed through the study of the influence of input geotechnical parameters and soil layer thickness.

Chapter 7 presents the procedure for mathematical model selection from a set of candidate models that better describes ground movement due to TBM tunneling. Data from the case study is used for assessment of the lower and upper bounds of the selected mathematical model. Later on, comparison of centrifuge test results, from literature, with the selected mathematical model is made. Finally, a procedure for assessing the physical meaning of the parameters of the mathematical model is shown.

Finally, conclusions and recommendations for further research are offered.

2 APPROACHES FOR THE ANALYSIS OF TUNNELS

2.1 PROBABILISTIC METHODS APPLIED IN TUNNELING

Whitman (1984), in the Seventeenth Terzaghi Lecture, highlighted that soil properties should not be recognized as a unique value for projecting a geotechnical, civil work, because soils are materials which differ from one place to the other. Due to their natural heterogeneity, uncertainties in the estimation of soil properties have to be considered, and for this reason, he encouraged the application of probability concepts as a new state of the art approach in geotechnical engineering.

Since then, statistical and probabilistic approaches have been applied in geotechnical fields such as: geotechnical investigation (Kulhawy, 1992; and Phoon & Kulhawy, 1999a,b), foundation (Griffiths & Fenton, 2007), lateral and earth support structures (Fenton & Griffiths, 2008), transportation (Swei et al., 2013), ground improvement (Bari & Shahin, 2014), slope stabilization (Griffiths & Fenton, 2007), geosynthetics (Lin et al., 2016) and contaminated site remediation (Xie et al., 2016).

Regarding tunneling, Mollon et al. (2013) investigated tunneling-induced ground movements due to a slurry shield machine through the application of a probabilistic method called the Collocation Based Stochastic Response Surface Method (CSRSM) in order to evaluate the impact of variability of several input variables that influence ground movements. Likewise, the use of probabilistic methods in tunneling has been studied in Brazil (Alarcón, 2014 and Napa-García et al., 2014).

This chapter will introduce the concepts used for the application of probabilistic methods in tunneling.

2.1.1 UNCERTAINTY IN GEOTECHNICS – SOIL VARIABILITY

When dealing with engineering problems, most engineers consider the behavior of physical phenomena or processes as deterministic (Baecher & Christian, 2005), because if input variables are known with precision, it is possible to forecast with precision the future state of the phenomena. However, the consideration of nature as deterministic has been changed to an assumption of a range of variability in the different scenarios of engineering practice, as first introduced by Whitman (1984).

In geotechnical engineering, the significant uncertainty for development of analysis of problems is related to the inherent variability of the soil for the estimation of soil properties (Ang & Tang, 1975). Even though the terms variability and uncertainty might be employed interchangeably due to a close concept relation, a clarification from the terminological point of view need to be specified. According to Uzielli et al. (2007), variability can be defined as a visible manifestation of heterogeneity of one or more physical parameters or processes. While uncertainty

reflects the decision (or necessity) to recognize and address the observed variability in or more soil properties of interest.

Regarding the term uncertainty, the DET NORSKE VERITAS (DNV) in its recommended practice guidance on Statistical Representation of Soil Data (DNV, 2012), specified two types of uncertainties: aleatory and epistemic uncertainty. Aleatory uncertainty refers to the natural randomness of a quantity such as the variability in the soil strength from point to point within a soil volume. While, epistemic uncertainty consists of statistical uncertainty, model uncertainty, and measurement uncertainty, which are all classified as a type of uncertainty associated with limited, insufficient or imprecise knowledge. This work will focus more on the uncertainty related to the natural variability of the soil.

In this respect, as a manner of comparison, Baecher & Christian (2005) pointed out that the degree of uncertainty associated with geotechnical characterization is much higher than the degree uncertainty associated in structural engineering.

Back to soil variability, Phoon & Kulhawy (1999a) described uncertainties in soil properties as the attribution of three sources: inherent variability, measurement error and transformation uncertainty (Figure 2.1). The first is the result of natural geological processes that produced and continually modified the soil mass in situ. The second is due to equipment, procedural operator, and random testing effects. Collectively, these two sources are described as data scatter. In situ measurements, also are influenced by statistical uncertainty or sampling error that result from limited amounts of information.

The third source of uncertainty is due when field or laboratory measurements are transformed into the design of soil properties using empirical or other correlation models. The relative contribution of these three sources to the overall uncertainty in the design of soil property depends on the site conditions, the degree of equipment and procedural control, and precision of the correlation model.

As a result of the conception of these sources, Phoon & Kulhawy (1999a), after Kulhawy (1992), indicated that soil properties could be described by the Coefficient of Variation (CoV) and the correlation distance (δ_v) or scale of fluctuation (Figure 2.2). This last one is more ap-
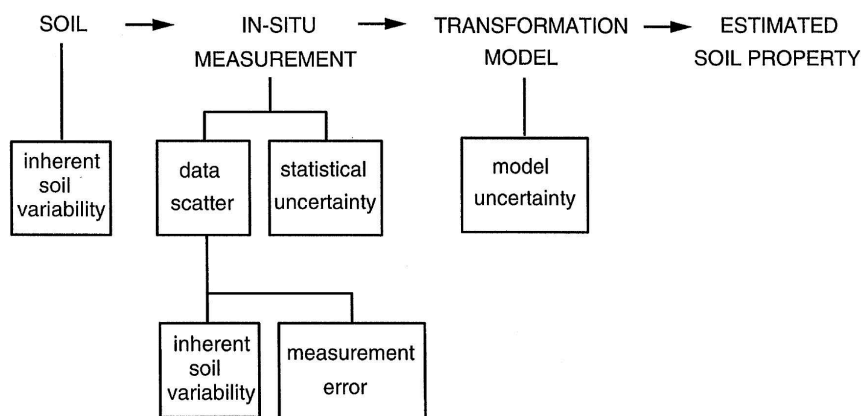
Figure 2.1 – Schematic representation of uncertainty for soil property estimation (Phoon & Kulhawy, 1999a).
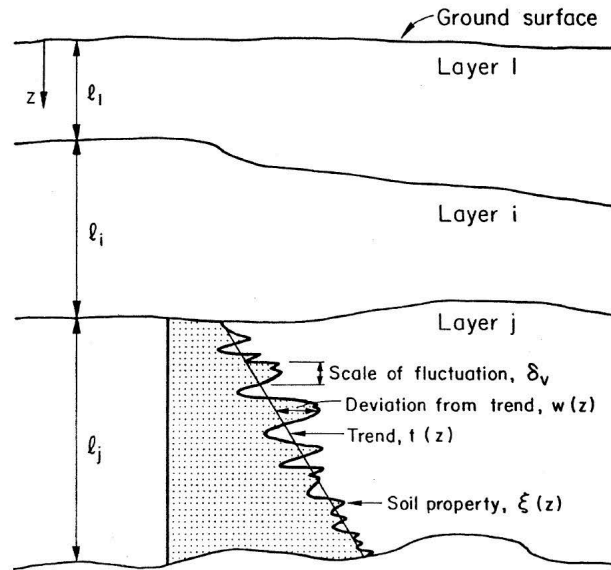
Figure 2.2 – Schematic representation of inherent soil variability – Scale of fluctuation (Phoon & Kulhawy, 1999a).

plied in geostatistical because it indicates the distance within which the property values showed a relatively strong correlation.

The CoV, on the other hand, is used as a tool to establish realistic statistical estimation of the variability of soil properties, in order, to quantify realistic "best case" and "worst case" scenarios and provide property guidelines for the calibration of the Reliability-Based Design (RBD) equations. Thus, the focus of this research is to work with the uncertainty of soil properties in terms of CoV.

Table 2.1 reports some typical ranges of coefficients of variation (CoV) of soil properties to provide an overview of the variability of soils.

2.1.2 STATISTICAL ESTIMATION METHODS

Because acceptance in civil engineering practice of the quality of information (parameters) obtained and used for the evaluation of physical phenomena or processes have some degree of uncertainty, it turns the necessity of employment of probabilistic methods to estimate population values from sample values, to describe from mathematical tools input parameters uncertainty that will provide a fit to the population data, given the sample from that population. Where, a population includes all of the elements from a set of data, and a sample consists one or more observations drawn from the population.

Uncertainties, as is the case of soil properties in geotechnical engineering, are described by probabilistic density functions (PDF).

Various methods can estimate the values of the parameters of these density functions. According to Gelder (2000), the methods, currently in circulation in civil engineering practice, are:

– The method of moments.

9

Table 2.1 – Approximate guidelines for Coefficients of Variations (CoV) of some design soil properties.

Property			Soil Type	CoV (%)	References
Specific unit weight	γ	[kN/m^3]	Clay and Silt	< 10	Uzielli et al. (2007) Assis (2002)
Effective cohesion	c'	[kPa]	Not reported	20 – 80	Assis (2002) Baecher & Christian (2005)
Effective angle of friction	φ'	[º]	Clay and Sand	5 – 15	Baecher & Christian (2005) Uzielli et al. (2007)
Young's modulus	E	[MPa]	Not reported	10 – 30	Mollon et al. (2013) Baecher & Christian (2005)
Coefficient of consolidation	C_v	[-]	Not reported	33 – 68	Uzielli et al. (2007)
Undrained shear strength	C_u	[kPa]	Clay	20 – 55	Uzielli et al. (2007)
Initial void ratio	e_0	[-]	All soil types	7 – 30	Uzielli et al. (2007)
Compression index	C_c	[-]	Not reported	10 – 37	Uzielli et al. (2007)
Overconsolidation ratio	OCR	[-]	Not reported	10 – 35	Uzielli et al. (2007) Baecher & Christian (2005)
Coef. of lateral earth pressure at rest	k_0	[-]	Clay	40 – 75	Phoon & Kulhawy (1999b)
Permeability coefficient	K	[m/s]	All soil types	200 – 300	Baecher & Christian (2005)

– The method of maximum likelihood.

– The method of least squares (on the original or on the linearized data).

– The method of bayesian estimation.

– The method of maximum entropy.

– The method of probability weighted moments, and.

– The method of L-method.

A brief review of the application of the above estimation methods will be introduced. For detail information about the traditional methods (first four), the reader might refer to textbooks such as: Benjamin & Cornell (1970); Ang & Tang (1975) and, recently, Faber (2012).

In general, it is hard to say which estimation method is the most appropriate method for a particular model and dataset. This depends on the size of the sample, the type of the distribution, the choice of the parameters of the distribution, the inhomogeneity embedded in the data, and of course the choice of the criterion (Gelder, 2000).

2.1.2.1 *The method of moments (MoM)*

Introduced by Karl Pearson in 1894, the method establishes that the moments of a distribution function, in terms of its parameters, are set to be equal to the moments of the observed sample. After the mean and variance of the sample (main descriptor of a random variable) have been estimated then the parameters of its probability density are determined.

The analytical expressions can be derived quite easily, but the estimators can be biased and not efficient. The moment estimators, however, can be used as a starting estimation in an iteration process.

The central moments of distribution are given by:

$$
\begin{aligned}
&\mu_j = E(x - \mu)^j = \int (x - \mu)^j f(x)\, dx \therefore j = 1, 2, 3, 4 \\
&Variance: \sigma^2 = \mu_2 = \int (x - \mu)^2 f(x)\, dx \\
&Skewness: \gamma = \frac{\mu_3}{\mu_2^{3/2}} \\
&Kurtosis: \kappa = \frac{\mu_4}{\mu_2^2}
\end{aligned}
\tag{2.1}
$$

The sample moments are given by:

$$
\begin{aligned}
&\overline{x} = \tfrac{1}{n} \sum x_i \\
&m_j = \tfrac{1}{n} \sum (x_i - \overline{x})^j
\end{aligned}
\tag{2.2}
$$

The sample mean $\overline{x}$ is a natural estimator for μ. The higher sample moments m_j are reasonable estimators of the μ_j, but they are not unbiased. Unbiased estimators are often used. In particular σ^2 is unbiasedly estimated by

$$
s^2 = \frac{1}{n-1}(x_i - \overline{x})^2
\tag{2.3}
$$

2.1.2.2 *The method of maximum likelihood (MML)*

Recommended by Ronald Fisher between 1912 and 1922 and then popularized, the method finds the parameter values of the distribution function that will maximize the likelihood of the observed data, which means that one must seek the value of the parameter vector that maximizes the likelihood function $L(x, \theta)$. For a PDF with two or more parameters, the parameters are estimated through the following equation:

$$
\frac{\partial L(x_1, \cdots, x_n; \theta_1, \cdots, \theta_m)}{\partial \theta_j} = 0 \therefore j = 1, \cdots, m
\tag{2.4}
$$

where $L(x, \theta)$ is the likelihood function. Once the parameters of the PDF that fitted the data are found, the mean and the standard deviation are calculated. This method gives an asymptotically

unbiased parameter estimation, and of all the unbiased estimators it has the smallest mean squared error.

The MML is extremely useful since it is often quite straightforward to evaluate the parameters and the collected information. Nonetheless, it is an approximation, and should only be trusted for large values of n (though the quality of the approximation will vary from model to model).

Analytical expressions for the parameter estimators are sometimes difficult to derive. In those cases, numerical optimization routines have to be used to determine the maximum of the likelihood function, which can also be quite tricky since the optimum of the likelihood function can be extremely flat for large sample sizes (Gelder, 2000).

2.1.2.3 *The method of least squares (MLS)*

Credited by Legendre in 1805 as an approach of regression analysis, the method uses the theory of this approach to find the parameter estimators of the PDF through the minimization of the error of estimation.

$$y_i = ax_i + b + e_i \tag{2.5}$$

In this way, this method allows to minimize the sum of squares of residues as:

$$S = \sum (e_i)^2 = \sum (y_i - ax_i - b)^2 \tag{2.6}$$

Minimization occurs by deriving S from a and b and then equating to zero $\frac{\partial S}{\partial a} = 0 \therefore \frac{\partial S}{\partial b} = 0$. This approach allows to find the values of a and b. Thus, given the observations $x = (x_1, x_2, \cdots, x_n)$ and $y = (y_1, y_2, \cdots, y_n)$ and assuming a PDF, regression techniques are employed to the data. In this way, its parameters can be estimated by assuming that the function can be linearized.

2.1.2.4 *The method of bayesian estimation (BEM)*

The method is based on the Bayesian Decision Theory, introduced by Bayes (1763), in which the unknown parameters of the PDF are assumed, to describe the random process which has generated the observed data.

$$f(\theta \mid x) = \frac{f(\theta) f(x \mid \theta)}{\int f(\theta) f(x \mid \theta) \, d\theta} \tag{2.7}$$

where $f(\theta)$ is the known or assumed PDF of the possible θ values which summarizes the prior beliefs about the possible values of the parameters of the PDF (like the λ and ζ parameters of the Lognormal PDF), $f(x|\theta)$ is the conditional probability, or likelihood of the data given θ and $f(\theta|x)$ is the posterior distribution of θ given the observed data x.

Density functions represent the prior and posterior distributions of θ. The joint probability distribution of the data and the parameter is given by $f(x|\theta)$ which is called the likelihood and is defined by:

$$f(x|\theta) = L(\theta) = \prod f(x_i|\theta) \tag{2.8}$$

Bayes theorem is applied multiplying the prior distribution by the likelihood function and then normalizing it, to get the posterior probability density, which is the conditional distribution of the uncertain quantity given the data. The posterior density summarizes the total information, after considering the new data, and provides a basis for posterior inference regarding θ.

In this way, by combining the prior PDF with the observed data, the PDF is updated obtaining a posterior PDF. After this procedure, the value of each parameter (assumed) which minimizes the posterior PDF will be the right estimated parameters.

2.1.2.5 *The method of maximum entropy (MME)*

Formulated by Jaynes (1957) as an approach for choosing a consistent PDF among all possible distributions, the method measures the uncertainty about a random variable. The concept of entropy provides a quantitative measure of this uncertainty. The maximum uncertainty corresponds to the maximum of entropy. Thus, for the estimation of PDF parameters, the PDF that maximizes the information entropy is the statistically most like to occur, because the more is the value of entropy, the higher is the information obtained from the data. For a continuous random variable, x, the entropy is defined as:

$$H[f(x)] = -\int_R f(x)\ln[f(x)]\,dx \tag{2.9}$$

where $f(x)$ denotes the probability density function (assumed), and R is the integral domain. Then the central moments of the PDF are determined by the following equations:

$$\int_{-\infty}^{\infty} f(x)\,dx = 1 \tag{2.10}$$

$$\int_{-\infty}^{\infty} x^i f(x)\,dx = m_i \therefore i = 1, 2, \cdots, N \tag{2.11}$$

where Eq. 2.9 represents the normalization condition and m_i in Eq. 2.10 are the moments of the density functions, and N represents the moment of highest order. Thus, by estimating these moments, the PDF parameters are then estimated.

The Euler – Lagrange equation can be applied to solve the problem. Thus, the function $f(x)$ is rewritten in the following form:

$$f(x) = \exp\left[-\lambda_0 - \sum_{i=1}^{N} \lambda_i x^i\right] \tag{2.12}$$

where λ_0, λ_i are the Lagrangian multipliers. It can be proved that this functional form is referred to as the most unbiased among all PDFs that satisfy the same set of conditions imposed on Eqs. 2.9 and 2.10.

2.1.2.6 *The method of probabilistic weighted moments (PWM)*

Introduced by Greenwood et al. (1979), the method considers that a cumulative distribution function $F(x) = Prob(X \leq x)$, can be characterized by:

$$M_{l,j,k} = \int_0^1 x^l F^j(x)(1-F(x))^k dF(x) \tag{2.13}$$

where l, j and k are real numbers. These moments can be seen as descriptive parameters of location, scale, and shape of a probability function, respectively. When j and k are set to zero, the moments $M_{l,0,0}$ correspond to the moment in the origin of order l.

Estimation based on probability weighted moments is often considered to be superior to standard moment-based estimates. They are sometimes used when maximum likelihood estimates are unavailable or difficult to compute (Landwehr et al., 1979), as are the cases of the Weibull, Gumbel, Generalized lambda, Logistic, Wakeby, and Kappa distribution function. A particular case is observed in the Weibull distribution function where the parameters λ and κ can be estimated by using the Maximum Likelihood Method (an implicit function is implemented on the κ parameter).

Greenwood et al. (1979) proposed this method to deal with the Wakeby distribution because it is a distribution function potentially useful to flood frequency analysis in particular and to flow frequency analysis in general for several reasons. First, it offers a simple explanation of the condition of separation. Second, it is characterized by five parameters suggesting better capability of fitting data than distributions characterized by fewer parameters.

2.1.2.7 *The method of L – moments (MLM)*

Introduced by Hosking (1990), the method emphasizes the construction of L-moments, through linear combinations, of the same statistic order of the traditional moments. The L-moments, for a probability density with cumulative distribution function $F(x)$, are estimated by the following equations:

$$
\begin{aligned}
\lambda_1 &= \int_0^1 x(F)\, dF \\[2mm]
\lambda_2 &= \int_0^1 x(F)(2F-1)\, dF \\[2mm]
\lambda_3 &= \int_0^1 x(F)(6F^2 - 6F + 1)\, dF \\[2mm]
\lambda_4 &= \int_0^1 x(F)(20F^3 - 30F^2 + 12F - 1)\, dF
\end{aligned}
\tag{2.14}
$$

where x is the real-valued random variables. These L – moments are related to the conventional moments through the following relations: Mean: $\lambda_1 = \mu$; Variance: $\lambda_2 = \sigma^2$; Skewness: $\tau_3 = \lambda_3/\lambda_2$; and Kurtosis: $\tau_4 = \lambda_4/\lambda_2 = \kappa$.

Analogously to the usual method of moments, the "method of L-moments" obtains the estimation of parameters by equating the unknown parameters to the corresponding population quantities.

As a final remark, L-moments are less subject to bias in estimation and approximate their asymptotic normal distribution more closely in finite samples. Estimated parameters obtained from L-moments are sometimes more accurate in small samples than even the maximum likelihood method.

2.1.3 DISTRIBUTION TYPES USED IN GEOTECHNICS

Statistical and probabilistic textbooks in geotechnical engineering were reviewed (Bury, 1999; Baecher & Christian, 2005; Griffiths & Fenton, 2007 and Faber, 2012) in order to identify which are the widespread probability distribution functions (PDF) used in the geotechnical field. Table 2.2 summarizes, in alphabetic order, these distribution functions. As it is possible to see, in Table 2.2 have also reported some statistical estimation method applied to the PDF and the geotechnical field where it was applied which of usage was according to the reviewed reference.

Table 2.2 – Some report of PDF applied in geotechnics.

Type of PDF	References	Type of Estimation Method	Geotechnical Field
Beta	Al-Homoud & Tahtamoni (2001) Bhattacharya et al. (2009)	MoM	Slope stability
Exponential	Li et al. (2012)	MME	Slope stability
	Chen et al. (2016)	MoM	
Gamma	Miranda (2007)	MBE	Rock mechanics
	Kulatilake et al. (1993)	MoM	
Generalized Pareto	Teena et al. (2012)	PWM	Offshore
	Vivekanandan (2015)	MLM	Dykes and leavees
Gumbel	Low & Phoon (2002)	MoM	Foundation
	Risi et al. (2013)		Dykes and leavees
Lognormal	Mollon et al. (2013)	MML	Tunneling
	Miro et al. (2015)		
Normal	Cecílio Jr et al. (2014)	MoM	Tunneling
	Miro et al. (2015)	MML	
Weibull	Scheffer et al. (2016)	MoM	Tunneling
	Lin et al. (2016)		Geosynthetics

2.1.4 PROBABILISTIC METHODS

Once the uncertainties, regarding the soil properties for a geotechnical problem, are defined as input variables in terms of mean (μ), standard deviation (σ) and probability density function (PDF), the next step should be to estimate the answer (output) of the problem under analysis. Because in geotechnical engineering as well as in many engineering fields, the estimation is made base on a deterministic analysis (i.e., Factor of safety for a slope stability analysis), only one value of the variables involved in the analysis is used at a time.

So, in order to be able to represent, through a probability density, all the spectrum of possible outputs generated by the combination of the statistical distribution of the input variables, a non-deterministic approach is needed. Figure 2.3 portrays a modification for the classification of the different non-deterministic approaches, found in the literature, and proposed by Nasekhian (2011).

An update of the scheme portrayed in Figure 2.3 was presented by Huber (2013). The standard methods and procedures such as MC (Monte Carlo simulation), FOSM (First Order Second Moment approximation), FORM (First Order Reliability Method). SORM (Second Order Reliability Method), Taylor Series Finite Difference Method and the PEM (Point Estimate Methods) can be found in standard textbooks (Haldar & Mahadevan, 2000; Assis, 2002; Baecher & Christian, 2005; Griffiths & Fenton, 2007 and Faber, 2012).

Regarding application on geotechnical engineering, some applications of the methods just
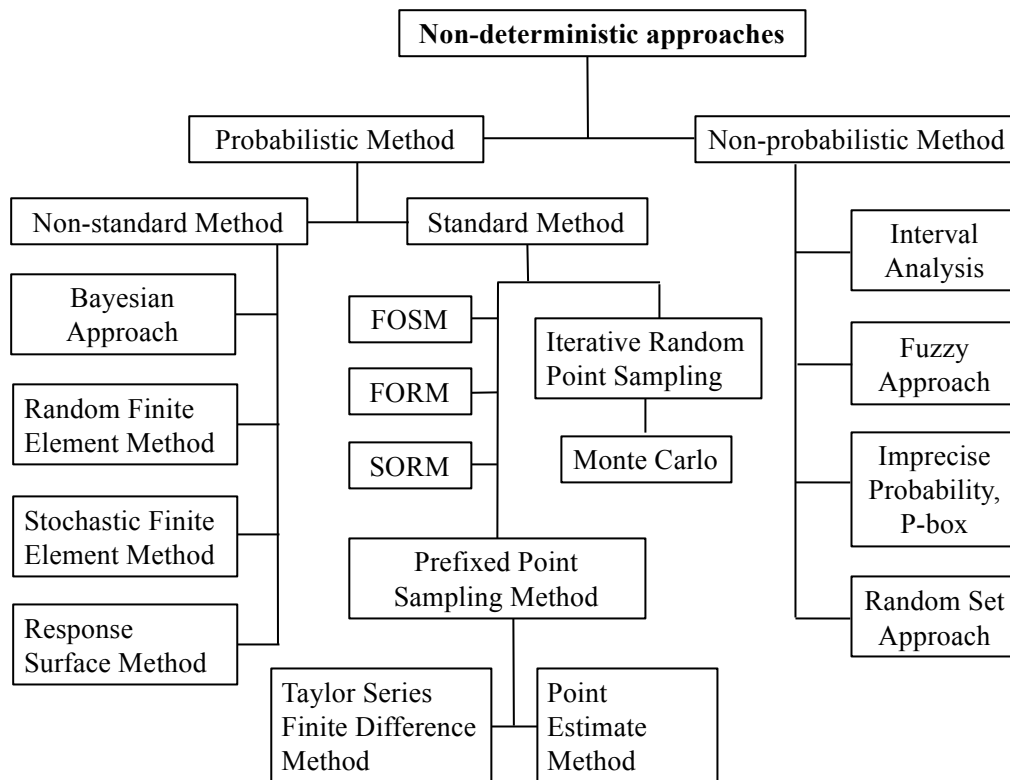
Figure 2.3 – Schematic classification of non-deterministic approaches (after Nasekhian, 2011).

mentioned previously are reported by:

- Monte Carlo: Cecílio Jr et al. (2014).

- FOSM: Alarcón (2014).

- FORM: and SORM: Napa-García et al. (2014) and Low (2014).

- Taylor series difference method: Phoon (2008).

- PEM: Charbel (2015) and Napa-García et al. (2017).

In relation to the others of non-deterministic approaches portrayed in Figure 2.3 a brief introduction of them will made herein after.

2.1.4.1 *The bayesian approach*

Based on the Bayes' theorem, the scope of this approach is to compute the estimation of the probability of failure of a system (Zhang, 2009). For this achievement, the output variable is inferred to have a PDF, and the values of its parameters are also assumed. A first assumption of the output information depends on engineering experience which can be linked to the use of the observational method, because the more data is available and accurately assessed the few subjective assumptions, about the probability density of the output random variable, is assigned and thus the better is the result for prediction of the system response.

In principle, the estimation of the probability of failure P^f, based on the gaining additional information Z, is:

$$P_{(F|Z)} = \int_{\Omega_Z} f_{X|Z}(x)\, dx \tag{2.15}$$

where Ω_Z is the updated failure region making the limit state functions conditional on Z. X is the prior random information data, and $f_{X|Z}(x)$ is the updated probability density function given the information Z, which can be estimated as:

$$f_{X|Z}(x) = \frac{L(Z|x)\, f(x)}{\int L(Z|x)\, f(x) dx} \tag{2.16}$$

where $L(Z|x)$ is the likelihood function of observing Z, given the variable X.

2.1.4.2 *The random finite element method*

This approach allows the consideration of the spatial variability of the soil parameters into the numerical modeling, thus neglecting the homogeneity of the soil layer. Soil parameters are modeled as random fields. The soil is divided into small elements employing finite element

discretization, and the sampling is implemented for each element (Griffiths & Fenton, 2007). Not to confuse these elements (material properties elements) with the finite element mesh used for modeling. Considering the spatial correlations length (which depends on soil characteristic) the soil property of the i_{th} element in the random field is assigned using different algorithms as:

– Moving Average method.

– Discrete Fourier Transformation method.

– Covariance Matrix Decomposition.

– Fast Fourier Transform method.

– Turning Bands method.

– Local Average Subdivision method.

Figure 2.4 illustrates better the application of the Random Finite Element Method for estimation of probability of failure of differential settlements (α) due to tunneling. Huber et al. (2010) started by constructing a single model where the material follows a random set distribution in order to take into account the spatial soil variability (only Modulus of Elasticity).

After that, numerical simulation of the tunnel model is made and the differential settlements of points X–Y is calculated. In order to describe the differential settlements in terms of mean (μ), standard deviation (σ) and PDF, the Monte Carlo approach was used. A total number of 300 numerical simulations were done, and finally the probability of failure was estimated.

2.1.4.3 *The stochastic finite element method*

Introduced by Ghanem & Spanos (1991), the method is an extension of the deterministic finite element method (FEM) where the properties and boundary conditions are random, and the result of this process is coupled with response surface techniques. Following this approach, several finite element simulations are performed, the solution of which define an approximation to the response surface, in order to achieve that a response surface technique is used (i.e., polynomial chaos expansion).

This process will allow representing the random output (i.e., the nodal displacement) as a polynomial series in the input variables of the response surface. The response of the system, which corresponds to a random vector of the unknown probability density function, is used to compute a statistical model of the response quantities, estimate the response PDF of the system as well as to compute the probability of failure of the system through the application of Monte Carlo simulations (Sudret & Der Kiureghian, 2000).
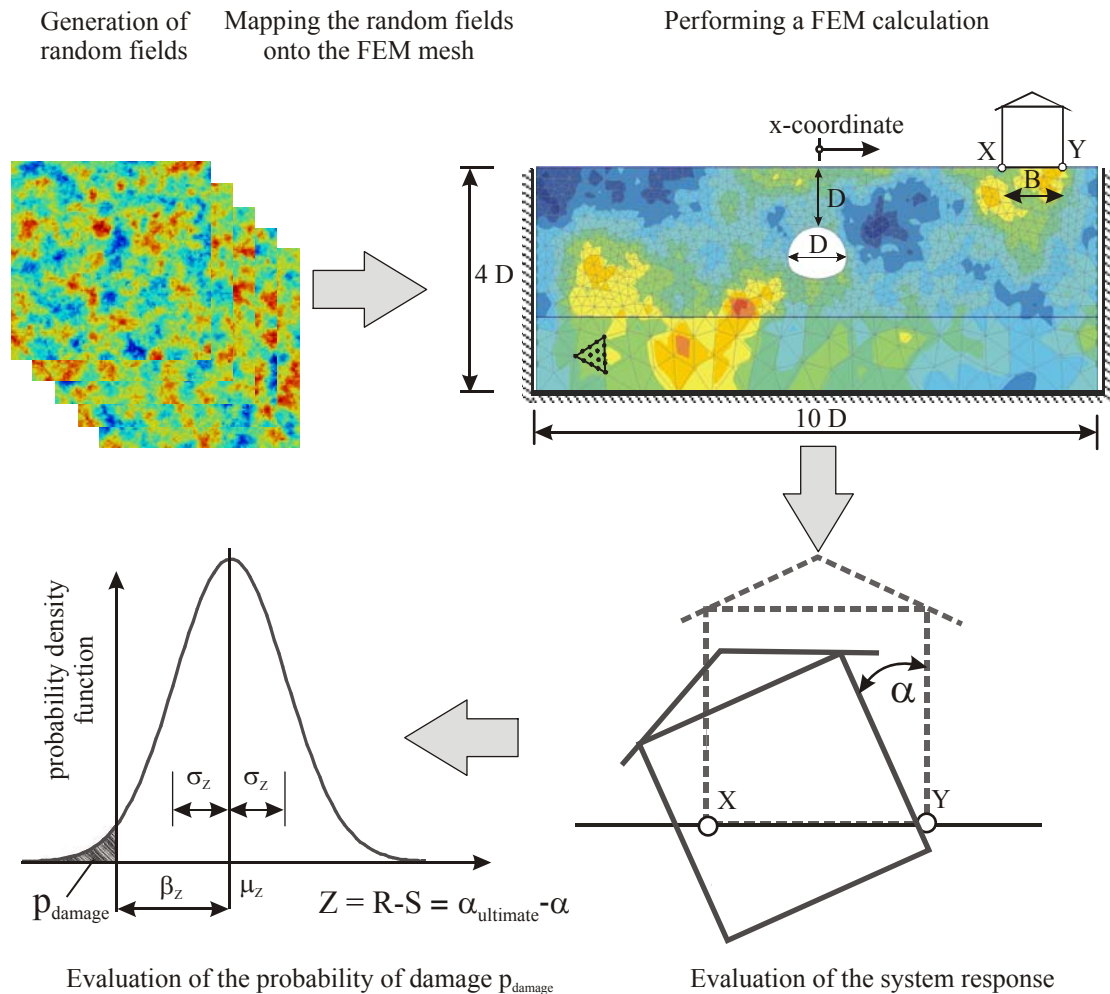
Figure 2.4 – Schematic approach for estimation of probability of failure of differential settlement due to tunneling (Huber et al., 2010).

2.1.4.4 *The response surface method*

Introduced by Box & Wilson (1951), the method is a collection of mathematical and statistical techniques for modeling and analysis where the response quantity of interest (i.e., surface settlement due to tunneling), represented by an unknown function is approximated by a known function chosen appropriately. This approximation can be based on the results of experiments and also on the results of numerical modeling, i.e., results obtained from finite element method (Griffiths & Fenton, 2007). In the case of numerical computations, a relationship between the model parameters $x_1, x_2, x_3, \cdots, x_n$, which are introduced as input data, and the values obtained as output data $y = f(x_1, x_2, x_3, \cdots, x_n)$ is defined. The function obtained by this method can replace the original model in uncertainty analysis.

According to Bucher (2009), there are different approaches to represent the response surface:

– Regression models (i.e. polynomials of varying degree or non-linear functions such as exponentials).
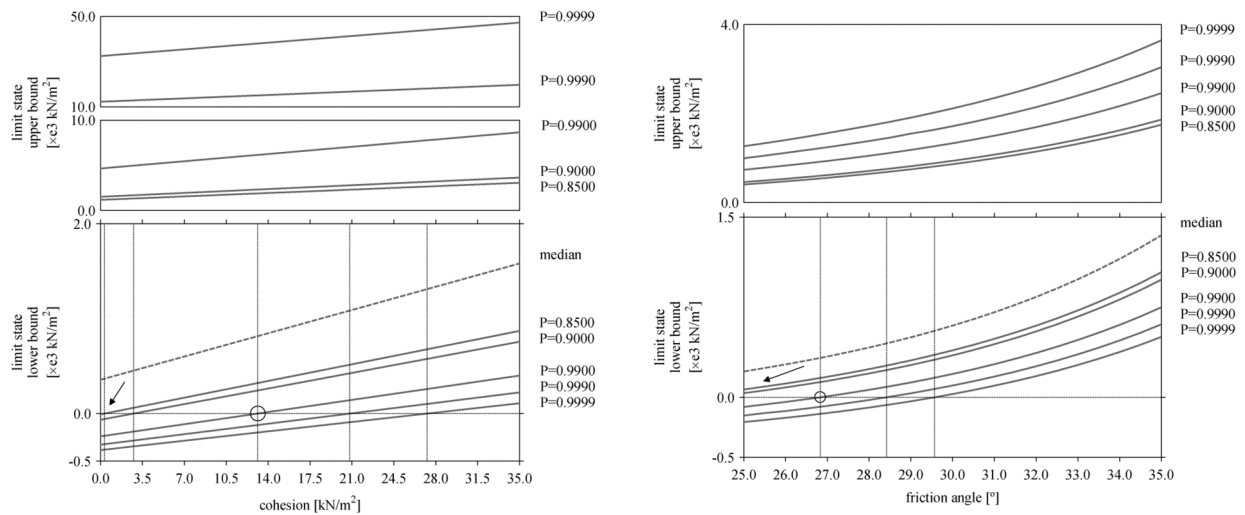
Figure 2.5 – Interval analysis of a limit state chart for safety assessment for the cohesion and friction angle, respectively (after Marques et al., 2015).

  – Artificial neural networks.

  – Support vector machines.

  – Kriging and radial basis functions.

  – Polynomial Chaos Expansion (for a stochastic version of the problem).

Then, the Monte Carlo simulation is applied to the response model in order to evaluate the system. With this approach, a PDF that represents the whole system response is defined, and information about its mean, variance and other statistical moments are also obtained. Moreover, this PDF can be used for the evaluation of the probability of failure of the system.

2.1.4.5 *Interval analysis*

Introduced by Moore (1969), the method seeks for represent interval numbers, vectors and matrices through a set of techniques in order to provide error analyses for computational results. The interval approach is used to describe parameters uncertainties either in geometry, loading and soil parameters as interval quantities. The uncertainty is assumed to be unknown. but bounded $[a, b] = \{x : a \leq x \leq b\}$.

Technics are used in order to obtain simultaneously upper and lower bounds to the exact solution of the system under analysis. Nasekhian (2011) describes the following technics: *i*) Combinatorial method, *ii*) Perturbation method, *iii*) Sensitivity analysis method, *iv*) Optimization method, *v*) Monte Carlo sampling method and *vi*) Interval arithmetic FEM.

In this way, instead of assuming a PDF to describe the limited data (PDF is considered unknown), an acceptable range of performance fluctuation is estimated. Figure 2.5 shows a representation of the above-stated where different levels of probability were estimated.

2.1.4.6 *Fuzzy approach*

Introduced by Zadeh (1965), the method involves the application of the concept named "Possibility Theory" as an alternative tool of probability theory to deal with uncertainties and is an extension of fuzzy sets and fuzzy logic. The uncertainties of geometry, loading and soil parameters and the lack of knowledge of the PDF type are then studied through the fuzzy set analysis.

A fuzzy set is a class of objects with a continuum of grades characterized by a membership function which assigns to each object a grade of membership ranging between zero and one. In the fuzzy set, the membership function can be expressed as being of various types, such as linear, bell type, triangular, ladder. The membership function explains the degree of uncertainty or fuzziness of an element (parameter), and so selecting the appropriate membership function is essential at the moment to apply fuzzy set theory (Figure 2.6).
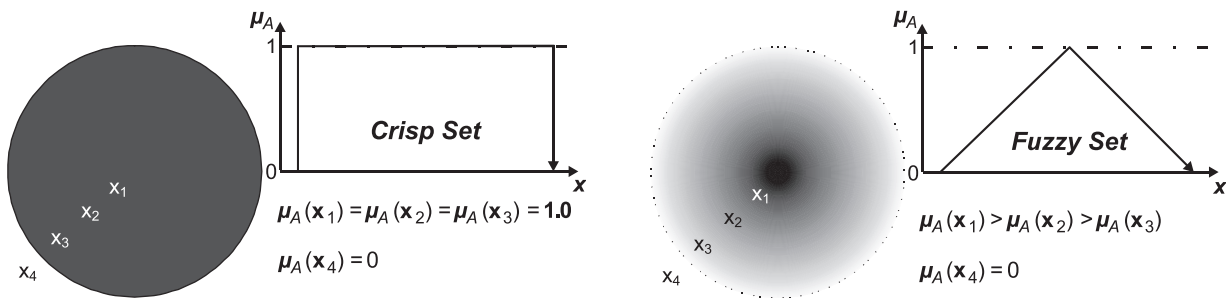
Figure 2.6 – Comparison of types of membership functions, crisp and fuzzy set, respectively (after Aydin, 2004).

Once the membership function is defined, the concept of possibility theory is then applied. In this step, fuzzy variables and distribution of possibility can be compared, respectively, to random variables and probability density functions in the probability theory. The following equation estimates the probability of failure (P_f) in the fuzzy approach:

$$P_f = P\left[Z \leq 0\right] = P\left[R \leq L\right] = \int_{L'}^{\infty} \mu_R\left(x\right) f_L\left(x\right) dx \tag{2.17}$$

where Z is the limit state function, R is the structural resistance, L is the load, $\mu_R(x)$ is the fuzzy membership function of resistance and $f_L(x)$ is the probability density function of load (assumed).

Figure 2.7 shows an example of an application of the fuzzy approach for assessing the occurrence of spalling in underground openings (Lee et al., 2013). From this figure, the letters L' and H' correspond to the fuzzy zones of lower and upper bounds for the spalling criteria. Deterministic and random (defined by a PDF) variables correspond the cases used for representing the load condition model.

2.1.4.7 *Imprecise probability, P-box*

The concept of imprecise probability was formalized/grouped by Walley (1991), to cover mathematical models such as upper and lower probabilities, upper and lower previsions (or expec-
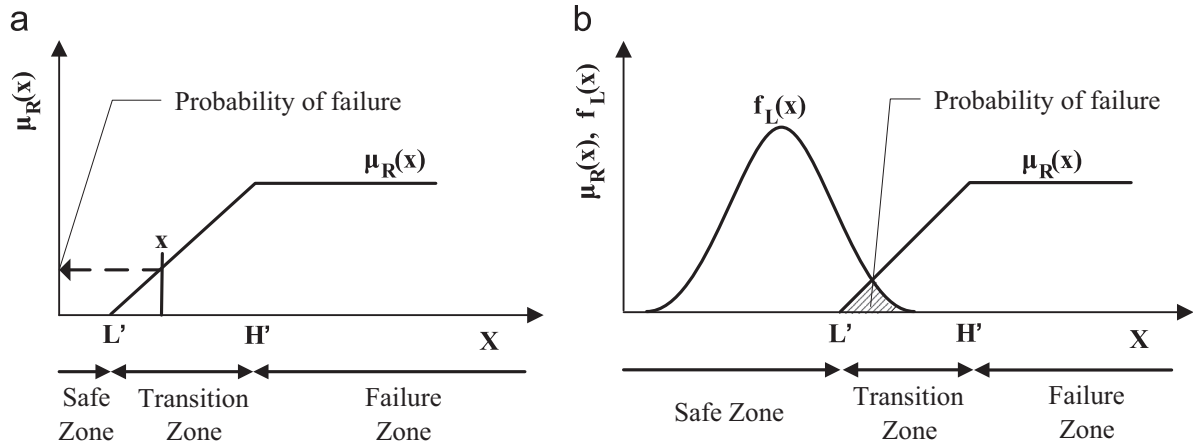
Figure 2.7 – Application of fuzzy approach for estimation occurrence of spalling, (a) Fuzzy criterion-deterministic load model, (b) Fuzzy criterion-random load model (after Lee et al., 2013).
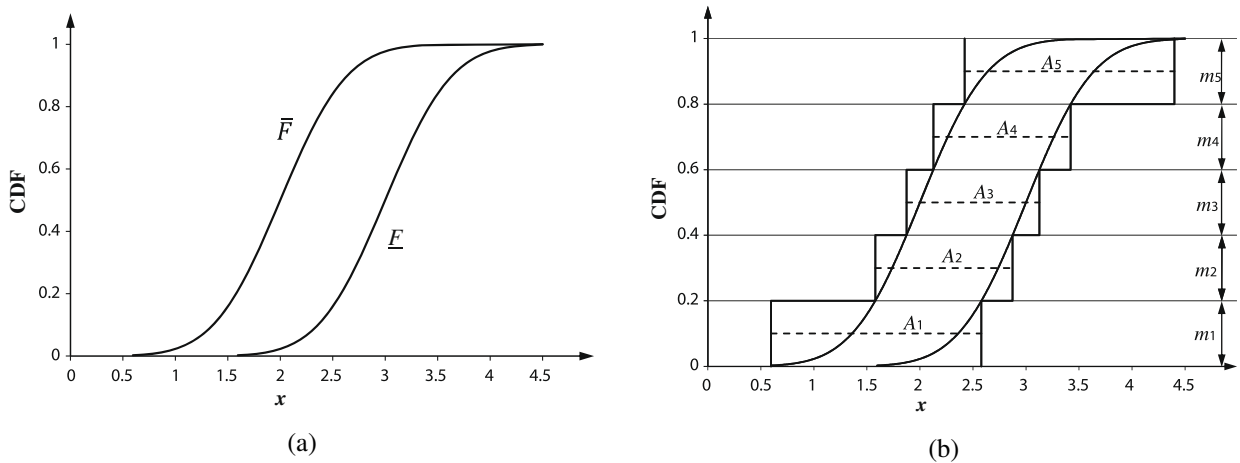
Figure 2.8 – Application of P-box approach, (a) Monte Carlo-based (Zhang et al., 2010b), (b) Discretized P-box (Zhang et al., 2010a).

tations), classes of additive probability measures partial preference orderings and other qualitative models. Before this, Williamson & Downs (1990) already introduced the interval-type bounds on Cumulative Distribution Functions (CDF), which later becomes known as "probability boxes" or "P-box". This method helps to represent, within a pair of CDF, the imprecise PDF of a random variable.

The method can consider all possible distribution types that might lie within the two bounds. Though, this representation is very similar to the random set approach. They are structurally different (Nasekhian, 2011).

The upper and lower CDF are first constructed by considering the limited data and by application of either two technics: *i*) Monte Carlo-based solution or *ii*) Discretized P-box approach (Figure 2.8). By adding more data (i.e., results of finite element analysis), then the bound curves can be refined.

2.1.4.8 *Random set approach*

According to Goutsias et al. (1997), Random set theory was independently conceived by Kendall (1974) and Matheron (1975) as a tool to study the probability of random elements enclosed on space of subsets. The mathematical foundation of random sets is mainly based on Choquet's capacity theorem, which characterizes the distribution of these set-valued random elements as non-additive set functions or "non-additive measures". In theoretical statistics and stochastic geometry, such non-additive measures are known as infinitely monotone, alternating capacities of infinite order, or Choquet capacities, whereas in expert systems theory they are more commonly known as belief measures. Plausibility measures, possibility measures. The study of random sets is, consequently, inseparable from the study of non-additive measures Goutsias et al. (1997).

Based on the measured data (imprecise data), the method allows providing an estimation of its range of probability by deriving the bounds of the original random variables. The bounds are built in terms of CDF and allow to comprise any distribution compatible with the existing data. Figure 2.9 shows a schematic representation of the range of probability for the random variables as well as its zone of the probability of failure.
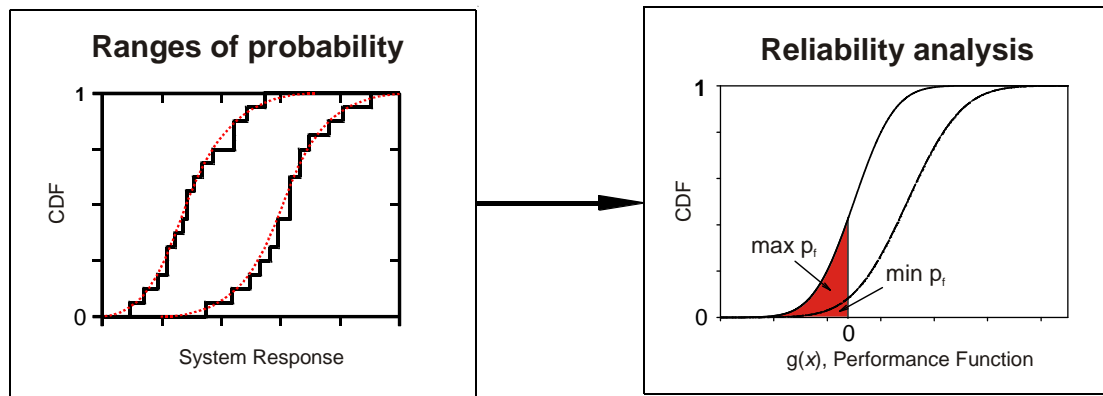
Figure 2.9 – Random set representation of upper and low bound cumulative distribution function (CDF) and the region of probability of failure (after Peschl, 2004).

2.1.5 HYBRID POINT ESTIMATE METHOD (HPEM)

The HPEM is a probabilistic approach that accommodates a multivariate function of numerous correlated and non-correlated, symmetric and non-symmetric input random variables. This method is based on the combination of the first order second-order moment (FOSM) approximation, and the point estimate method (PEM). This method was introduced by Gitirana Jr. (2005), and is mathematically similar to that proposed by Li (1992), but with a different theoretical basis.

The output response, for non-correlated and symmetric input random variables, the first and second statistical moments of $f(X)$ are obtained as follows:

$$\mu\left[f\left(X\right)\right] = f\left(\mu\left[X\right]\right) + \sum_{i=1}^{n}\left[p_i^+ f\left(x_i^+\right) + p_i^- f\left(x_i^-\right) - f\left(\mu\left[X\right]\right)\right] \qquad (2.18)$$

23

$$Var\left[f\left(X\right)\right] = \sigma^2\left[f(X)\right] = \left\{f\left(\mu\left[X\right]\right) - \mu\left[f\left(X\right)\right]\right\}^2$$

$$+ \sum_{i=1}^{n}\left[\begin{array}{l} p_i^+\left\{f\left(x_i^+\right) - \mu\left[f\left(X\right)\right]\right\}^2 + p_i^-\left\{f\left(x_i^-\right) - \mu\left[f\left(X\right)\right]\right\}^2 \\[3mm] -\left\{f\left(\mu\left[X\right]\right) - \mu\left[f\left(X\right)\right]\right\}^2 \end{array}\right] \qquad (2.19)$$

where $X = $ set of n input random variables, $x_1, x_2, \ldots, x_n$; $p_i^\pm = 0.5$ for normally distributed variables; $f(x_i^\pm) = f(\mu[x_1], \ldots x_i^\pm, \ldots \mu[x_n])$; $x_i^\pm = \mu[x_i] \pm \sigma[x_i]$ assuming a normal distribution and n is the number of input random variables.

According to Gitirana Jr. (2005), Equations 2.18 and 2.19 require a small number of computations of $f(X)$ ($2n + 1$ for uncorrelated variable), when compared to the PEM (i.e., 2^n). He, also, demonstrated that these equations have a superior efficiency and same accuracy respect to the conventional PEM, since the same moment-matching estimate points were adopted.

Unlike the Monte Carlo method, where it is necessary to know the PDF of the independent input variables, in the HPEM is just enough to know the values of $\mu[x_i]$ and $\sigma[x_i]$ of the independent variables responsible for generating the dependent output variables.

The computation of this method allows the application of sensitivity analysis through the representation of tornado diagrams, which are commonly used in Decisions Analysis. These diagrams indicate which variables need more attention from the decision maker because they have the more significant influence on the process and which variables can be considered as fix variables because their uncertainty has little influence on the problem in respect (Clemen, 1996).

Two types of tornado diagrams can be used for this purpose, deterministic and probabilistic event tornado diagrams. The deterministic event tornado diagram shows how much uncertainty would be in the performance function if that variable were the only uncertainty in the model. Therefore, correlations are not considered. On the other hand, the probabilistic tornado diagram shows how much uncertainty of a solely variable would be in the performance function when removed from the set of variables of the model. In this case, the correlation of that variable with the other is kept. As no correlation will be considered in the analysis of input variables, this research will focus on the implementation of the deterministic event tornado diagram.

A typical representation of the deterministic event tornado diagram is presented in Figure 2.10. Each diagram bar is constructed by the followings steps:

a) The uncertainty of one input variables (i^{th} variable) is considered and the first and second moments of the performance function are calculated based on the modification of Eqs. 2.18 and 2.19, respectively, for that specific variable as follows:

$$\mu[f\left(X\right)]_i = p_i^+ f\left(x_i^+\right) + p_i^- f\left(x_i^-\right) \qquad (2.20)$$

$$Var[f\left(X\right)]_i = \sigma^2\left[f(X)\right]_i = p_i^+\left(f\left(x_i^+\right) - \mu[f\left(X\right)]_i\right)^2 + p_i^-\left(f\left(x_i^-\right) - \mu[f\left(X\right)]_i\right)^2 \qquad (2.21)$$
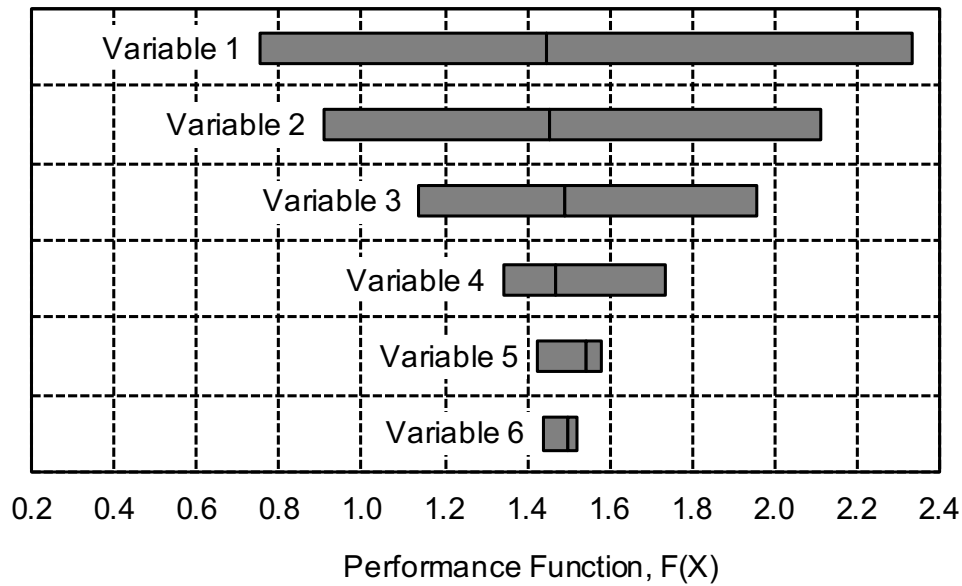
Figure 2.10 – Presentation of deterministic tornado diagram.

b) Computation of the 10th, 50th and 90th percentiles is made from Eqs. 2.20 and 2.21. The Lognormal distribution is assumed for the performance function in order to compute the percentiles;

c) Steps "a" and "b" are repeated for all random input variables;

d) A bar is created on the tornado diagram for each run perfomed from steps "a" to "c". Each bars corresponds to the input random variables whose unceratainty was considered. The ends of the bars correspond to the 10th and 90th percentiles of F and the line in the middled of each bar indicates the 50th;

e) Finally, the bars are sorted from widest to narrowest, resulting in the tornado-shaped appearance. The larger the size of a bar, the more sensitive is the performance function to the input variable corresponding to that bar.

2.1.6 MONTE CARLO (MC) APPROACH

The Monte Carlo method allows obtaining the probability density function (PDF) of a dependent variable through the successive process simulation of several combinations random of set input variables $X = (X_1, X_2, \cdots, X_n)$. Each input variable X_i is characterized to have its PDF. Thus, at every simulation, a particular set of values of the random input variables X_i randomly generated, is used to obtain a corresponding value of the dependent variable F_i. The set of values obtained after the completion of the process simulation helps to defined the Probability Density Function of F (Figure 2.11). In some cases, some variables are considered as deterministic input variables, which remained as constant variables in the simulation process.

The main advantage of this method is the ability to obtain the complete PDF of the dependent variable, which is why the method is referred to as an accurate method. As a disadvantage, the

$$F = f(D_1, X_1, ..., X_n, ..., D_n)$$
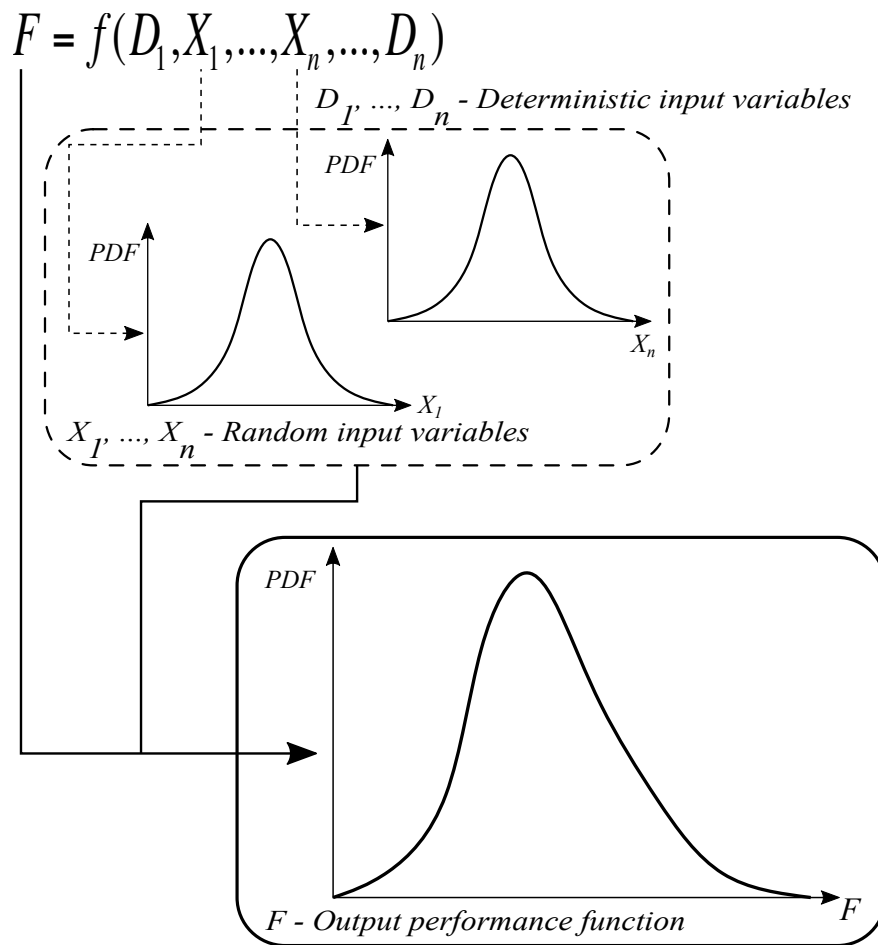
Figure 2.11 – Schematic representation of application of the Monte Carlo method.

long time to perform a large number of trials in the simulations is cited, especially in analyses that involved Finite Element models (Assis, 2002).

Good examples of the application of the Monte Carlo method in tunneling can be observed on the Works of Mollon et al. (2013) and Miro et al. (2015). These authors provided a methodology for evaluating the influence of uncertainties of soil parameters on surface settlements due to tunneling (Figure 2.12). Firstly, the authors idealized a 3D numerical model for tunnel simulation to obtain the settlement trough. The obtained transversal and longitudinal settlement curve were converted, respectively, into a mathematical formulation in terms of geotechnical parameters (e.g., cohesion, friction angle, Young's modulus) by the employment of Surface Response technics. Finally, the Monte Carlo method was applied to these formulations to obtain the PDF of the dependent variable (Settlement trough) after the trial simulation process of the random input variables (e.g., cohesion. friction angle. Young's modulus).

Finally, to conclude with this chapter, the employment of the HPEM is justified on the premise that this method was not be applied before in tunneling studies and, also, because allow fast and reliable computation of numerical models, while the MC method will be employed in the forthcoming analytical expressions.
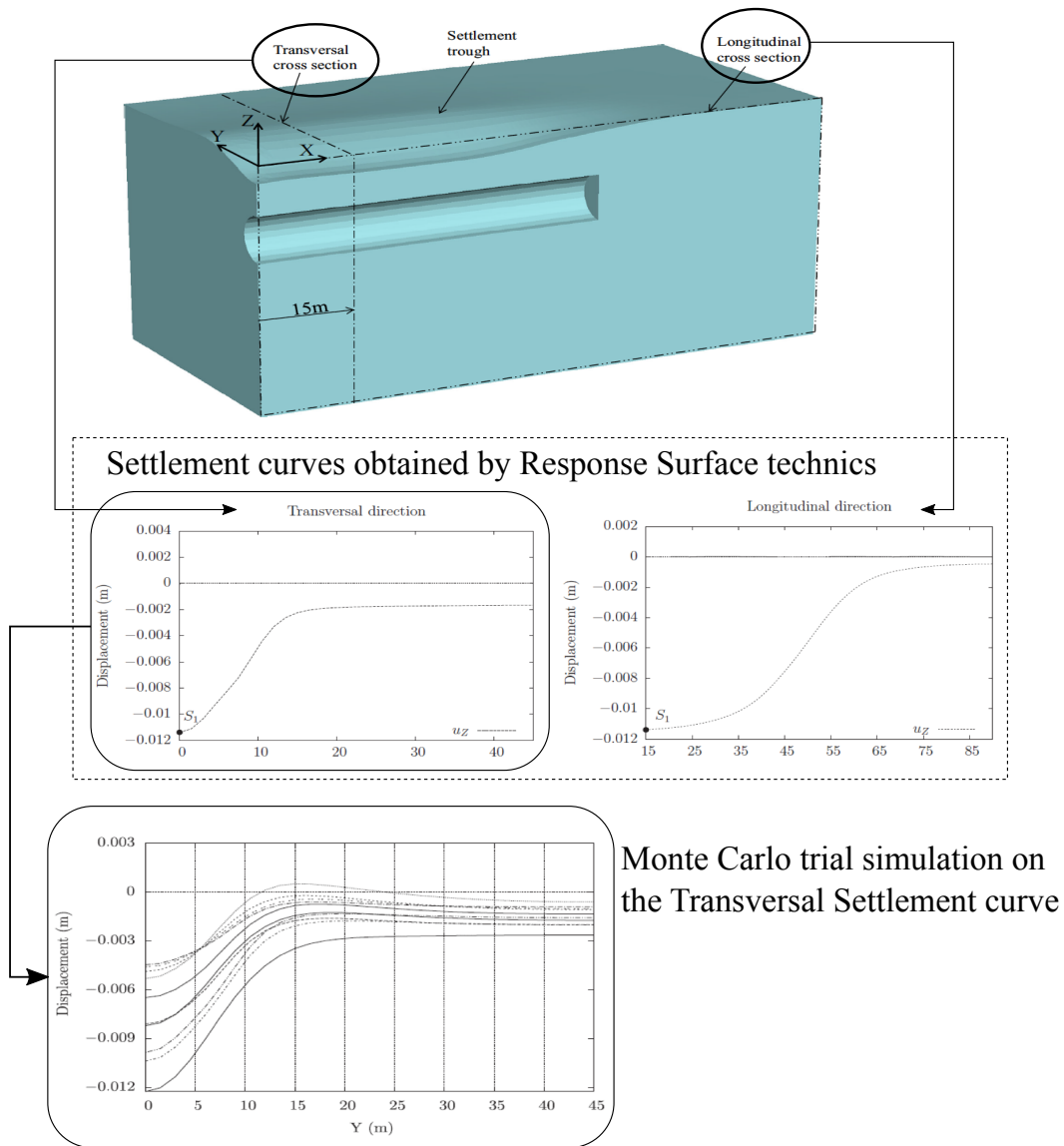
Figure 2.12 – Schematic Monte Carlo analysis on surface settlement due to tunneling (after Miro et al., 2015).

2.1.7 DISCUSSION AND ADOPTED APPROACH

The main topic of this chapter was to provide a general overview and brief definition of the different statistical methods, for estimation of Probability Density Function (PDF) of input parameters, as well as the currently probabilistic methods employed in geotechnical engineering for estimation of mean (μ), standard deviation (σ) and PDF of output variables.

So, as in any engineering field as in the geotechnical field, these technics constitute the necessary tools to deal with uncertainty and soil parameter variability. The choice of either the appropriate type of statistical estimation method or probabilistic method to use will depend on too many factors. Such factors like the expertise of the engineer with the methods, the type of geotechnical problem to deal with (i.e., slope stability, surface settlement, etc.), the size of the variables to work with, the type of PDF assumed for the variables and, lastly, the probability of failure (P_f) of the output variable to perform reliability analysis.

Another approach, that was mentioned to deal with soil variability, is the use of geostatistics, which allows analyzing from the spatial point of view the variation of soil properties. Thus, in geostatistic a set of statistical tools are employed in order to describe and estimate, through correlation, the spatial features of a data set (Isaaks & Srivastava, 1989). Variogram models, based on the data set, are employed to reduce the error variance of continuity (correlation distance $- \delta_v$) between nearby samples. In other words, in variogram models, the changes in spatial continuity with distance and direction are described.

In this study, the use of geostatistical tools for estimation of soil variability on surface settlement due to TBM tunneling will not be employed. As already mentioned in Chapter 1, surface settlement is a subject of interest in urban areas resulted from a combination of geotechnical parameters of groundmass. Thus, the author believes that input soil parameters as those indicated in Table 2.1 can be better treated with geostatistical technics. Even so, the efficiency on the estimation of the output response of surface settlements may not be well assessed. Additionally, in order to apply this approach correctly, it is also necessary to have sufficient data related to the correlation length of each input variable, which sometimes is not available (Isaaks & Srivastava, 1989).

Therefore, the focus of this research will be to work with the uncertainty of soil properties in terms of CoV on the input soil properties in order to assess the output variables (e.g., surface settlement), also, in terms of CoV.

Regarding the use of probabilistic density function (PDF) in this research. Table 2.2 summarized all the types of distribution which will be used for the description of the sample data, from the statistical point of view. So, in order to facilitate these analyses, the distribution fitting toolbox embedded in MATLAB R2015a will be employed at every PDF, to estimate their respective values of the mean (μ) and standard deviation (σ). The type of statistical estimation methods offered within this software, to solve the analyses, is the method of maximum likelihood (MML).

The MATLAB distribution fitting toolbox comprises a collection of various and widely used of distribution functions in statistic converting it in a popular choice for fitting distribution function parameters. The software also allows to manage a lot of data and computationally find out the distribution parameters in a very efficient manner.

Once again, the short description of probabilistic approaches presented in section 2.1.4 was the author intended to provide a general overview of the current methodologies for the evaluation of uncertainty in geotechnical problems. So far, many of these probabilistic methods cannot be found easily compiled in statistical and probabilistic textbooks applied in geotechnics. Thus, even though these approaches can be used to analyze the problem stated in this research, none of them will be later discussed in the following chapters.

For this research, the employment of the Hybrid Point Estimate Method (HPEM) and Monte Carlo (MC) methods will be more than enough to describe, in statistical terms, the output variable of the problem (Surface settlement due to tunneling). In the following, a summary of these approaches is described.

2.2 TUNNEL CONSTRUCTION – TUNNEL FACE STABILITY

The constructions of tunnels in urban areas induce ground movement that might represent a hazard or produce damage of buildings, infrastructures or service networks near the excavation. Therefore, the most critical aspect in the construction of tunnels in urban areas is the control of these movements.

According to Leca & New (2007), the surface settlements manifest primarily as a consequence of the rupture of the groundmass stability, which begins at the tunnel face. Depending on the type of soil to be excavated, two types of rupture are formed for cohesive and non-cohesive soils, respectively. Figure 2.13 shows the mechanisms of rupture proposed by Leca & New (2007), supported by the use of laboratory tests with geotechnical centrifuges. Recently with the use of 3D numerical analyses, it has been confirmed a similar failure mechanism for these types of soils (Mollon, 2010).

(a)

(b)
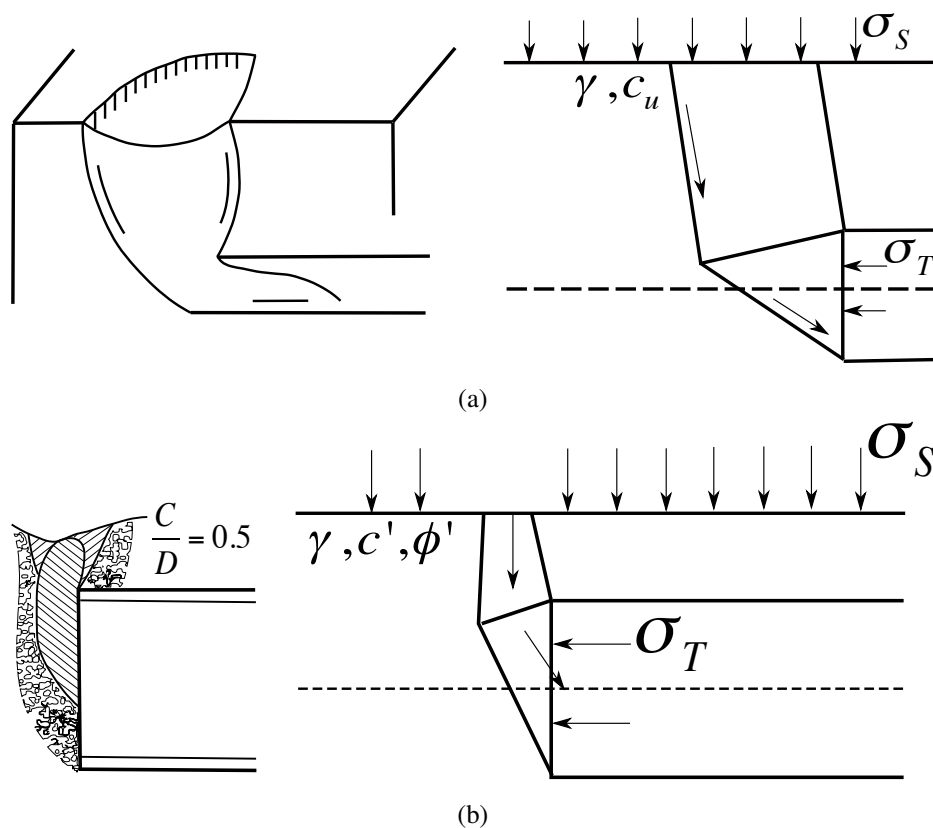
Figure 2.13 – Schematic representation of groundmass failure mechanism due to tunnel face instability. (a) Cohesive soil. and (b) Non-cohesive soils (after Leca & New, 2007).

In the case of cohesive soils (Figure 2.13a) face failure involves a large volume of ground ahead of the working front. This mechanism leads to the formation of a sinkhole at the ground surface, for non-cohesive soils (Figure 2.13b), failure tends to propagate along a chimney acting above the tunnel face. Both types of failure mechanisms produce horizontal and vertical displacements in the groundmass that manifest themselves on the surface in the form of settlement trough. Through this is defined and formulated the volume lost.
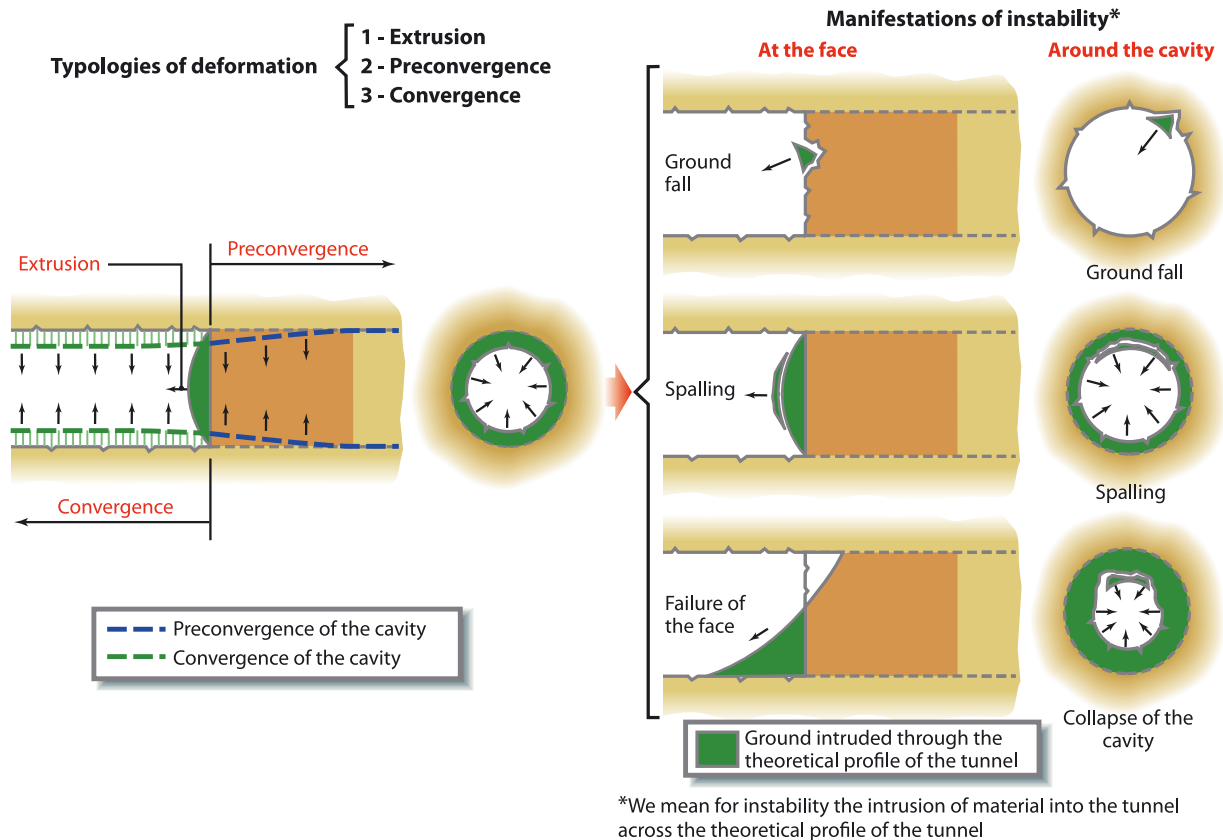
Figure 2.14 – Schematic representation of groundmass deformation at the face and around the tunnel (Lunardi, 2008).

However, although failure occurs at the limit state condition of the groundmass, it is also possible the occurrence of surface settlements, even if the ultimate limit state of the ground is not achieved. These settlements would be the result of the mobilization of the ground strength before achieving failure.

Regarding the deformation at the tunnel face and around the tunnel. Lunardi (2008) observed three types of phenomena (Figure 2.14):

– Extrusion at the face, which can manifest with either a more or less axial symmetric geometry (enlarge of the face) or a gravitational churning geometry (rotation of the face), depending on the type of material and the existing stress state;

– Preconvergence of the cavity, understood as the convergence of the theoretical profile of the tunnel ahead of the face, strictly dependent on the relationship between the strength and deformation properties of the advanced core and its original stress state; and

– Converge of the cavity, which manifests as a decrease in the size of the theoretical cross section of the excavation after the passage of the face.

Thus, the tunnel face stability is closely linked to the type of excavation method which could be the sequential method or the tunnel boring machines (TBM). Sequential excavation methods apply this by either face reinforcement or partial excavation, while TBMs apply this by directly

pressurizing the chamber. A brief description of the tunnel excavation methods will be introduced as well as the type of calculations used to estimate tunnel face stability.

2.2.1 SEQUENTIAL EXCAVATION METHODS

The sequential excavation methods regards those excavations that are carried out at atmospheric pressure through the application of a series of ground treatments at the tunnel face and around the external tunnel profile in order to improve the groundmass condition and allow a safe work environment. This type of tunnel construction method is also know as the New Austrian Tunneling Method (NATM), the Sprayed Concrete Lining (SCL) method, or the conventional tunneling method.

The tunnel excavation is carried out by small section excavation increments. The increments are supported by shotcrete immediately applied after exposure of the ground, followed by the installation of the lining support consisted of steel welded wire mesh, steel arches or also shotcrete. The lining has a defined stiffness to allow controlled stress relaxation around the opening, minimizing the section forces and hence allowing a cost-effective structural design. Thus, different types of sequential excavation methods can be applied for the same project (Figure 2.15).
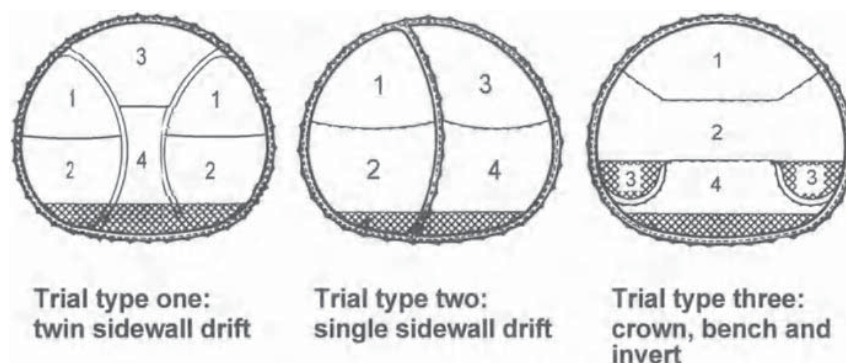
Figure 2.15 – Different types of sequential excavation methods for the Heathrow tunnel construction (New & Bowers, 1994).

Besides, various ground support, face support, pre-support and ground improvement measures are implemented to ensure the stability and safety of the tunneling operation and minimize settlements at the surface (Figure 2.16).

During construction, the deformations in the tunnel, groundmass and the surface are continuously recorded, monitored and interpreted to verify the design assumptions and assess the stability and fitness of the applied excavation sequence and support elements. The interpretation of the monitoring data is fed back to the ongoing construction and adjustments can be made if necessary. The tunnels, constructed through this type of excavation method, are characterized by having a short length and mostly a non-circular shape.

Taking a step back to ground deformation, the experimental and numerical research on the deformation of the ground (extrusion, pre-convergence, and convergence) when a tunnel is excavated lies on the deformability of the advance core (Lunardi, 2008).

Ancona – Bari railway line – "Vasto" tunnel

Solution by means of jet-grouting   **Silty sands and sandy silts**

Solution by means of mechanical precutting + FGT   **Clays**

Solution by means of FGT + FGT   **Clayey silts and silty clays**

12.00 m

FGT = Fibre glass tubes
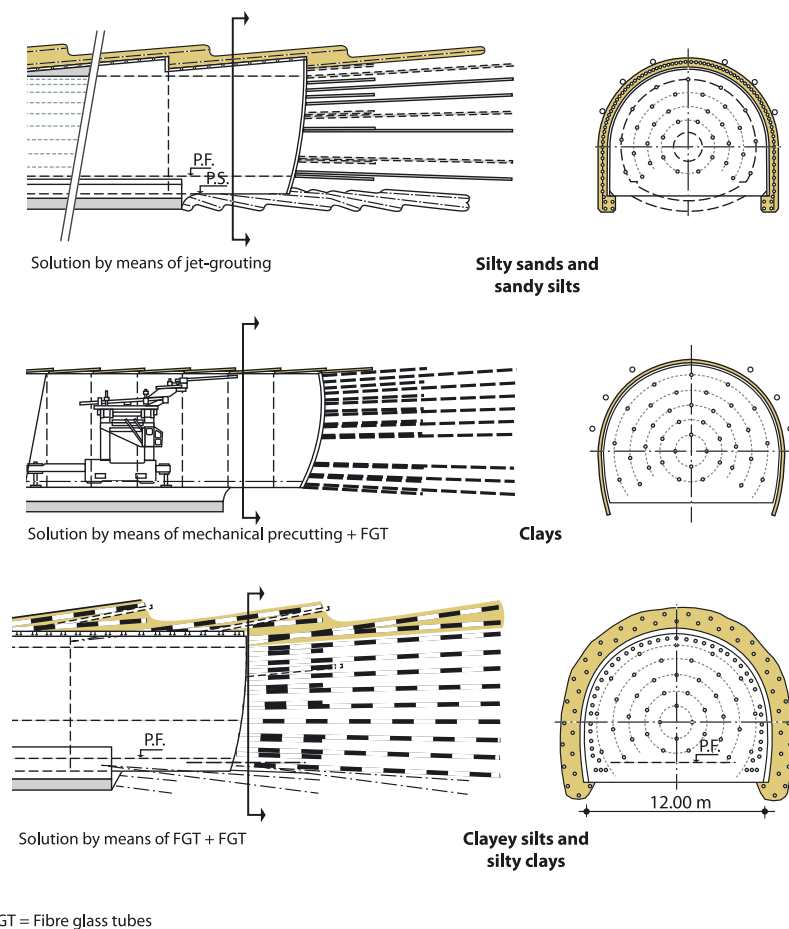
Figure 2.16 – Different types of ground treatments for tunnel construction (Lunardi, 2008).

Therefore, it is necessary the applications of support actions (ground treatment) as those shown in Figure 2.16 to control the deformation due to tunneling. Figure 2.17 shows a representation of the types of control (ahead and down the tunnel face) to avoid significant deformation of the ground.

– Ahead of the face, by regulating the rigidity of the advance core using appropriate preconfinement techniques; and

– Down from the face, by controlling the manner in which the advance core itself extrudes using tunnel confinement techniques capable of providing immediate continuous active confinement of the cavity close to the face.

Finally, as conclusion, an overview on the state of the art of this type of tunneling method was provided. For detail information about the convergence confinement for undestanding the process to design the stiffness and time to install the support, and the construction procedure of this method, the reader might refer to ICE (1996), Kolymbas (2005), Lunardi (2008), Chapman et al. (2017) and Maidl et al. (2013).

Control

Control of deformation response is achieved by regulating the rigidity of the advance core ahead of the face and how it extrudes through the face into the tunnel

Ahead of the face

By regulating the rigidity of the advance core

By means of preconfinement of the cavity using the followings instruments of control:

A   A-A

- The protection of the core

A

A   A-A

- The reinforcement of the core

A

Down from the face

By regulating how the advance core extrudes

By means of confinement of the cavity using the following instrument of control:

- Closing the ring and making the preliminary lining rigid near the face

Figure 2.17 – Schematic representation of ground treatment to control deformation at the face and around the tunnel (Lunardi, 2008).

2.2.2   TUNNEL BORING MACHINE (TBM)

Tunnel Boring Machine consists of the use of a type of machine to construct tunnels with a circular cross-section. These machines, at the front, are equipped with cutting tools to cut the ground. The excavated soil is then mixed with some chemical agents to improve the consistency of the excavated soil. This approach allows to apply a continuous support pressure at the tunnel face to avoid face instability of the ground and at the same time to allow better removal of the excavated material from the excavation chamber. The continuously applied pressure also helps to prevent water from entering into the tunnel if the excavation is made under the water table.

For excavation of soft ground, there are two types of TBM: Earth Pressure Balance machines (EPB) and Slurry Shield (SS) machines. EPB machines use the excavated material to balance the pressure at the tunnel face with the external groundmass by the addition of chemical additives as foams, polymers or bentonite. In SS machines, the cutterhead is filled with pressurized slurry which applies hydrostatic pressure to the excavation face. Figure 2.18 shows a schematic representation of an EPB and SS machine, respectively.

TBMs have the advantages of limiting the disturbance of the surrounding ground and producing a smooth tunnel wall. This significantly reduces the cost of tunnel lining thickness and makes them suitable to use in heavily dense urbanized areas.

Regarding the ground deformation, for the specific case of mechanized tunneling, the magnitude of the movements causing the ground deformation are:
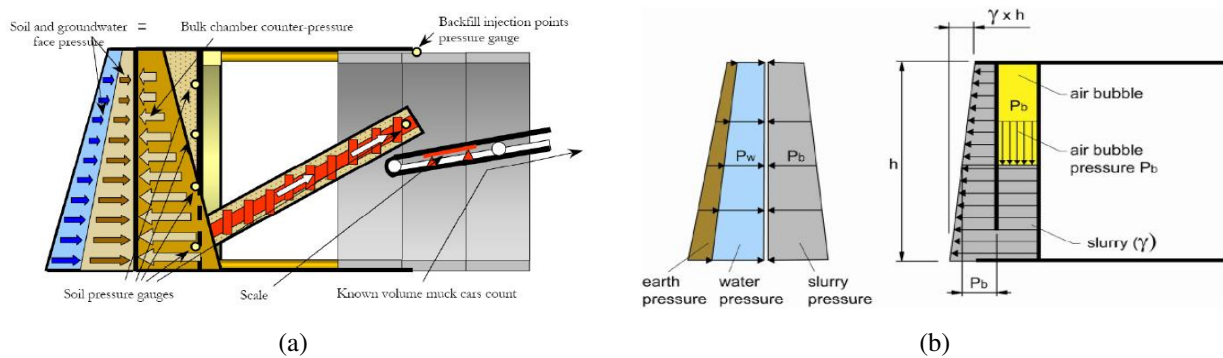
Figure 2.18 – Schematic representation of applied face pressure of TBMs for the excavation soft grounds, (a) Earth Pressure Balance – EPB and (b) Slurry Shield – SS.

– Face loss (extrusion): due to the continuous process of excavation, the ground protrudes out of the tunnel face (Figure 2.19a);

– Radial loss on the shield: this type of deformation is produced by the conical shape of the shield, to allow advance in a straight path, or by the slightly TBM cutterhead over-excavation, to allow advance in a curve path. Guglielmetti et al. (2008) indicated that the deformation due to the conical shape of the TBM is called partial radial (Figure 2.19b) loss and the combination of both factors is called total radial loss (Figure 2.19c); and

– Annular radial loss: is the movement of the ground due to the lack of properly grout injection in the annular gap, and the significant difference in diameter from the back of the shield to the extrados of the lining (Figure 2.19d).

Adequate TBM driving procedures can adequately control both face loss and radial loss. TBM face loss is very limited if the tunnel face is adequately pressurized and the annular radial loss controlled by injection of an adequate volume of grout at the right pressure, with a proper grouting mix design, and through regularly maintained injection lines to avoid plugging.

However, to prevent the face loss requires both a properly application of pressure at the tunnel face as well as a deep understanding of the potential failure mechanisms of the ground due to TBM tunneling, in order to define the most appropriate range of operational pressure distribution applied at the tunnel face according to the encountered geology, the groundwater height, and the depth of the tunnel (Guglielmetti et al., 2008).

Another key aspect for controlling face loss is the extraction mechanism. EPBs extract the mixture mechanically, so the consistency of the mixture is the most important issue. If it is too fluid, it will pass like water through the screw and the face pressure will drop. If it is too sticky or rigid, it will not slide through the screw. In SS machines, this problem does not exist, as the mixture is basically fluid extracted hydraulically.

To conclude, for more detail information about this method, the reader might refer to Guglielmetti et al. (2008) and Maidl et al. (2012).
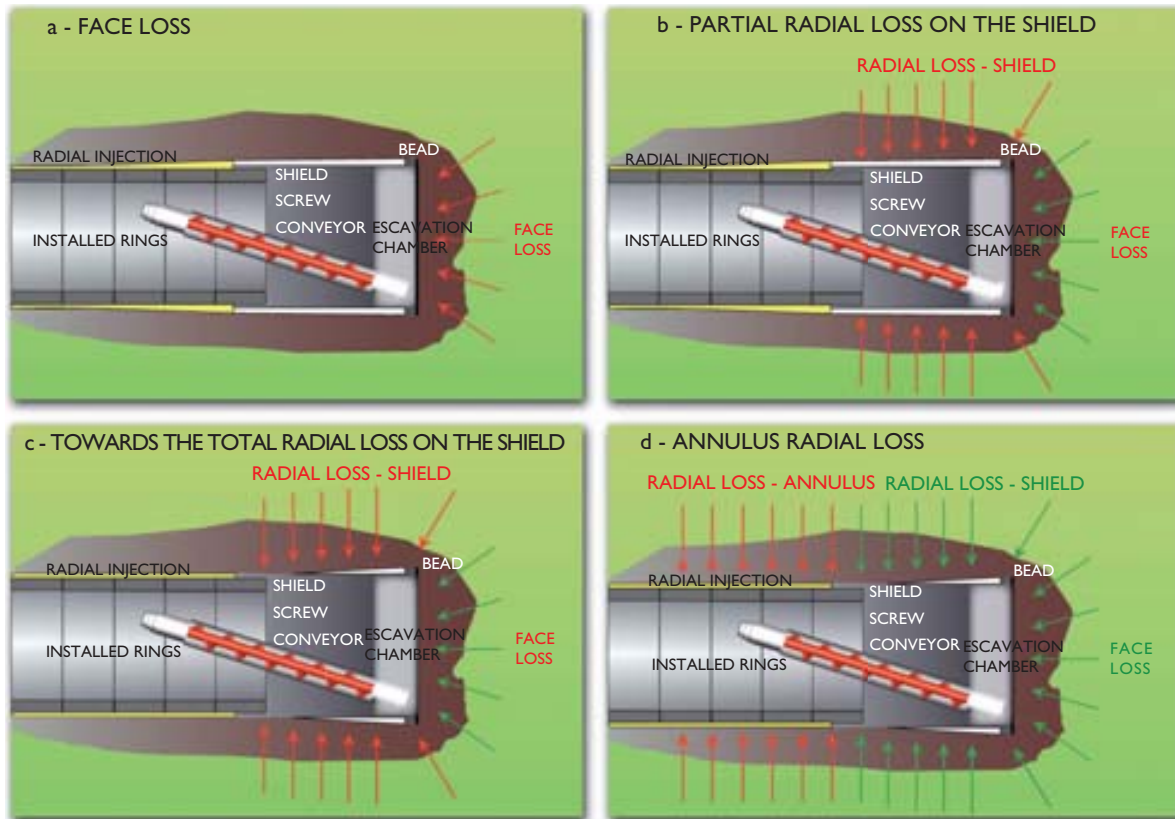
Figure 2.19 – Schematic representation of ground deformation around mechanized tunneling (Guglielmetti et al., 2008).

2.2.3 EVALUATION OF TUNNEL FACE STABILITY

Because tunnel construction in soft ground and highly dense urban areas is becoming very employed, the need for keeping tunnel face stability has become the analysis of vital importance. Besides this, other priorities needed during excavation in the urban environment include *i*) Control of surface settlement, to preserve pre-existing structures, and *ii*) Maintenance of the hydro-geologic equilibrium.

Thus, for the calculation of the face support pressure, two types of calculation approaches are used: *i*) Analytical Methods, and *ii*) Numerical Methods.

2.2.3.1 *Analytical methods*

In the analytical methods, the calculations are based in the use of the global Limit Equilibrium Methods (LEM) or in the Limit Analysis Stress Methods (LASM), which are based in the upper and lower bound solutions of the theory of plasticity. Table 2.3 shows a list of the analytical methods most implemented for estimation of the face support pressure.

In the following. some of the methods indicated in Table 2.3 will be shortly described.

Table 2.3 – List of analytical methods for estimation of face support pressure (after Guglielmetti et al., 2008)

Model/method	Analysis type*	Failure surface	Failure criterion
1. Horn model (Horn, 1961)	GE 3D	Linear (Wedge + silo)	–
2. Murayama method (Murayama et al., 1966)	GE 2D	Spiral logarithmic	MC
3. Broms and Bennemark method (Broms & Bennermark, 1967)	GE 2D	Not defined	TR
4. Atkinson and Potts method (Atkinson & Potts, 1977)	St 2D	Not defined	MC
5. Davis et al. method (Davis et al., 1980)	St 2D	Not defined	TR
6. Krause method (Krause, 1987)	GE 2D – 3D	Circular	MC
7. Mohkam method (Mohkam & Bouyat, 1984, 1985 Mohkam & Wong, 1989)	GE 2D – 3D	Spiral logarithmic + Cylindrical	MC
8. Leca and Dormieux method (Leca & Dormieux, 1990)	St 3D	Solid conical blocks	MC
9. Jancsecz and Steiner method (Jancsecz & Steiner, 1994)	GE 3D	Linear (Wedge + silo)	MC
10. Anagnostou and Kovari method (Anagnostou & Kovári, 1994, 1996)	GE 3D	Linear (Wedge + silo)	MC
11. W. Broere method (Broere, 2001)	GE 3D	Linear (Wedge + silo)	MC
12. Caquot method (Caquot & Kérisel, 1956) implemented by C.Carranza-Torres (Carranza-Torres, 2004)	St 3D	Not defined	MC – HB
13. Mollon method (Mollon, 2010)	St 3D	Solid conical blocks	MC

* GE = Global Equilibrium; St = Stress method; 2D, 3D = analytical formulation derived from 2D, 3D numerical analyses; MC = Mohr–Coulomb; TR = Tresca; HB = Hoek-Brown.

The Mollon method

The method of Mollon (2010) is an update of the Leca and Dormieux method (Leca & Dormieux, 1990), which is based on the upper bound solution of plasticity theory. This method takes into consideration a rigid circular tunnel of diameter D driven under a depth of cover C (Depth: $H = C + D/2$).

Regarding the failure mechanism, this method considers three failure mechanisms (Figure 3.8) denominated MI, MII, and MIII. The firsts two are collapse mechanism, and the third is named blow-out (ground heave).

The upper bound solution for these failure mechanisms are written as:

$$N_S Q_S + N_\gamma Q_\gamma \leq Q_T \tag{2.22}$$

for collapse mechanisms MI and MII and

$$N_S Q_S + N_\gamma Q_\gamma \geq Q_T \tag{2.23}$$
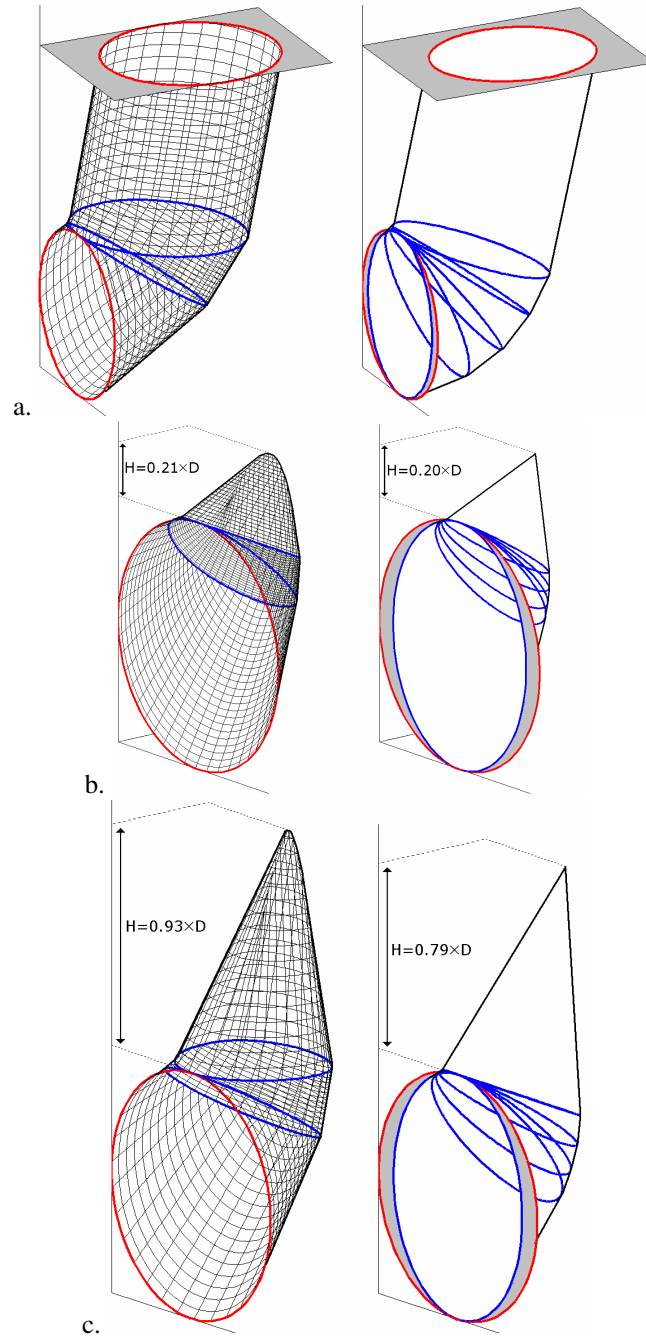
Figure 2.20 – Failure mechanism: (a) MIII, (b) MII and (c) MI (after Mollon, 2010).

for blow-out mechanism MIII, N_S and N_γ are weighting coefficients that depend on the angle α between the axis of the cone adjacent to the tunnel and the horizontal. Q_S, Q_γ and Q_T are loading parameters defined, respectively, as:

$$Q_S = (K_P - 1)\frac{\sigma_S}{\sigma_C} + 1$$

$$Q_\gamma = (K_P - 1)\frac{\gamma D}{\sigma_C} \tag{2.24}$$

$$Q_T = (K_P - 1)\frac{\sigma_T}{\sigma_C} + 1$$

where: K_P: is the Rankine earth pressure coefficient (passive),

σ_C: is the unconfined compression strength,

σ_S: is the surcharge pressure,

σ_T: is the Tunnel pressure, and

γ: is the saturate soil unit weight.

The Anagnostou & Kovári method

This method uses the limit equilibrium method and considers drained soil properties for stability solution. The method is based on the silo theory (Janssen, 1895) and on employs a three-dimensional wedge model of the sliding mechanism proposed by Horn (1961).

Anagnostou & Kovári (1994) investigated the effects of slurry infiltration into the soil mass ahead of the tunnel face on the face stability of slurry shield driven tunnels and quantified the loss of the face support pressure caused by slurry infiltration.

Later, Anagnostou & Kovári (1996) proposed a solution for the required effective face support pressure that consists of four dimensionless factors that consider tunnel diameter, cohesion, piezometric head difference between the excavation chamber and the surrounding soil, and the cross effect of cohesion and the head difference in the flow domain ahead of tunnel face and above the crown.

Figure 2.21 shows the limit equilibrium of forces acting on the model, where G' is the submerged weight of the wedge, V' is the vertical force acting on the wedge-prism interface, F_X and F_Z are the seepage forces, N' and T are the normal and shear forces acting on the slip plane, and the S' is the effective face support force, effective face support pressure. σ_T', multiplied by the face area, A. The lateral earth pressure coefficient was assumed to be 0.4 for the wedge and 0.8 for the prism.

The required face support pressure is then a function of model geometry (tunnel diameter, cover depth and the inclination angle of slip surface) and ground properties (cohesion, friction angle and unit weight of the ground). Based on the force equilibrium of the system, required face support pressure is calculated, and the wedge inclination angle (β) is determined by iterative evaluation, in which the support pressure is maximized.

Alternatively, to this approach. the authors also provide an equation for estimating the required effective face support pressure at limit equilibrium state, which is:

$$\sigma_T' = F_0 \gamma' D - F_1 c + F_2 \gamma' \Delta h - F_3 c \frac{\Delta h}{D} \tag{2.25}$$

where F_0, F_1, F_2 and F_3 are non-dimensional factors derived from nomograms, which are function of H/D and ϕ'. Figure 2.22 shows estimation of coefficients F_0 and F_2.

Analytically, the soil is idealized as a rigid-plastic material obeying the Mohr-Coulomb failure condition with cohesion c and angle of internal friction ϕ. Figure 2.23 shows the forces acting on the wedge which allows the estimation of the minimum support pressure for equilibrium.
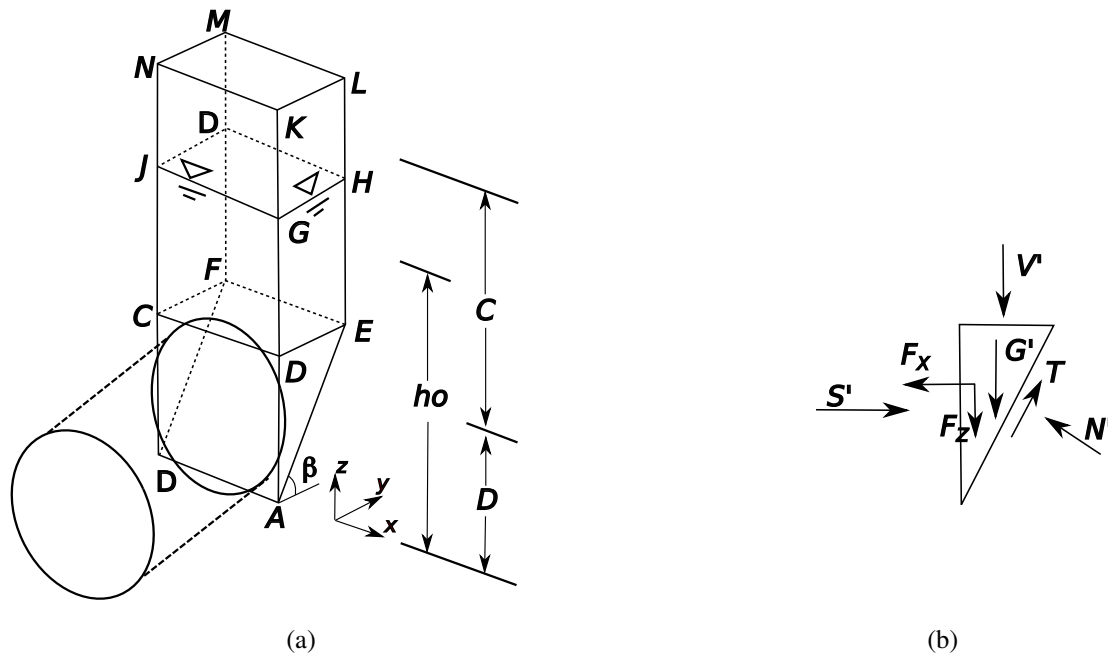
Figure 2.21 – Anagnostou and Kovári's method, (a) Sliding mechanism and (b) Diagram of forces acting on the wedge in front of the tunnel face (after Anagnostou & Kovári, 1996).

Another necessary assumption if that the face of the wedge is failing so that the angle that the resultant force has with the normal is equal to the friction angle. Therefore, the evaluation of the minimum support pressure is carried out using the following procedure:

$$S \geq \eta_W.W + \eta_E.E \qquad (2.26)$$

where S is the resulting force of stabilizing pressure, W is the resulting force of water pressure, E is the resulting force of horizontal spatial earth pressure, η_E is the safety factor of earth pressure equals to 1.50 and η_W is the safety factor of water pressure equals to 1.05. The estimation of E and W, respectively, are:
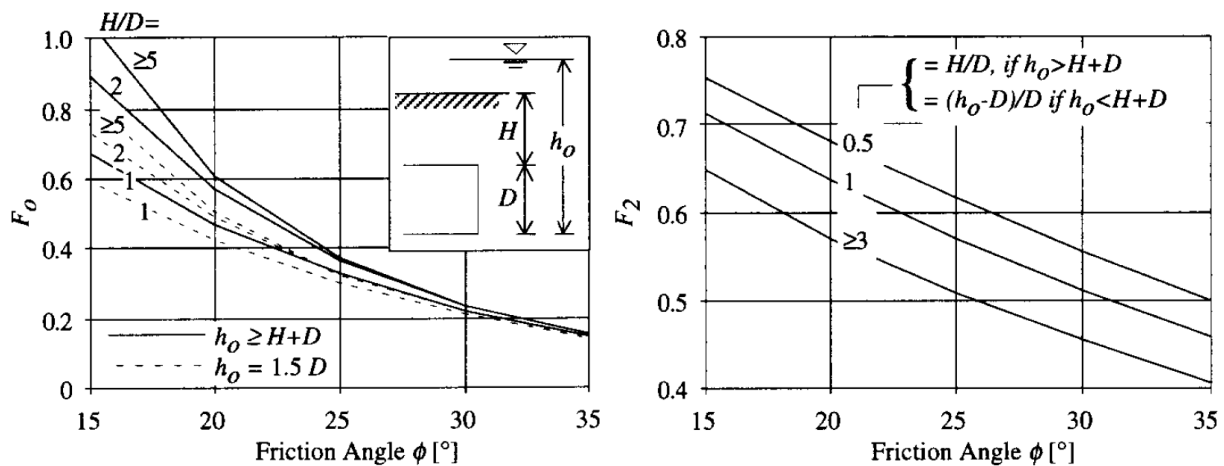
Figure 2.22 – Nomograms for coefficients F_0 and F_2 (Anagnostou & Kovári, 1996).
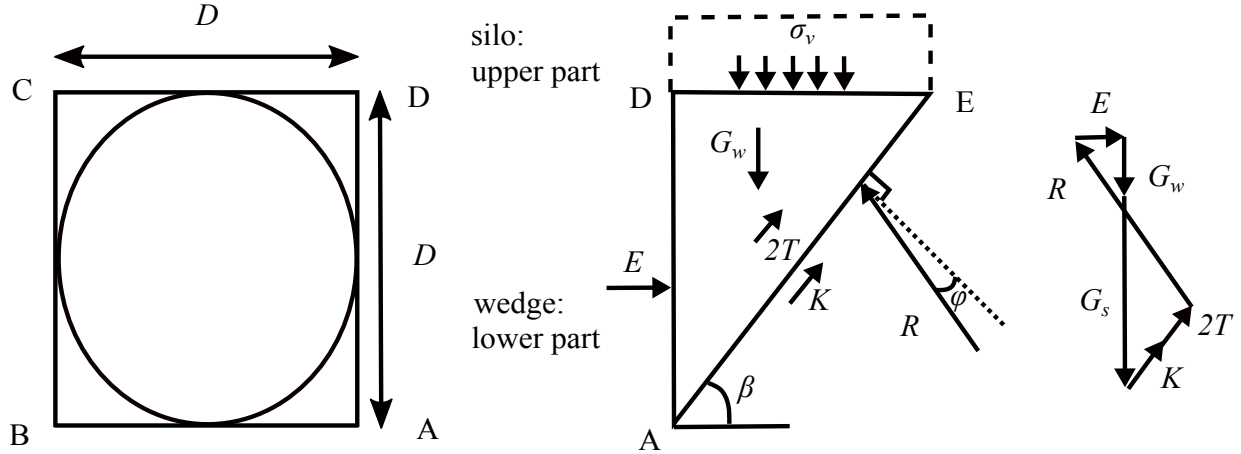
Figure 2.23 – Circular tunnel front approximated by square + force equilibrium on wedge (after Anagnostou & Kovári, 1994).

$$E = \frac{(G_W + G_S)(\sin\beta - \cos\beta\tan\phi) - (K + 2T)}{\sin\beta\tan\phi + \cos\beta} \qquad (2.27)$$

$$W = \gamma_w \left(h_{w,crown} + \frac{D}{2} \right) D^2 \qquad (2.28)$$

where:

$G_W = \frac{1}{2}\gamma' D^3 \cot\beta$

$G_S = \sigma'_V D^2 \cot\beta$

$K = \frac{cD^2}{\sin\beta}$

$T = K_a \left(\frac{1}{3}\gamma' D + \frac{2}{3}\sigma'_V \right) \tan\phi \frac{1}{2} D^2 \cot\beta$

Consequently, the required support pressure at the tunnel crown is calculated as:

$$S_{crown} = \frac{S}{\frac{\pi D^2}{4}} - \gamma_S \frac{D}{2} \qquad (2.29)$$

where γ_S is the unit weight of the support medium (kN/m^3), which is a value that has to be assumed.

The Broere method

Broere (2001) pointed out some significant limitations of the current analytical methods and, consequently, developed a solution (Figure 2.24) which can take into account the following relevant features:

– The heterogeneity of the ground at the face;

– The soil arching effect in the evaluation of the vertical load; and

– The effect of the penetration of the support medium into the tunnel face in terms of excess pore water pressure.
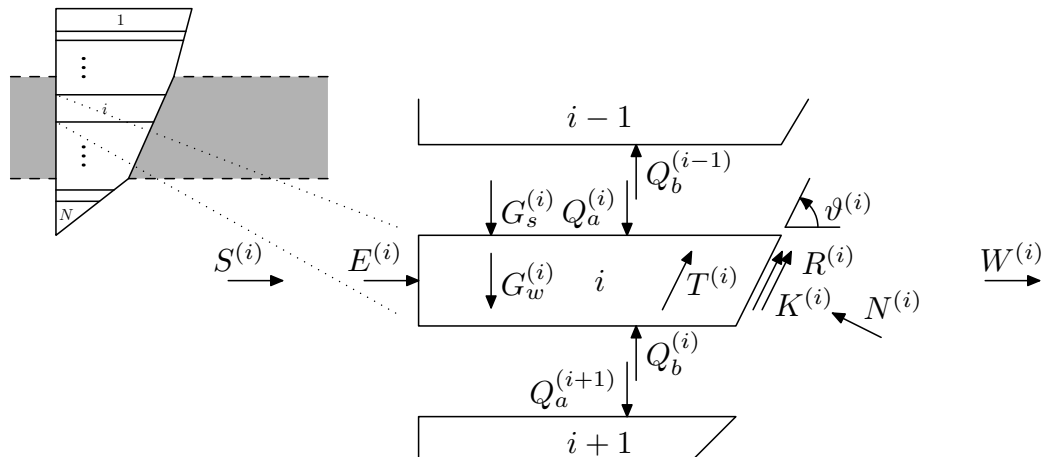
Figure 2.24 – Definition of symbols in the multilayered wedge model (Broere, 2001).

The heterogeneity of the ground created, for example, by the presence of different stratified soils, is analyzed by assigning a set of geotechnical properties and calculating the relative weights and the forces, which are acting at each homogeneous layer, at each interface, and along the sliding surfaces.

A particularity of this method in regards with the Anagnostou and Kovári's method is that the penetration of the medium during the excavation, either by Slurry or EPB, may produce an excess in the pore pressure in front of the TBM, as well as a reduction of the effective support force. This phenomenon is considered significant when excavating soils with permeability in the range of $10^{-5} - 10^{-3}$ m/s. As a consequence, the required support pressure could be significantly higher than that predicted by Anagnostou and Kovári's method.

Thus, the author developed specific equations to evaluate the distribution of the pore pressure in the penetrated ground, as a function of the support pressure, as well as of the pore pressure at rest, time and property of the soil and the muck.

An intense monitoring program from the surface supported by COB (the Dutch Centre Underground Construction) during the construction of three tunnels in Netherlands (2 tunnels by Slurry Shield and 1 tunnel by EPB) gave the possibility to verify a good correspondence between the predicted and measured values of excess pore pressure, confirming this type of occurrence up to about 30 m in advance of the tunnel face (Broere, 2001).

The Caquot-Karisel method

The Caquot-Karisel's method or Caquot's solution is a statically admissible solution based on the lower bound of plasticity theory (known as limit analysis). The solution allows determination of the minimum internal support pressure required to maintain the stability of the shallow tunnel. Caquot's solution considers that after excavation, stresses around a circular tunnel redistribute around a concentric circular domain with a radius that extends from the crown of the tunnel to the ground surface without developing shear stress and considering that the hoop stress is significant principal stresses and the radial stresses are minor.

Caquot's model considers the equilibrium condition for material undergoing failure above the crown of a shallow circular (cylindrical or spherical) cavity. The material has a unit weight γ and a shear strength defined by Mohr-Coulomb parameters c (cohesion) and ϕ (friction angle), while the distribution of vertical stresses before excavation is lithostatic and the ratio of horizontal to vertical stress is 1. A support pressure P_s can be applied inside the tunnel, while a surcharge q_s (from infrastructures or embankments) acts on the ground surface. For the case presented in Figure 2.25.
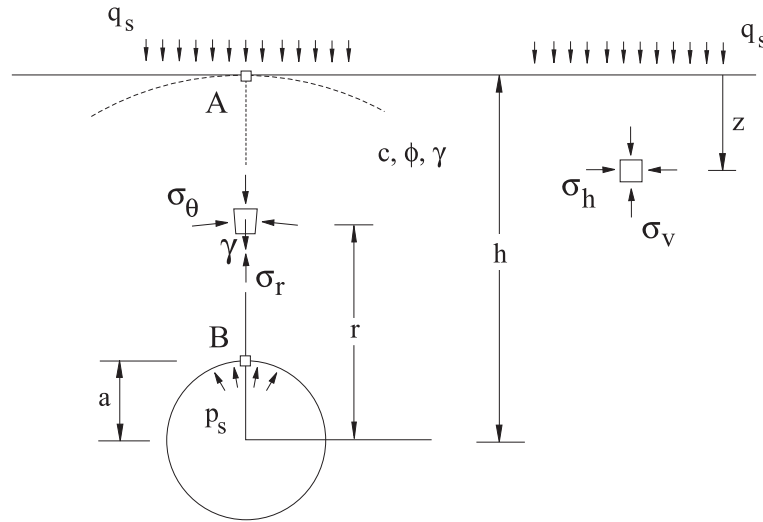
Figure 2.25 – Basic scheme for the Caquot-Kerisel's method (Carranza-Torres, 2004).

Caquot's solution defines the value of internal pressure (P_s) as the minimum or critical pressure in which the tunnel will collapse. Figure 2.25 represents, also, the Caquot's generalized solution for dry conditions (which include the factor of safety – FS), and can be represented by the following equation developed by Carranza-Torres (2004):

$$\frac{P_S}{\gamma a} = \left(\frac{q_S}{\gamma a} + \frac{c}{\gamma a} \frac{1}{\tan \phi} \right) \left(\frac{h}{a} \right)^{-k\left(N_\phi^{FS}-1\right)}$$

$$- \frac{1}{k\left(N_\phi^{FS}-1\right)-1} \left[\left(\frac{h}{a} \right)^{1-k\left(N_\phi^{FS}-1\right)} - 1 \right] - \frac{c}{\gamma a} \frac{1}{\tan \phi} \quad (2.30)$$

where a = the tunnel radius; h = axis depth below the surface; k = parameter that dictates the type of excavation (1 = cylindrical tunnel; 2 = spherical cavity).

It should be pointed out that the equation above (Eq. 2.30) is valid only when the given Mohr-Coulomb parameters lead to collapse. In general, the strength of the material will be larger than the strength associated with the critical equilibrium state of the cavity.

The factor of safety FS is defined as "the ratio of actual Mohr-Coulomb parameters to the critical Mohr-Coulomb parameters", as expressed in the following equation:

$$N_\phi^{FS} = \frac{1 + \sin\left(\tan^{-1}\frac{\tan\phi}{FS}\right)}{1 - \sin\left(\tan^{-1}\frac{\tan\phi}{FS}\right)} \therefore FS = \frac{c}{c^{cr}} = \frac{\tan\phi}{\tan\phi^{cr}} \quad (2.31)$$

As indicated in Figure 2.26, this approach assumes a proportional reduction of the Mohr-Coulomb parameters.

$$FS = \frac{c}{c^{cr}} = \frac{\tan \phi}{\tan \phi^{cr}}$$
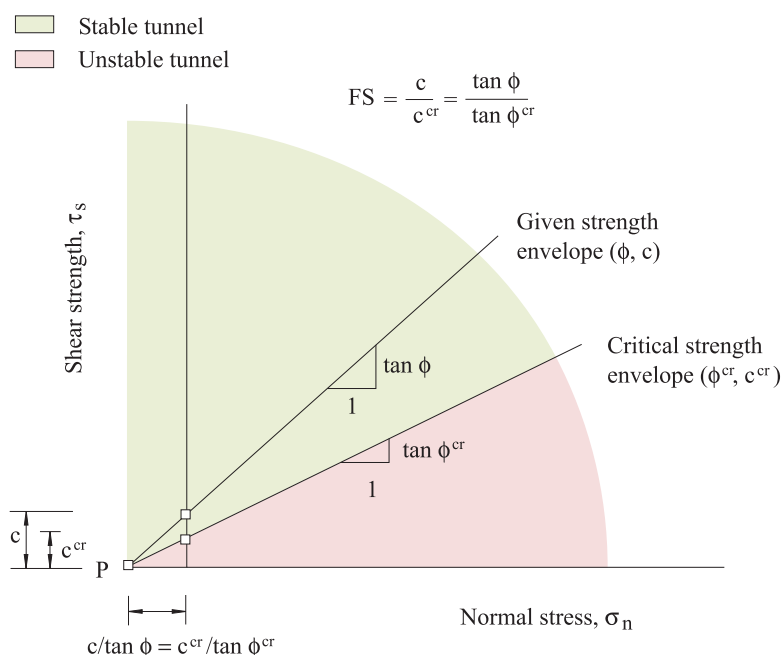
Figure 2.26 – Scheme of shear reduction used to compute factor of safety values (Carranza-Torres, 2004).

2.2.3.2 *Numerical methods*

In the numerical methods, calculation programs based mainly on the Finite Difference Method (FDM) and Finite Element Method (FEM) are used to model problems both in two-dimension (2D) and three-dimension (3D), since they allow the use of a sophisticated constitutive models. According to Vermeer et al. (2002), the tunnels are analyzed mostly by the use of 2D simulations because 3D requires a lot of computing time. 3D numerical modeling not only allows to calculate the face support pressure but also to estimate the surface settlements.

Regarding tunnel excavation, Lambrughi et al. (2012) highlighted that some critical aspects could be simulated only when the 3D numerical model is employed, such as:

– Behavior of the excavation front;

– 3D arching;

– Longitudinal settlement trough; and

– Intermediate conditions, like the temporary heave of the ground surface in case high values of the face support pressure are applied.

Useful sets of parametric analyses are presented in Franzius & Potts (2005) and Franzius et al. (2005), where the influence of mesh geometry, soil anisotropy and of the coefficient of

earth pressure at rest are evaluated. Also, regarding model geometry, Lambrughi et al. (2012) proposed that the minimum model dimension for calculation and computer time optimization can be expressed in the following manner (Figure 2.27):

– (H+4D). for the mesh height;

– 2(H+4D). for the mesh length; and

– 2(H+4D). for the mesh width.

where H is the tunnel axis depth and D is the tunnel diameter.

Results on the influence of gap grouting properties, cover depth and face pressure can instead be found in Kasper & Meschke (2006a,b). The authors stated that although the decrease of the settlements with increasing face pressure or grouting pressure are usually accepted, generalization should not be made without further investigation.

Finally, Kavvadas et al. (2017) investigated the effect of face pressure in controlling face stability by calculating the magnitude of face extrusion (average axial displacement of the excavation face) in a large set of parametric analyses. Additionally, The authors developed a 3D numerical model to simulate important components of the TBM excavation process including variable muck pressure on the excavation face, cuttherhead overcut and shield conicity, installation of a jointed segment lining with a tail gap, tail grouting gradual setting of the grout and effect of jointing on the segment lining.

2.2.4 DISCUSSION AND ADOPTED APPROACH

In this section, an introduction of the two main type of failure mechanism due to tunneling was made. Each failure mechanism depends on the type of soil to be excavated, which eventually are cohesive or non-cohesive soils.

The sequential excavation method and Tunnel Boring Machine (TBM) were also introduced as the most type of excavation methods employed for tunneling in soft ground. Each of these types considers methodologies and technical features of excavation for application of support to achieve stability of the tunnel face.

In terms of face stability estimation, various analytical and numerical techniques that are typically employed to assess the face and to head stability were indicated.

The analytical methods proposed by Anagnostou & Kovári (1994, 1996) and Carranza-Torres (2004) will be employed in this study because it constitutes the most widely used tools for estimating face stability. The method presented by Mollon (2010) is not considered because, about the two previously mentioned before, it does not consider the presence of a water level in it.

Regarding the numerical analysis, the finite element method (FEM) via the commercial code ABAQUS in which the Elastic and Mohr-Coulomb constitutive models are going to be used.

Detail description and procedure will be indicated in Chapter 4.
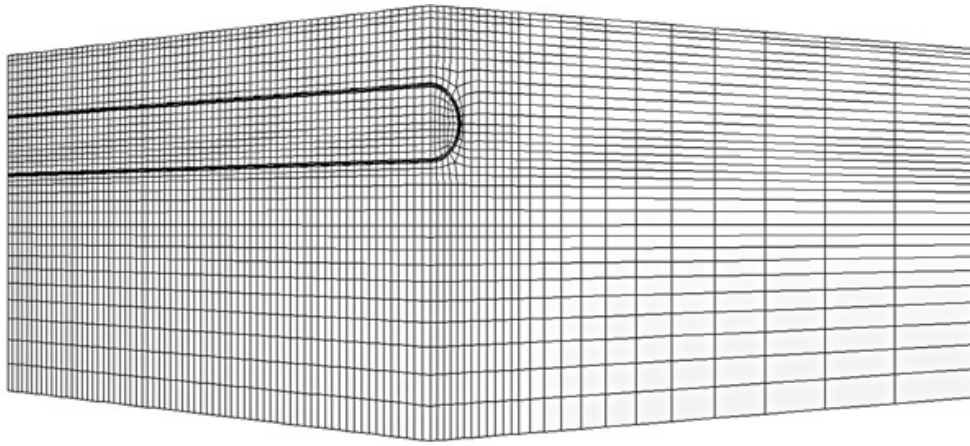
(a)
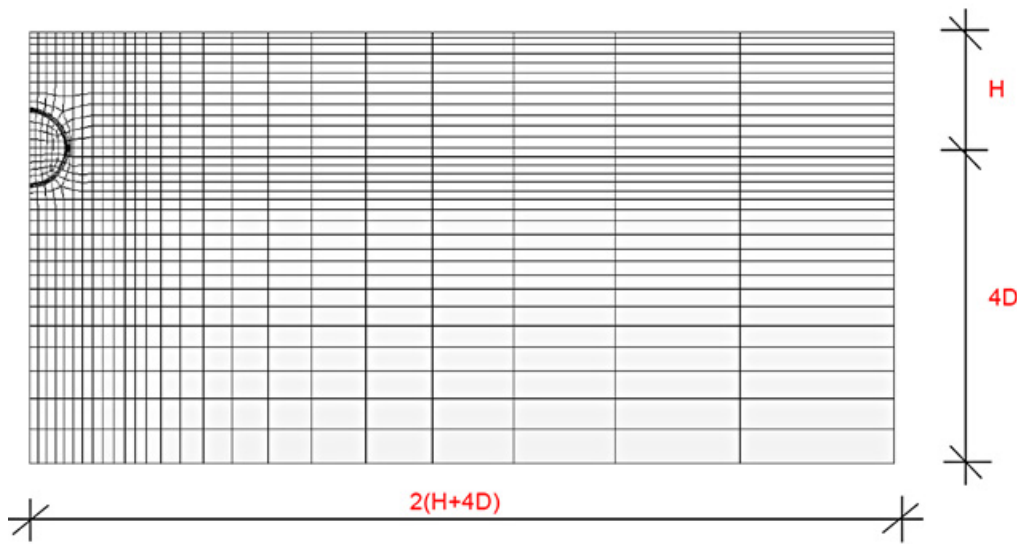
(b)
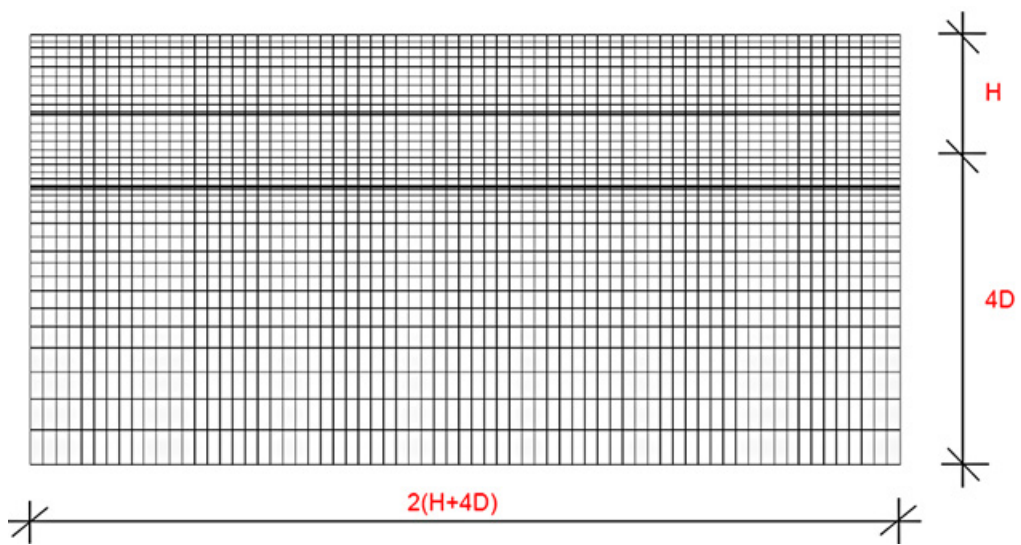
(c)

Figure 2.27 – Sketches of the proposed mesh dimension, (a) Isometric view, (b) Front view and (c) Lateral view (Lambrughi et al., 2012).

2.3   GROUND MOVEMENTS DUE TO TUNNELING

The most fundamental factors of ground response in any soft ground tunneling project is that the soil moves towards the opening since this is where the stress relief occurs. Furthermore, if the soil is under the water table, change on the initial water pressure condition by water inflow towards the opening may occur. Beyond this simple concept, the details of the ground response will vary depending on the type of tunneling technique used. The objective of this chapter is to introduce the key aspects of ground response caused by shield tunneling in order to predict and describe ground deformations, from a quantitative point of view. Finally, it will be discussed and indicated the approach adopted.

2.3.1   DEVELOPMENT OF GROUND MOVEMENTS

According to Wong & Kaiser (1987), the ground behavior in soft ground, from the tunnel to the surface, may be characterized by two distinct modes yielding (Modes I and II), separated by a critical k_0–value (k_{cr}). For mode I ($k_0 < k_{cr}$), yielding induced by stress relief is initiated at the shoulders of a tunnel and localized yield zones propagated to the surface with further stress relief (Figure 2.28a). For mode II ($k_0 > k_{cr}$), a continuous yield zone surrounds the tunnel opening takes place (Figure 2.28b).
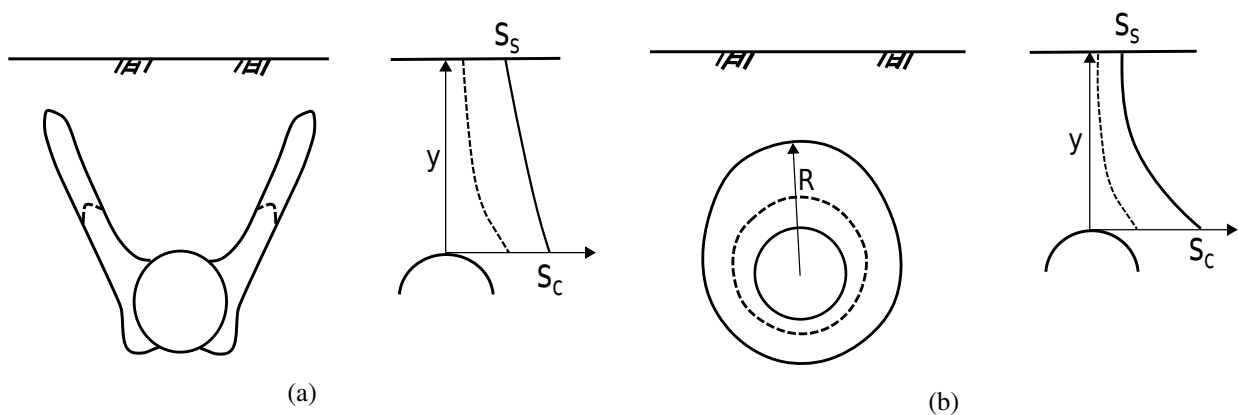
Figure 2.28 – Schematic representation of ground movement around tunnel for (a) mode I and (b) mode II (after Wong & Kaiser, 1987).

It is intuitively expected that Modes I and II will display distinctly different features in their settlement profiles because they represent different subsurface displacement patterns if the settlement at tunnel crown (S_c) is small. The vertical settlement profiles of Modes I and II are initially very similar, but the magnitude of settlement is larger in Mode I than in Mode II. Small displacement occurs in the elastic zone and large plastic straining within the yield zone.

For excessive S_c (i.e., the yield zone reaching the surface), Modes I and II exhibit distinct differences in vertical settlement profile above the crown. In Mode I, two localized shear planes develop, and the soil block displaces toward the opening as a rigid body. The soil block remains elastic so that the differential strain and displacement between the crown and the surface are small,

In Mode II, a plastic zone develops around the opening and is surrounded by the elastic ground, the elastic zone area is small, and most of the straining will occur within the plastic zone. Near collapse, the ratio of surface and crown displacement (S_s/S_c) tends toward unity for both modes, but at a faster rate for Mode I (Wong & Kaiser, 1987).

Recently works made by Rowe & Lee (1992), Osman et al. (2006), Standing & Selemetas (2013) and Avgerinos et al. (2018) confirmed such transversal ground behavior around the tunnel presented by Wong & Kaiser (1987).

From a longitudinal point of view, the displacements on the groundmass, especially at the surface, due to changes in the stress state of the ground are generated as the result of different sources produced during the excavation (Figure 2.29), for excavation with TBM, these sources can be grouped as:

– Face loss (u^*_{3d}), ground movement towards the face due to stress relief. For TBMs, this is normally associated to low face pressure;

– Shield loss (ω), ground deformation around the shield due to passing of the TBM. The presence of an over-cutting edge combined with any tendency of the machine to deviate from its strait path can result in a significant radial ground movement as well as shearing of the soil by friction;

– Tail void loss (G_p), deformation of ground due to a existence of a gap between the tail of the shield and the final precast lining;
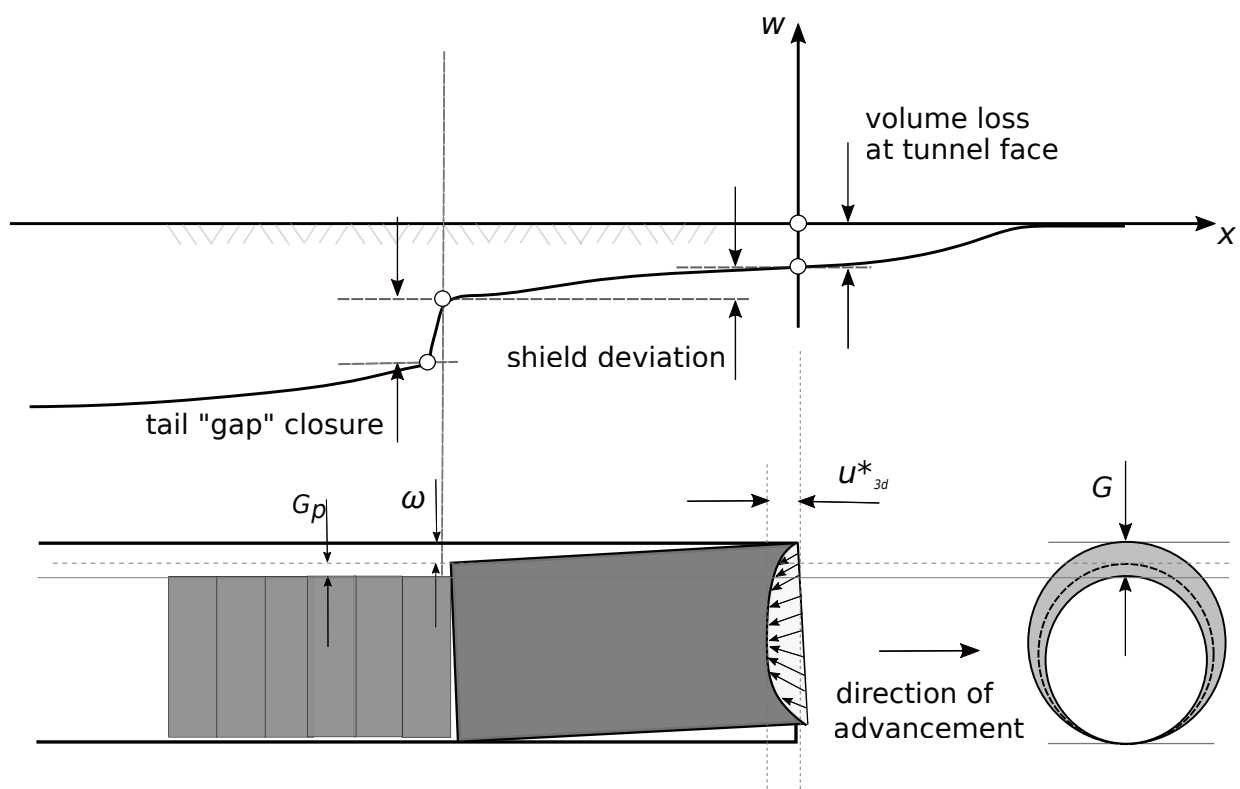
Figure 2.29 – Sources of longitudinal ground movements due to TBM tunneling (after Lee et al., 1992).

47

– Lining loss, ground movement due to deflection of the lining as the ground pressure increases as a consequence of soil closure on the lining. For tunnels lined with thick pre-cast concrete segments, this is normally a small source of movement; and

– Consolidation, correspond to the ground movement due to new equilibrium of pore pressure regime due to changes in the drainage condition.

By combining the transversal and longitudinal profiles, a 3D perspective is shown on Figure 2.30 as the response of the ground movement at the surface due to tunnel construction, which is manifested into a trough shape extending laterally and ahead of the advancing face. Therefore, through the understanding of groundmass behavior due to tunneling, either from the transversal and longitudinal point of view is possible to measure the generated surface settlement.

2.3.2 EVALUATION OF GROUND MOVEMENTS

Peck (1969) and later Attewell & Woodman (1982) were the first to represent the settlement at surface considering the shape of surface deformation as a settlement trough. Figure 2.30 shows that representation of settlement trough formed due to excavation. The depth of the tunnel center-line is set to z_0 and the origin of the x, y coordinate system is set any monitoring section establish by the engineer, and x_i is the distance of the tunnel portal, x_f is the distance of the tunnel face.

Following the authors mentioned above, many studies have been made since then. From that beginning until now, three types of approaches for estimating ground deformation exists and will be introduced in the following.

2.3.2.1 *Empirical relationships*

In every tunnel construction project, field measurements are made to monitor, among other things, the groundmass behavior during the excavation process. At the surface, the monitoring regards the installation of instruments transversely to the tunnel path. The trend values obtained from the measurement are then mathematically fit in order to have a mathematical approximation of the settlement data. Therefore, Table 2.4 summarizes in chronological order the different types of formulations for the estimation of surface settlement that provide an excellent fit to the settlement data, where S_{max} represents the maximum settlement and i represents trough width parameter (valid for the formulations presented in the Table).

In the Gaussian curve (Peck, 1969), the settlement trough is defined by a combination of the Gaussian probability distribution function that describes the settlement shape in the transverse direction ($y - axis$) and the Gaussian cumulative distribution function to describe it in the longitudinal direction ($x - axis$). Furthermore, the expression $\Phi(\cdot)$ represents the standard normal cumulative distribution function. So, the tunnel portal distance (x_i) is considered to be far from the tunnel face, i.e. $x_i = -\infty$, then the term in the formulation of the Gaussian curve that contains x_i will be $\Phi(+\infty) = 1$.
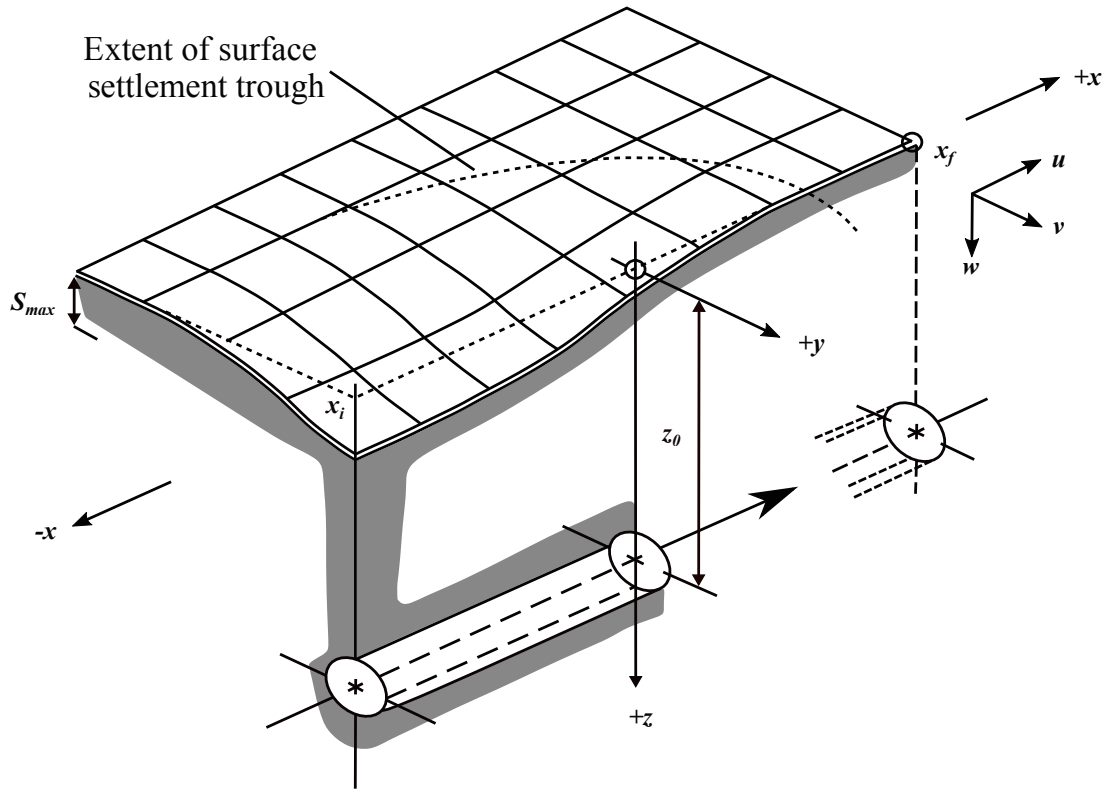
Figure 2.30 – Schematic representation of settlement trough due to tunneling (after Attewell et al., 1986).

Table 2.4 – Type of curve for estimation of settlement trough (after Marshall et al., 2012).

Reference	Type of analysis	Formulation	Eq. #
Peck (1969), Attewell & Woodman (1982) Gausian curve	2D – 3D	$S = S_{\max}e^{\left(-\frac{y^2}{2i^2}\right)}\left[\Phi\left(\frac{x-x_i}{i}\right) - \Phi\left(\frac{x-x_f}{i}\right)\right]$	(2.32)
Celestino et al. (2000) Yield density curve	2D Transverse section	$S = \dfrac{S_{\max}}{1 + \left(\frac{|x|}{a}\right)^b}$	(2.33)
Jacobsz et al. (2004) Modified settlement trough curve	2D Transverse section	$S = S_{\max}e^{\left(-\frac{1}{3}\left(\frac{|x|}{i'}\right)^{1.5}\right)}$	(2.34)
Vorster et al. (2005) Modified gaussian curve	2D Transverse section	$S = \dfrac{\eta}{(\eta-1) + e^{\left[\alpha\left(\frac{x}{i}\right)^2\right]}}S_{\max}$	(2.35)

Moreover, S_{max} can be expressed as:

$$S_{\max} = \frac{\left(\frac{\pi D^2}{4}\right)V_{loss}}{\sqrt{2\pi}i} \tag{2.36}$$

where D is the tunnel diameter and V_{loss} is the volume ground loss per unit. The term in parenthesis represents the cross-section area of a circular tunnel. If the tunnel is not circular, the area to be used has to be estimated.

The Yield density curve (Celestino et al., 2000) represents the transversal shape of the settle-

49
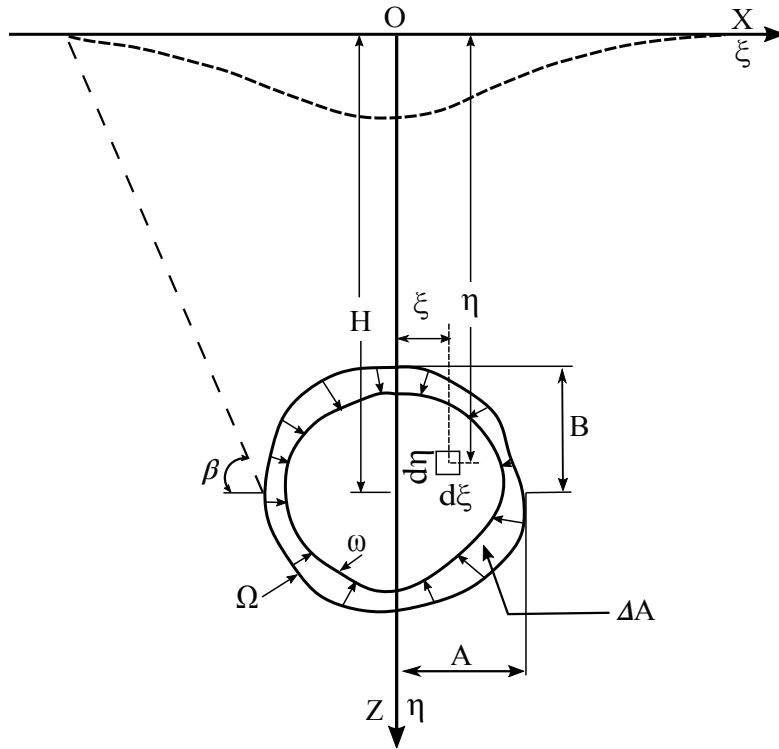
Figure 2.31 – Schematic representation of tunnel excavation by application of the Stochastic Medium Theory (after Yang et al., 2004).

ment trough. In this formulation three parameters (S_{max}, a – length dimension and b – dimensionless) are used providing an additional degree of freedom, respect to the Gaussian curve, thus giving more flexibility to the shape of the curve.

Finally, the formulations proposed by Jacobsz et al. (2004) (2004) and Vorster et al. (2005) are both based on centrifuge tests to study the effect of tunneling on nearby single pile foundation and pipelines, respectively.

2.3.2.2 *Analytical solutions*

Several analytical solutions were proposed in the past for the evaluation of the ground surface settlement induced by tunneling. Here, some examples of these methods will be recalled.

Litwiszyn (1957) proposed a method called the Stochastic Medium Theory which is a rigorous mathematical method developed to predict the soil deformation induced by tunneling. According to the stochastic medium theory, it is assumed that the underground excavation is composed of numerous infinitesimal excavation elements and the total soil deformation due to excavation is equal to the sum of the soil deformation induced by each excavation element (Figure 2.31).

By assuming that after excavation, the cross section will converge, equally in all radial directions, from Ω to region ω, then the ground settlement at surface, $w(x)$, is estimated by the following expression:

$$w\left(x\right) = \int_a^b \int_c^d \frac{\tan\beta}{\eta} e^{\left[-\frac{\pi\tan^2\beta}{\eta^2}(x-\xi)^2\right]} d\xi d\eta - \int_e^f \int_g^h \frac{\tan\beta}{\eta} e^{\left[-\frac{\pi\tan^2\beta}{\eta^2}(x-\xi)^2\right]} d\xi d\eta \qquad (2.37)$$

where β is the angle of influence zone of ground settlement. For a circular tunnel, $A = B$, with radial convergence of ΔA, the limits integration are:

$$a = H - B, b = H + B, c = -\sqrt{A^2 - (H - \eta)^2}, d = -ce = H - (A - \Delta A),$$

$$f = H - (A - \Delta A), g = -\sqrt{(A - \Delta A)^2 - (H - \eta)^2}, h = -g.$$

Regarding its application, Yang et al. (2004) and Zeng & Huang (2016) have implemented this method both in some tunneling projects in China (with circular and non-circular cross-section) and concluded that the results obtained agree well with the observed values. Furthermore, Yang et al. (2004) concluded that the input parameters could be estimated using the available information as well as semi-empirical relations. For accurate determinations of the input parameters, it is recommended that correlations between input parameters and soil/tunnel conditions have to be established. For the development of such correlations, an extensive database of field settlement profiles is needed for back analyses.

Regarding the implementation of elastic theory, Sagaseta (1987) performed a closed form solution for an isotropic and homogeneous incompressible soil. Later, Verruijt & Booker (1996) presented a generalization of Sagaseta's solution for a homogeneous elastic half-space. However, the analytical solution of Verruijt & Booker was unable to provide a satisfactory agreement with the measured settlement profile.

In an attempt to refine the solution of Verruijt & Booker (1996) and Loganathan & Poulos (1998) incorporated the similar ground loss concept into the analytical solution for tunnels in clays (Figure 4.6). In the solution, the equivalent undrained ground loss parameter was defined based on the gap parameter proposed by Lee et al. (1992). In this solution, the relationship between settlement trough width and the tunnel depth is expressed as a horizontal angle, $\beta = 45°$. Furthermore, it is considered that the surface settlement above the tunnel axis is the resultant of the complete cumulative equivalent ground loss ($100\%\varepsilon_0$) around the tunnel and the surface settlement at the horizontal distance ($H + R$) is the resultant of partial cumulative ground loss ($25\%\varepsilon_0$). Their boundary conditions are also shown in Figure 2.32.

Thus, by applying the boundary conditions and deriving the formulation. the prediction of surface settlement is expressed as:

$$U_{Z=0} = 4\left(1 - \nu\right) R^2 \frac{H}{H^2 + x^2} \frac{4gR + g^2}{R^2} e^{\left[-\frac{1.38x^2}{(H+R)^2}\right]} \qquad (2.38)$$

where ν is the Poisson's ration and g is the gap parameter.

Chi et al. (2001) extended the equivalent ground loss model of Loganathan & Poulos (1998) to clayey and sandy soils. In the analysis, the effect of soil consolidation was neglected. The analytical solution was used to conduct back analyses for 29 case records. The back analyses were performed to obtain the key parameters of influence zone angle (β) and gap parameter that
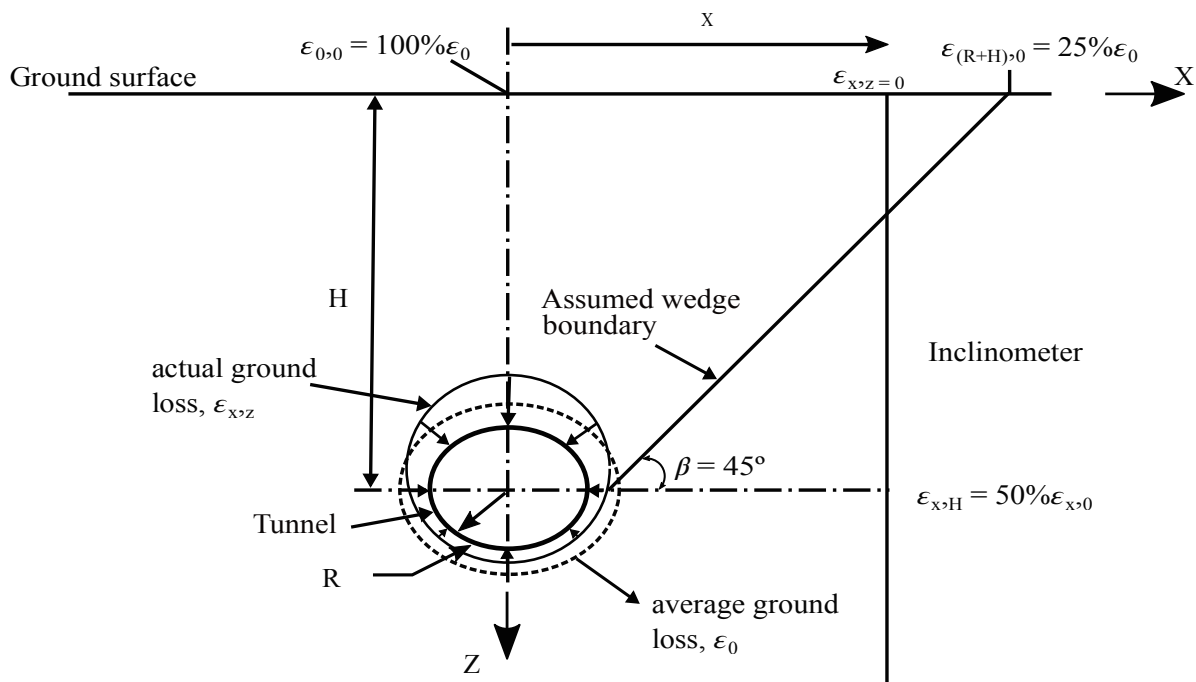
Figure 2.32 – Ground movement and ground loss boundary conditions (after Loganathan & Poulos, 1998).

provide the best fit to the measured ground settlement profiles. The results of the prediction were very encouraging.

Later, Hosseini et al. (2012) performed a numerical and analytical analysis on Teheran 7th line subway. The results of the analysis revealed that predictions using the Finite Differential Method (FDM) and Loganathan-Poulos' solution were in excellent agreement with a marginal difference of 9.5%.

2.3.2.3 *Numerical models*

Numerical models relating surface settlements due to tunneling can be traced back to the work of Rowe et al. (1983) and Rowe & Kack (1983), who compare the results they obtained with monitored in situ data. Lee & Rowe (1989) indicated the importance of considering soil anisotropy to cope with the drawbacks of numerical simulation of tunnel excavations, which often leads to broader settlement troughs than real.

Lee et al. (1992) and Rowe & Lee (1992) defined a detailed procedure for the evaluation of ground displacements, through the definition of a gap parameter, which is used to quantify all ground loss factors.

Three dimensional numerical analyses can be very demanding. due to the much higher computational effort required. Results obtained by means of three dimensional models have been presented by Lee & Rowe (1991), Augarde et al. (1995), Akagi & Komiya (1996), Broere & Brinkgreve (2002) and Fargnoli et al. (2015).

Komiya et al. (1999) in their two-dimensional model proposed a procedure for simulating the

behavior of the excavation front and its interaction with the shield. Also, a contribution came from Ng & Lee (2005) who considered full three-dimensional coupled consolidation analyses.

Kasper & Meschke (2004) proposed a modeling procedure for non-rectilinear paths for TBM, as well as a procedure for the progressive aging of gap grouting.

Tamagnini et al. (2005) introduced a two-dimensional procedure that considers the ovalization of the tunnel excavation and its, significant, effect on the shape of the settlement trough.

2.3.3 DISCUSSION AND ADOPTED APPROACH

A description of the development and estimation of ground movement due to tunneling were presented in this chapter. According to the type of ground, when a tunnel is under construction, two types of mechanisms of ground movements toward surface exist (Wong & Kaiser, 1987). Nonetheless, despite the type of groundmass, propagation of stress-strain relief toward the surface is finally observed in the form of settlement. From the longitudinal point of view, this displacement is well identified due to different sources during the excavation process.

Based on the literature, three approaches were identified for the estimation of ground displacement at surface: empirical, analytical and numerical solutions.

The empirical solution proposed by Peck (1969) and then improve by Attewell & Woodman (1982) has proved to be the more appropriate formulation as it fits when modeling surface settlement in real-world practice.

Few developments have been documented regarding the analytical solution proposed by Litwiszyn (1957). No attempts have been made so far to relate the mathematical parameters used in this formulation with physical variables. On the other hand, the formulation proposed by Loganathan & Poulos (1998) is limited to elastic material providing. Therefore, decidedly narrower results concerning the real case.

Regarding numerical analysis, these are useful for indicating the general form of the settlement trough as the formulation proposed by Peck (1969) does. 2D analyses do not contemplate realistic 3D groundmass behavior due to tunneling, and depending on the degree of excavation of steps modeled a good approximation may be achieved on the estimation of surface settlement. Otherwise, 3D analyses are used to improve the limitations encountered in the 2D analysis even if all the aspects of tunneling cannot be replicated. Approximation of surface settlement is better assessed when using 3D numerical analysis.

Furthermore, the focus of this study will be given to the employment of the empirical formulation proposed by Peck (1969) complemented with the realization of numerical analyses in 2D and 3D.

Finally, the review presented here did not consider the presence of a water table in the groundmass. Therefore, detail description concerning the consideration of water in the groundmass will be given in Chapter 4.

2.4 MATHEMATICAL APPROACH FOR MODELING IN TUNNELING

The following section intends to introduce the basic definitions for describing a tunneling problems in mathematical terms. Furthermore, information regarding previous related works that employed centrifuge tests, analytical solution and consideration of variability of soil properties are going to be presented where correlation of the applied face support pressure with the surface settlement is studied. The scope will be to provide the necessary ideas for proposing an approach for assessment of tunneling-induced surface settlements.

2.4.1 BASIC CONCEPTS OF MATHEMATICAL MODELING

Generally speaking, mathematical modeling consists of representation of the behavior of a system or object. According to Velten (2009), nature is a complex system that, in geotechnical engineering as in any other field of engineering or science, demands a need for the understanding, development or simulation of the phenomena or system. The complexity is inherent of the system under consideration made possible the introduction of a model as a scientific approach to provide an adequate tool for representing the complexity and make the problem tractable.

Figure 2.33 shows an elementary depiction of the scientific method on how is conceived the relation between the real world and conceptual world.
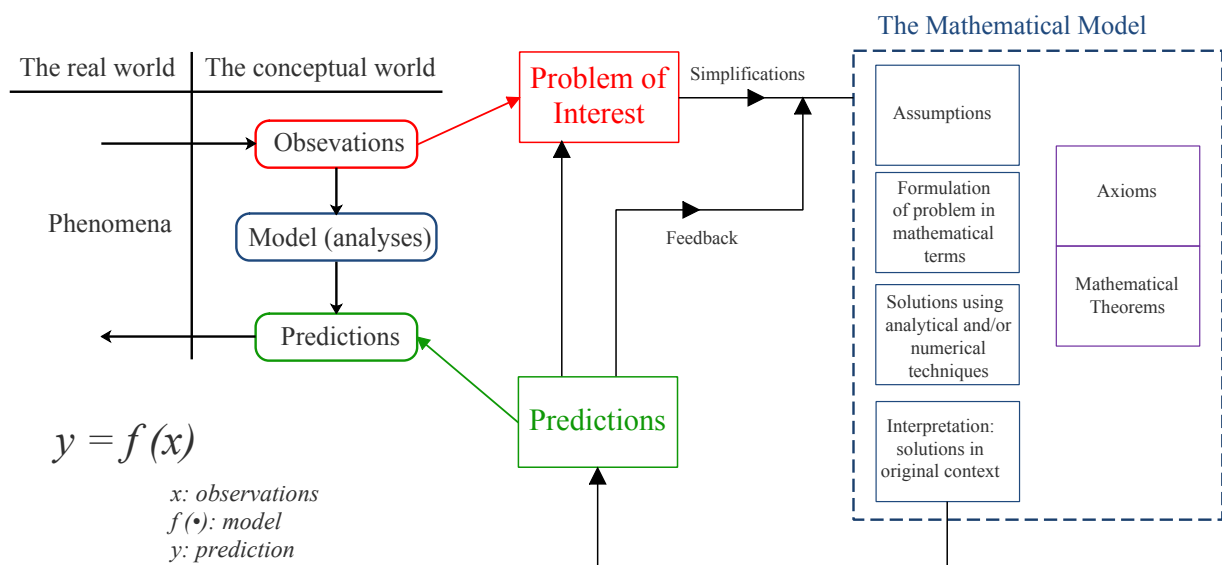
Figure 2.33 – Elementary depiction of scientific method for modeling (after Dym, 2004).

The basic conception of the scientific method is that in the real world, the various phenomena and behavior whether natural or produced by artifacts are observed. Nevertheless, in the conceptual world, three stages are needed to understand the phenomena: observation, modeling, and prediction. In the observation part, measurements are done. In the modeling part, the observation is analyzed to described the behavior or observed results. Finally, in the prediction part, the model is tested to predict events that confirm the behavior of the phenomena (Dym, 2004).

In mathematical terms. the observations can be seen as input variables x and the prediction as output variable y where $y = f(x)$. The model $f(\cdot)$ will be a simplified representation of the phenomena / real system (Velten, 2009).

Modeling starts, first of all, with a philosophical approach where questions of principles and methods have to be made in order to represent the system accurately. Figure 2.34 portrays a general approach for formulating or building a mathematical model, a list of questions and instructions are presented in the form of iterative loop to re-examine the assumptions. Known parameter values, principles are chosen, hypothesis assumed and means for calculation of the model.


```
                    ┌────────────────┐
                    │  OBJECT/SYSTEM │
                    └────────────────┘
                Why? What are we looking for?
                Find? What do we want to know?

                ┌──────────────────────┐
                │        MODEL         │◄ ─ ─ ─ ─ ─ ─ ─ ─ ─ ─ ─
                │ VARIABLES, PARAMETERS │                       │
                └──────────────────────┘                       │

 Given? What do we know?      How? How should we look at this model?
 Assume? What can we assume?

                               Improve? How can we improve the model?

 Predict? What will
        our model predict?

                      Valid? Are the predictions valid?

        ┌───────────────────┐                    ┌──────┐
        │ MODEL PREDICTIONS │◄───────────────────│ TEST │
        └───────────────────┘                    └──────┘

                 Verified? Are the predictions good?

        ┌────────────────────────────┐
        │ VALID, ACCEPTED PREDICTIONS │
        └────────────────────────────┘
        Use? How will we exercise the model?
```

Figure 2.34 – First order view to approach the development of a model (after Dym, 2004).

Another aspect to consider when formulating a mathematical model is to know the scale of the system to be reproduced. Herrera & Pinder (2012) described that there are two approaches the microscopic approach, which studies molecules, atoms, and elemental particles; and the macroscopic approach, which studies large systems. Prediction of the behavior of microscopic particles is the subject of quantum mechanics (no further description on this subject will be presented), while predicting the behavior of large system is approached by applying the concepts drawn from the mechanics of continuous media (i.e., civil engineering, oil industry, weather prediction, mechanics of human bones, etc.).

2.4.2 TYPES OF MODELS

In order to accomplish the task of building a model, that in a simplified way, allows to understand and reproduce or approximate the behavior of a complex system, it is necessary to identify how the system could be represented. In this regard, different types of modeling technics might arrive satisfactorily to the representation of the system's behavior. The primary type of modeling

technics, according to Gershenfeld & Gershenfeld (1999), are grouped in: analytical, numerical and observational models.

2.4.2.1 *Analytical models*

Analytical models are models that have a closed form solution, i.e., the solution to the equations used to describe changes in a system can be expressed as a mathematical analytic function. This type of approach is more aesthetically pleasing since an inspection of the mathematical function can give information about the system's behavior without the need for graphing or generating a table of values. Analytical models involve the application of ordinary differential equations, partial differential equations, as well as the use of probabilistic techniques to deal with stochastic system's behavior.

Regarding tunneling, some application of this approach was employed by Litwiszyn (1957) as well as Loganathan & Poulos (1998) to develop a solution for addressing a prediction of surface settlement due to excavation. The formulation proposed by these authors is based on a rigorous mathematical method and linear elastic soil behavior, respectively.

2.4.2.2 *Numerical models*

Numerical models are used to obtain an approximated solution of the system for cases in which analytical models are unproductive. However, the numerical model usually needs to be carefully calibrated and validated against pre-existing data and analytical results. Colorful, impressive graphic presentation of a sophisticated software package does not necessarily provide accurate numerical results.

It is important to highlight that although the widespread access to fast computers has perhaps led to an over-reliance on numerical answers when there are other possibilities and a corresponding false sense of security about the possibility of numerical severe problems or errors, it is now possible without too much trouble to find solutions to most equations that are routinely encountered.

For the simulation of a system with numerical modeling the use of algorithms, finite differences methods, finite elements methods or cellular automata technics are implemented. Some application of this type of model in tunneling can be mentioned, again, on the works of Rowe & Kack (1983), Lee & Rowe (1991), Ng & Lee (2005), Fargnoli et al. (2015) and Kavvadas et al. (2017).

2.4.2.3 *Observational models*

Observational models are those built from measurement data, treating the system as a black box, that is, without using any information about the internal processes occurring inside the system when input values – x provide output values – y (Velten, 2009). Still, some inference about

the internal process of the system can be made. In this manner, the model may be used to characterize and classify the data. To generalize from measurements in order to make predictions about new observations, or most ambitiously to learn something about the rules underlying the observed behavior.

In these types of models, engineers or scientists may use laboratory and in situ tests from which information to develop empirical or semi-empirical algorithms for real application are obtained. Many tools are implemented in order to build these types of models such as statistic and probabilistic methods, regression analysis, neural networks or fuzzy methods. Some example of application of this type of model on tunneling can be observed, again, on the works of Peck (1969), Celestino et al. (2000), Meguid et al. (2008) and Marshall et al. (2012).

Nowadays, either for science or engineering purpose, predicting the behavior of a system of interest is not entirely the competence of a specific modeling technic. Many are the cases where an application of a model's couple integration, between mathematical and computational tools, is necessary. According to Herrera & Pinder (2012), an optimal approach will be to successively construct a conceptual model, a mathematical model, a numerical model and a computational model, which usually consists of a computational computer program or code.

The conceptual model establishes the purpose for, and scope of the model to be developed; furthermore, it also identifies the processes and phenomena that will be incorporated in the mathematical model. Using numerical methods and algebraic matrix algorithms, this latter model is transformed into a numerical model. Then, a computational code is developed that permits solving the numerical equations with a resource to suitable computational hardware.

2.4.3 MODEL SELECTION

Burnham & Anderson (2002) mentioned that several models could give a good representation of a system; such models constitute the set of candidate models. As a manner of example from the biology field, is shown in Table 2.5 a set of candidate models that fit in the studied of patterns of avian species-accumulation rate among forested landscapes in the USA.

Once the set of candidate models have been chosen, statistical analyses are implemented to allow the selection of the best of these models. Model selection techniques are considered estimators of some physical quantity, such as the probability of the model producing the given data, and thus their approach will be to balance goodness of fit with simplicity.

Model selection techniques are also based on information theory, which is a mathematical representation of the conditions and parameters affecting the transmission and processing of information. So, it offers an estimate of the relative information lost when a given model is used to represent the process that generated the data. A key measure in information theory is "entropy". Entropy quantifies the amount of uncertainty involved in the value of a random variable or the outcome of a random process.

Among the model selection techniques, it is possible to mention:

Table 2.5 – Examples of the set of candidate models of avian-species accumulation curves from Breeding Bird Survey index data for Indiana and Ohio Burnham & Anderson (2002).

Model structure	Number of parameters (k)*
$E(y) = ax^b$	3
$E(y) = a + b\log(x)$	3
$E(y) = a(x/(b+x))$	3
$E(y) = a(1 - e^{-bx})$	3
$E(y) = a - bc^x$	4
$E(y) = (a + bx)/(1 + cx)$	4
$E(y) = a(1 - e^{-bx})^c$	4
$E(y) = a(1 - \left[1 + (x/c)^d\right]^{-b})$	5
$E(y) = a\left[1 - e^{-b(x-c)^d}\right]$	5

* k is the number parameters in the model plus 1 for σ^2.
Assumed: $y = E(y) + e$, $E(e) = 0$, $V(e) = \sigma^2$

– Akaike Information Criterion (AIC);

– Bayesian Information Criterion (BIC); and

– Minimum Description Length (MDL).

2.4.3.1 *The AIC and BIC*

The Akaike Information Criterion – AIC (Akaike, 1974) is a measure for evaluating general statistical models for a given set of data; in other words, AIC is a tool to compare different models on a given outcome. As indicated above, the selection of the model is essential, as under-fitting a model may not adequately capture the true nature of what determines the variable of interest, while an over-fitted model may increase variability in the estimated equation or lead to information loss in increased degrees of freedom. AIC is then a way to select the model that best balances these drawbacks. Once the best model is selected, traditional null-hypothesis testing can then be used on the best model to determine the relationship between specific variables and the outcome of interest.

As well, the Bayesian Information Criterion – BIC (Stone, 1979) is another criterion for model selection that measures the trade-off between model fit and complexity of the model. The two criteria are very similar in form but arise from very different assumptions. The AIC is derived from information theory, and it is designed to pick the model that produces a probability distribution with the smallest discrepancy from the actual distribution. The BIC has derived from a large sample asymptotic approximation to the full Bayesian model comparison. The following equations are used to estimate the AIC and BIC of a model, respectively:

$$AIC = -2\ln\left[L\left(\widehat{\theta}\middle|y\right)\right] + 2k \tag{2.39}$$

$$BIC = -2\ln\left[L\left(\widehat{\theta}\middle|y\right)\right] + \log(n)k \tag{2.40}$$

where $L(\widehat{\theta}|y)$ denotes the maximum likelihood, k is the number of estimable parameters in an approximating model, and n is the number of observable data.

Hurvich & Tsai (1989) observed that AIC might perform poorly if there are too many parameters concerning the size of the sample, generally when the ratio of n/k < 40. Therefore, they recommended the use of the following expression, when the above relation applies:

$$AIC = -2\ln\left[L\left(\widehat{\theta}\middle|y\right)\right] + 2k + \frac{2k(k+1)}{n-k-1} \tag{2.41}$$

Burnham & Anderson (2002) indicated that both tools are based on the principle of Parsimony in which ideally, a model would be able to capture the true relationship between the variables of interest while not losing generality from over-fitting the data.

For both techniques, the AIC and BIC, each of the set candidate models are evaluated, and the best model will be the one with the smallest value. Table 2.6 shows the results of application AIC to the example provide in Table 2.5.

Table 2.6 – Examples of the set of candidate models of avian-species accumulation curves from Breeding Bird Survey index data for Indiana and Ohio Burnham & Anderson (2002).

Model structure	Number of parameters (k)*	AIC value	Adjusted R^2
$E(y) = ax^b$	3	227.64	0.962
$E(y) = a + b\log(x)$	3	91.56	0.986
$E(y) = a(x/(b+x))$	3	350.40	0.903
$E(y) = a(1 - e^{-bx})$	3	529.17	0.624
$E(y) = a - bc^x$	4	223.53	0.960
$E(y) = (a + bx)/(1 + cx)$	4	57.53	0.989
$E(y) = a(1 - e^{-bx})^c$	4	-42.85	0.995
$E(y) = a(1 - \left[1 + (x/c)^d\right]^{-b})$	5	-422.08	0.999
$E(y) = a\left[1 - e^{-b(x-c)^d}\right]$	5	-585.48	0.999

* k is the number parameters in the model plus 1 for σ^2.

Regarding tunneling, an example of applications of these criteria can be observed on the work of Fuentes (2015), where they presented a method for calculating internal force distribution of underground structures based on displacement measurements, by applying the principle of virtual work. At this respect, Figure 2.35 shows the result of the method proposed by Fuentes (2015). High order polynomial functions were used to calculate theoretical bending moments and compare it with the measured value.

The author based the polynomial order of the functions on the case of other structures as: 5th to 9th from singly propped walls, 6th to 10th from multi-propped walls and 4th to 8th from cantilever walls and laterally loaded piles. Finally, the AIC was implemented to evaluate which of the polynomial functions fitted better to the measured value.

Furthermore, Liu et al. (2017) made a risk analysis on six pre-existing buildings located near the tunnel axis of the new construction of Wuhan Yangtze River Metro Tunnel in China. A number of 180 Finite Element simulations were made to construct different copula functions to
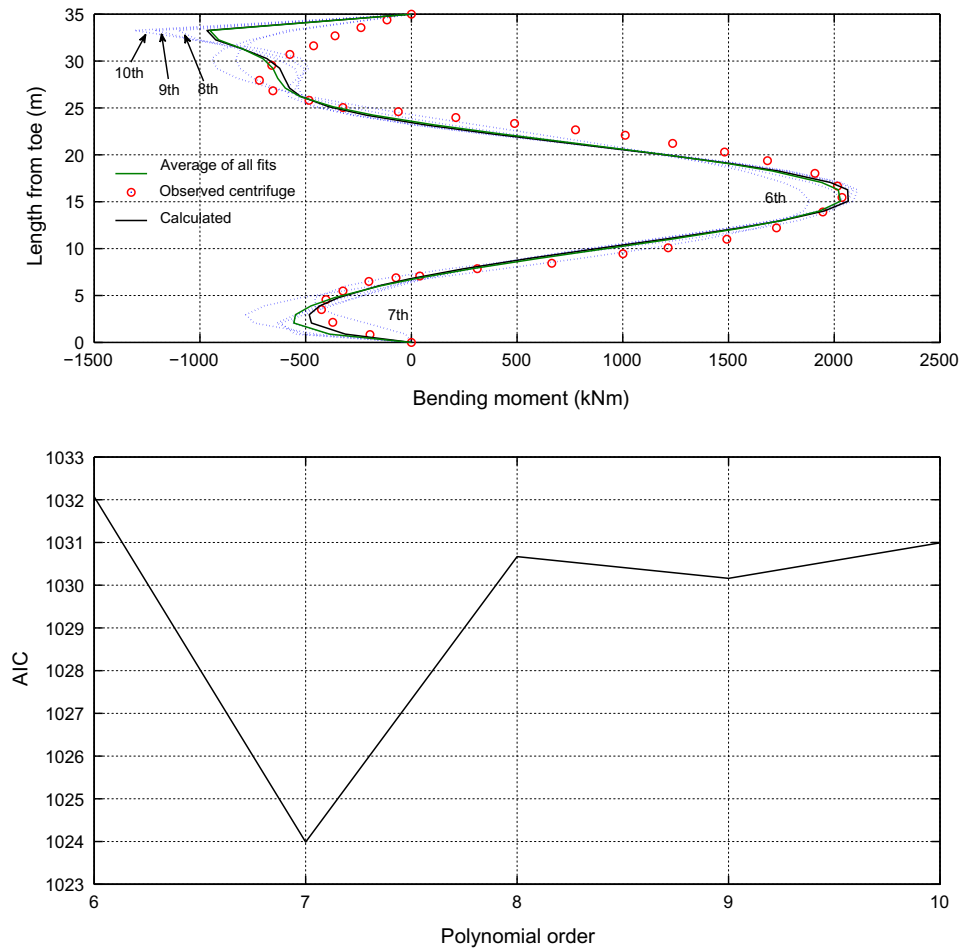
Figure 2.35 – High order polynomila functions for representing bending moment distribution on a retaining wall for an urban excavation and development of AIC according to the polynomial order (Fuentes, 2015).

each output variable, the maximum settlement adjacent to the building (S_{max}) and the maximum inclination rate of the building (I_{max}). Then, the best-fitted copula was identified by the AIC and BIC. Finally, the safety risk levels of the six concerned buildings were evaluated by considering both the importance of the examined buildings and the limited value of building reliability index β.

2.4.3.2 *The MDL*

The Minimum Description Length (MDL), introduced by Rissanen (1978), is a criterion for statistical model selection also based on information theory. The mathematical formulation of this method is based on the philosophical principle of *Occam's razor*, which states that "simple explanations of a given phenomenon are to be preferred over complex ones" (Nishii et al., 2014). This includes the information to specify both the form of the model and the values of the parameters.

The MDL measures the complexity of models by introducing the stochastic complexity theory of a set concerning a class of models as the shortest code length or description length (Claeskens & Hjort, 2008). The most basic recognition here is that there is necessarily one to one correspon-

dence between code for data compression and a probability distribution of the data. So, in order to pursue the shortest code length, each of the candidate set models is transformed into a code by a process called data compression (mechanism used to describe the data in a short manner).

In this way, by making the procedure, the number of parameters involved in the model are reduced allowing to know if the model is over-fitted. Then, by applying the notion of stochastic complexity (a type of statistical inference), the description length of the data is obtained. The minimum value of the description length of all the models will be the preferred one.

2.4.4   RELATED MATHEMATICAL MODELS TO THE PROPOSE RESEARCH

Regarding the studies related to the correlation between applied face support pressure and surface settlement, it is highlighted that low information was found in the literature. For example, Vermeer et al. (2002), used the construction of a tunnel by the sequential method as a case study, and proposed a 3D numerical analysis approach, by the application of the finite element method (FEM), to estimate the development of surface settlements, and thus reduce the computer time consumption for modeling. The authors made no further analyses regarding the face support pressure and its interaction with surface settlement obtained from the 3D numerical analysis.

Regarding laboratory modeling, Ahmed (2011) realized experimental analyses for measurements of tunnel face support pressure and associated ground movements by using a small-scale model with transparent soil and associated image processing techniques to simulate shield tunneling in medium dense, saturated sand (Figure 2.36).
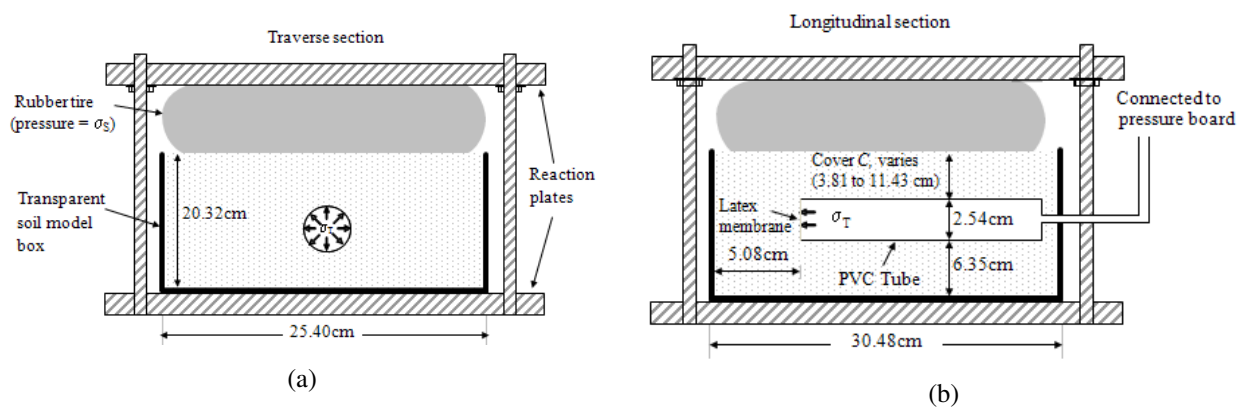
Figure 2.36 – Schematic representation of small – scale model, (a) transversal and (b) longitudinal section (Ahmed, 2011).

In this study, Ahmed (2011), for the case of face support pressure, confirmed a failure mechanism of a prismatic wedge in front of the tunnel face and a vertical chimney of soil above. Concerning the surface settlements, the author observed that the results were consistent with the well extended Gaussian curve. In this study, no attempt for correlation between the face support pressure and the surface settlement was made. These parameters were studied separately.

Macklin (1999), based on the concept of load factor (L_F) proposed by Kimura & Mair (1981) from results geotechnical centrifuge test, proposed a relationship to estimate the volume loss.

Later, Atkinson (2007) proposed a new application of the load factor concept as a tool to relate the applied face support pressure with the volume loss. Figure 2.37 shows the expected behavior of these two variables. Parameters as vertical stress (σ_z), ultimate limit stress (σ_{tc}) and the applied tunnel support pressure (σ_t) are introduced in the analysis for the estimation of the load factor. As the load factor approximates to the unity, the settlements become very large, which is the result of the collapse of the tunnel face.

$$L_f = \frac{\sigma_z - \sigma_t}{\sigma_z - \sigma_{tc}}$$
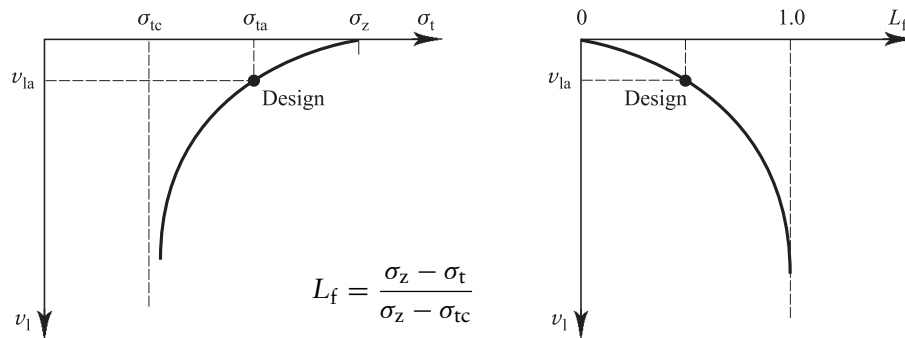
Figure 2.37 – Relationship between tunnel support and ground settlements (Atkinson, 2007).

By designating a value for load factor, its interception with the curve allows to estimate the volume loss (V_{la}), and thus the allowable support pressure (σ_{ta}) is estimated. This approach requires the application of a series of laboratory tests (centrifuge test) to build a relationship which then will be applied to a particular tunneling project.
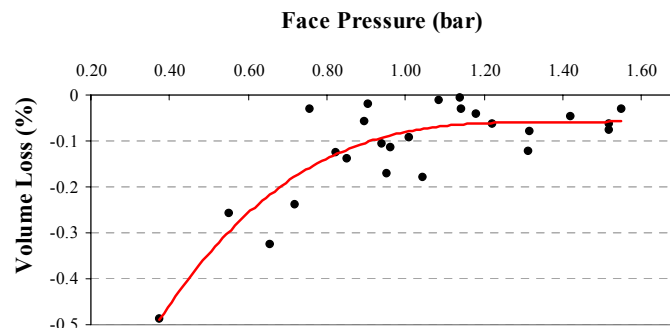
Figure 2.38 – Face support pressure vs Volume loss (Repetto et al., 2006).

Another reference that was found is related to Repetto et al. (2006). In this work, the authors were involved in the construction of a 7 km railway tunnel under the city of Bologna – Italy, to study the performance of an EPB–TBM. Through back analyses and the implementation of analytical and probabilistic methods, the authors presented a diagram to correlate the face support pressure with the volume loss. Figure 2.38 shows a diagram of the correlation between these two main parameters. This curve is the result of the realization of a regression analysis technics.

As it was the case of the work presented by Atkinson (2007), and also presented by Repetto et al. (2006), the nature of the correlation expected is that a low face pressure would cause large settlement and if a high face pressure is applied this would produce a smaller surface settlement. Nevertheless, as it can be seen from Figure 2.38 a dispersion on the correlated parameters, which could be linked to the inherent variability of soil properties.

From the analytical point of view, Osman et al. (2006) proposed a simplified closed-form solution, based on the upper bound theorem of plasticity, for the prediction of maximum surface ground settlement given the applied tunnel support pressure. A series of five centrifuge test analyses on plane-strain unlined tunnels in kaolin clay were conducted to validate this formulation. Osman et al. (2006) observed a close correspondence between experimental and theoretical for the case of deep tunnels, $C = D > 3$ (Figure 2.39a) but a poor correlation for the case of shallow tunnels, C=D < 3 (Figure 2.39b).
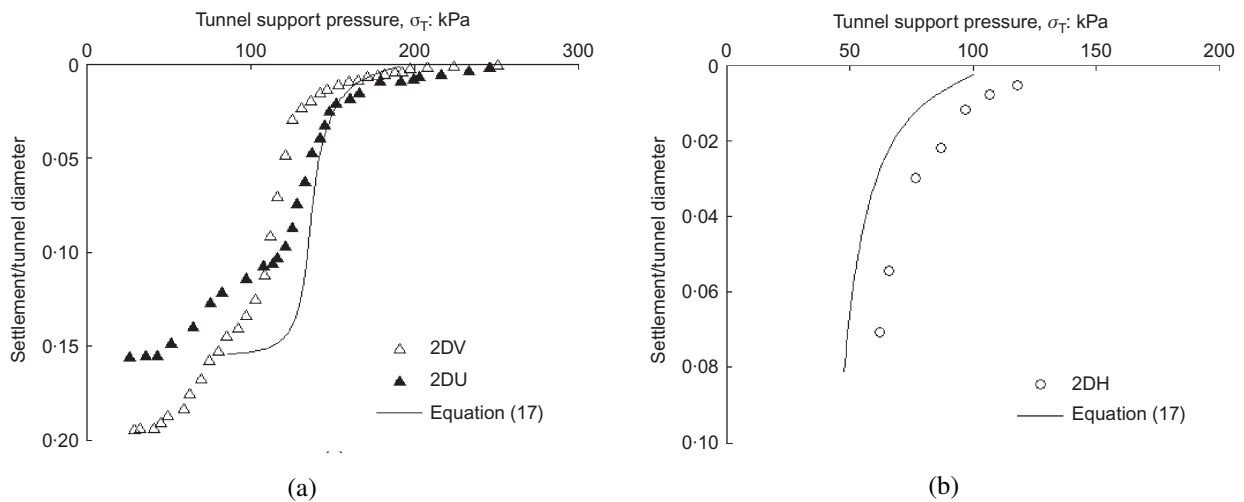
Figure 2.39 – Predicted values surface settlement by using proposed equation of Osman et al. (2006), (a) $C/D = 3.11$ and (b) $C/D = 1.80$. 2DV, 2DU and 2DH are the names given by the author to each centrifuge test.

Regarding the soil properties variability, a similar result was presented by Suwansawat & Einstein (2006) from the Bangkok Mass Rapid Transit Authority (MRTA) project, a 20 km twin tunnel constructed by EPB-TBM. Figure 2.40 shows the correlation between measured face pressure and maximum surface settlement. As it is possible to see from this figure, due to uncertainty in soil properties, a variation of correlated data is observed. Nevertheless, a behavior of the phenomena still can be followed.

Lastly, a study made by Fargnoli et al. (2013) about settlements induced by TBM tunneling for a new metro line in Milan – Italy is mentioned. In this study, an attempt was made to relate surface settlement (with available monitoring sections) with the applied TBM face pressure. The authors did not find a direct correlation from the few analyzed monitoring data (Figure 2.41). Even so, they concluded that the data indicates that face pressure contributes to limiting the surface settlements.

2.4.5 DISCUSSION AND ADOPTED APPROACH

Through this section, a series of definitions regarding the mathematical approach for modeling a system are given. In a general form, it was described the elementary basis needed as a scientist/engineer to represent a system mathematically. Three main types of modeling techniques (analytical, numerical and observational) may be adopted simultaneously to describe the problem. All of them will be employed in the pursuit of analyzing the system from different perspectives.
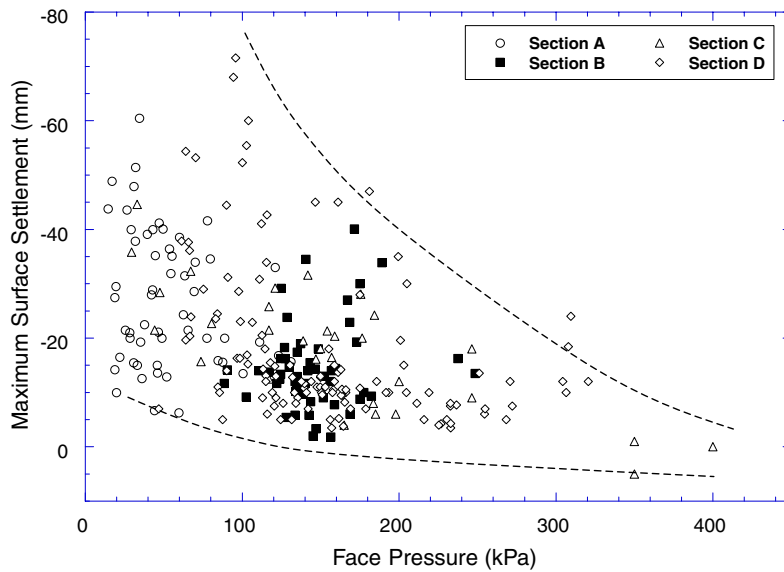
Figure 2.40 – Face pressure versus Maximum surface settlement (Suwansawat & Einstein, 2006).
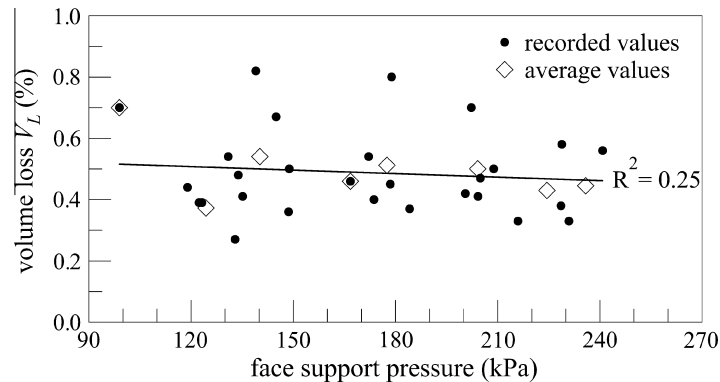
Figure 2.41 – Face pressure versus Volume loss (Fargnoli et al., 2013).

Therefore, a set of candidate models, each model with different mathematical expression (e.g., linear, polynomial, exponential equations) and several parameters involved, are generated.

The system subject of interest in this research is the one represented in Figure 2.42, in which a nonlinear behavior of ground due to applied TBM support pressure is observed. During tunneling, if the applied TBM support pressure, P, equals the estimated initial support pressure for face stability, P_0, thus the surface settlement will be negligible.

By reducing P is observed that the soil deforms following an elastic behavior. After that, the limit is reached, and then the development of soil plastic behavior begins to be noticed, meaning in a large formation of surface settlement which will not be more recoverable. Larger settlements or tunnel face collapse is achieved when the applied TBM support pressure reaches a minimum value, P_{min}, that cannot be zero.

Literature, already, offers a variety of mathematical formulations where this type of asymptotic type of behavior is observed, without any physical connection to the problem here proposed to study. Among all, the following are described:
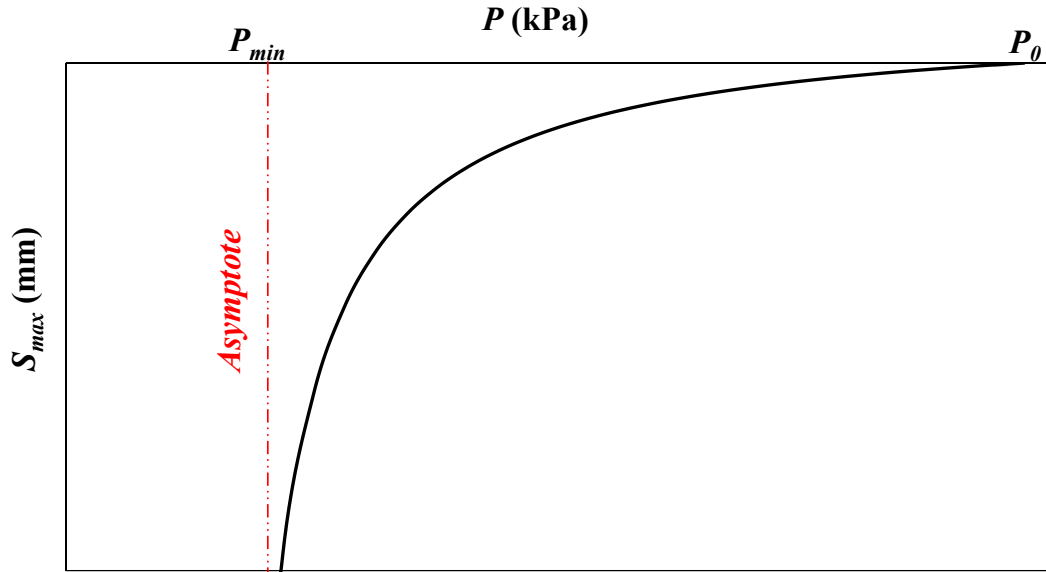
Figure 2.42 – Behavior of immediate surface settlement due to TBM tunneling.

2.4.5.1 *The nonlinear relationship of stress and stress in soils*

Based on the work of Kondner (1963), Duncan & Chang (1970) proposed a nonlinear stress-strain relationship for soils, based on the hyperbolic equation through the following expression:

$$(\sigma_1 - \sigma_3) = \frac{\varepsilon}{a + b\varepsilon} \tag{2.42}$$

where σ_1 and σ_3 are the major and minor principal stresses, ε is the axial strains, and a and b are constants values determined experimentally. Figure 2.43 shows the estimation of these constant, where Ei is the initial tangential modulus and $(\sigma_1 - \sigma_3)_{ult}$ is the asymptotic value of stress difference.

The importance of this formulation is that incorporates three fundamental aspects of the stress-strain behavior of soils; nonlinearity, stress-dependency, and inelasticity, and it provides simple techniques for interpreting the results of laboratory tests which may be used very conveniently in finite element stress analyses of soil masses.

2.4.5.2 *The soil stiffness with suction relationship*

Alonso et al. (1990) presented a constitutive model for describing the stress-strain behavior of partially saturated soils. In this model, the stiffness parameter, $\lambda(s)$, responsible of the elasto-plastic strains is expressed as a function of suction, s, by the following equation:

$$\lambda(s) = \lambda(0) \left[(1 - r) e^{-\beta s} + r \right] \tag{2.43}$$

where β is the parameter controlling the rate of increase of soil stiffness with suction and r is a constant related the maximum soil stiffness. Figure 2.44 shows the influence of β parameter on
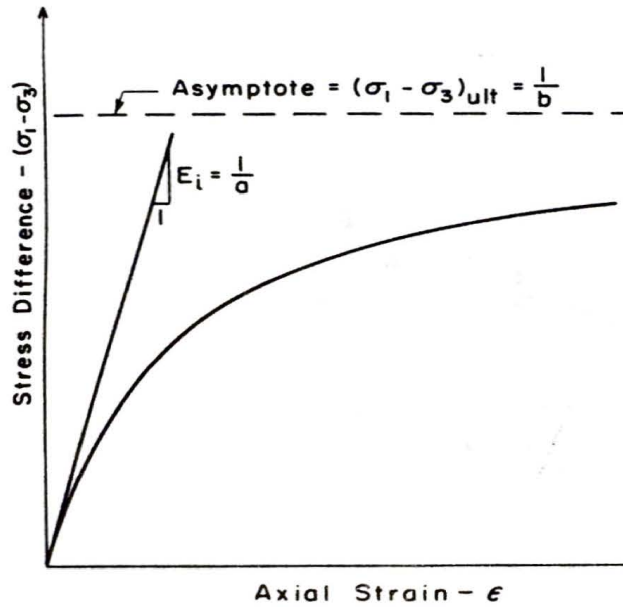
Figure 2.43 – Hyperbolic stress-strain curve Duncan & Chang (1970).

the $\lambda(s)$ curve (for $r = 0.5$). As it is possible to see, by increasing the suction value, there is a tendency for the stiffness parameter to keep constant.
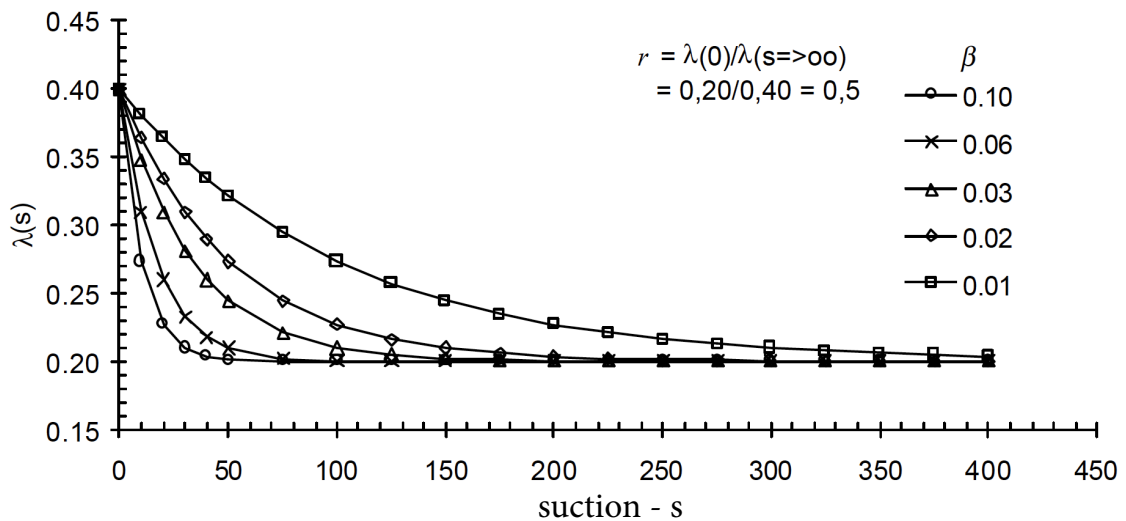
Figure 2.44 – Variation of $\lambda(s)$ curve for different values of β parameter (after Gitirana Jr., 1999).

2.4.5.3 *The infiltration rate curve*

Infiltration is the process whereby water enters the soil producing a downward flux that changes the water content with depth. The sources of water available for infiltration can be from rain, snowmelt, or irrigation. Koorevaar et al. (1983) showed an equation for computation of the infiltration rate, I, with time, t, as:

$$I = I_0 t^{-\alpha} \tag{2.44}$$

66

where I_0 is the initial infiltration rate, and α is an empirical constant experimentally determined for the site of interest. Figure 2.45 shows that during a period of constant precipitation, the rate of infiltration decreases with time until a constant rate is reached. This constant rate is called infiltration capacity and is equal to the saturated coefficient of permeability, k_{sat}^w.
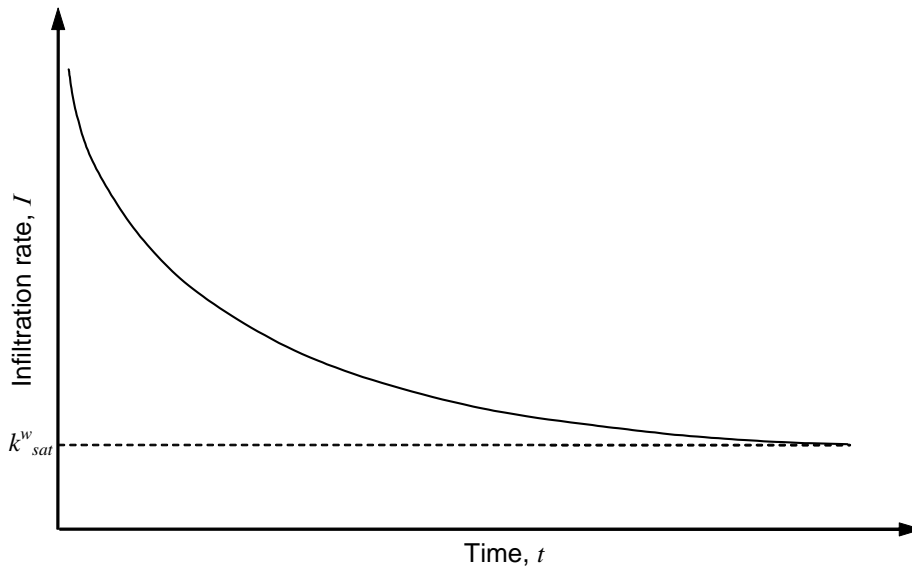
Figure 2.45 – Infilration rate with time (after Gitirana Jr., 2005).

2.4.5.4 *The exponential variogram model*

In geostatistics, the exponential variogram model is a function that describes the degree of spatial dependence of a spatial random field. Isaaks & Srivastava (1989) showed that this function has the following expression:

$$\widetilde{\gamma}(h) = \begin{cases} 0 & if \ \ |h| = 0 \\ C_0 + C_1 \left(1 - e^{-\frac{3|h|}{a}}\right) & if \ \ |h| > 0 \end{cases} \tag{2.45}$$

where $\widetilde{\gamma}(h)$ is the variogram of between points separated at distance h, C_0 which provides a discontinuity at origin, a which provides the distance beyond which the variogram value remains essentially constant and $C_0 + C_1$ which is the variogram value for very large distances, $\widetilde{\gamma}(\infty)$. Figure 2.46 an example of the exponential variogram model. As it possible to see as h increases $\widetilde{\gamma}$ approaches a sill asymptotically constant value.

2.4.5.5 *The idealized strain-strain diagram*

The Brazilian Association of Technical Norms (ABNT) published a proceed for the design of concrete structures (NBR 6118:2003), in which a stress-strain relationship for the design of concrete structures is indicated (Figure 2.47). As it is possible to see, a linear strain behavior develops on the concrete as the level of stress increases, then after a particular value of stress plastic deformation starts to appear to become later constant.
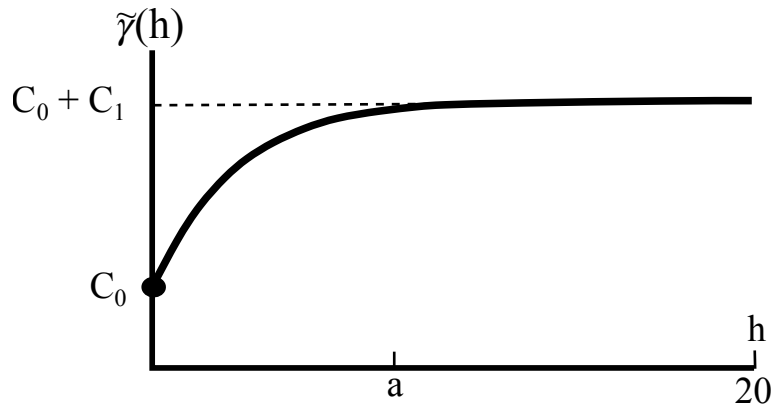
Figure 2.46 – Example of exponential variogram model (after Isaaks & Srivastava, 1989).

$$\sigma_c = 0,85 \, f_{cd} \left[1 - \left(1 - \frac{\varepsilon_c}{2\,\%_o}\right)^2\right]$$
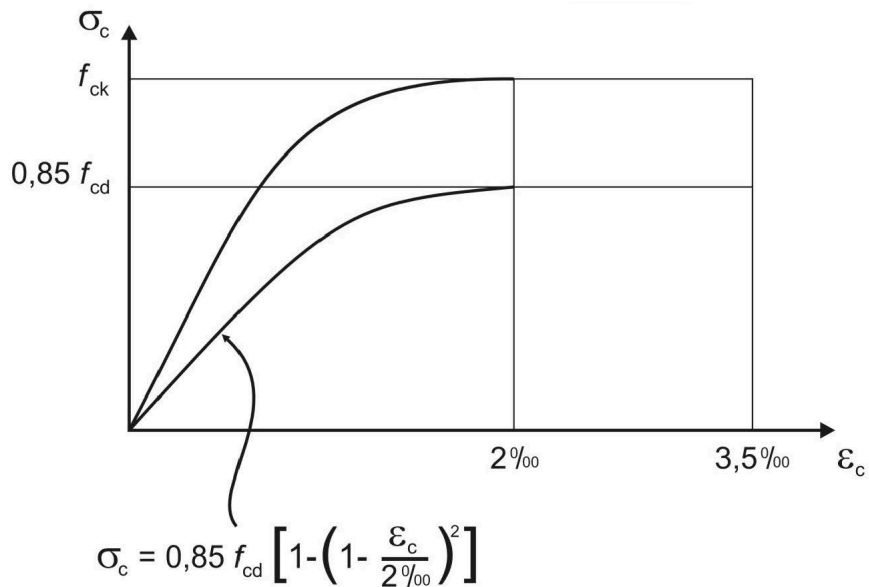
Figure 2.47 – idealized strain-strain diagram (NBR 6118:2003).

Finally, concerning model selection, Information theory became the basis for the establishment of the Akaike Information Criterion - AIC (Akaike, 1974), an excellent analysis tool for the selection of complex models. Even though, the Minimum Description Length - MDL is, till now, the most sophisticated tool to better describe a model in terms of its complexity and number of parameter embedded in it, not references of its application were found in tunneling or geotechnical engineering. Therefore, in this study, the AIC will be preferred as it provides a fastest and also reliable result.

3 CASE STUDY: EXTENSION WORKS OF SÃO PAULO METRO LINE 5

The construction of the São Paulo Metro System started, in the mid-1960s, with the first viability studies for the implementation of a metro system. The construction of the metro lines began in 1968 and the commercial operation in 1974. Currently, five lines make up the São Metro System, totalizing 68.5 km of track (mostly underground).

Regarding Line 5 – Lilacs, it can be said that it was inaugurated in 2002 with the entry into operation between the Capão Redondo and Largo Treze Stations, in the south region of the metropolitan city of São Paulo (9.3 km of track). From May 2011, the works for the extension of this line began. As described in the Management Business Planning Report of São Paulo Metro (GPE, 2013), the line extension works involve the stretch between Largo Treze and Chácara Stations, as well as Pátio Guido Caloi depot (Figure 3.1).

The total length of Line 5 Extension is of 11.5 km, of which 0.63 km was executed by the sequential method, 5.13 km correspond to single-tracks tunnels executed by two TBMs of Ø 6.9 m and, finally, 5.74 km correspond to a double-track tunnel executed also by a TBM of Ø 10.6 m. After finalization, this Line links to Line 1 – Blue at Santa Cruz Station. Line 2 – Green at Chácara Klabin Station and with Future Line 17 – Gold at Campo Belo Station. The Line, when completed, will have a total of 19.9 km of track, 17 Stations and 2 depots.
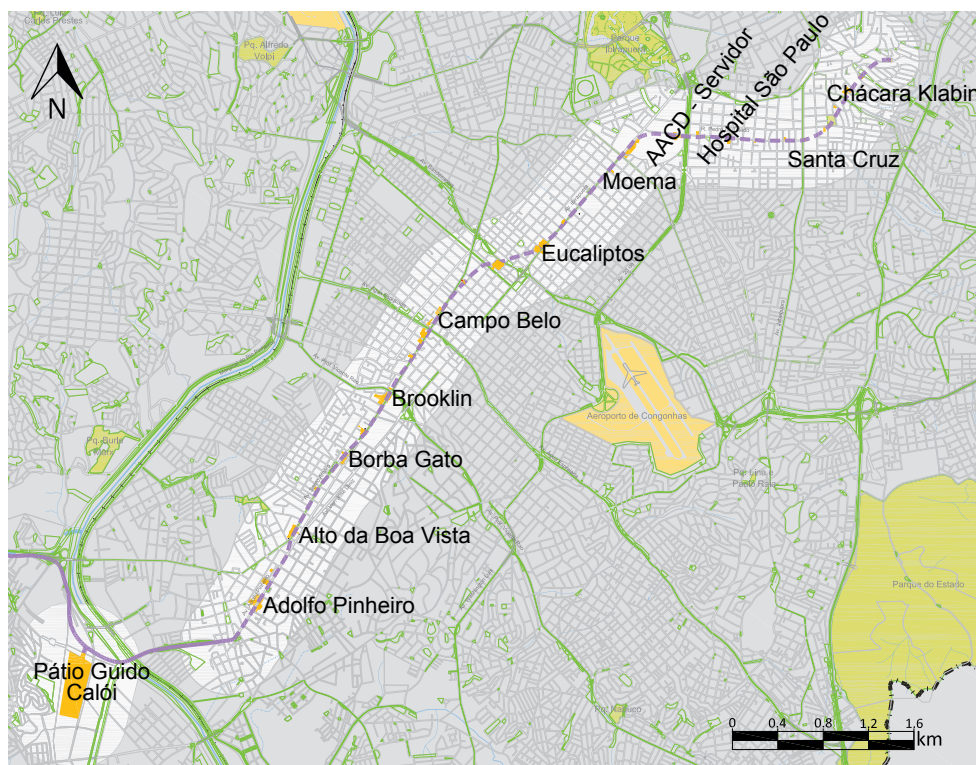
Figure 3.1 – São Paulo Metro line 5 – Lilacs route map, disposition of stations and depot (after PBA, 2010).

The tunnel stretch purpose of this study corresponds to the double-track tunnel between the Ventilation and Emergency Exit Shafts Bandeirantes and Dionísio Da Costa (points A and B respectively from Figure 3.2). Along this route, the 5.96 km double-track tunnel passes below a residential area in Jardim Novo Mundo neighborhood, continues along Ibirapuera Avenue, then passes under the Pedro Toledo Street, and finally passes beneath several residential areas in Vila Mariana neighborhood. The joint venture CM5 is responsible for the execution of this work and is composed of the construction companies: Odebrecht, OAS and Queiroz Galvão.

Figure 3.2 – Double-track tunnel from Ventilation and Emergency Exit Shafts Bandeirantes (point A) to Dionísio Da Costa (point B).

This tunnel stretch presents a series of factors that have made it a good choice as a case study for this research. Among these factors, the followings are mentioned: *i*) The intense instrumentation campaign carried out along the stretch of the Line, *ii*) The relative simplicity of construction methodology because is to a double-track tunnel executed by TBM, *iii*) Excavation done mostly between the contact of soils of São Paulo Formation (upper part of the tunnel) and soils of Resende Formation (lower part of the tunnel), *iv*) The reuse of the TBM previously used for the construction of Line 4, where geology was, mostly, similar to this stretch Line and because of that no modification was made to the TBM cutting wheel and, finally, *v*) The use of the same crew that made the excavation of Line 4 that allow an optimization of excavation due to familiarity with geology and machine.

3.1 GEOLOGICAL DESCRIPTION ALONG THE TUNNEL PATH

In order to establish the geological characteristic of the groundmass along the tunnel path, Standard Penetration Test (SPT) campaigns were carried out at intervals of 30 and 40 m. In general, the surveys reached depths of 55 m, is the largest of them of 58.5 m in correspondence of the crossing between the Alfonso Celso and the Jorge Tibirçá Street, in Vila Mariana neighborhood. With the elaboration of the geological profile, it was verified that along the excavation of the tunnel two types of geological conditions will be crossed: São Paulo and Resende Formation.

The sedimentary soils of Resende Formation consist of facies of clays and sands both subdi-

vided into three texturally different units. The clays of this formation are commonly known as the Taguá; these clays have grayish-green color, present a stiff consistency, highly overconsolidated due to erosive processes and low permeability (Massad, 2013). The sands, in general, have a medium granulometry and appear in confined lenses.

On the other hand, the soils of São Paulo Formation are constituted by two main facies, one clayey (red and variegated) and the other sandy. These two facies are also subdivided into several others according to their texture composition. In comparison with Resende Formation, the soils of São Paulo Formation are generally milder, and their sands are usually more clayey, with lower permeability coefficients and longer auto-sustention times. Both red and variegated clays are overconsolidated due to phenomena associated with clay fraction, like particle cementation due to sedimentation and drying cycles of soils (Massad, 2013).

From Bandeirantes Shaft (starting point of tunnel excavation) to Moema Station, the tunnel develops a topographic elevation through the soils of Resende Formation. From Moema Station until the end in Dionísio Da Costa Shaft, the tunnel passes through both Formations (Figure 5.1).

In addition to these materials, it was observed that the tunnel partially passes through quaternary sediments, which are presents in some areas along the path as is the case in Armando de Virgillís street next to Chácara - Klabin Station. According to Silva (2011), the quaternary sediments are materials of low geotechnical quality for the construction of tunnels due to the low cohesion and high permeability.

Regarding the phreatic level, it was observed that along the tunnel path, the phreatic level is in between 2 and 4 m below the surface. By taking into account the upper geratrix of the transversal tunnel section, a minimum of 5 m water column was detected in the vicinity of Chácara Klabin Station, and a maximum of 34 m water column was read between Santa Crux Station and Jorge de Melo Shaft. The average water column along the tunnel path is of 20 m, from what it is concluded that the groundmass around the tunnel is considered as saturated.

For detailed and comprehensive information regarding the geology, geomorphology, and Hydrogeology of the city of São Paulo, the reader may refer to ABMS (2013).

3.2 GEOTECHNICAL CHARACTERIZATION OF THE TUNNEL PATH

In order to quantify the geotechnical characteristic of the groundmass to study the ground behavior due to tunneling all along the route, a series of in situ and laboratory tests are needed. From the extensive in situ and laboratory tests performed by São Paulo Metro, were chosen those tests that provided the necessary information to accomplish the objectives in this work.

In this regard, for the tunnel route between Bandeirantes Shaft and Dionísio Da Costa Shaft, the São Paulo Metro performed 168 Standard Penetrations Test (SPT), 17 Flat Dilatometer Test (DMT), 1 Pressuremeter Test (PMT), 11 Piezocone Penetration Test (CPTu) and 60 Piezometer Shafts for water level measurement.

Regarding the laboratory tests, São Paulo Metro informed that for the construction of Line 5 – Lilacs were executed two survey campaigns for collecting samples and, later, triaxial tests were carried out. The samples were collected in correspondence of São Paulo Formation for the construction of the Pinheiros Station and São Sebastião Shaft. These structures belong to other groups of operas of Line 5 out of the section under study. In addition to these tests, the results of tests carried out for the construction of other Metro Lines were used, to have a more comprehensive database of soil parameters along the tunnel route.

In Chapter 5, the results of processing and statistical analysis of the information here mentioned will be presented in order to obtain the necessary parameters required for the accomplishment of this study.

3.3 TUNNEL CONSTRUCTION PROCESS

As indicated at the beginning of this chapter, the excavation of the tunnel stretch object of this study correspond to a tunnel of 5.96 km of track that will start from Bandeirantes Shaft to Dionísio Da Costa Shaft (points A and B respectively from Figure 3.2). The construction of this tunnel began on 09/09/2013, by using Tunnel Boring Machine (TBM).

The machine used for this purpose was an Earth Pressure Balance (EPB) machine (HER-RENKNECHT model S-733), designed to excavate the type of soils foreseen in this tunnel route, as well as to keep the water level at its initial condition. Figure 3.3 shows a layout of a general representation of an EPB machine. This type of machine applies two main support pressures: *i)* The face support pressure (P) at the front of the TBM and *ii)* The grout injection pressure (P_{inj}) behind the shield, that allows a reduction of ground movement by restricting the relaxation of the natural stress state of the soil mass. Disposition of pressure sensors allocation, either for face support and grout, is presented in Figure 4.2.

Both types of applied support pressure develop a dissipation of their respective pressures around the shield in the form of a triangular diagram. In this way, it is avoided the migration between the materials which are used for the application of the support pressure (i.e., injected grout toward the front shield).

Table 3.1 below shows a summary of the main characteristics of the TBM.

In order to allow an excellent TBM performance, in situations of TBM starting or arrival into station or shaft, ground treatment works were realized in order to reduce considerable permeability and to increase the ground strength around these particular areas. For this purpose, the type of ground treatment utilized was the use of Jet-Grouting columns. The geometric configuration of Jet-Grouting columns will depend on how is positioned the structure with the groundmass. Figure 3.4 shows the Jet-Grouting geometric configuration used for the ground treatment in Moema Station in order to allow the starting of TBM excavation to next Station (AACD – Servidor).

Regarding the construction of the tunnel route by the use of TBM, it is necessary to mention
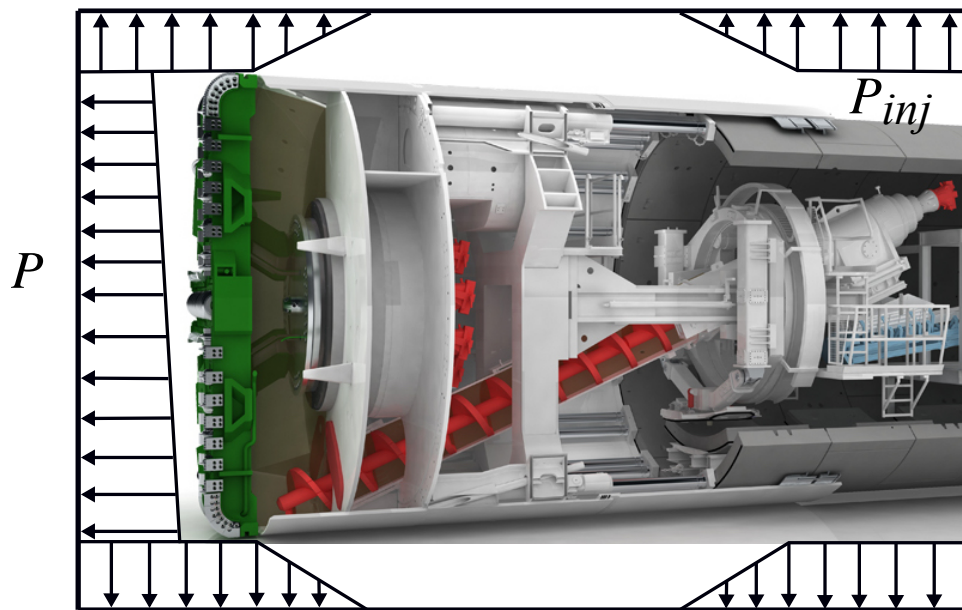
Figure 3.3 – Schematic representation of a EPB machine with the diagram of support pressure at the front face and at the tail shield.

Table 3.1 – Summary of TBM main features.

TBM MAIN CHARACTERISTICS	
Cutting wheel diameter (m)	10.58
TBM shield length (m)	12.54
TBM total weight (ton)	1500
Total weight of Back up (ton)	400
Number of thrust cylinders (-)	16 pairs
Number of EPB sensors (-)	7
Number of grout injection lines (-)	6
Number of extracted weight material balance (-)	2
Number of ground conditioning injection lines (-)	12

that the use of this type of construction method requires the continuous application of pressures to achieve general stability of the groundmass and low deformability. For that, it is mandatory for the elaboration of a project to define such operational pressures all along the tunnel route. The required pressure for this purpose is the tunnel face pressure and grout injection pressure. These types of pressures have a direct impact on surface settlements induced by tunneling. Besides these parameters, other parameters are also taken into account to evaluate ground mass stability like grout injection volume and weight of extracted material.

In this respect, for the definition of the tunnel face pressure, several analytical methods are considered in order to provide an optimal reference pressure. For the definition of tunnel face pressure of São Paulo Metro Line 5 were considered:

– Earth pressure at rest method (Rankine theory);

– COB (Dutch Onderground Bowen Center) method;
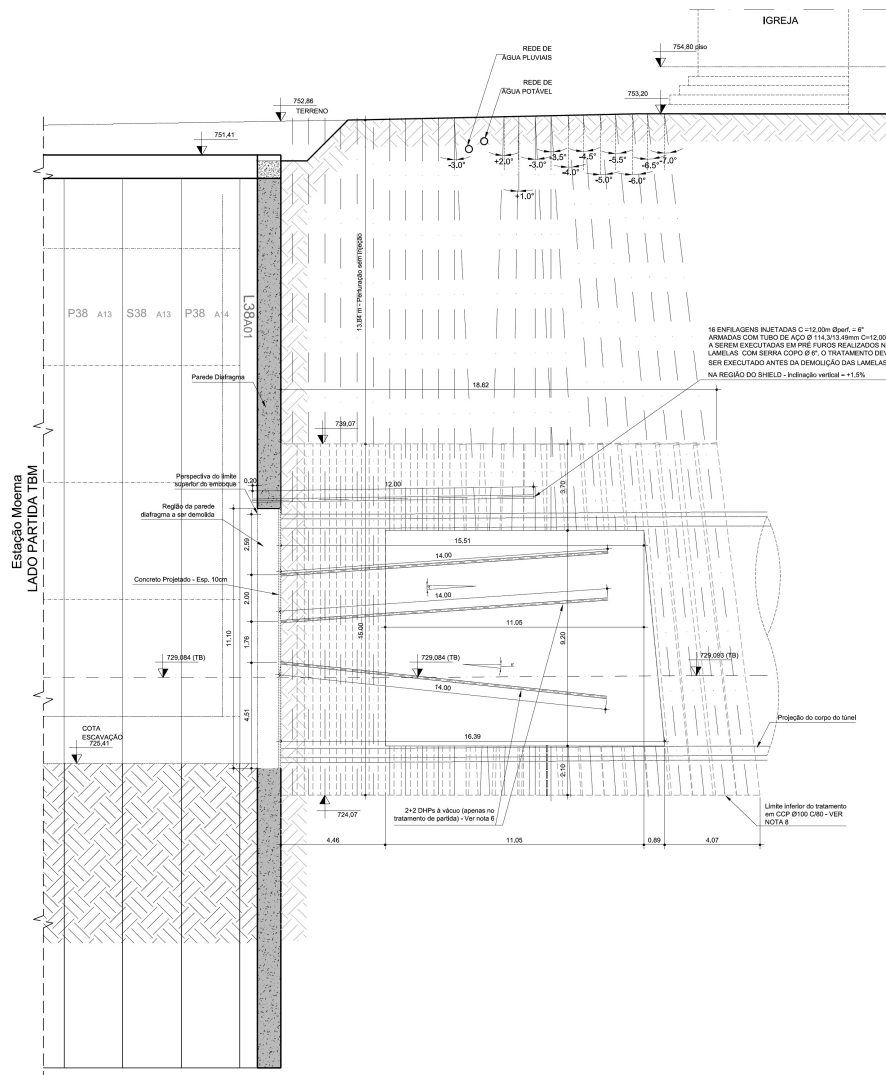
Figure 3.4 – Jet-Grouting columns executed from surface to allow starting TBM excavation to next Station (AACD – Servidor).

– Anagnostou and Kovari method; and

– Caquot-Kerisel method.

After comparative analysis among these methods, the designer of São Paulo Metro hired for this project recommended the use of Caquot–Kerisel method because it provides more conservative values and thus reduces possible effects of significant settlements at the surface. Chapter 6 will show a verification of these methods.

Regarding the grout injection pressure used for the filling of the annular gap between the excavated ground and the outer concrete tunnel ring. The value of applied grout injection pressure was 30 kPa more than the corresponding tunnel face pressure. This approach is due to the following considerations:

– Assure that grout is being injected into the annular gap; and
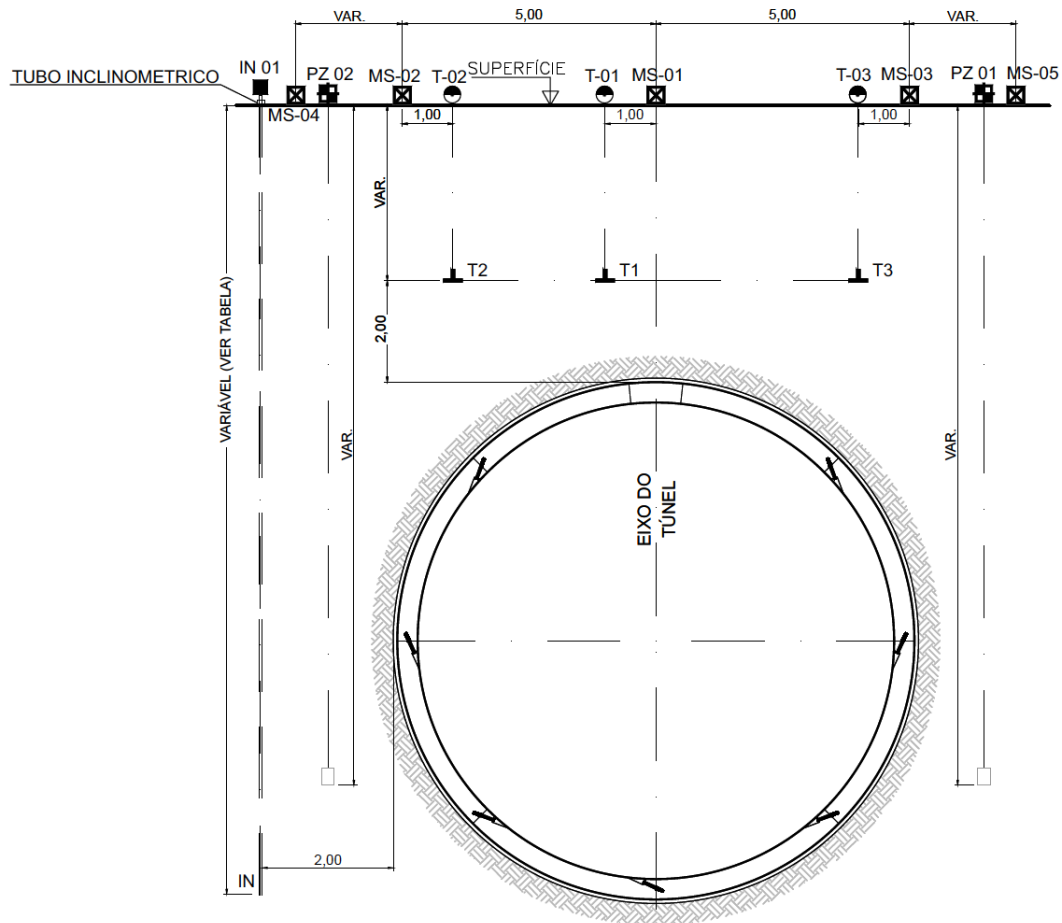
Figure 3.5 – Schematic representation of type A monitoring section.

− Avoid the transference of excavated material from the face to the tail shield.

Finally, concerning the volume of injected grout and the weight of extracted material, it is of common approach that the values of these parameters are estimated as a function of the annular space and the specific weight of the material, respectively. The volume of the annular gap (m^3) is estimated by considering the space between excavation surface profile and the outer tunnel lining per 1 m of TBM advancement. The weight of extracted material (tons) is estimated by considering the density of the material and the volume of excavation (transversal tunnel section per 1 m of advancement).

3.4   TUNNEL PATH MONITORING DESIGN

The use of the monitoring system plays an essential role in tunneling because it allows following and, consequently, control the development of deformations in the groundmass and the influence in nearby structures due to excavation. This is done to verify the design parameters hypothesis in terms of displacements, structural behavior of the tunnel during its construction and accompanied the influence of this construction on the nearest building.

By considering the stated above, a series of monitoring instrument was defined and installed all along the tunnel route between Bandeirantes shaft and Dionísio Da Costa Shaft.

Transversal monitoring sections were established for the arrangement of the installation of the instruments, at every 25 m, all along the tunnel route. Three types of monitoring sections (A. B and C) were defined as follow:

- Type A section — 5 MS, 3 T, 1 PZE, 1 PZM and 1 IN, every 100 m;

- Type B section — 3 MS and 1 T, every 50 m; and

- Type C section -– 3 MS. every 25 m.

Figure 3.5 shows a schematic representation of the type A monitoring section, indicating the disposition of monitoring instrument installation.

Table 3.2 shows a summary of the main instruments implemented for the accompanied of the tunnel construction.

Table 3.2 – Summary of monitoring instruments foreseen for accompanied of tunnel route excavation.

Instrument	Code	Parameter observed	Positioning
Levelling Point	MS	Surface Settlements	At surface near the tunnel
Tassometer	T	Settlements at depth	In the ground mass in correspondence with the tunnels axis 2 m ahead of tunnel roof and tunnel sides
Inclinometer	IN	Horizontal displacements	Ground around the tunnel
Electric piezometer	PZE	Water pressure	Ground around the tunnel
Piezometer (Casagrande)	PZM	Water level	Ground around the tunnel

To conclude, with these three types of sections configuration defined for the construction of this tunnel route, the registered surface settlements will be approximated to the theoretical Gauss distribution curve by the use of linear regression analysis, and thus, estimating the volume lost.

However, measurements were also made in the other monitoring instruments; it is pointed out that, for the objectives foreseen in this study, these readings will not be analyzed.

4 METHODOLOGICAL APPROACH

In order to accomplish the main objective proposed in this research, a series of sequential steps with the necessary information for that achievement will be presented. Firstly, it is presented the proposed sequential steps following, in a certain way, the concepts previously described all along Chapter 2 to 5. The proposed methodological approach is shown in Figure 4.1 is divided into four steps in which a detailed analysis will be made. After that, information about the extension works of Line 5 of São Paulo Metro will be introduced, as a case study to frame this research into a real case scenario and, in this way, to be able to validate the proposed formulation.

Data acquisition and processing	Probabilistic analysis of soil properties	Analytical and numerical analysis	Mathematical modeling approach
- Geological and geotechnical - TBM - Monitoring	- Preliminary selection of soil properties by analysis of coefficient of variation (CoV)	- Face support pressure - Settlement trough - 2D and 3D numerical analyses	- Mathematical representation of surface settlement due to TBM through the application of different techniques

Figure 4.1 – Propose methodological approach.

4.1 DATA ACQUISITION AND PROCESSING

Correspond to all the necessary information required for the proper development of the research. This regards information about geological and geotechnical features of the ground, TBM performance and monitoring measures recorded during tunneling.

4.1.1 GEOLOGICAL AND GEOTECHNICAL DATA

As previously mentioned, tunneling induces ground movements which predominantly depends on the mechanical properties of the soil. Acknowledging that soils are subject to uncertainties, it turns out necessary an appropriate processing of these uncertainties for application of ground movement analysis.

Therefore, the first step consists in to organize and quantify the results of in situ and laboratory tests that provided as well as the reference material of previous tunnel line projects (i.e., Line 2 and 4 of São Paulo Metro). After that, analysis and designation of the test results to the local geology units need to be made.

Next step, will be to identify the main geotechnical parameters and to search for its respective value of the coefficient of variation (CoV), in order to evaluate the influence of soils parameter uncertainties on the induce of immediate surface settlements by tunneling.

Finally, a list of input geotechnical parameters to use in this research as well as its respective value of CoV has to be presented. With this information, soil variability uncertainty will be considered to perform later numerical and probabilistic analysis.

4.1.2 MONITORING DATA

Monitoring programs are essential to control ground behavior before, during and after construction. Their results can be used to minimized uncertainties, to control the quality of production and to guide new plans of actions as well as to confirm the performance of excavation (Guglielmetti et al., 2008).

Therefore, the scope in this step will consist of the estimation of the volume loss along the tunnel path. The first thing to do will be to quantify and select the monitoring sections installed that could provide significant information about the transverse surface settlements. Following thing will be to verify of settlement trough curve as those presented in Table 2.4 adjust better to the settlement results of the monitoring sections.

After that, the estimation of the volume loss is made and then a statistical analysis will be applied for the estimation of mean (μ), standard deviation (σ) and the coefficient of variation (CoV) of the volume loss, maximum surface settlement and other parameters of the settlement trough curve.

In this sense, the total length of the tunnel path should be split in various parts to create zones in which, at least, from the statistical point of view, the ground movements within these zones will behave homogeneously due to tunneling. Thus, the zone with a better-homogenized behavior will be considered as a reference for the subsequent analyses.

4.1.3 TBM DATA

Tunnel Boring Machines (TBMs) are formed mostly by mechanical, hydraulic, electric and electronic parts. In this respect, the use of TBMs requires the presence of sensors in order to allow TBM technicians and operators to make a proper accompany of the machine performance during excavation.

A typical procedure is that during TBM operation, a computer registers at every instant the values indicated by the sensors. Each TBM parameter is then related to its respective sensor. The total number of samples for a single TBM parameter will depend on the number of concrete rings installed during tunnel construction.

Usually, the sensors are divided into the following categories:

– TBM guidance;

– TBM hydraulic system;

– Ground conditioning;

- Grout injection;

- Earth pressure;

- Extracted material;

- Electric system;

- Cooling system;

- Shield mechanics jacks;

- TBM thrust advance;

- Cutterhead torque;

- TBM velocity;

- Cutterhead penetration rate;

- Cutting tools wear detector;

- Lubrification grease system;

- Nocive gas detector; and

- Safety equipment detectors.

As the TBM face support pressure and grout injection pressure constitute the main components of a TBM to achieve ground stability during tunneling, attention to the sensors related to these components is given. Figure 4.2 shows the location of TBM Earth Pressure Balance Sensors and Grout Injection Pressure Sensors in the machine. Earth Pressure sensors (denoted with S) are installed on the bulkhead and their configuration of position allow the operator to manage the proper face-confinement pressure, to verify the distribution of pressure in the bulkhead and to detect any possible drop or increase of pressure in a localize part of the bulkhead. On the other hand, Grout Injection sensors (denoted with P) help to assure that grout is being injected properly.

Following the process of this analysis, related technical papers (Kasper & Meschke, 2006a,b; Mollon et al., 2013) as well as TBM books (Guglielmetti et al., 2008; Maidl et al., 2012) will be reviewed in order to evaluate the influence of other TBM parameters on the ground mass behavior besides the two main parameters previously indicated.

After preliminary analysis of TBM parameters, on the influence of reaction of ground mass behavior, a statistical and probabilistic analysis on these parameters will be made. Histogram and the best fitted probabilistic density function (PDF) will be estimated for each parameter.

To accomplish this task, the distribution fitting tool embedded in MATLAB R2016a will be used to obtain the PDFs and estimate their respective mean (μ) and standard deviation (σ) values. After that, the Kolmogorov-Smirnov test will be implemented in order to estimate the best fitted
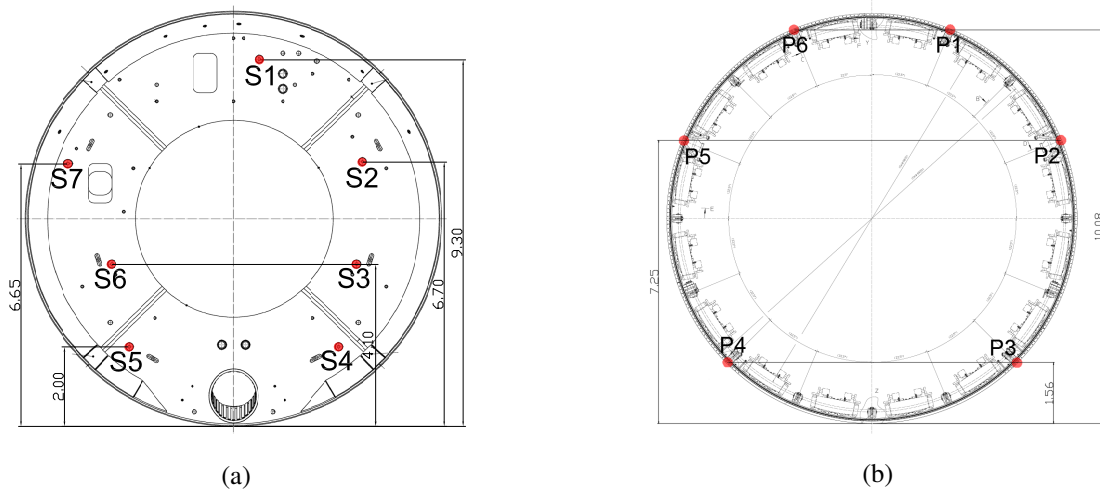
Figure 4.2 – Location of TBM Pressure Sensors, (a) Earth Pressure Balance sensors and (b) Grout Injection Pressure sensros.

PDF among the selected. The Normal, Lognormal, Gamma and Weibull probability density function will be used, which according to Baecher & Christian (2005) are the most implemented PDF in the geotechnical engineering field.

Finally, coefficient of variation (CoV) will be estimated for two cases: by considering first all the tunnel stretch, and second by considering homogeneous tunnel zones (between the main metro infrastructures), in order to estimate the tunnel section with less variability.

4.2   SENSITIVITY ANALYSIS OF SOIL PROPERTIES

This step consists of sensitivity analysis for the selection of soil property uncertainties which later will be used in this research for the performing of numerical and probabilistic analyses. In this regard, the representation of uncertainty of soil properties as random variables will be defined by employing their respective mean (μ) and CoV.

Therefore, based on the works of Mollon et al. (2013) and Miro et al. (2015), a methodology for evaluating the influence of uncertainties in soil parameters on surface settlements due to tunneling is going to be implemented with a slightly different approach. Due to the lack of real monitoring data to work with, these authors, firstly, idealized a 3D model for tunnel simulation to obtain a settlement trough. By performing a probabilistic analysis called the Response Surface Method, an evaluation of the propagation of the uncertainty from the input (soil properties) to the output variables (settlement trough) of the numerical model was made.

Unlike the procedure applied by these authors, in the approach here proposed, information about monitoring data is available from the case study, which is introduced later. Next, a 2D numerical model is implemented; subsequently, probabilistic analysis, based on the APEM, will be performed to analyze the influence of input parameters and finally, a statistical inference analysis is made to justify the proper CoV selection to apply for representing soil properties variability.

This procedure will be made through the conduction of sensitivity analyses which results will be presented in the form of a deterministic tornado diagram.

Besides considering geotechnical parameters as input variables, it will also be considered in the analysis of the influence of soil layers thickness. Figure 4.3 portrays a typical geological profile, resulted from site investigations, and tunnel path along with the profile. The random field theory is used to describe their spatial variability, as El Gonnouni et al. (2005) and Wang et al. (2016) did. Despite the capabilities of a random field to represent the spatial variability of soil properties, this type of analysis will not be considered.

As an alternative to that type of analysis, a simplified procedure for considering stratigraphic variability is here described. For that, the overall longitudinal direction of the geological model is assumed to have an equivalent transverse section. So from the available boreholes, the position of soil interfaces is statistically estimated in terms of their respective mean (μ) and standard deviation (σ). The normal distribution function will be assumed to these input variables. This consideration will undoubtedly represent an upgrade for a complete understanding of groundmass behavior on surface settlement due to tunneling.

The 2D numerical analysis is preferred, in this step, over the 3D simulation because the output variables response as maximum settlement (S_{max}), volume loss (V_{loss}) and inflection point (i), embedded in the transversal settlement curve, are of interest for comparison with their respective output variables obtained from the real monitoring data.

Three probabilistic scenarios for considering the randomness of soil property uncertainties are considered for the evaluation of the output variables response in the numerical analysis. These scenarios are the optimistic, neutral and pessimistic which are based on the range of applicability of CoV of the soil properties. The scenario is, thus, an indicator of the so-called epistemic error
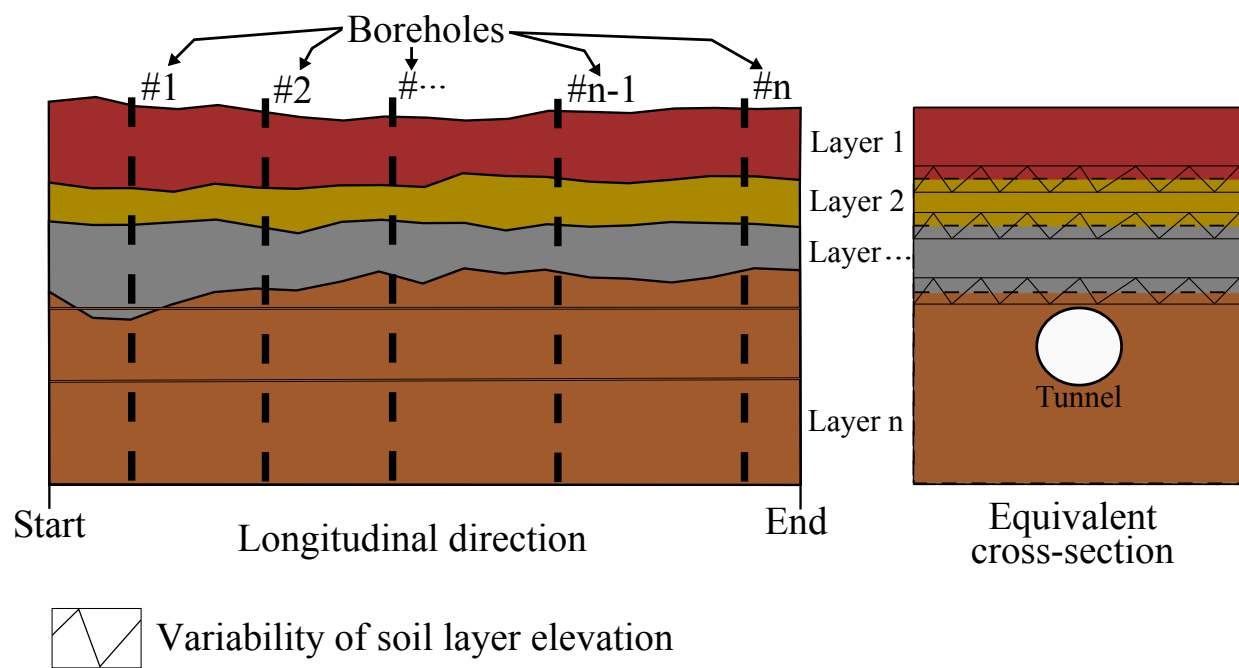
Figure 4.3 – Schematic representation of a longitudinal geologic profile and equivalent transverse section.

(related to lack of knowledge), rather than of the natural variability of the soil.

Therefore, the idea of performing the HPEM on a 2D numerical model will be to analyze the influence of variation of soil properties in the output variables for estimation of the transversal settlement curve.

By knowing the real behavior of the soil due to tunneling in terms of the variables of the transversal settlement curve, a comparison with the results obtained from the probabilistic analysis is made through the application of a statistical inference analysis like the Test of Hypothesis to establish which scenario will embrace an optimal consideration of soil variability for the behavior of immediate surface settlements due to tunneling.

Concerning the use of the HPEM over other probabilistic method and consequently tornado diagrams, their use is justified due to the quickness of application of these probabilistic technics. Neither, these types of approach were applied before in tunneling, until now. Thus, this could represent an excellent tool for evaluating soil property uncertainties.

The part of the zone to use for this analysis and further analyses will be the one obtained from field measurements with a better homogenized behavior in terms of ground movements.

4.3 ANALYTICAL AND NUMERICAL APPROACH

By considering the results obtained in the sensitivity analysis approach, a series of analytical and further numerical analyses should be made in order to gain a better comprehension of the development of ground movement due to TBM tunneling. Analytical analysis regarding tunnel face stability and settlement trough are, firstly, used to make the estimation of these parameters and secondly to compare them with the results of the further 2D and 3D numerical analysis.

Regarding the numerical approach, The numerical analyses will be carried out considering the drained condition with steady-state flow. According to Atkinson (2007), drained conditions may be assumed under typical excavation times if the materials have permeabilities higher than 10^{-6} m/s. The local materials are characterized as tropical residual soils. Pedogenic processes produce highly weathered soils that present macropores, resulting in relatively high values of permeability (Blight & Leong, 2012; Huat et al., 2012). Soils $3Agp_1$, $3Ag_{1,2}$ and $3Ar_{1,2}$ have permeabilities that range between $5.00 \times 10^{-6} - 1.00 \times 10^{-4}$ m/s. Therefore, the hydraulic behavior of these tropical residual soils warrants drained analyses.

4.3.1 ANALYSIS OF FACE SUPPORT PRESSURE

Some of the analytical methods shown in Table 2.3 as the Anagnostou & Kovari and the Caquot methods will be used for the analysis of tunnel face stability. The idea will be to estimate, by two different approaches, the values of face support pressures, related to each method, and in this manner, foresee which method allows to provide a better approximation to a real situation.

The proposed analytical methods will be analyzed by applying a statistical approach where after estimation of the mean (μ) and standard deviation (σ) of the face support pressure, a statistical inference analysis like the Test of Hypothesis will be implemented for comparison with the real case scenario, obtained from the TBM data.

4.3.2   ANALYSIS OF SETTLEMENT TROUGH

As expressed in section 2.3.3, that the analytical formulations for analysis of ground movement will not be used. The following analysis is already integrated with the application of the empirical formulations propose to be used in section 4.1.2, for the estimation of the settlement curve parameters.

4.3.3   2D AND 3D NUMERICAL ANALYSIS

It is the intention to use the well know software package ABAQUS®, which is available in the Department of Civil and Environmental Engineering of this University and is based on the Finite Element Method (FEM).

Other than estimating stress distribution around the tunnel, the 2D numerical analysis will allow checking input soil properties by comparison with the analytical solution for the development analysis of transverse surface settlements (section 4.2).

The 2D FE analysis will be made by considering the model in-plane strain and greenfield condition. The numerical analysis steps adopted in order to simulate tunnel excavation by a TBM are shown in Figure 4.4, which are: geostatic condition (Figure 4.4a), reduction of tunnel core stiffness (Figure 4.4b), removal of core, total normal stress boundary condition applied to the excavation perimeter and injection of grout for filling the gap (Figure 4.4c) and installation of tunnel lining (Figure 4.4d).

Attewell & Woodman (1982) indicated that surface settlement directly above the tunnel face corresponds to $0.5 S_{max}$. Thus, in order to be coherent with their conclusion, the stiffness reduction method proposed by Swoboda (1979) was used in the numerical analysis, where the elasticity modulus in the excavation area is reduced (Figure 4.4b). Regarding the step in Figure 4.4c, following the recommendation indicated by Guglielmetti et al. (2008), a higher grout injection pressure of 30 kPa respect to the TBM face pressure was applied. The analytical method proposed by Anagnostou & Kovári (1996), which is based on the limit equilibrium method, was implemented for the estimation of the TBM face support pressure.

On the other hand, the 3D numerical analysis will be made in order to study the development of ground movement by reduction of the TBM face support pressure. This type of analysis provides a direct relation between these two parameters.

Regarding the 3D numerical analysis, values of face support pressure will be chosen to apply in the simulation. These values will be taken from the results obtained from section 4.3.1. Thus, for a given realization of face pressure as an input value, it is expected a ground response, which

(a) Groundmass initial condition.

(b) 50% core stiffness reduction.

(c) Grout injection around the tunnel.

(d) Tunnel lining installed.
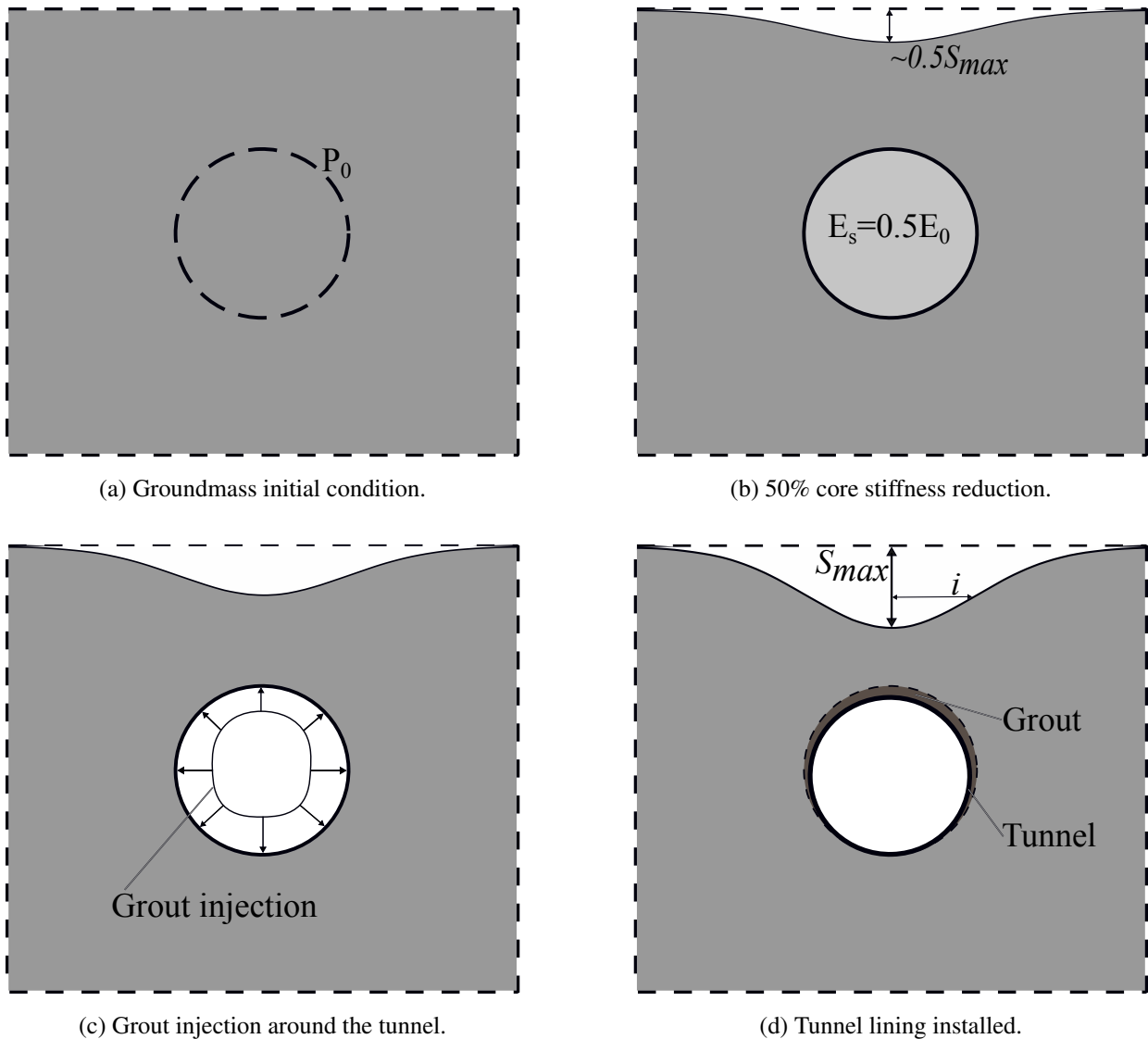
Figure 4.4 – 2D numerical analysis approach.

will allow building a semi-empirical relationship between these two parameters (face pressure and surface settlement).

For a shield is driven tunneling constructions method, a consistent 3D finite element model, based on the work of Kavvadas et al. (2017), will be performed. This includes several features of EPB tunneling such as face support pressure, conically-shaped shield with a shield-ground interface, tail gap, grout filling of gap and segment lining. In this respect, Figure 4.5 illustrates the features for performing a shield driven tunnel excavation in the 3D numerical model.

The distribution of face support pressure will be added in the analysis as a linearly distributed load with depth, which value at the top of the tunnel came from the previous analysis (Section 4.3.1). Shield conicity and the annular gap will be modeled following the TBM geometry indicated in Table 3.1 from the case study. As the shield will not share nodes with the surrounding soil, the interaction between corresponding nodes of the shield and the ground will be modeled by employing a pressure-overclosure interface. The "Softened" exponential pressure-overclosure re-
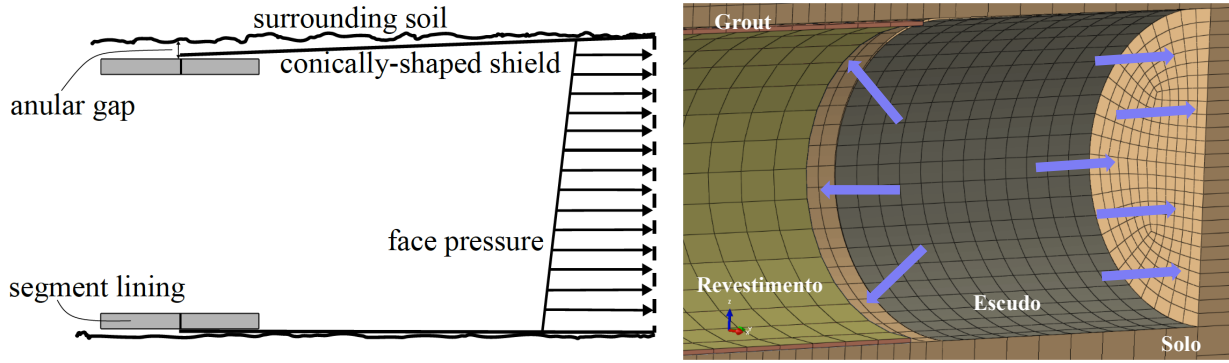
Figure 4.5 – Sketch for modeling shield driven tunneling.

lationship type contact is preferred over the "Hard" contact type because it allows better numerical stability.

As depicted in Figure 4.6, the transference of pressure stars when the normal distance between the two surfaces falls below a prescribed small positive value of C_0 and the contact pressure reaches a prescribed value of P_0 then the two surfaces came in contact. A frictionless horizontal interaction between the shield and surrounding soil will be considered as usually during tunnel construction lubrication is used.
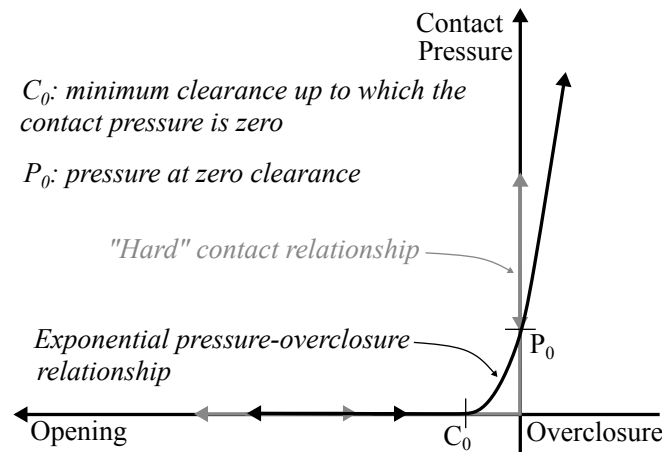
Figure 4.6 – "Hard" contact and "Softened" exponential pressure-overclosure relationship types of contacts (after ABAQUS, 2016).

In order to simulate the filling of the annular gap, pressure against the surrounding soil will be employed which will represent the fact of injecting cement grout, later this pressure is substituted by a grout element with a prescribed E-modulus corresponded at 48 hours of hardening, following the time-dependent elastic modulus of grout according to FIB (2013):

$$E_{ci}(t) = \beta_E(t) E_{ci}$$
$$\beta_E(t) = [\beta_{cc}(t)]^{0.5}$$
$$\beta_{cc}(t) = \exp\left\{0.38\left[1 - \left(\frac{28}{t}\right)^{0.5}\right]\right\}$$

(4.1)

where $E_{ci}(t)$ is the modulus of elasticity in MPa at an age t in days; E_{ci} is the modulus of elasticity in MPa at the age of 28 days; $\beta_E(t)$ is a coefficient which depends on the age of concrete, t in days and $\beta_{cc}(t)$ is a function that describes the strength development with time.

The segment lining, on the other hand, will be considered as a continuous linear elastic shell.

By considering the features mentioned above, the numerical modeling of the excavation process adopted considers the following steps:

– The excavation is advanced by one ring length (1.5 m), via removal of soil element at tunnel face;

– The whole shield is moved forward the one ring length;

– The prescribed face support pressure is applied on the new excavation face;

– The grout injection is applied around the side wall of the tunnel ;and

– The grout element is activated as well as the segment lining.

4.4 MATHEMATICAL AND MODELING APPROACH

By using the monitoring and TBM data, from the case study, it is proposed an attempt for building a semi-empirical formulation. To achieve that, the results of the various performed numerical analysis, as well as the observed data, will be used to build a series of set candidate models that, satisfactorily, may provide a good representation of the problem.

In this regard, Figure 4.7 shows the steps proposed for the mathematical modeling of surface settlement due to tunneling.
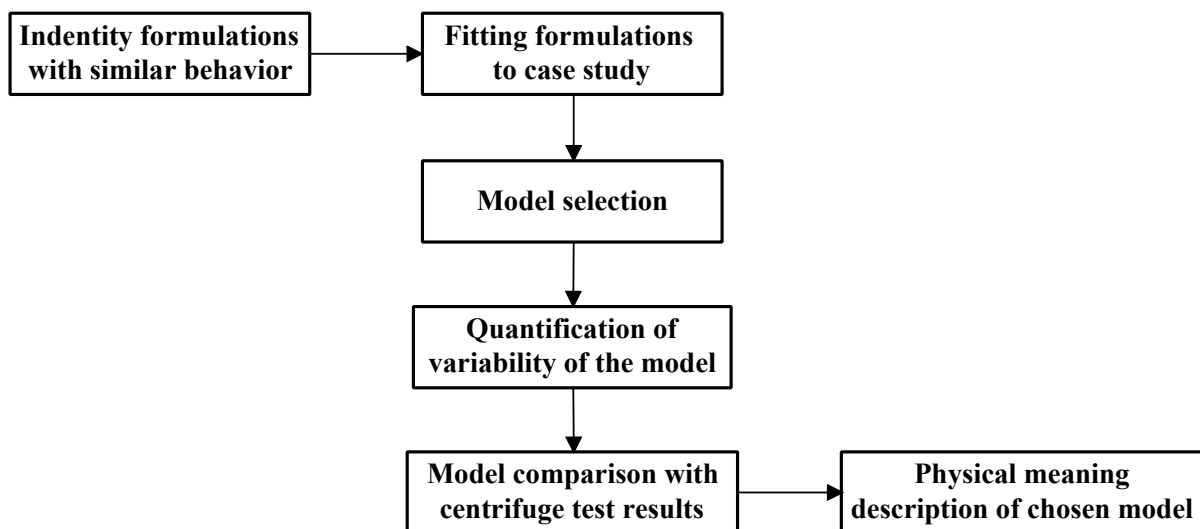
Figure 4.7 – Proposed approach for mathematical modeling.

In the first step, an identification of formulations that describes a similar behavior of the system will be adapted to the present case, that is, a set of candidates models are proposed. The second step regards the process of fitting parameters of every set of candidate models to real values from the case study, which will be performed through nonlinear regression techniques.

Third, the Akaike Information Criterion (AIC) is going to be used in order to choose the candidate model that fit the most. Fourth, due to nature itself of the system where high variability between settlement trough and face support pressure exists, an upper bound and lower bound is suggested to represent this variability which is based on the concept of confidence limits.

Then, various references where centrifuge test analyses, were performed for the study of surface settlement due to tunnel face support pressure, are used for comparison with the selected model.

Finally, a description for the derivation of the physical parameters of the selected model is offered.

5 PROBABILISTIC AND SENSITIVITY ANALYSES

Probabilistic and sensitivity analyses regarding the topics of this research are presented from here on. The presentation of these results is shown following the steps initially proposed in the methodological approach (Chapter 4).

5.1 ANALYSIS AND DISCUSSION OF DATA

São Paulo Metro provided all the information required for the development of this research through its various departments. The Design and Engineering department provided data of geological and geotechnical parameters, the TBM data operation by the construction and supervision department and the monitoring data through authorized access to the SACI software package (Instrumentation System for Interactive Monitoring and Control).

In the following, a proposed approach for the treatment of the data will be introduced.

5.1.1 GEOLOGICAL AND GEOTECHNICAL DATA - CHOICE OF PARAMETERS

To characterize the geotechnical parameters of the materials involved in this research, the study and analysis of the geological and geotechnical information, provided by São Paulo Metro, was performed. In this manner, by taking into account the series of in-situ test, laboratory test and reference material previously detailed in section 4.1.1, is presented the different geological units involved in the excavation of the Tunnel Metro Line. Table 5.1 shows a summary of the main units found during the geological surveys made for the design and construction of this Line.

As a manner of visualization, Figure 5.1 shows the geological profile between Hospital São Paulo and Santa Cruz stations indicating, majorly, the geological units mentioned in Table 5.1.

It is highlighted that the terminology used for the geological and geotechnical soil characterization of the metropolitan city of São Paulo is based on the standardized system developed by Metro São Paulo, from the establishment of the basic design of Metro Line 4 – Yellow (Monteiro et al., 2013).

5.1.1.1 *Description of in-situ tests*

Considering the large number of in-situ tests collected and provided by São Paulo Metro to this research, firstly, the flat dilatometer test (DMT) is discussed. The DMT allows to obtain for every measure made, and relatively quickly, values of the main geotechnical parameters. This is because of the correlation derived from the dilatometer indices measured during the test: Material Index – I_D, Horizontal Stress Index – K_D and the Dilatometer Modulus – E_D (Schnaid, 2009).
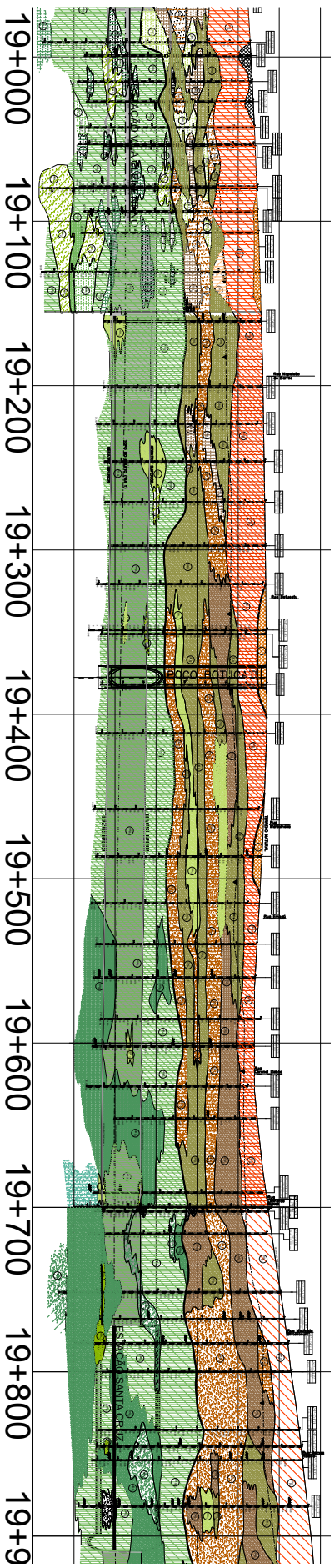
GEOLOGICAL PROFILE:

① TECNOGENIC DEPOSITS

EARTHFILL WITH VARIOUS MATERIALS AND WITH THE PREDOMINANCE OF SILTY CLAY WITH SAND

③ SÃO PAULO FORMATION (TERCIARY)

.CLAY LAYERS

(3Ag₀) SILTY CLAY WITH SAND, SOFT CONSISTENCY TO MEDIUM

(3Ag₁) SILTY CLAY WITH SAND, MEDIUM CONSISTENCY TO HARD

(3Ag₁) SANDY CLAY

(3Ag₂) SANDY CLAY WITH SILT

.SAND LAYERS

(3Ar₁) FINE TO MEDIUM CLAYEY SAND

(3Ar₂) MEDIUM SAND WITH BOULDERS

④ RESENDE FORMATION (TERCIARY)

.CLAY LAYERS

(4Ag₁) SILTY CLAY, WITH FINE TO MEDIUM SAND

(4Ag₂) SANDY CLAY, FINE TO MEDIUM SAND

.SAND LAYERS

(4Ar₁) FINE TO MEDIUM CLAYEY SAND

(4Ar₂) MEDIUM TO COARSE SAND

Figure 5.1 – Geological profile between Hospital São Paulo and Santa Cruz stations.

90

Table 5.1 – Summary of principal geologic units identified along the tunnel.

Unit	Geologic Classification	Description
1	Tecnogenic Deposits	Earthfill with various materials and with the predominance of Sandy silty Clay, some boulders and organic matter.
$3Agp_1$	São Paulo Formation (Terciary)	Sandy silty Clay, porous. soft consistency to medium, red and yellow.
$3Ag_1$		Sandy silty Clay, stiff consistency to hard, variegated (yellow, gray and red).
$3Ag_2$		Silty sandy Clay, medium consistency to hard, variegated (yellow, gray and red).
$3Ar_1$		Fine to medium clayey Sand, moderately compact to compact, yellow and red.
$3Ar_2$		Medium sand with boulders, moderately compact to compact, red.
$4Ag_1$	Resende Formation (Terciary)	Sandy silty Clay (fine to medium sand), moderately plastic to plastic, stiff consistency to hard, greenish gray.
$4Ag_2$		Sandy Clay (fine to medium sand), slightly micaceus, little plastic to moderately. stiff consistency to hard, gray.
$4Ag_3$		Silty sandy Clay with boulders, moderately plastic to plastic, stiff consistency to hard, brown gray.
$4Ar_1$		Fine to medium clayey Sand, little silty and little plastic, little compact to compact, gray to yellow.
$4Ar_2$		Medium to coarse Sand, little silty, medium to very compact, yellow gray.

Among the geotechnical parameters, derived from the correlations with the dilatometer indices, can be mentioned:

– Overconsolidation ration, OCR;

– Coefficient of lateral earth pressure at rest, k_0;

– Undrained shear strength, C_u;

– Effective friction angle, φ'; and

– Young modulus, E.

Monnet (2015) presented the corralation of geotechnical parameters with dilatometer indices, previously mentioned, as:

$$OCR = (0.5K_D)^{1.56} \qquad for \ I_D < 1.2$$
$$OCR = (0.67K_D)^{1.91} \qquad for \ 1.2 < I_D < 2.0$$
$$OCR = (mK_D) \qquad for \ I_D > 2.0$$

where:
$m = 0.5 + 0.17P$
$n = 1.56 + 0.35P$
$P = \frac{I_D - 1.2}{0.8}$

$$k_0 = \left(\frac{K_D}{1.5}\right)^{0.47} - 0.6$$

$$C_u = 0.22\sigma'_{v0}(0.5K_D)^{1.25}$$

$$\varphi' = 28° + 14.6\log(K_D) - 1.21[\log(K_D)]^2$$

$$E = 0.8R_m E_D$$

where:

$R_m = 0.14 + 2.13\log(K_D)$	$for\ I_D \leq 0.6$
$R_m = R_{m0} + (2.5 - R_{m0})\log(K_D)$	$for\ 0.6 < I_D < 3.0$
$R_m = 0.5 + 2\log(K_D)$	$for\ 3.0 \leq I_D < 10.0$
$R_m = 0.32 + 2.18\log(K_D)$	$for\ I_D \geq 10.0$

Figures 5.2 to 5.5 shown the depth values of geotechnical parameters obtained through correlation with DMT index parameters, previously indicated, for the investigation surveys SP-55534, SP-55597, SP-55754, and SP-55784, respectively.

Figure 5.2 refers to investigation surveys made in correspondence with the future Ventilation and Emergency Exit Shaft Conde de Itu, part of the Line 5 Extension. The test was carried out until a depth of 29 m. Along this test, the instrument passed, predominantly, through the $3Agp_1$ and $3Ar_2$ units. Units $3Ag_1$, $3Ag_2$ and $3Ar_1$, which codes are described in Table 5.1, were also identified along the test. By observing the results, it can be concluded the values of OCR and k_0 parameters are very high, especially the OCR, at the surface and with the increasing of depth the parameters kept constant with values of 2.0 and 0.6, respectively.

Regarding the Undrained Shear Strength Resistance (C_u), it can be said that for the $3Agp_1$ unit the parameter has high values at the surface and with increasing of depth the parameter kept constant around 15 kPa, for the other clay units, specially $3Ag_1$, the shear resistance varies from 20 – 90 kPa. Meanwhile, the friction angle (φ') shows values between 25° and 35°. Finally, the Young modulus (E) shows a tendency to increase with depth, especially after 25 m, the values vary between 30 – 70 MPa.

Figure 5.3 refers to investigation surveys made in correspondence with the future Metro Station of Borga Gato, part of the Line 5 Extension. The test was carry until a depth of 18 m. Along this depth was established that the instrument passed, predominantly, through the sand and clay soils of São Paulo Formation ($3Agp_1$, $3Ag_1$, and $3Ar_1$) and the clay soils of Resende Formation ($4Ag_1$ and $4Ag_2$). It can be observed that in the first 6 m of depth, the parameters OCR, C_u and E show constant values of 1.2, 11.5 kPa and 8 MPa, respectively. After 6 m, the parameters are shown scattered variation with no tendency. For the k_0 and φ', it is observed that until 11 m of depth these parameters showed a relatively constant value of 0.8 and 35°, respectively. After 11 m, occurs an increase of the value on both parameters to 1.8 and 40°, respectively.

Finally, Figure 5.3 and Figure 5.4 refer to investigation surveys made in correspondence with the future Metro Station of Moema and AACD-Servidor Parking Train station, respectively, both
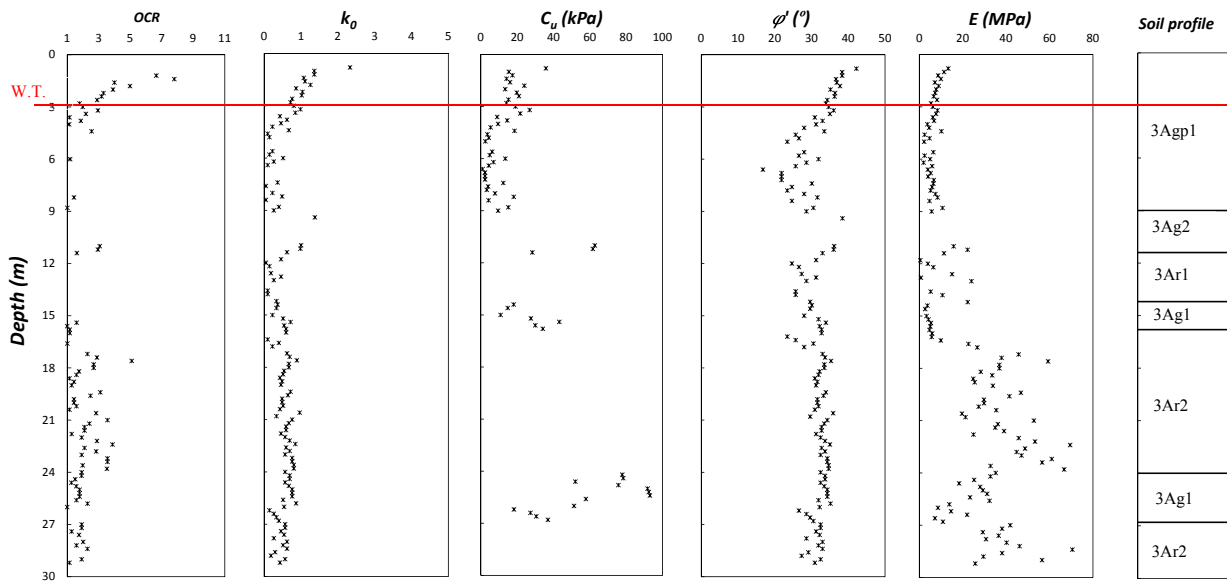
Figure 5.2 – Geotechnical Parameters, defined through dilatometric indices correlation, from investigation survey SP-55534, from 0 to 30 m, for construction of Conde de Itu Shaft, part of Line 5 Extension.
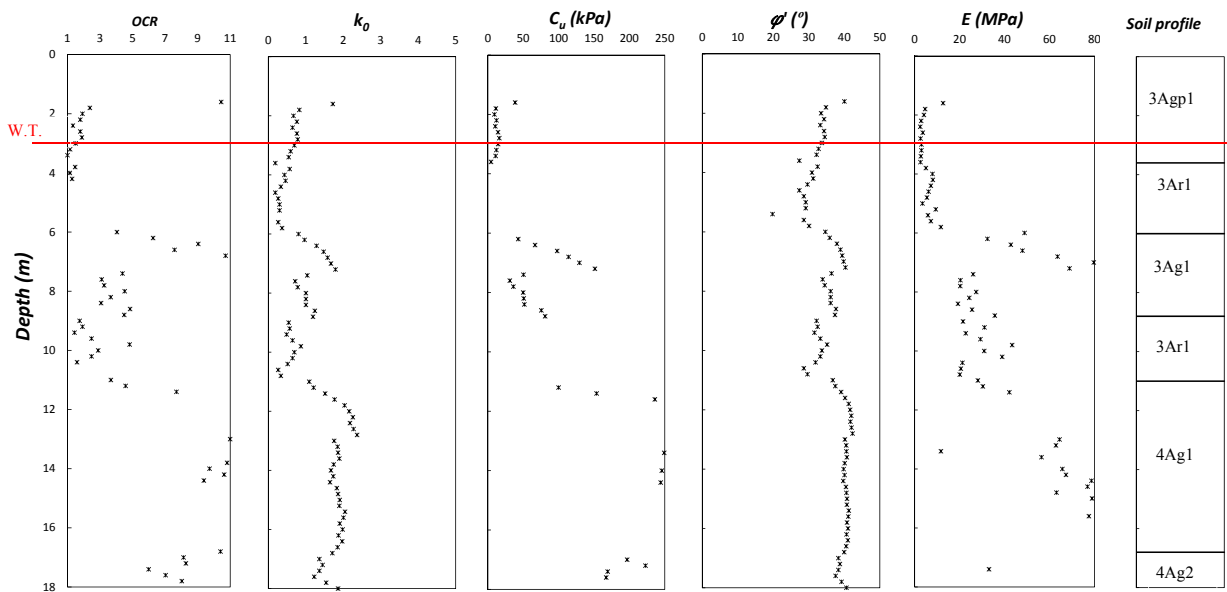
Figure 5.3 – Geotechnical Parameters. defined through dilatometric indices correlation, from investigation survey SP-55597, from 0 to 18 m, for construction of Borba Gato station, part of Line 5 Extension.

also part of the Line 5 Extension. The depth of the test carried out in each location was 12 m and 16 m, respectively.

While in Moema station were identified, predominantly, $3Ag_1$, $3Ar_1$ and $3Ar_2$ units, in AACD-Servidor station were identified units from all type of geologic conditions: unit 1 from Tecnogenic Deposits, units $3Ag_1$ and $3Ar_1$ from São Paulo Formation and unit $4Ar_1$ from Resende Formation.

From the geotechnical point of view, in both figures, it is possible to see that the parameters OCR, C_u and E show a wide dispersion on the values not making possible a correlation of their respective parameters with depth.
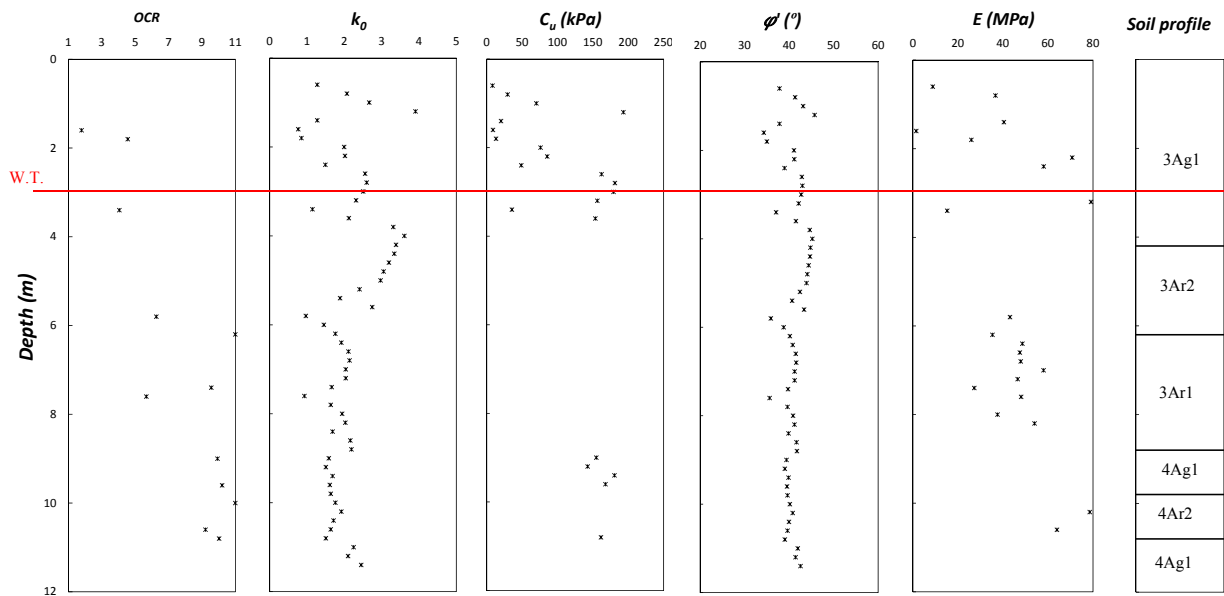
Figure 5.4 – Geotechnical Parameters. defined through dilatometric indices correlation, from investigation survey SP-55754, from 0 to 12 m, for construction of Moema station. part of Line 5 Extension.
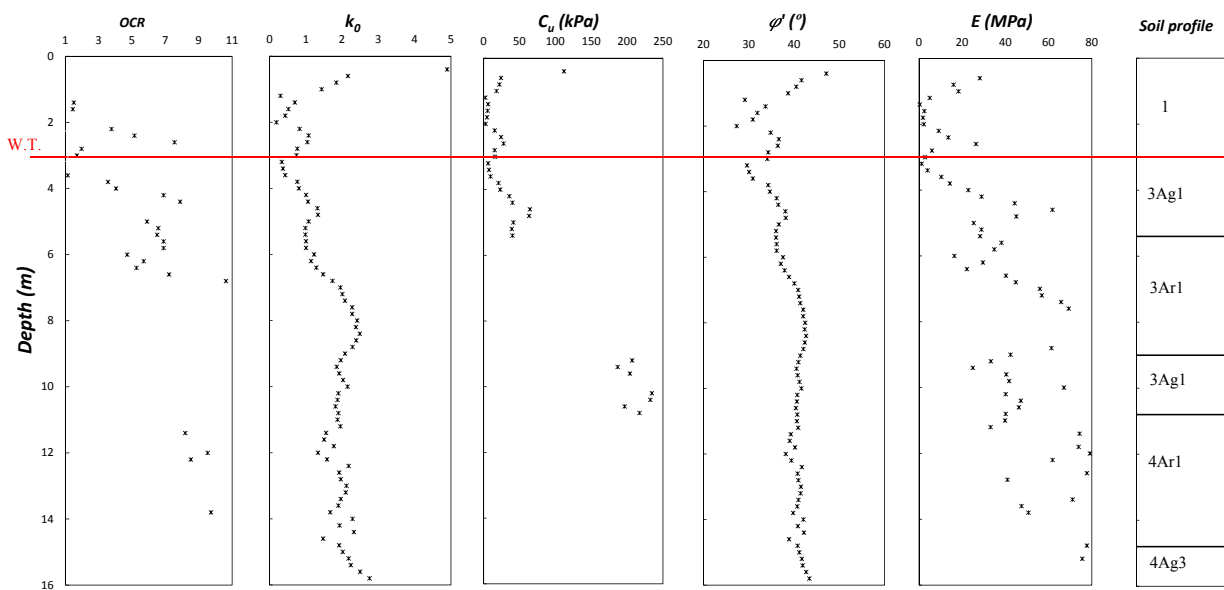
Figure 5.5 – Geotechnical Parameters, defined through dilatometric indices correlation, from investigation survey SP-55784, from 0 to 16 m, for construction of AACD-Servidor Parking Train station, part of Line 5 Extension.

On the other hand, the parameters k_0 and φ', in both figures, shown a visible range of values with depth independently of the geologic unit. For example, in Moema station, the parameters k_0 and φ' vary between 1.5 – 2.2 and 35º – 45º, respectively. While for AACD-Servidor station, the parameters k_0 and φ' vary between 1.3 – 2.7 and 36º – 43º, respectively.

In general, the geotechnical parameters herein presented through the use of correlation with the dilatometer indices don't show a strong agreement with literature (ABMS, 2013).

Regarding the Pressuremeter Test (PMT). Figure 5.6 shows the results of in-situ pressumeter test (PMT) performed in correspondence with the future AACD-Servidor Parking Train station.

The depth of the borehore was carried out until 30 m and the tests were made at 4, 10, 12, 14, 16, 18, 20, 22, 26, 28 and 30 m. During borehole were identified some soils from all the geologic conditions: unit 1 from Tecnogenic Deposits; units $2Ag_1$ and $2Ar_1$, $3Agp_1$, $3Ag_1$ and $3Ar_2$ from São Paulo Formation and unit $4Ag_1$ from Resende Formation.
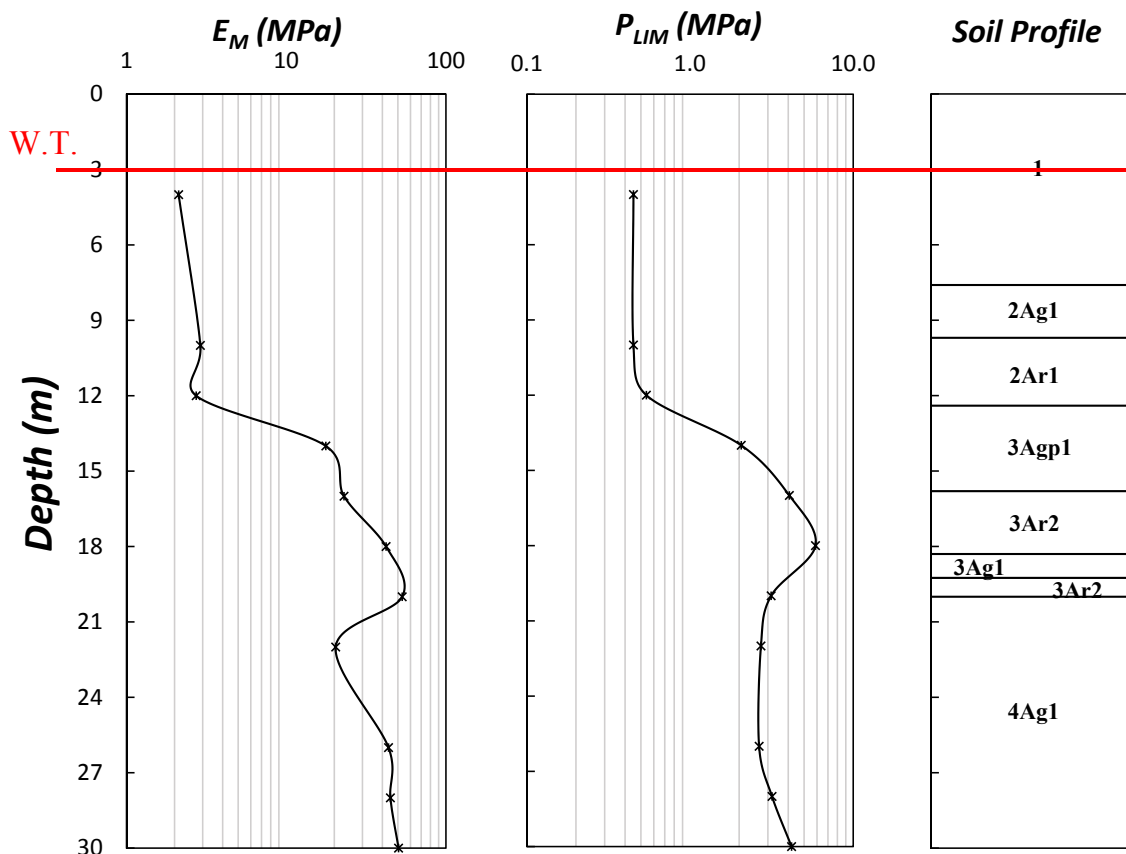
Figure 5.6 – Pressuremeter test results. from investigation survey SP-55774, from 0 to 30 m, for construction of AACD-Servidor Parking Train station, part of Line 5 Extension.

In the PMT test, the parameters: Soil Shear Deformation Modulus (E_M) and Pressure Limit (P_{LIM}), which is linked to the resistance of soil shearing, are obtained through the application of equal increments of pressure at equal intervals of time. Each pressure increment is maintained for 60 secs with readings of volume change measured at 15, 30 and 60 secs after pressure application. The test starts immediately after the probe is in place at the prescribed depth with the membrane expanded to reach full contact with the borehole wall (Schnaid, 2009).

In Figure 5.6, it is possible to see an increase tendency with depth of E_M and P_{LIM} parameters. A minimum value of the deformation modulus of 2.12 MPa was registered in correspondence of geological unit 1, and a maximum value of 53.20 MPa was registered in correspondence of geological unit $3Ar_2$. Concerning the pressure limit parameter, a minimum value of 0.45 MPa was registered in correspondence of geological unit 1, and a maximum value of 5.87 MPa was registered in correspondence of geological unit $3Ar_2$.

It is also possible to see that the test at 18 m depth follows different behavior respect to others where an increase of pressure the volume deformation has small variations. It is known that

the geological material related at this is clayey Sand (3Ar$_2$) while at other depth the geological material is predominantly composed by Clay: unit 1 at 4 m, unit 3Agp$_1$ at 14 m and 4Ag$_1$ unit at 22 and 30 m, respectively. Finally, it is possible to see that not unloading-reloading cycles were applied during these tests which made difficult to know the in-situ behavior of the materials from an elastoplastic point of view.

As a concluding remark, the flat dilatometer test (DMT), the scattered variation of the geotechnical parameters with depth which presumes three possible factors in getting meaningful values from this test: *i*) Lack of personal experience in making the test, *ii*) In-situ difficulties condition for making the test and *iii*) Reliability of registered values (measurement errors). Regarding the pressuremeter test (PMT), even if the pressuremeter modulus doesn't reflect true elastic strains of soils as Young modulus does, it helps to provide specific knowledge of the elastoplastic soil behavior.

5.1.1.2 *Description of laboratory tests*

For the characterization of geotechnical parameters, the São Paulo metro performed for the construction of their Lines, laboratory tests, mostly, the Consolidated Undrained Triaxial Compression Tests (CU). As a manner of illustration, Figure 5.7 and 5.8 shown the results of a CU test applied to a soil sample collected in correspondence with the future Ventilation and Emergency Exit Shat São Sebastião, which is part of the new extension Line 5.
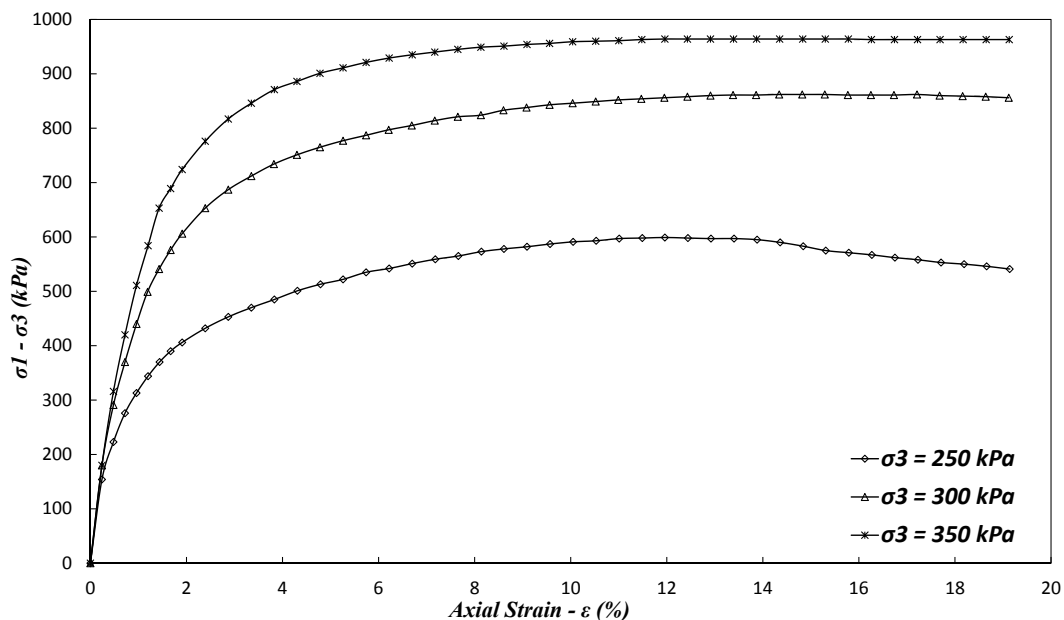
Figure 5.7 – Consolidate Undrained Triaxial Compression Tests (CU) at different confine pressures: 250, 300 and 350 kPa, respectively. Soil sample São Sebastião Shaft, part of Line 5 Extension.

The soil samples were collected between 15.0 – 16.7 m deep. At this depth, the geologic material is formed by fine to medium clayey Sand (3Ar$_1$) unit. The confine pressures applied for the test were at 250, 300 and 350 kPa, respectively. From Figure 5.7, it is possible to see the development of os stress-strain behavior for the different confine pressures. The values of

tangent Young modulus obtained for the different stages were 75.1 MPa, 89.2 MPa, and 100.3 MPa, respectively. This indicates a progressive increase of the Young modulus with the rise of the confining pressure applied to the soil sample.

Figure 5.8 shows in the p'-q plane the failure point tensions. By designing a tendency line (K_f line), the c and φ' parameters are determined. In this plane, every point represents the value of stress in which the soil failed at the different confine pressures. For this specific case, the soil samples, characterized as $3Ar_1$ unit, it was determined a cohesion of 0 kPa and a friction angle of 15°.
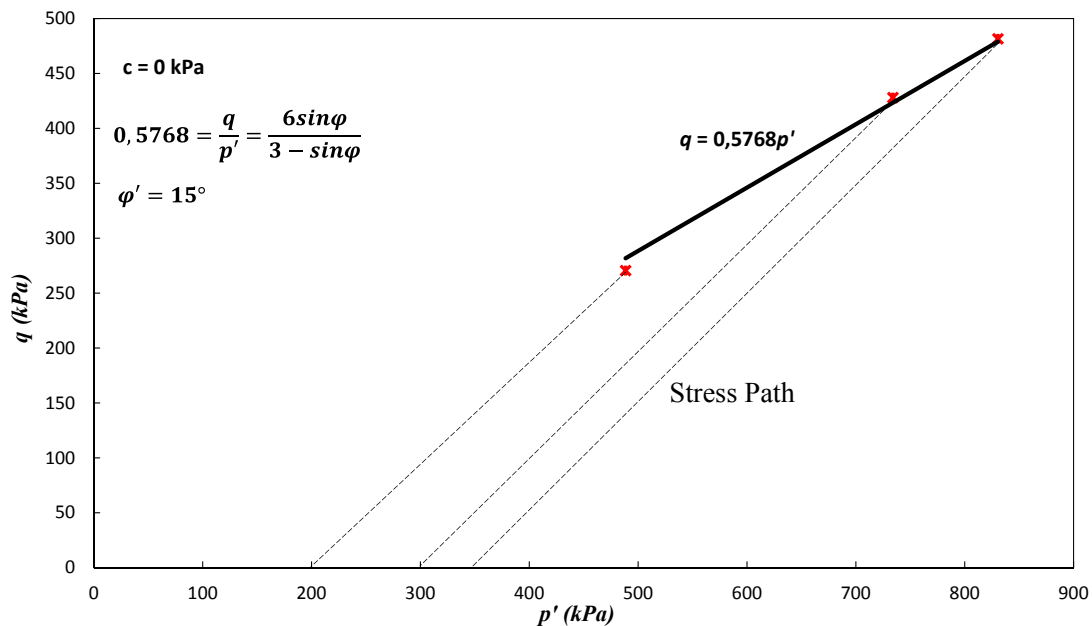
Figure 5.8 – p'-q plane representation of the soil samples previously tested under CU condition.

Most of the laboratory test performed and provided by Metro São Paulo for their infrastructure and the use in the present research were based on the use of the Consolidated Undrained Triaxial Compression Tests (CU), which mean that so few geotechnical parameters can be obtained from this test. As an example of previously mentioned, that can be seen from Figure 5.8 is that not unloading/reloading condition was performed, and this is observed in the other data. Regarding tunnel construction not further comprehensive laboratory test was conceived to represent a more realistic behavior of soils like the use of the elastoplastic model to implement in numerical analysis.

5.1.1.3 *Preliminary representation of geotechnical parameters variability*

As previously mentioned in the introduction and subsequently in the following chapters, the construction of tunnels induces ground movements that predominantly depends on the mechanical properties of the excavated soil. Remembering that soil properties are subject to uncertainties, it turns necessary an appropriate description of these uncertainties and evaluation for generating ground movements that are of substantial interest for shallow tunnel projects.

Table 5.2 – Values of range of geotechnical parameters adopted.

Geotechnical Parameters		1	3Ag$_{p1}$	3Ar$_1$	3Ar$_2$	3Ag$_1$	3Ag$_2$	4Ar$_1$	4Ar$_2$	4Ag$_1$	4Ag$_2$	4Ag$_3$
γ	kN/m³	16-18	13.3-18.0	19-20	19-20	17-20	17-20	18.7-20.6	18.7-20.6	18.8-21.6	18.8-21.6	18.8-21.6
c'	kPa	5.0-10.0	8.0-30.0	3.0-10.0	1.0-10.0	15-100	25-100	3.0-5.0	2.0-3.0	15-150	40-100	>25
φ'	°	20-25	20-28	30-40	30-35	21-27	21-27	30-35	30-40	20-27	20-24	27
E	MPa	4-32	10-35	15-265	10-250	15-200	30-175	25-300	25-350	15-300	40-135	180-360
C_v	cm²/s	-	5.00E-02	-	-	5.00E-02	5.00E-02	-	-	5.00E-03	5.00E-03	5.00E-03
C_u	kPa	-	30-70	-	-	80-250	80-250	-	-	100-400	100-400	150-500
e_0	-	-	1.0-1.8	0.70-0.95	0.8-0.9	0.5-1.2	0.5-1.2	0.85	0.85	0.5-1.4	0.5-1.4	0.5-1.2
$C_c/(1+e_0)$	-	0.07	0.16-0.25	0.05-0.18	0.05-0.18	0.08-0.22	0.08-0.22	0.05-0.18	0.05-0.18	0.10-0.20	0.10-0.20	0.10-0.20
$C_r/(1+e_0)$	-	-	0.016-0.025	0.005-0.018	0.005-0.018	0.008-0.022	0.008-0.022	0.005-0.018	0.005-0.018	0.01-0.02	0.01-0.02	0.01-0.02
OCR	-	-	1.1-2.0	1.5-3.0	1.5-3.0	2.5-3.0	2.5-3.0	1.7-3.3	1.7-3.3	1.7-3.3	1.7-3.3	>4
k_0	-	0.83	0.55-0.73	0.35-0.87	0.43-0.87	0.66-1.00	0.66-1.00	0.66-1.00	0.43-0.80	0.36-0.80	0.7-2.6	0.7-2.6
k	cm/s	1.00E-04	5.00E-04	5E-4 - 1E-2	5E-4 - 1E-2	5E-4 - 1E-3	5.00E-04	1E-4 - 9E-3	1E-4 - 9E-3	1.00E-06	1.00E-06	1.00E-06

Therefore, following the considerations of Phoon & Kulhawy (1999a) about inherent soil variability, the uncertainty of geotechnical parameters are presented as random variables under the form of Coefficient of Variation (CoV). In this regard, Mollon et al. (2013) and later Miro et al. (2015) presented a comprehensive study and methodology for evaluating the influences of soil parameter uncertainties on surface settlements induced by the tunneling process, by using a 3D finite element simulation and a probabilistic method called the Response Surface Method.

Hence, with the scope to have a significant quantity of information, the use of the past geological and geotechnical technical reports provided by São Paulo Metro helped also as reference material for the construction of a database of geotechnical parameters, aside from the results of in-situ and laboratory test. In Table 5.2 is presented the range of values of geotechnical parameters for the different geological units involved in this study.

In this regard, the input geotechnical parameters here presented are considered as random variables while the other input variable, necessary for the numerical simulation, are considered as deterministic. As part of probabilistic analysis, three probabilistic scenarios, optimistic, neutral and pessimistic, are proposed in this study as a first attempt to estimate the better assumption for soil parameters applied to tunneling. These considerations were taken due to accuracy unknown of the chosen input random variables.

According to Mollon et al. (2013), the scenarios are indicators of the so-called epistemic error (related to lack of knowledge), rather than the natural variability of the soil; it should be emphasized that the scenarios are closely linked not only to the quantity but also to the quality of the soil investigation.

In Table 5.3 the mean values, coefficients of variation, and the ranges of uncertainty parameters are shown for the adopted scenarios. The values of CoV for these parameters were chosen according to the results proposed by Uzielli et al. (2007), for the three scenarios.

Table 5.3 – Mean and CoV values of input geotechnical parameters.

Geotechnical Parameters		μ				CoV (%)		
		$3Agp_1$	$3Ag_{1,2}$	$3Ar_{1,2}$	$4Ag_1$	Optimistic	Neutral	Pessimistic
γ	kN/m^3	16.6	18.5	19.5	20.2	2	5	8
c'	kPa	18	40	7	80	20	40	60
ϕ'	°	24	24	32	26	5	10	15
E	MPa	20	120	185	230	10	20	30
ν	-	0.26	0.30	0.31	0.28	10	15	20
k_0	-	0.67	0.93	0.82	0.90	40	55	70

5.1.2 MONITORING DATA - VOLUME LOSS ESTIMATION

In the following, it is presented and discussed some of the monitoring data registered by the instrumentation which were installed along the tunnel path. As stated in section 3, from all monitoring instruments implemented for the following of the tunnel excavation, only the leveling points were analyzed as they provide information about the surface settlement. In this regard, the transverse cross-section settlement trough is studied to estimate the volume loss due to tunneling.

From all monitoring sections installed along the tunnel section, 103 sections provided significant information for the construction of the transverse settlement curve. Among the empirical approaches presented in Table 2.4, it was verified that the Gaussian curve adjusted better to the settlement measures of all the 103 monitoring sections.

The maximum value of settlement registered was of 26.40 mm in correspondence of the section SC_21+103 between Chácara Klabin station and Dionísio da Costa Shaft. The point of inflection estimated, by applying regression analysis of the Gaussian curve was 5.57 m. Finally, the maximum value of Volume Loss determined was of 0.67 % in correspondence with Section SC_17+660 between the future Moema station and AACD_Servidor station and the point of inflection estimated for this section was of 17.30 m.

Figure 5.9 shows the estimation of the settlement through the use of the transverse Gaussian curve for the sections with the maximum settlement (SC_21+103) and with the maximum volume loss (SC_17+660).
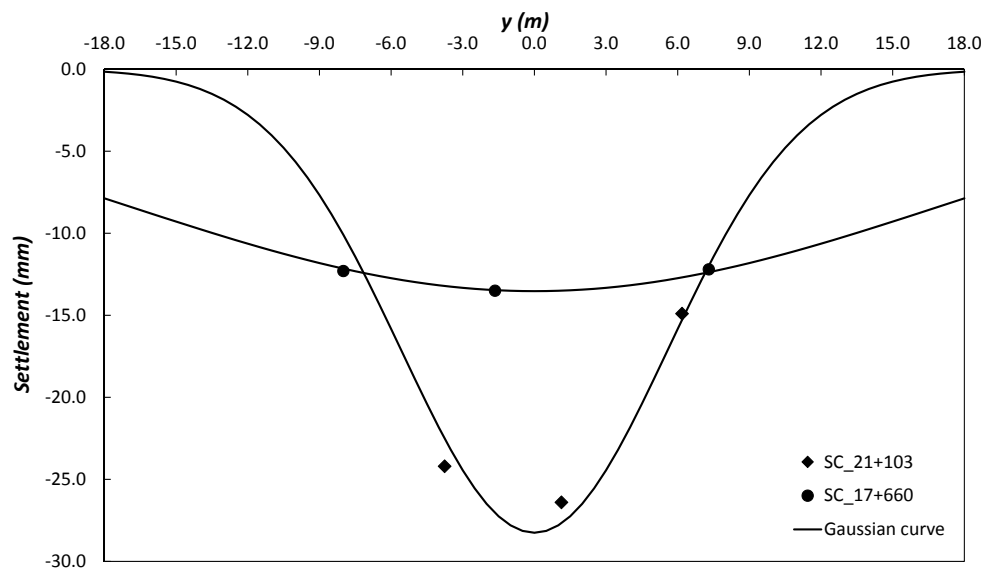
Figure 5.9 – Transverse Gaussian curves for monitoring sections SC_21+103 and SC_17+660.

Table 7.4, on the other hand, shows a statistical approach applied to the 92 monitoring sections that provided information on settlement trough. The total length of the Tunnel Line (5.74 km) was split into 7 zones to homogenize ground behavior. These zones are delimitated as follow (see Figure 4.2):

1 BAN – EUC: Bandeirante ventilation and emergency exit shaft – Eucalipto station (483 m length);

2 EUC – MOE: Eucalipto Ssation – Moema station (840 m length);

3 MOE – SER: Moema station – AACD-Servidor station (1174 m length);

4 SER – HSP: AACD-Servidor station – Hospital São Paulo station (518 m length);

5 HSP – SCR: Hospital São Paulo station – Santa Cruz station (665 m length);

6 SCR – CKB: Santa Cruz station – Chacára Klabin station (880 m length); and

7 CKB – DDC: Chácara Klabin station – Dionísio da Costa ventilation and emergency exit Shaft (362 m length).

Table 5.4 – Summary of estimation of Gaussian curve parameters.

Zone	Tot. Monit. Sections	Sections with Ground Loss	S_{max} (mm)			i (m)			V_{loss} (%)		
			μ	σ	CoV (%)	μ	σ	CoV (%)	μ	σ	CoV (%)
BAN - EUC	19	4	5.33	1.873	35	11.64	5.699	49	0.16	0.065	40
EUC - MOE	42	16	2.40	1.219	51	10.35	4.984	48	0.07	0.051	74
MOE - SER	39	24	3.00	2.654	88	6.83	2.975	44	0.06	0.048	86
SER - HSP	20	12	2.01	1.057	53	6.30	2.195	35	0.04	0.031	78
HSP - SCR	**31**	**19**	**2.69**	**1.246**	**46**	**8.20**	**3.575**	**44**	**0.07**	**0.043**	**64**
SCR - CKB	16	10	3.90	4.226	108	6.73	3.307	49	0.07	0.068	100
CKB - DDC	9	7	5.55	9.293	168	7.03	3.15	45	0.1	0.145	149

As it is possible to see from Table 5.4, the minimum value of Coefficient of Variation (CoV) for the maximum settlement (S_{max}) as well as for the Volume Loss (V_{loss}) parameters were obtained in the first zone (BAN – EUC). However, due to the low quantity of available samples (5) on this zone, a conclusion on the behavior of the settlement trough, from a statistical point of view, is negligible.

By considering the number of sections that provide information of ground loss in comparison with the total number of sections installed for their respective zone, the fifth zone (HSP – SCR) provided a better result in terms of CoV, which could be interpreted as better homogenized behavior of the ground in comparison to the other zones.

5.1.3 TBM DATA - SELECTION OF MAIN PARAMETERS

Data of TBM excavation parameters, all along the tunnel length, was provided by the personnel of the department of construction supervision of São Paulo Metro. For the excavation of the tunnel Line, a total of 3285 concrete segment rings were used which mean that the TBM computer system recorded, for every ring, 335 machine parameters.

Due to the necessity to perform ground treatment works in areas near stations and shafts, to avoid instability of these structures due to TBM operation, no reliable information was obtained from the TBM recording system in those areas, and so, from this total quantity of rings, a number of 2977 rings were analyzed which represents the ordinary conditions of TBM advance.

Briefly remembering of what was mentioned in section 4.1.3, the total numbers of sensors installed in the TBM for controlling of tunneling performance is 335. All these quantities of sensors allow the operator to know the condition of the machine in terms of guidance, excavation process, grout injection, ground conditioning, hydraulic and lubrication of mechanical parts as well as health and safety warnings.

So, in this regard, from this total amount, only 11 sensors, seven from EPB face pressure and four from Grout Injection Pressure were considered for analysis in this research. These parameters directly influence groundmass reaction due to the active ground support pressure by them applied (Guglielmetti et al., 2008; Maidl et al., 2012; Mollon et al., 2013).

Other TBM parameters like TBM Thrust Force, Cutterhead Torque, Cutterhead Penetration Rate, and TBM Advance Velocity are not considered here. However, these parameters may induce some effect in the groundmass reaction, but these are more related to TBM performance. To clarify what was said previously, as long as soil type is constant, the torque used to cut through the ground will be higher if the ground is stiffer. The Thrust Force used to move forward the machine, help also to balance the earth pressure surrounding the tunnel.

With applied earth pressure and torque at constant and manageable levels, the increasing thrust will generally increase Penetration Rates. If the operator maintains the same level of applied earth pressure and thrust and the TBM enters a much stiffer material, the torque will increase. Excessively high levels of torque for long periods will place strain on the motors and also result in increased wear and tear on the cutter head and cutter tools (O'Carroll, 2005).

Figures 5.10 and 5.11 shown the results of the application of best-fitted probability density function (PDF) for the TBM Earth and Grout Injection Pressures applied for excavation of the all tunnel line. For these analyses were utilized the Normal, Lognormal, Gamma and Weibull Probability Density Function, which according to Baecher & Christian (2005) are the most implemented in the geotechnical engineering field.

Regarding the Grout Injection, it is necessary to highlight that no data was registered in sensors P3 and P4 since contractor manifested that it was not required to use these injections line for the tunnel line construction.

These figures showed, first of all, the values of pressure applied during tunneling and registered by the respective sensors. The Earth and Grout Pressure were represented in the form of histograms. After that, the four PDFs are used to estimate the best-fitted distribution function for the data. As it is possible to see from these figures, the order of best-fitted function is from high to low as indicated in the respective legend for every sensor pressure.

Another consideration to make is that due to the variability of registered pressure a unique PDF could not be attributed to these values. Though, the two most recurrent functions were the Normal and Gamma probability density functions. Table 7.5 shows a summary of the best-fitted PDF for every pressure sensor of the TBM registered during tunneling along the tunnel length. As can be seen, variation on the best-fitted PDF is observed for every pressure sensor. Also, from this table, significant values of coefficient of variation (CoV > 30%), so significant variability were obtained from the Grout Injection Pressure sensors respect to the Earth Pressure sensors (CoV < 20%).

Table 5.6 and 5.7 shown a detail estimation analysis of CoV for every TBM Earth Pressure and Grout Injection Pressure sensor during tunneling, at each tunnel zone. From the comparison of these tables, it is still noticed that significant values of CoV were estimated in the Grout sensors.
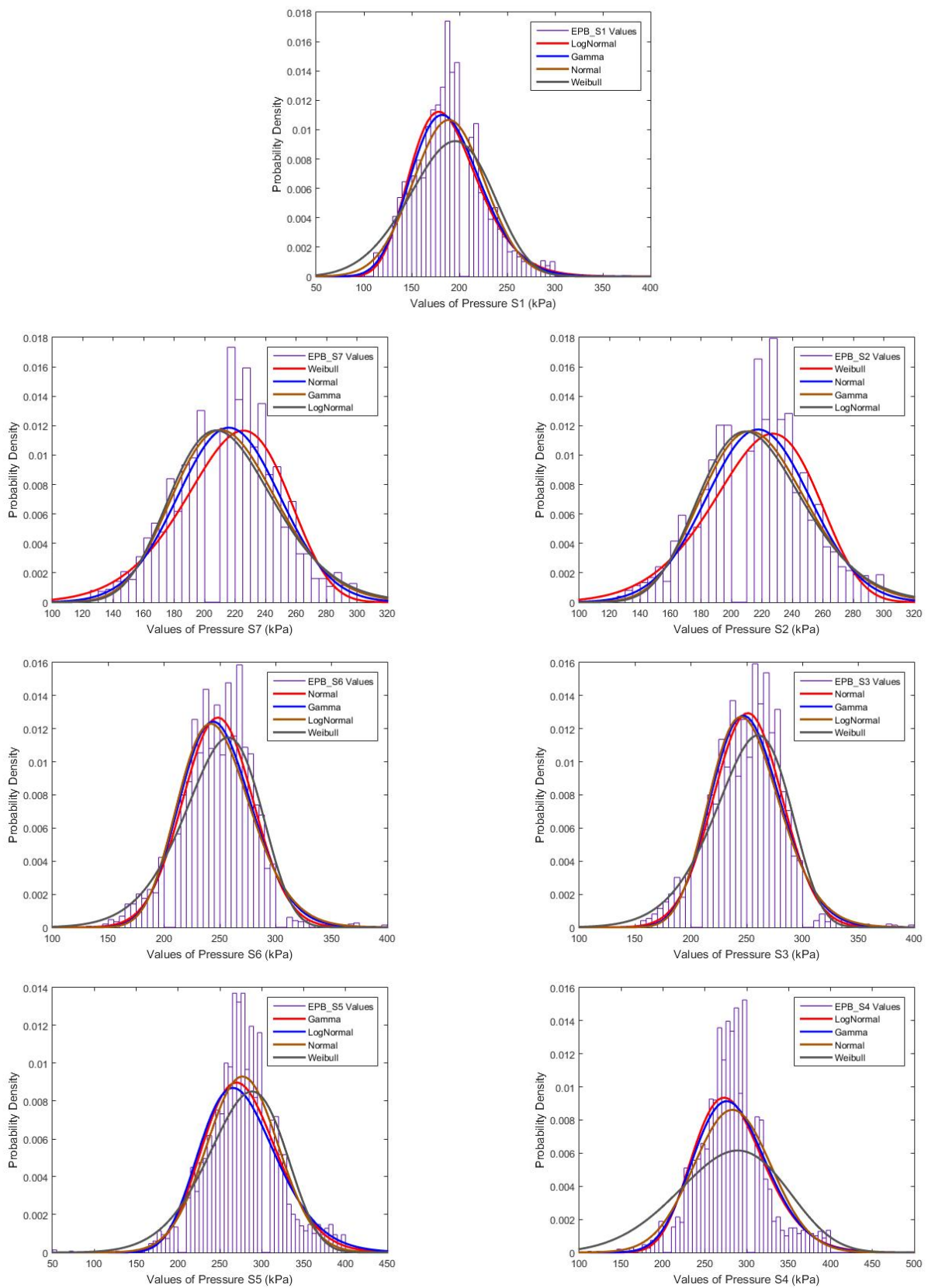
Figure 5.10 – Probability density function (PDF) of TBM Earth Pressure sensors along the all tunnel length (Positions according to Figure 4.2a).
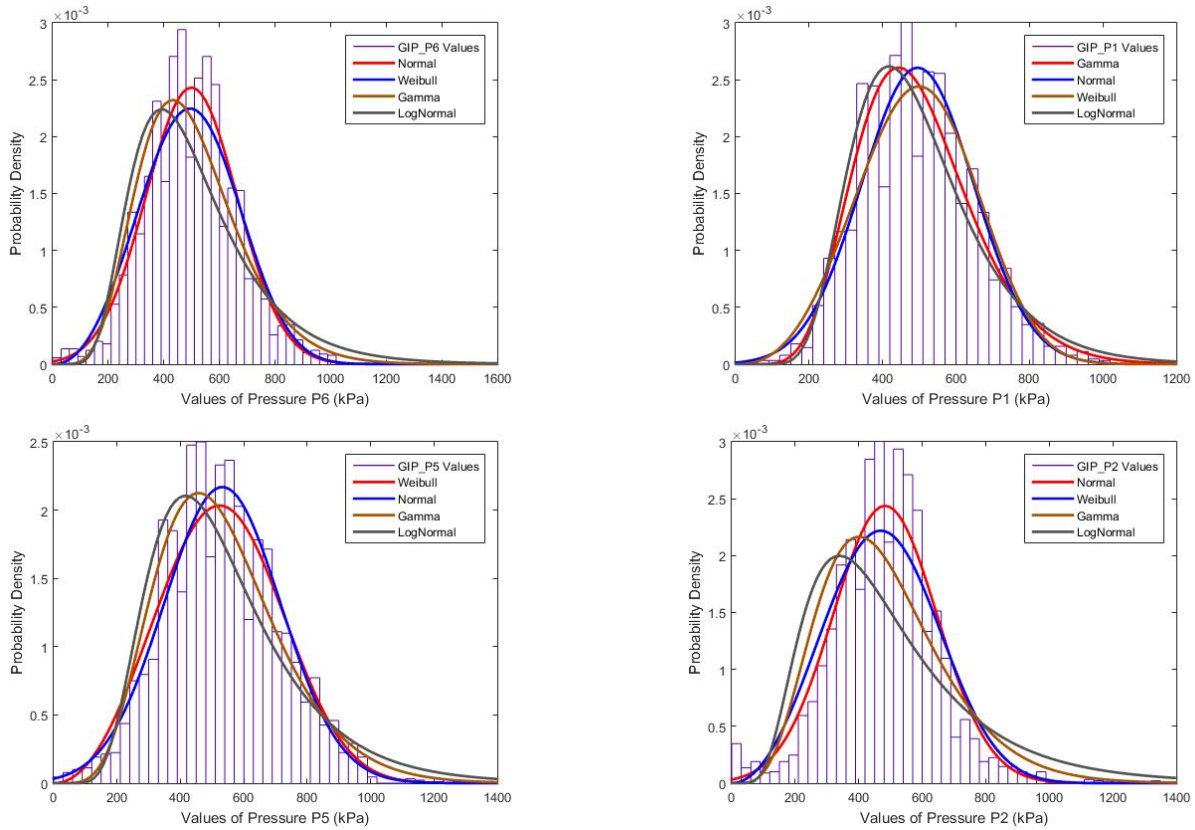
Figure 5.11 – Probability density function (PDF) of TBM Grout Injection Pressure sensors along the all tunnel length (Possitions according to Figure 4.2b).

Table 5.5 – Summary of best Fitted PDF for TBM Pressure Sensors along the all tunnel path.

TBM Sensors	PDF	Parameters Max. Likelihood	Mean (kPa)	Std Dev (kPa)	CoV (%)
EPB - S1	LogNormal	μ= 5.22225 σ= 0.195442	188	37.212	20
EPB - S2	Weibull	α= 7.15073 β= 231.885	217	35.771	16
EPB - S3	Normal	μ= 250.92 σ= 30.8159	251	30.816	12
EPB - S4	LogNormal	μ= 5.63268 σ= 0.154504	283	43.951	16
EPB - S5	Gamma	$a(Shape) = 38.0527$ $b(Scale) = 7.2786$	277	44.899	16
EPB - S6	Normal	μ= 248.152 σ= 31.4733	248	31.473	13
EPB - S7	Weibull	α= 7.22592 β= 230.101	216	35.172	16
GIP - P1	Gamma	$a(Shape) = 9.57866$ $b(Scale) = 0.517337$	496	1.6011	32
GIP - P2	Normal	μ= 482.855 σ= 163.655	483	163.655	34
GIP - P5	Weibull	α= 3.09583 β= 593.933	531	187.668	35
GIP - P6	Normal	μ= 499.344 σ= 164.12	499	164.12	32

Table 5.6 – Coefficient of variation (CoV) at every Earth Pressure sensor at each tunnel zone (Order according to Figure 4.2a).

Zone	EPB-S1 (kPa)		
	μ	σ	CoV (%)
BAN - EUC	184.88	17.91	10
EUC - MOE	192.05	23.63	12
MOE - SER	169.55	40.15	24
SER - HSP	180.01	26.73	15
HSP - SCR	182.18	17.86	10
SCR - CKB	203.31	37.56	19
CKB - DDC	172.15	19.16	11

Zone	EPB-S7 (kPa)			EPB-S2 (kPa)		
	μ	σ	CoV (%)	μ	σ	CoV (%)
BAN - EUC	214.84	20.41	10	214.76	20.36	9
EUC - MOE	220.09	21.75	10	215.76	22.27	10
MOE - SER	195.52	27.63	14	198.33	28.41	14
SER - HSP	206.87	29.82	14	211.25	30.5	14
HSP - SCR	202.68	19.76	10	205.69	20.04	10
SCR - CKB	225.48	37.45	17	227.81	37.78	17
CKB - DDC	195.01	18.77	10	197.8	19.15	10

Zone	EPB-S6 (kPa)			EPB-S3 (kPa)		
	μ	σ	CoV (%)	μ	σ	CoV (%)
BAN - EUC	255.29	22.17	9	256.58	21.43	8
EUC - MOE	255.91	21.12	8	257.62	21.64	8
MOE - SER	233.34	29.05	12	235.99	28.16	12
SER - HSP	245.39	34.84	14	248.4	33.93	14
HSP - SCR	234.58	22.97	10	237.2	21.26	9
SCR - CKB	251.48	41.94	17	256.02	40.28	16
CKB - DDC	232.07	20.51	9	233.66	28.2	12

Zone	EPB-S5 (kPa)			EPB-S4 (kPa)		
	μ	σ	CoV (%)	μ	σ	CoV (%)
BAN - EUC	238.56	40.3	17	299.83	76.11	25
EUC - MOE	290.1	26.78	9	292.63	22.53	8
MOE - SER	266.43	33.96	13	265.64	28.35	11
SER - HSP	275.87	45.02	16	281.01	36.67	13
HSP - SCR	270.28	21.12	8	270.5	25.06	9
SCR - CKB	273.95	42.85	16	267.58	35.55	13
CKB - DDC	267.45	25.95	10	265.04	51.06	19

Table 5.7 – Coefficient of variation (CoV) at every Grout Injection Pressure sensor at each tunnel zone (Order according to Figure 4.2b).

Zone	Grout-P6 (kPa)			Grout-P1 (kPa)		
	μ	σ	CoV (%)	μ	σ	CoV (%)
BAN - EUC	443.85	125.95	28.38	454.65	148.56	32.68
EUC - MOE	503.7	172.85	34.32	576.11	163.89	28.45
MOE - SER	559.05	180.47	32.28	532.59	150.7	28.29
SER - HSP	511.36	131.03	25.62	504.99	139.99	27.72
HSP - SCR	685.11	210.52	30.73	493.52	146.46	29.68
SCR - CKB	557.5	164.8	29.56	414.44	109.83	26.5
CKB - DDC	372.38	151.8	40.76	381.84	125.43	32.85

Zone	Grout-P5 (kPa)			Grout-P2 (kPa)		
	μ	σ	CoV (%)	μ	σ	CoV (%)
BAN - EUC	485.88	123.9	25.5	447.41	123.18	27.53
EUC - MOE	573.48	164.78	28.73	514.1	148.07	28.8
MOE - SER	482.88	139.87	28.97	505.93	123.26	24.36
SER - HSP	482.62	166.1	34.42	453.51	223.79	49.35
HSP - SCR	480.45	172	35.8	538.47	222.75	41.37
SCR - CKB	512.17	172.81	33.74	446.6	136.08	30.47
CKB - DDC	355.4	167.45	47.12	379.86	157.81	41.54

5.2 SENSITIVITY ANALYSIS OF SOIL PROPERTIES

This section introduces the application of a probabilistic and sensitivity analysis approach of input geotechnical parameters for the assessment of tunneling-induced ground movements. To accomplish this goal, 2D finite element (FE) numerical analysis will be implemented, which were carried out under the drained condition with the steady-state flow.

Therefore, according to the analysis presented in the previous section, the implementation of the proposed analysis will be made, specifically, in a zone of the tunnel path between Hospital São Paulo and Santa Cruz stations. The tunnel length in this stretch zone is characterized to be 670 m long. From the statistical analysis of the geological survey, a total of six layers were encountered to be assumed in the numerical model.

5.2.1 STATISTICAL ANALYSIS OF SOIL LAYER INTERFACES

Figure 5.1 shows the geological profile along this zone, from which it is possible to notice the spatial variability of the geological units. 29 drilling borehole geological survey campaigns, executed in this zone, allowed to identify and quantify, from top to bottom, the depth interface between soil layers. Consequently, through a statistical approach, values of soil layer depth, in terms of mean (μ) and standard deviation (σ), were estimated which allow to build the 2D numerical model to be used.

Furthermore, an evaluation of the influence of a soil layer thickness over the others was made

and is shown in Figure 5.12. The Pearson correlation analysis indicates low values of correlation between soil layers depth position. However, a moderate correlation between soil Layer 1 and soil Layer 2 ($r_{L1,L2}$) is observed, this result brouht to the conclusion that wouldn't be necessary to consider in the probabilistic analysis a correlation between soil layer thickness as input variables.

r_{L1L2}	0.65
r_{L1L3}	0.30
r_{L1L4}	0.28
r_{L1L5}	0.18
r_{L2L3}	0.13
r_{L2L4}	0.23
r_{L2L5}	-0.23
r_{L3L4}	0.39
r_{L3L5}	-0.09
r_{L4L5}	0.40
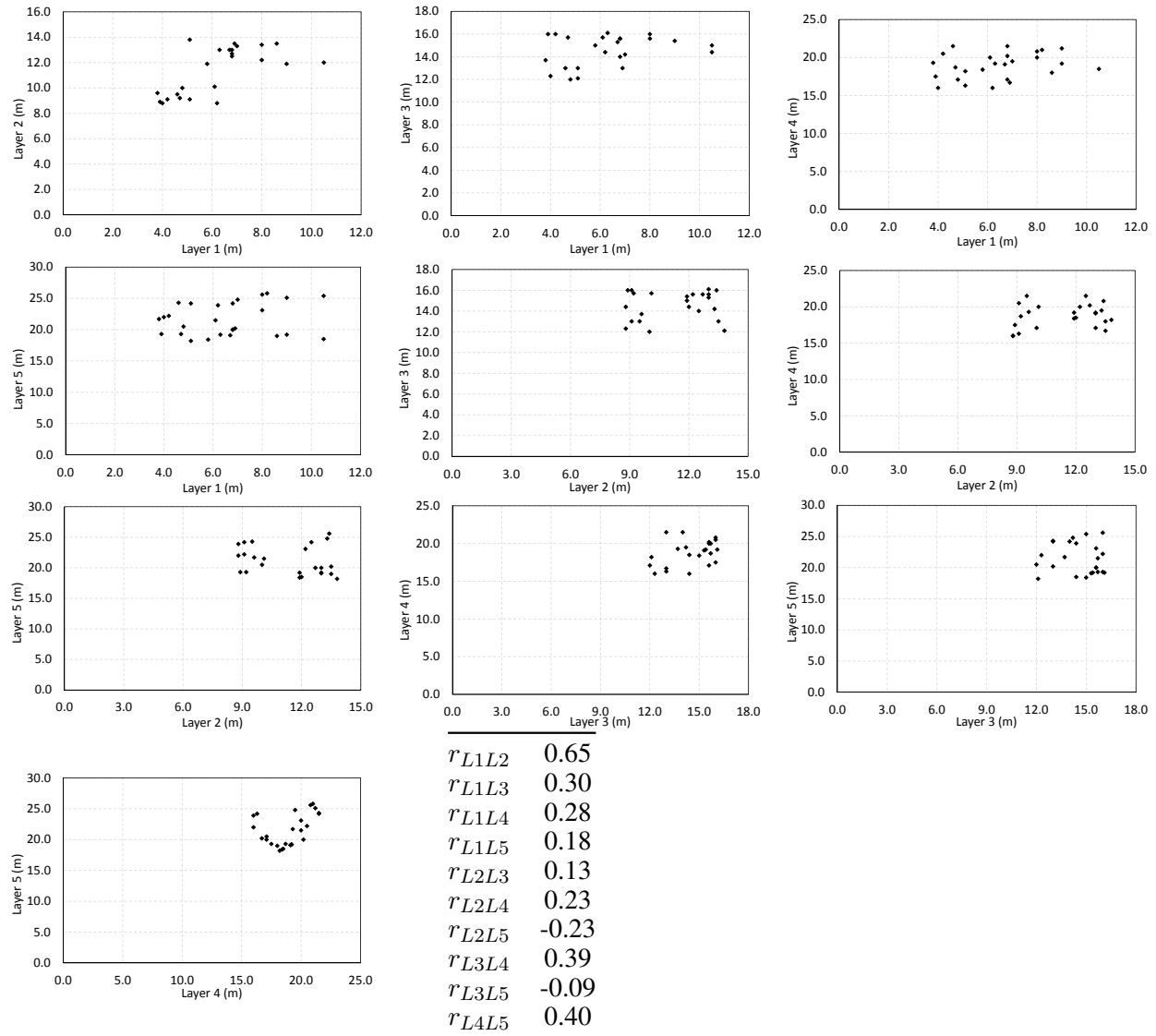
Figure 5.12 – Results of Pearson correlation analysis between soil layers depth position.

5.2.2 FE MODEL GEOMETRY SET UP

Following the previous analysis, for the numerical analysis, Figure 5.13 shows the geometrical representation of the 2D numerical model adopted for the FE analysis. Information about the number of soil layers (expressed in μ and σ terms), depth of their respective layer, depth of tunnel axis (H), TBM diameter (D) and position of water level (w.l.) are also indicated in the figure.

Therefore, the numerical steps, for estimation of ground movement due to tunneling, proposed in section 4.3.3 were applied to estimate the effect of input parameters uncertainty.

Furthermore, in Table 5.8 have summarized the structural tunnel properties adopted for the numerical analysis.
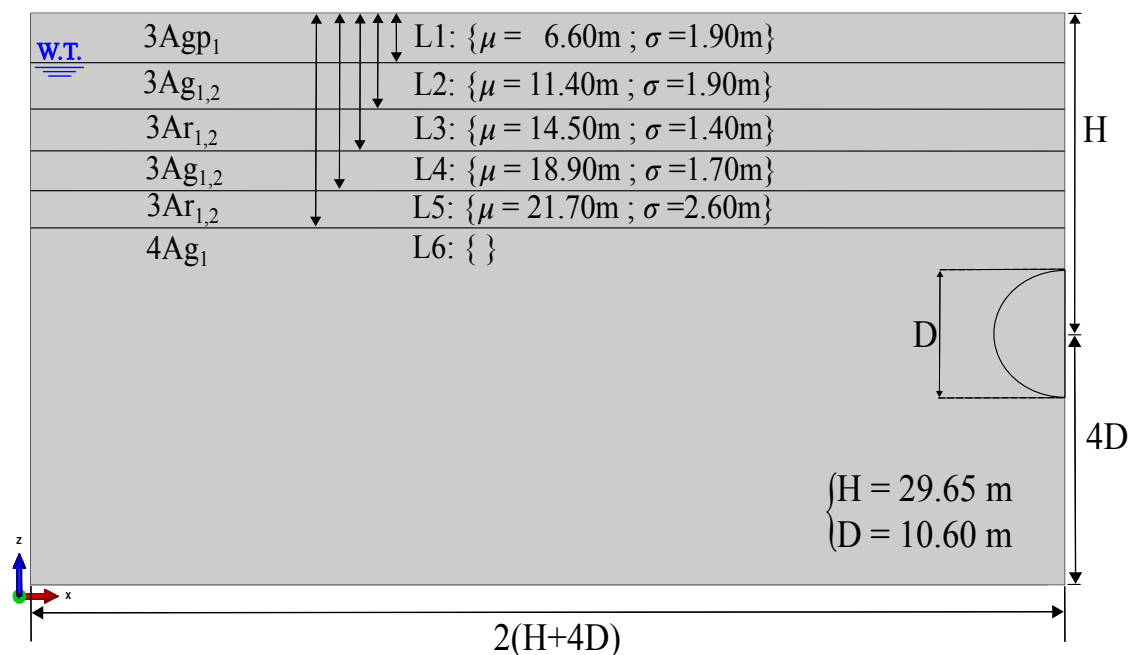
Figure 5.13 – Geometry and size of the 2D numerical model.

Table 5.8 – Material properties of tunnel.

Materials	γ (kN/m^3)	ν (-)	E (MPa)
Grout	25	0.22	5.94
Segment Lining	25	0.22	32800

5.2.3 TUNNELING-INDUCED GROUND MOVEMENTS

Once defined the FE numerical analysis approach, the probabilistic and sensitivity analysis of input parameters is then conducted and presented in the form of tornado diagram as shown in section 4.2.

Figure 5.14 shows the results of a typical numerical simulation employed on the APEM, in terms of the effective vertical stress and total displacement, according to the steps indicated in section 4.3.3.

Figure 5.15 shows the result of the HPEM for the proposed probabilistic scenarios, where a normal probability distribution was assumed for the input variables. In total, 11 input variables were adopted for the analysis, six geotechnical parameters presented in Table 5.3 and five variables related to the position of soil layers at the bottom as depicted in Figure 5.13.

The tornado diagrams of optimistic, neutral and pessimistic scenarios presented in Figures 5.15a, 5.15b and 5.15c, respectively, show that the variables whose uncertainty has the greatest

S, S22
Bottom, (fraction = −1.0)
(Avg: 75%)
+7.375e−01
−3.439e+04
−6.879e+04
−1.032e+05
−1.376e+05
−1.720e+05
−2.064e+05
−2.408e+05
−2.751e+05
−3.095e+05
−3.439e+05
−3.783e+05
−4.127e+05
−4.471e+05
−4.815e+05
−5.159e+05
−5.503e+05
−5.847e+05
−6.191e+05
−6.535e+05
−6.879e+05
−7.223e+05
−7.566e+05

U, Magnitude
+9.157e−03
+8.740e−03
+8.324e−03
+7.908e−03
+7.492e−03
+7.076e−03
+6.659e−03
+6.243e−03
+5.827e−03
+5.411e−03
+4.995e−03
+4.578e−03
+4.162e−03
+3.746e−03
+3.330e−03
+2.913e−03
+2.497e−03
+2.081e−03
+1.665e−03
+1.249e−03
+8.324e−04
+4.162e−04
+0.000e+00

Figure 5.14 – Representation of effective vertical stress and total displacement, respectively for the different simulation steps: (a) Geostatic condition, (b) 50% reduction of tunnel core stiffness, (c) Grout injection around the tunnel and (c) Tunnel lining installation.

109
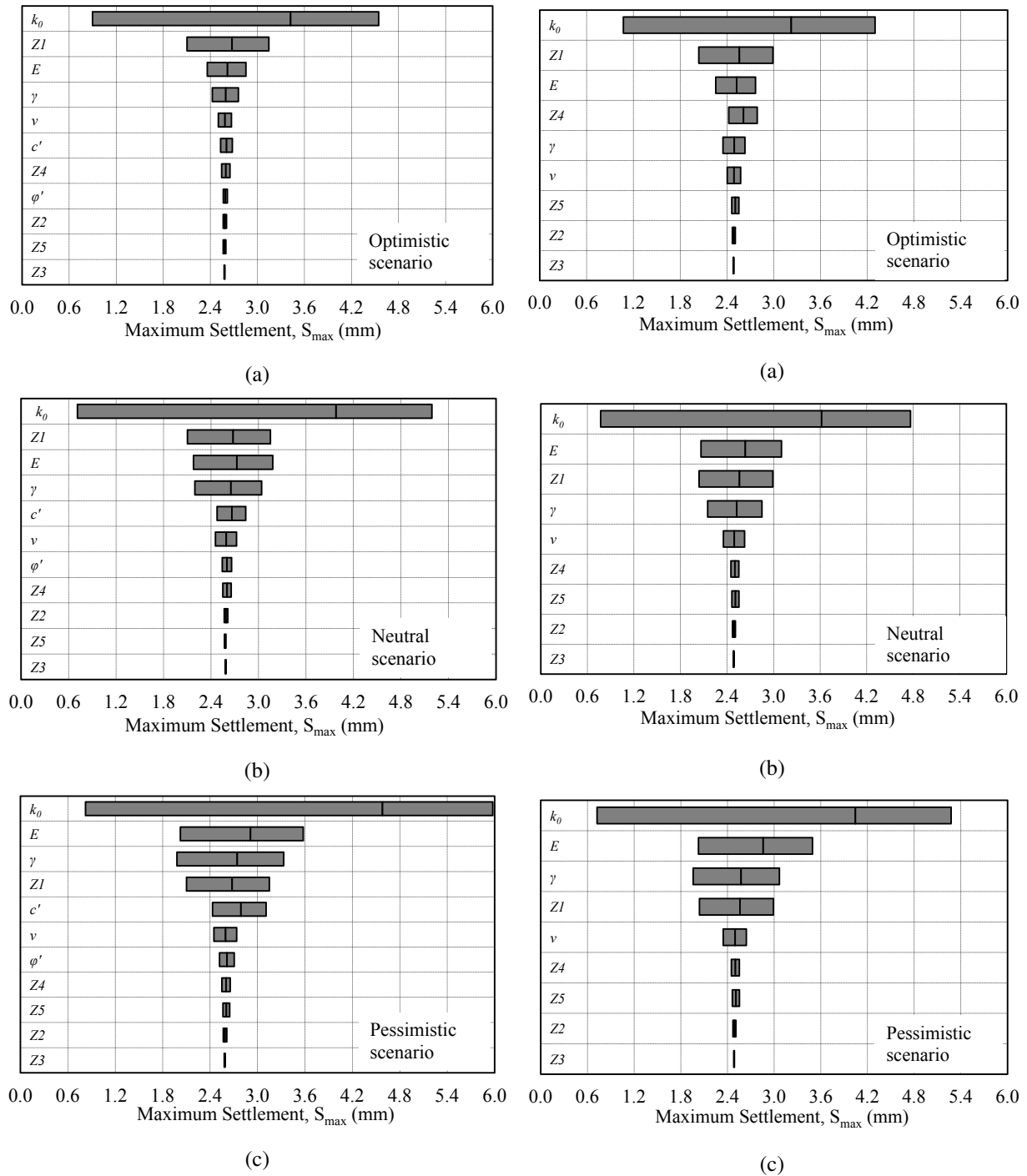
Figure 5.15 – Sensitivity analysis considering CAP model (a) and Mohr-Coulomb model (b and c).

Figure 5.16 – Sensitivity analysis considering the Linear-Elastic model.

effect on the uncertainty of S_{max} are the coefficient of earth pressure at rest (k_0), the depth of the bottom of the 1st layer, Young's modulus (E) and the specific weight (γ). The variable k_0 presents a major contribution in all scenarios analyzed. The significant influence of k_0 and the relatively low influence of cohesion (c') and friction angle (ϕ') indicate that the tunnel excavation with TBM in this type of groundmass can be adequately simulated by considering a linear elastic behavior.

Figure 5.16 shows again the sensitive analysis conducted this time by adopting a linear elastic behavior of soils in all three probabilistic scenarios. As in the previous analysis, the most sensitive variables continue to be k_0, the position of the 1st layer, E and γ.

Finally, to establish which probabilistic scenario fit the best the behavior of groundmass due to TBM tunneling, a statistical inference analysis as the hypothesis test is conducted. From one side, there is a sample of the population of the real behavior of groundmass which is represented by the measured surface settlement data, and from the other hand, there are three samples of the population of simulated groundmass behavior which are represented by the optimistic, neutral and pessimistic probabilistic scenarios.

Table 5.9 shows the results of hypothesis test, where a student's t-distribution was assumed, and the null hypothesis ($H_0 : \mu_{mon} = \mu_{HPEM}$) and alternative hypothesis ($H_a : \mu_{mon} \neq \mu_{HPEM}$) were also defined. Statistically speaking, the tests indicated that all three null hypotheses are accepted, yet the optimistic scenario is preferred over the other scenarios because by assuming low values of CoV for input parameters, their variability can embrace the tunneling-induced ground movements problem satisfactorily.

Table 5.9 – Hypothesis test analysis of probabilistic scenarios.

		Optimistic	Neutral	Pessimistic
μ_{mon}	(mm)		2.695	
$(\sigma_{mon})^2$	(mm)		1.553	
n_{mon}	(-)		19	
μ_{HPEM}	(mm)	2.642	2.575	2.906
$(\sigma_{HPEM})^2$	(mm)	2.321	4.395	6.321
n_{HPEM}	(-)	19	19	19
$g.l$		18	18	18
t		**0.116**	0.214	-0.329
$t_{critical}$		± 2.101	± 2.101	± 2.101

6 ANALYTICAL AND NUMERICAL ANALYSIS

Analysis of tunnel face stability and ground movements through analytical or numerical methods will be presented here on, to understand and provide a similar tool that might allow establishing a relationship among the variables involved in the construction of shallow tunnels.

6.1 TUNNEL FACE STABILITY ANALYSIS

The computation of minimum internal support pressure required to maintain the stability of the tunnel is presented according to the analytical methods mentioned in the methodological approach (section 4.3.1). These methods consider the Mohr-Coulomb failure criterion for the estimation of the minimum support pressure.

6.1.1 THE ANAGNOSTOU & KOVÁRI METHOD

Figure 6.1 shows the scheme for estimation of the vertical stress (σ_V') expressed in Equation 2.27.
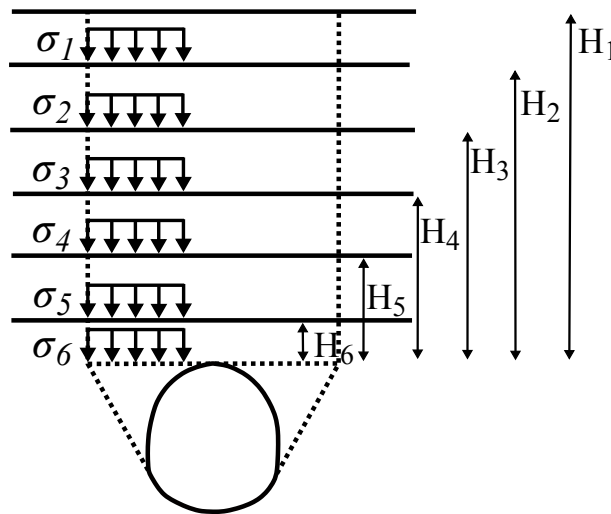
Figure 6.1 – Model geometry with six layers for estimation of σ_V' according to Anagnostou & Kovári (1994).

So, the computation of σ_V' was obtained through the following expression:

$$
\begin{aligned}
\sigma_v ={} & \frac{\gamma_1 r - c_1}{\lambda_1 \tan \varphi_1} \left(e^{-\lambda_2 \tan \varphi_2 \frac{H_2}{r}} - e^{-\lambda_1 \tan \varphi_1 \frac{H_1}{r}} \right) + \frac{\gamma_2 r - c_2}{\lambda_2 \tan \varphi_2} \left(e^{-\lambda_3 \tan \varphi_3 \frac{H_3}{r}} - e^{-\lambda_2 \tan \varphi_2 \frac{H_2}{r}} \right) \\
& + \frac{\gamma_3 r - c_3}{\lambda_3 \tan \varphi_3} \left(e^{-\lambda_4 \tan \varphi_4 \frac{H_4}{r}} - e^{-\lambda_3 \tan \varphi_3 \frac{H_3}{r}} \right) + \frac{\gamma_4 r - c_4}{\lambda_4 \tan \varphi_4} \left(e^{-\lambda_5 \tan \varphi_5 \frac{H_5}{r}} - e^{-\lambda_6 \tan \varphi_6 \frac{H_6}{r}} \right) \quad (6.1) \\
& + \frac{\gamma_5 r - c_5}{\lambda_5 \tan \varphi_5} \left(e^{-\lambda_6 \tan \varphi_6 \frac{H_6}{r}} - e^{-\lambda_5 \tan \varphi_5 \frac{H_5}{r}} \right) + \frac{\gamma_6 r - c_6}{\lambda_6 \tan \varphi_6} \left(1 - e^{-\lambda_6 \tan \varphi_6 \frac{H_6}{r}} \right)
\end{aligned}
$$

where $r = 0.5D\tan\omega/(1 + \tan\omega)$ and $\omega = 90° - \beta$.

Therefore, by taking the geotechnical parameters from Table 5.3 and the related formulation of this method presented in section 2.2.3.1, the value of support pressure at tunnel axis obtained was of 308 kPa.

6.1.2 THE CAQUOT-KÉRISEL METHOD

According to Carranza-Torres (2004), Caquot's model can be applied in various conditions in which groundwater exists and dry or wet condition inside the tunnel section. In this manner, Figure 6.2 represents the condition that majorly fits with the case study.
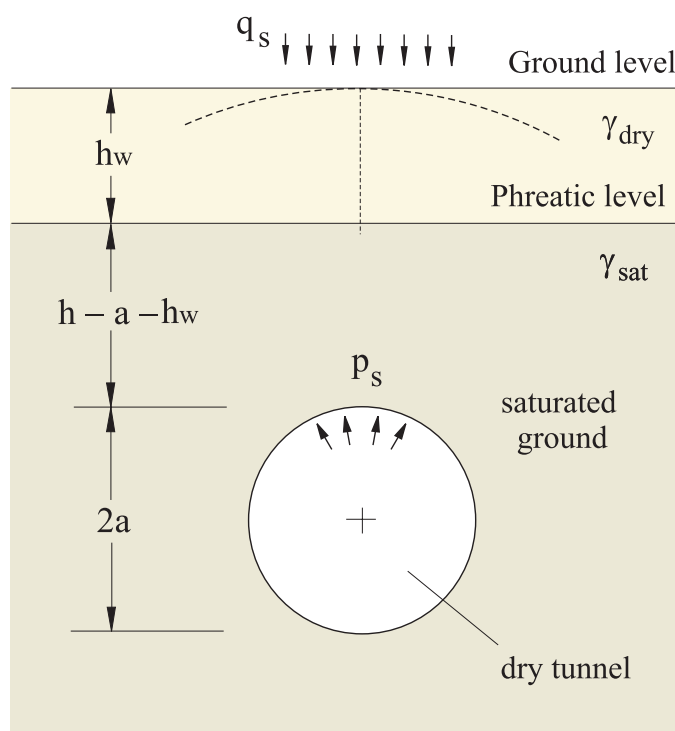
Figure 6.2 – Schematic representation of stability model for the case phreatic level below ground level and dry condition of tunnel.

Under this condition the estimation of the support pressure is given through the following expressions:

$$
\left.\frac{p_S}{\gamma h}\right|^* = \left(\left.\frac{q_S}{\gamma h}\right|^* + 2\left.\frac{c}{\gamma h}\right|^* \frac{\sqrt{N_\phi}}{N_\phi - 1}\right)\left(\frac{h}{a}\right)^{-k\left(N_\phi^{FS}-1\right)}
$$
$$
- \frac{1}{k\left(N_\phi^{FS} - 1\right) - 1}\left[\left(\frac{h}{a}\right)^{-k\left(N_\phi^{FS}-1\right)} - \left(\frac{h}{a}\right)^{-1}\right] - 2\left.\frac{c}{\gamma h}\right|^* \frac{\sqrt{N_\phi}}{N_\phi - 1}
$$

(6.2)

$$
\left.\frac{\gamma h}{c}\right|^* = \frac{\gamma_d h}{c}\frac{\left|\frac{h_w}{h}\right|}{1 - \frac{a}{h}} + \frac{\gamma_d h}{c}\frac{1 - \frac{a}{h} - \left|\frac{h_w}{h}\right|}{1 - \frac{a}{h}}\left(\frac{\gamma_S}{\gamma_d} - \frac{\gamma_w}{\gamma_d}\right)
$$

(6.3)

$$\left.\frac{q_s}{\gamma h}\right|^* = \frac{q_s}{\gamma_d h} \frac{\frac{\gamma_d h}{c}}{\left.\frac{\gamma h}{c}\right|^*} \tag{6.4}$$

$$\left.\frac{p_s}{\gamma h}\right|^* = \frac{p_s}{\gamma_d h} \frac{\frac{\gamma_d h}{c}}{\left.\frac{\gamma h}{c}\right|^*} - \frac{\gamma_w}{\gamma_d} \left(1 - \frac{a}{h} - \left|\frac{h_w}{h}\right|\right) \frac{\frac{\gamma_d h}{c}}{\left.\frac{\gamma h}{c}\right|^*} \tag{6.5}$$

Table 6.1 shows the values of input parameters used for the estimation of the support pressure. The value of the specific weight, cohesion and friction angle indicated in the table correspond to the estimated weighted average from the six soil layers of the numerical model.

Table 6.1 – Input parameters for estimation of support pressure according to the Caquot-Karisel method.

γ_s (kN/m^3)	γ_d (kN/m^3)	γ_w (kN/m^3)	c' (kPa)	ϕ' (°)	a (m)	h (m)	hw (m)	FS	q_s (kPa)	k
19.27	9.27	10	41	28	5.3	29.65	6.6	1	0	1

Thus, the value of support pressure obtained was of 328 kPa.

As expected, the previous analytical analyses confirmed that for the same factor of safety equals to 1, by employing the lower bound plasticity theory (Caquot-Karisel method), in tunneling, the required support pressure necessary at the tunnel face is higher than that from the limit equilibrium theory (Anagnostou & Kovári method). This because the first approach is based on statically admissible solution (a solution that nowhere violates the equilibrium conditions nor the yield condition of the material) while, the second considers minimum support pressure for the equilibrium of a region in the vicinity of the tunnel front to avoid face collapse.

6.1.3   ANALYSIS OF FACE STABILITY IN 2D NUMERICAL MODEL

To analyze the influence of applied support pressure on the stability around the tunnel, a series of 2D numerical analyses were performed. Figure 6.3 shows the result five analyses of decreasing of support pressure, where five scenarios were considered 0 %, 25 %, 50 %, 75 % and 100 %, respectively, from the reference pressure assumed, which was the one obtained from LEM analysis.

As it is possible to see from this figure, only the 0 % of the assumed reference support pressure generated a small plastic zone around the tunnel of 2.43 m in correspondence of the tunnel side wall. The 25 % of applied support pressure produce negligible plastic zone and from this percentage to the 100 % no plastic zone formed around the tunnel. This result brought to the conclusion that TBM tunneling could be performed without application of support pressure and water inflow in the tunnel is prevented thanks to water tightness of the TBM shield and tunnel lining.

It is essential to highlight that even if the lack of application of support pressure will generate small plastic zone around the tunnel, this approach will produce that the values of the surface settlement will be larger than the values registered from the monitoring campaign.
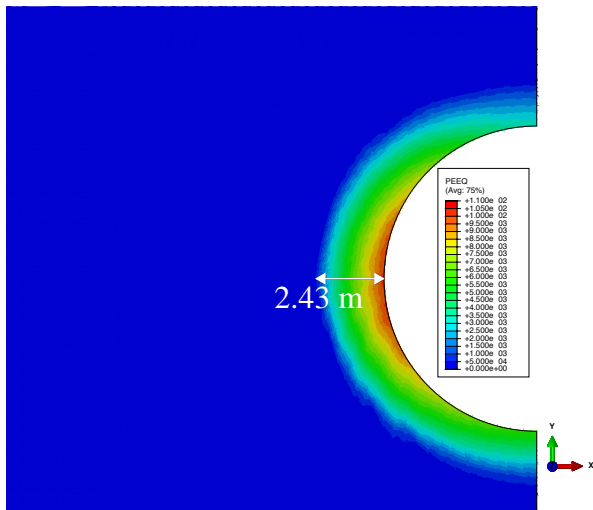
(a) 0 % of LEM analysis (0 kPa).
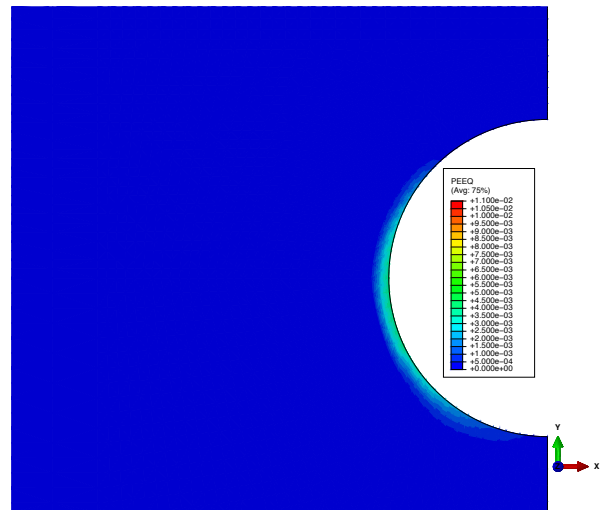
(b) 25 % of LEM analysis (77 kPa).
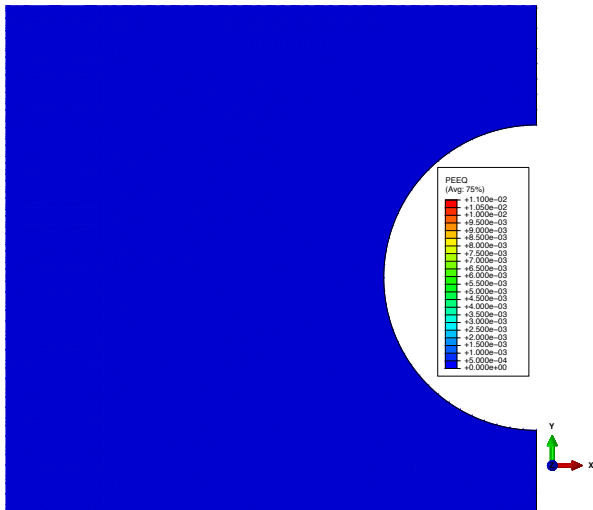
(c) 50 % of LEM analysis (154 kPa).
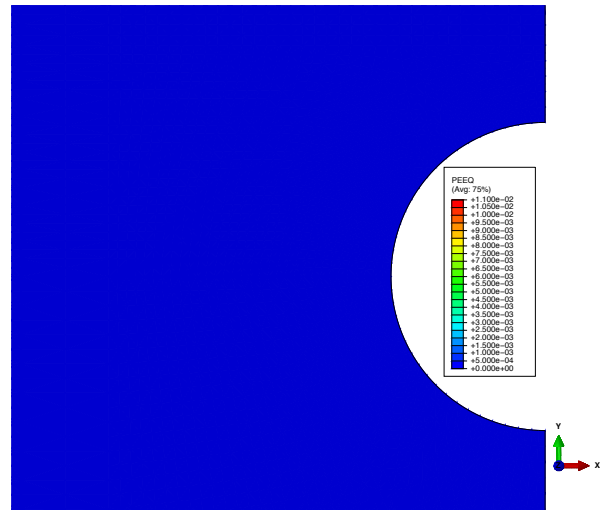
(d) 75 % of LEM analysis (231 kPa).
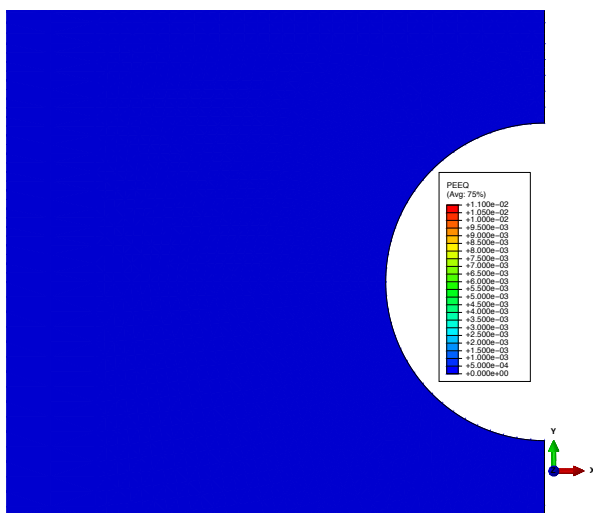
(e) 100 % of LEM analysis (308 kPa).

Figure 6.3 – Sequence of internal support pressure reduction in the ABAQUS model where the M-C failure criterion was assumed.

6.2 GROUND MOVEMENT ANALYSIS

Estimated the influence of input geotechnical parameters (Section 5.2), the optimistic scenario and the γ, k_0, E and $Z1$ input variables were considered for conducting a sensitivity analysis of tunneling-induced ground movements. Based on the HPEM, nine simulations were computed by evaluation of the variability of the input parameters. A 3D finite element model for shield driven tunneling is made for the analysis of surface ground movement in the transverse direction and the longitudinal direction.

This numerical approach includes several of the features of the EPB tunneling features considered by Kavvadas et al. (2017) as cutterhead overcut, conically-shaped shield with the shield-ground interface, tail gap, grout injection for annular gap filling and continuously cylindrical shell of segment lining. A grout injection pressure to that obtained in Section 6.1.1 was used.

Figure 6.4 shows the results of a typical 3D numerical analysis of tunneling in terms of the distribution of vertical displacement and plastic deformation of groundmass around the tunnel. Propagation of vertical movement occurs from the tunnel crown to the surface whereas an uplift of groundmass develops in the zone of the tunnel invert. It is also possible to notice that ground-mass displacements start to develop in correspondence of the tunnel face and reach equilibrium approximately after 30 m from the tunnel face.
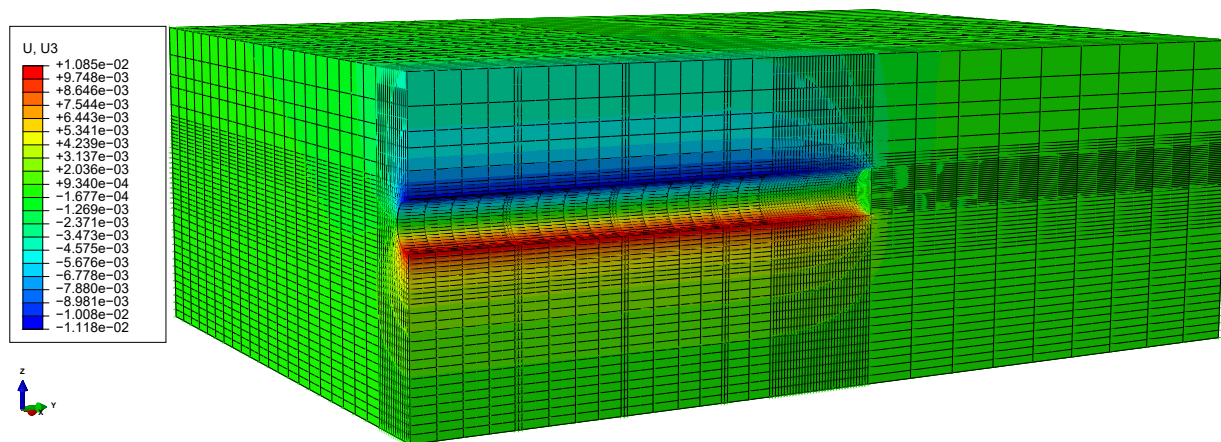
Figure 6.4 – 3D numerical analysis of tunneling, contour plots of vertical displacement.

Figure 6.5 shows the variability of the settlement curves in the transverse and longitudinal direction. Typical behavior of surface settlement introduced by Peck (1969) and Attewell & Woodman (1982) is observed where the Gaussian probability density function describes the settlement shape in the transverse direction (Figure 6.5a), and the Gaussian cumulative distribution function describes it in the longitudinal direction (Figure 6.5b). As seen in Figure 6.5a, k_0 not only delimits the bound of the transverse settlement curves but also indicates the distance where the inflection of the settlement curve occurs, which is around 20 m from the tunnel axis. Computation of ground movements through evaluation of k_0 will converge to the same distance of settlement curves inflection. Therefore, it may be interpreted that the variability of k_0 represents a pivot to evaluate the sensitivity of surface settlement curve parameters due to tunneling.
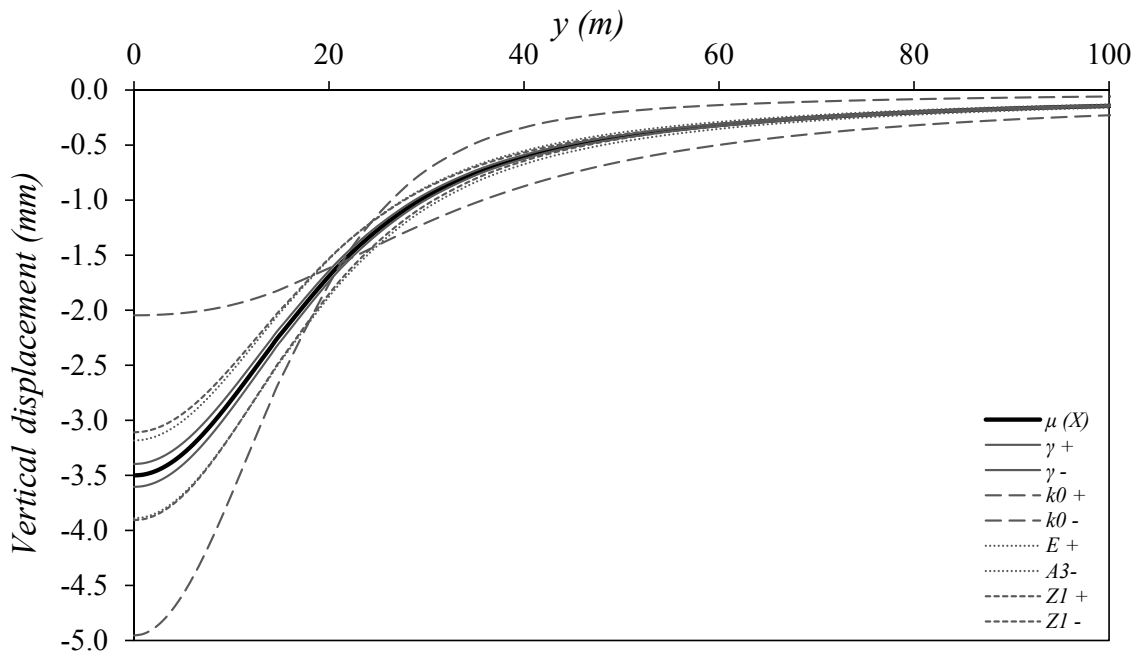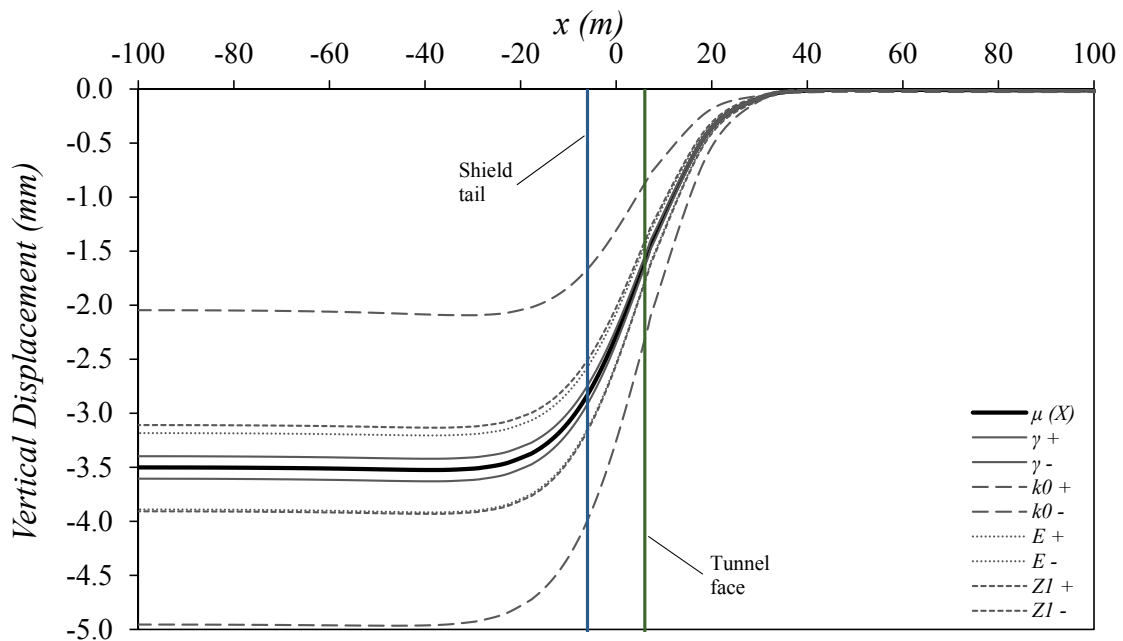
Figure 6.5 – Settlement curves of random input variables along the transverse direction (a) and longitudinal direction (b).

From another perspective, Figure 6.5b shows that ground movement started to develop around 20 m ahead of the tunnel face. It seems no influence of grout injection is observed on the longitudinal settlement curves in correspondence of the TBM shield tail. Stability of settlements occurs around 20 m behind the shield tail. Furthermore, it is possible to see that the variable k_0 exerts significant influence on the slope of the settlement curves; thus, providing the limits of the variability of ground movements.
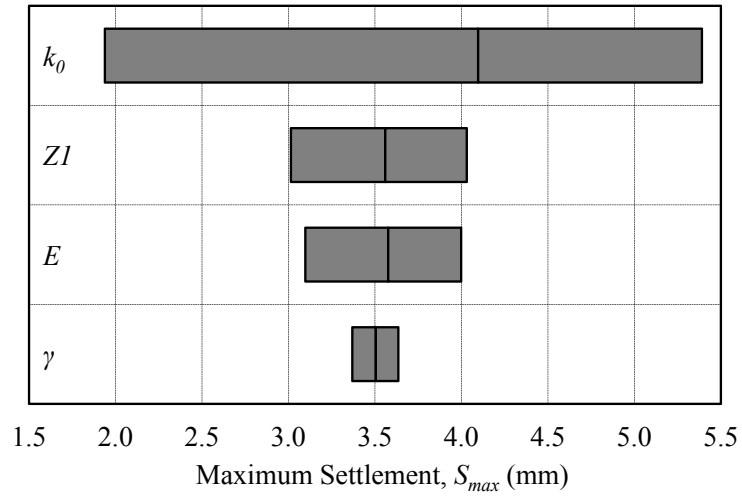
(a)
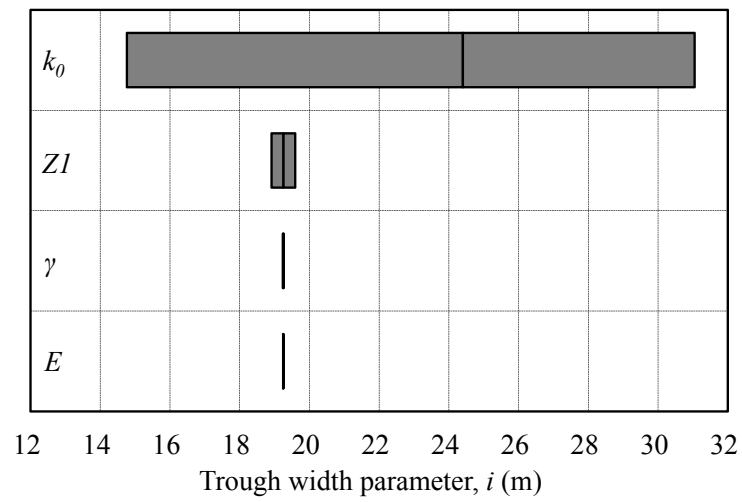
(b)
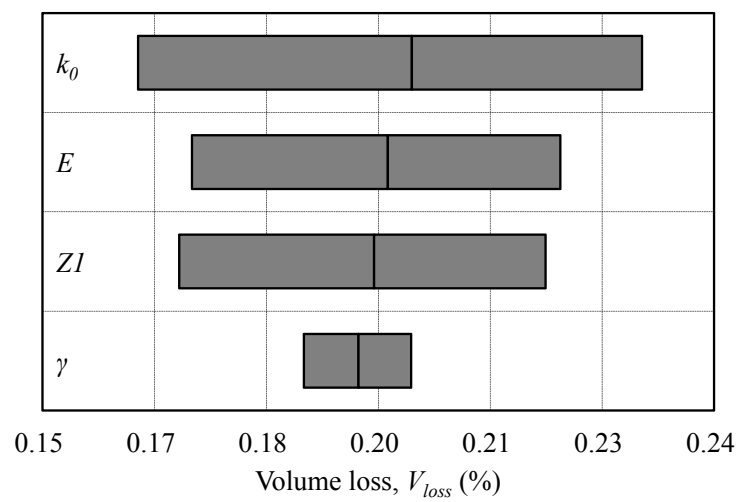
(c)

Figure 6.6 – Tornado diagram of settlement curve parameters; (a) Surface settlement, (b) Trough width parameter and (c) Volume loss.

Figure 6.6 shows the sensitivity analysis of settlement curves parameters. It can be seen from Figures 6.6a and 6.6b that the maximum surface settlement (S_{max}) and trough width parameter (i), respectively, are very sensitive to k_0 followed by the depth of 1st layer ($Z1$). It can be assumed that the reason these variables have an impact on ground movement could be since k_0 is related to changes of stress-strain in the horizontal direction and $Z1$ is practically the zone where the ground movement takes place. Variability of E, which is directly related to the stress-strain relationship, produces negligible impact. The same can be said about the variable γ.

Regarding the Volume loss, V_{loss} (Figure 6.6c), it is observed that k_0 continues to be an input variable of great influence on ground movements whereas a decrease of the influence of $Z1$ is noticed, due to the increase of influence of E. The input variable γ constitutes the last parameter on the tornado diagram that exerts some impact on V_{loss}. As V_{loss} is a dependent variable resulted from the relationship between S_{max} and i variations of the order of influence of E, $Z1$ and γ is different from that observed in S_{max} (Figure 6.6a) and i (Figure 6.6b). Also, unlike the tornado diagram observed in the parameters S_{max} and i, the tornado diagram in the parameter V_{loss} seems to have a better uniform distribution of effects of the input variables.

7 MATHEMATICAL MODEL FOR ESTIMATION OF SURFACE SETTLEMENT

This chapter presents the selection of a mathematical model for the estimation of immediate surface settlement due to TBM tunneling. A set of candidate models is proposed for representing the effect of immediate surface settlement due to TBM tunneling; after that, a criterion for selecting the best model is employed and, finally, an analysis of the fitting parameters is made. The bases of theory and approach here employed were provided along with the previous chapters. Information about the case study used in this research allowed, therefore, to ensure a strong representation of the groundmass behavior.

Real tunnel construction develops in heterogeneous groundmass with various stratigraphy and also below water level. Herein, it was assumed to work with a single equivalent groundmass, which heterogeneity is considered by taking into account the concept of spatial variability. Furthermore, the presence of a phreatic level is considered.

The procedure used is represented, below, through the following steps.

7.1 SET CANDIDATE MODELS

Following the system behavior described in Figure 2.41, Table 7.1 presents the set of candidate models proposed which equally represents the development of ground movement, in the form of maximum surface settlement (S_{max}), due to the applied TBM face support pressure (P).

From this table, P_0 correspond to the estimated value of TBM support pressure for face stability, and a and b, at this stage, are the curve-fitting parameters. Once the best model is chosen, an attempt for describing the physical meaning of these variables will be made.

7.2 FITTING EQUATIONS TO DATA FROM CASE STUDY

Measured values of either maximum surface settlement (S_{max}) and applied TBM face support pressure (P) were used to evaluate the capability of candidate models to fit in real case scenarios. The analyses of ground movement (Section 5.1.2) and TBM performance (Section 5.1.3), along the tunnel length, allowed to consider the stretch between HSP – SCR (presented in Table 5.4) as the best option to work with.

Concerning fit analysis, it is well known that, within the mathematical literature, the coefficient of determination of R-squared is an inadequate measure for the goodness of fit to apply directly in nonlinear models, as the those presented in Table 7.1. Nevertheless, it is still a standard

Table 7.1 – Proposed set of candidate models for estimation immediate surface settlement due to TBM tunneling.

Reference	Re-adapted formulation	Eq. #
Duncan & Chang (1970) Section 2.4.5.1	$S_{\max} = \dfrac{a(P_0 - P)}{b(P_0 - P) - 1}$	(7.1)
Alonso et al. (1990) Section 2.4.5.2	$S_{\max} = \dfrac{1}{b}\left[LN\left(\dfrac{P}{P_0} - a\right) - LN\left(1 - a\right)\right]$	(7.2)
Koorevaar et al. (1983) Section 2.4.5.3	$S_{\max} = a\left[1 - \left(\dfrac{P}{P_0}\right)^{-b}\right]$	(7.3)
Isaaks & Srivastava (1989) Section 2.4.5.4	$S_{\max} = a\left[1 - e^{b\left(\frac{P_0}{P} - 1\right)^c}\right]$	(7.4)
NBR 6118:2003 (2003) Section 2.4.5.5	$S_{\max} = -a\left[\dfrac{(P_0 - P)^b}{P}\right]$	(7.5)
Author proposal	$S_{\max} = -aLN\left(\dfrac{P_0}{P}\right)^b$	(7.6)

tool used for the analysis and interpretation of nonlinear fitting to data.

An example, to the mentioned above, is given by Spiess & Neumeyer (2010) which study on pharmacological and biological data allowed them to conclude that the use of R-squared tool to evaluate the fit of nonlinear models leads to an incorrect interpretation. So, in order to consider the use of R-squared on a nonlinear model, a mathematical approach is applied for the estimation of the sum of squared error (SSE), by applying the concept of maximum and minimum values with partial derivative on the fitting function $y = f(x|\widehat{\theta})$, as follows:

$$
\begin{aligned}
SSE &= \sum_{i}^{n} [y_i - y_i']^2 = \sum_{i}^{n} \left[f\left(x_i \left|\widehat{\theta}\right.\right) - y_i' \right]^2 \quad \therefore \quad \widehat{\theta} = \theta_1, \theta_2, \ldots, \theta_m \\
\frac{\partial SSE}{\partial \theta_j} &= 0 \qquad\qquad\qquad\qquad\qquad\qquad \therefore \quad j = 1, 2, \ldots, m
\end{aligned}
\tag{7.7}
$$

where $\widehat{\theta}$ is the vector containing the parameters of the fitting function $f(x|\widehat{\theta})$, n is number of samples, m is the number of parameters involved the fitting function, y_i is the value of the fitting function evaluated in x_i and y_i' is the observed value related to its respective x_i. This approach allows not only the estimation of the parameters of fitting function but also to estimate the minimum value of SSE that can be obtained. Therefore, an optimized estimation of the variance (σ^2) is made allowing a better fitting for each nonlinear model.

Figure 7.1 presents the best-fit curve of each candidate model with the measured data along the tunnel stretch between HSP – SCR stations. As expected, due to the variability of the variables of interest, a low coefficient of determination (R^2) is observed in the proposed models.

Yet, it proves that a nonlinear relation between the applied TBM support pressure and surface ground movement exist as indicated by Atkinson (2007). Additionally, as presented in Section 6.1.1, the value of support pressure at tunnels axis of 308 kPa was used for fitting the candidate models.
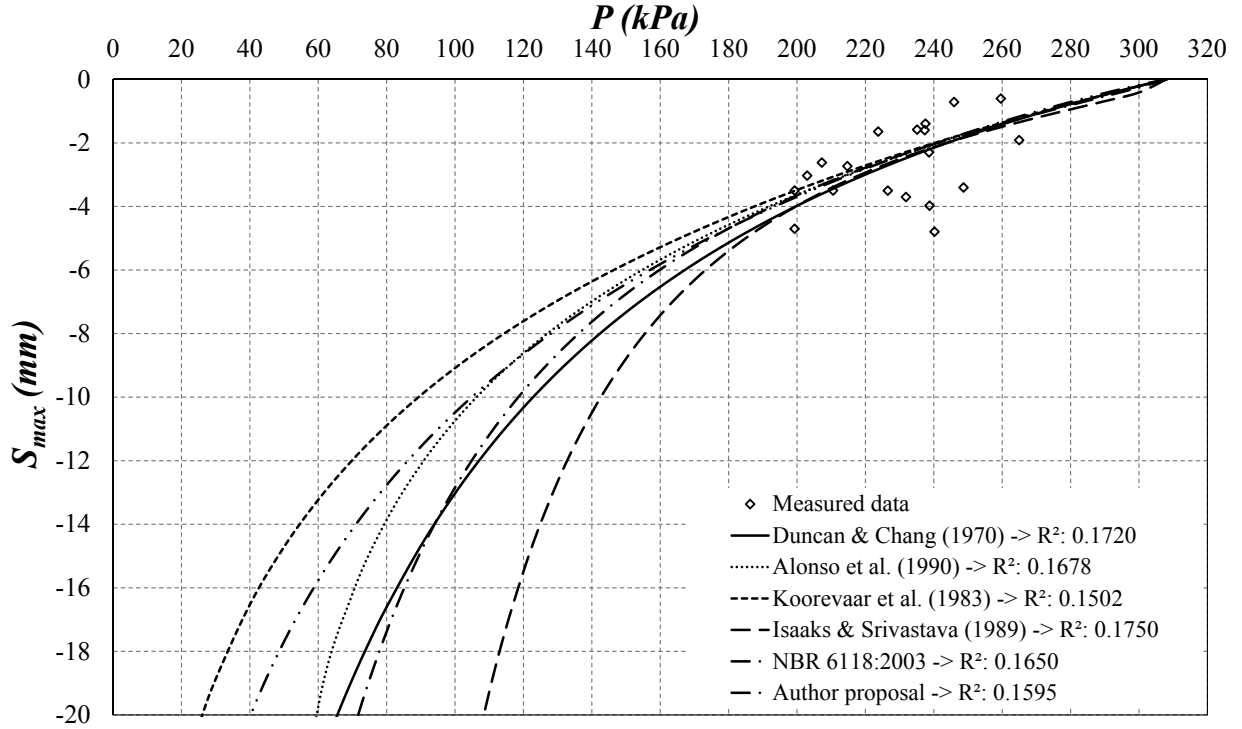
Figure 7.1 – Set candidate models fitted to measured data along the tunnel stretch between HSP – SCR stations.

7.3 MODEL SELECTION - AIC

In order to apply the Akaike Information Criterion (AIC) presented in Equation 2.41, the log-likelihood function ($L(\widehat{\theta}|y)$) needs to be solved. In order to do that, it is necessary to attribute a distribution function to the sample vector ($y : y_1, y_2, \cdots, y_n$). For this research, the normal distribution function, where the parameter vertor is formed by: $\widehat{\theta} = [\mu\ \sigma]$. Therefore, the likelihood function is expressed as:

$$
\begin{aligned}
L\left(\widehat{\theta}\middle|y\right) &= f\left(y, \widehat{\theta}\right) \\
&= \prod_{i=1}^{n} f\left(y_i; \mu, \sigma\right) \\
&= \prod_{i=1}^{n} \left(2\pi\sigma^2\right)^{-1/2} e^{-\frac{1}{2}\frac{(y_i-\mu)^2}{\sigma^2}} \\
&= \left(2\pi\sigma^2\right)^{-n/2} e^{-\frac{1}{2\sigma^2}\sum_{i=1}^{n}(y_i-\mu)^2}
\end{aligned}
\tag{7.8}
$$

Then, the expression $-2\ln\left[L\left(\widehat{\theta}\middle|y\right)\right]$ becomes:

$$
\begin{aligned}
-2\ln\left[L\left(\widehat{\theta}\middle|y\right)\right] &= -2\ln\left[\left(2\pi\sigma^2\right)^{-n/2} e^{-\frac{1}{2\sigma^2}\sum_{i=1}^{n}(y_i-\mu)^2}\right] \\
&= n\ln(2\pi) + n\ln\left(\sigma^2\right) + \frac{1}{2\sigma^2}\sum_{i=1}^{n}(y_i-\mu)^2
\end{aligned}
\tag{7.9}
$$

because the third term in Equation 7.9 is close to zero, this term is unconsidered. Whereas the first term is also unconsidered because it corresponds to a constant value which will have the same value for all the evaluated models. Thus, the computation of the AIC is expressed as:

$$AIC = n \ln \left(\sigma^2 \right) + 2k + \frac{2k \left(k + 1 \right)}{n - k - 1} \tag{7.10}$$

where $\sigma^2 = SSE/n$; SSE is the sum of squared-error of each candidate model. According to the number of data evaluated between HSP – SCR stations, $n = 19$.

Table 7.2 – Summary of model selection by AIC.

Model		Number of parameters k [*]	SSE	AIC	Estimated R^2
Eq. 7.1	$S_{\max} = \dfrac{a(P_0 - P)}{b(P_0 - P) - 1}$	3	23.1461	11.3504	0.1720
Eq. 7.2	$S_{\max} = \dfrac{1}{b} \left[LN \left(\dfrac{P}{P_0} - a \right) - LN \left(1 - a \right) \right]$	3	23.2629	11.4460	0.1678
Eq. 7.3	$S_{\max} = a \left[1 - \left(\dfrac{P}{P_0} \right)^{-b} \right]$	3	23.7659	11.8452	0.1502
Eq. 7.4	$S_{\max} = a \left[1 - e^{b \left(\frac{P_0}{P} - 1 \right)^c} \right]$	4	23.0632	14.5393	0.1750
Eq. 7.5	$S_{\max} = -a \left[\dfrac{(P_0 - P)^b}{P} \right]$	3	23.3419	11.5104	0.1650
Eq. 7.6	$S_{\max} = -aLN \left(\dfrac{P_0}{P} \right)^b$	3	23.4975	11.6366	0.1595

[*] k is the number of parameters in the regression model plus 1.

Table 7.2 shows the results of the application of the Akaike Information Criterion (AIC) for model selection of the best immediate surface settlement curve due to TBM tunneling for the present case study. Furthermore, the estimated R^2 was added in order to provide a better analysis. As mentioned in Section 2.4.3.1, the model with the lowest value of AIC represents the best candidate model for the data. Therefore, Equation 7.1 resulted in being the best model for this analysis. The fitting values of parameters a and b, for this equation, were 3.480 and 0.151, respectively.

It should be noticed that Equation 7.4 shows a better estimation in terms of R^2, but from the AIC point of view, the value is higher due to the penalty occasioned for the increment on the number of parameters.

7.4 PARAMETRIC ANALYSIS OF CHOSEN EQUATION

In order to analyze the impact of parameters of the selected model (Equation 7.1), a series of parametric studies are made to describe this influence. Figures 7.2 and 7.3 show the effects of

variation when changing one parameter while keeping the other fixed.

By analogy with the formulation proposed by Duncan & Chang (1970), It can be seen that parameter a controls the slope of the curve (Figure 7.2), where a significant range of values (from 0.05 to 22) produce little effect on the variation of the curve slope. In relation to parameter b (Figure 7.3), small range of applied values (from 0.04 to 0.3) shown a rapid tendency for large settlements.
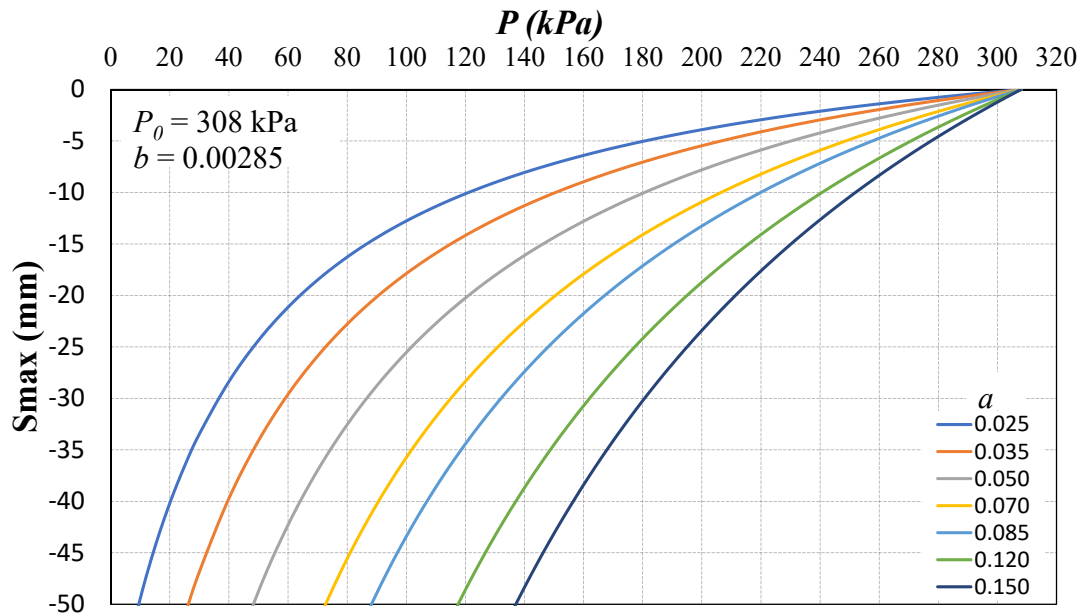
Figure 7.2 – Effect of changing fitting parameters a on selected equation.
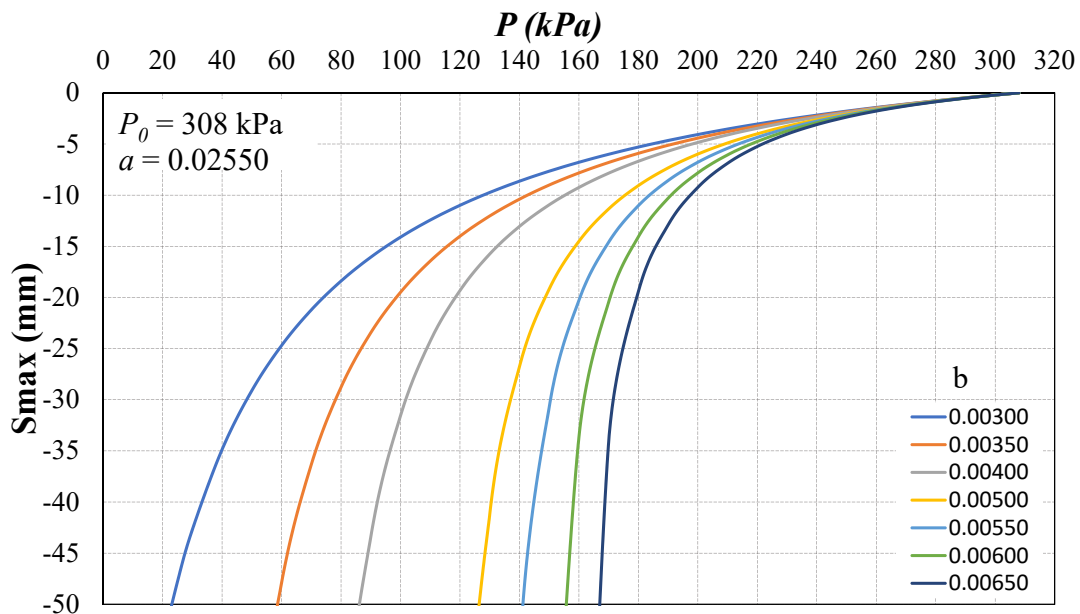
Figure 7.3 – Effect of changing fitting parameters b on selected equation.

Table 7.3 – Limits of fitting parameters.

Fitting parameters	μ	σ	min 10th percentile	max 90th percentile
a	0.02550	0.000138	0.0132	0.0406
b	0.00285	0.000002	0.0015	0.0072

7.5 QUANTIFICATION OF VARIABILITY OF EQUATION PARAMETERS

The following analysis is based on the work of Zhai & Rahardjo (2013), which procedure for the variability representation of the Soil Water Characteristic Curve (SWCC) fitting parameters, may be considered to be perfectly applied in this case.

The idea of this method will be to represent the variability within the upper and lower bounds of the selected equation (Equation 7.1). According to Kool et al. (1987), the bounds of a model is directly correlated to the confidence limits of the parameters involved in the equation, in which the normal distribution represents the parameters.

For this case, the parameters a and b are assumed to be represented by the Lognormal probabilistic distribution function. Therefore, the lower and upper bound of the model are found by estimating the 10th and 90th percentiles of the distribution function of each variable. Table 7.3 shows the lower and upper bounds of fitting parameters by considering the value of the coefficient of variation (CoV) of 46%. This value is taken from the results of registered values of maximum surface settlement (S_{max}) presented in Table 5.4 for the tunnel stretch between HSP – SCR.

Thus, by the combination of the maximum and minimum values of the fitting parameters on the selected equation (Equation 7.1), the upper and lower confidence limits can be obtained. Figure 7.4 shows the correlation between the maximum surface settlement with fitting parameters a and b, respectively.

As it is possible to see, the combination of a_{max} and b_{max} will give the upper bound while the combination of a_{min} b_{min} will give the lower confidence limit. The model bounds are expressed as follow:
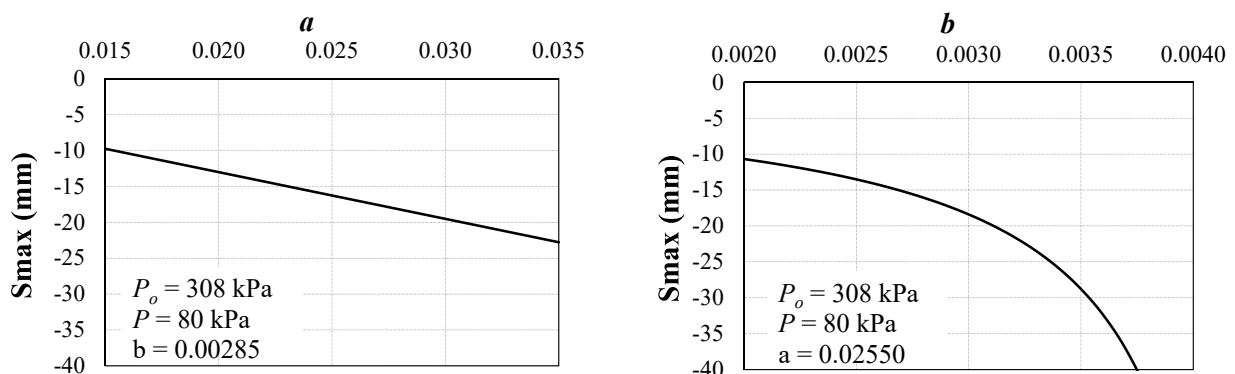
Figure 7.4 – Relationships between maximum surface settlement (S_{max}) and fitting parameters a and b, respectively.

$$Upper : S_{\max} = \frac{a_{\max}(P_0 - P)}{b_{\max}(P_0 - P) - 1}$$

(7.11)

$$Lower : S_{\max} = \frac{a_{\min}(P_0 - P)}{b_{\min}(P_0 - P) - 1}$$

Finally, Figure 7.5 shows the variability of the selected equation through a series of computation of the upper and lower limits by considering CoV of 10 %, 20 %, 30 %, 40 % and 46 %. It is observed that a CoV of 46 % provides a good fit of the lower and upper bounds to the registered values.
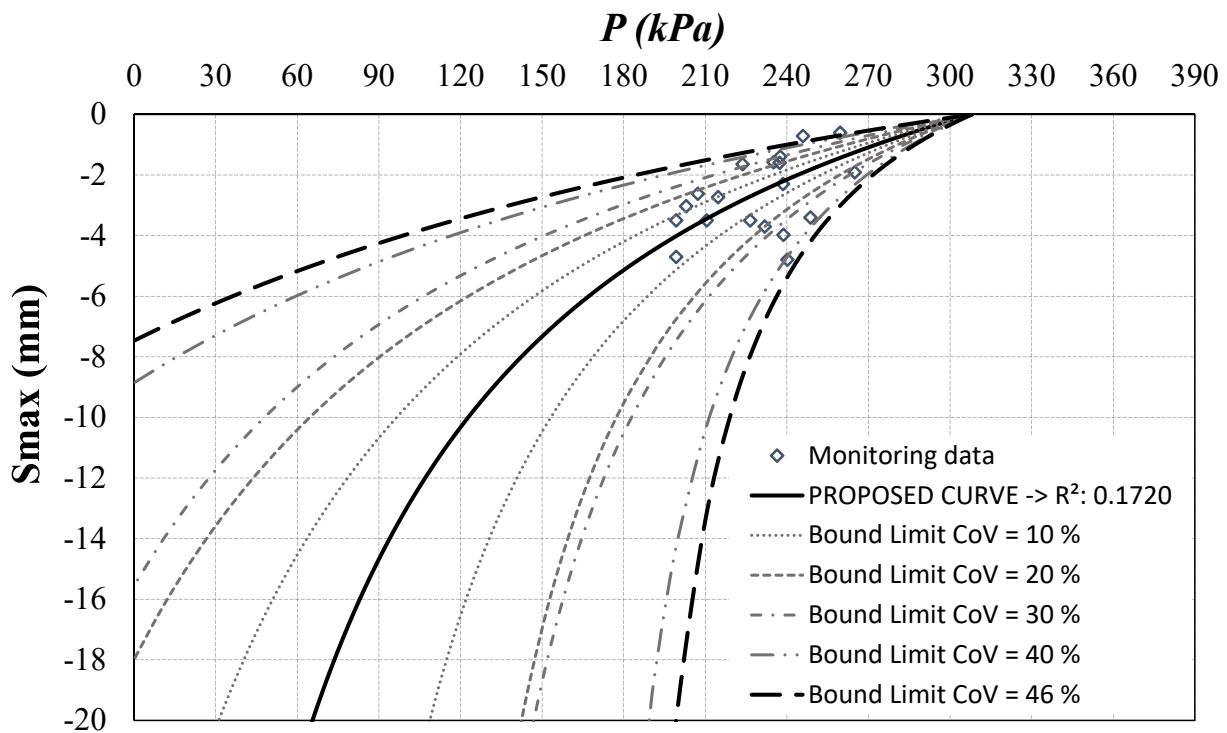
Figure 7.5 – Illustration of selected equation, upper and lower bounds of S_{max} settlement between HSP - SCR.

7.6 MODEL COMPARISON WITH CENTRIFUGE TEST RESULTS

Centrifuge model is a type of physical model that allows a better approximation of stress-strain behavior in good agreement with reality (Janin & Dias, 2014). To this aim, the following section presents five published references concerning centrifuge model test results, for analysis of tunnel face stability and ground movement, selected for comparison with chosen equation (Eq. 7.1).

Figure 7.6 shows the centrifuge test result performed by Lee & Rowe (1989). A relationship between the applied tunnel support pressure with surface settlement is presented. The test was carried out on a Kaolin clay by considering an Overburden (C) and Tunnel Diameter (D) relationship of C/D = 1.67 (D = 36 mm). The proposed curve is also shown in this figure, where the

assumed value for P_0 was of 130 kPa. As is possible to see, a good agreement between the result presented by Lee & Rowe (1989) and the proposed model is observed.
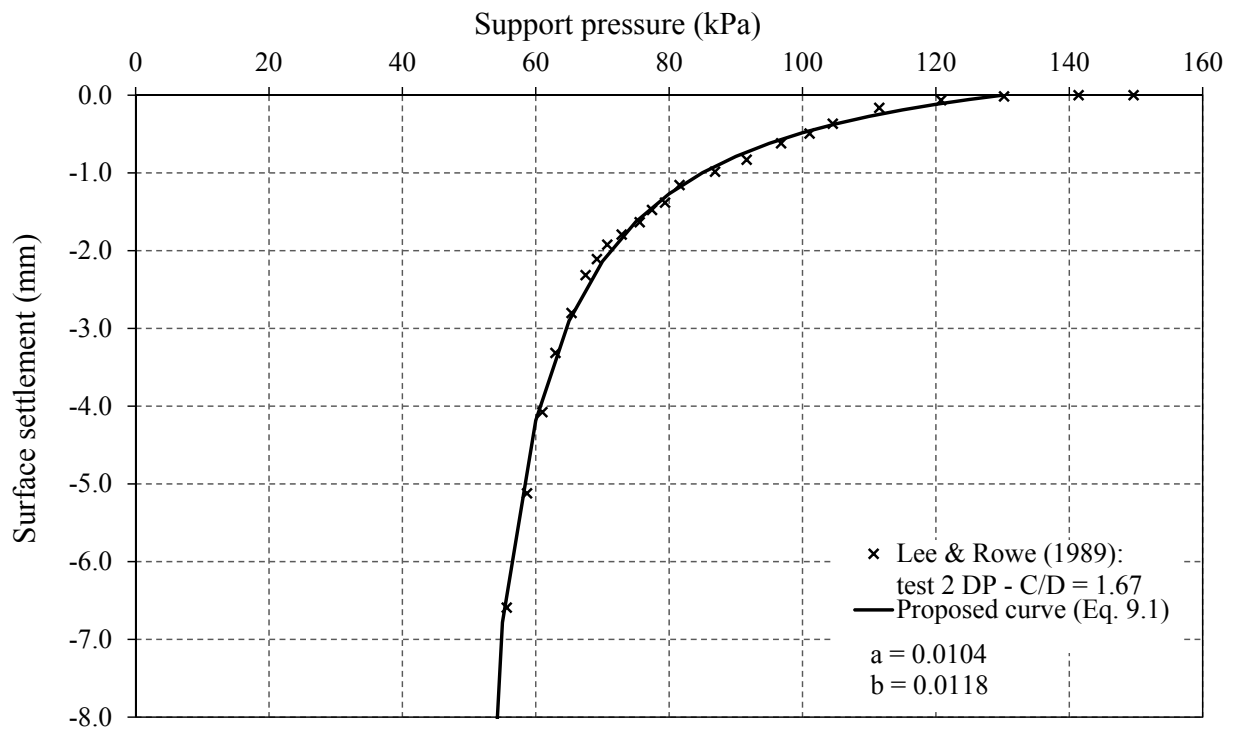
Figure 7.6 – Proposed curve and evolution of surface settlement above tunnel face (after Lee & Rowe, 1989).

Figure 7.7 shows the centrifuge test result performed by Chambon & Corté (1994), where the relationship between surface settlement and support pressure is displayed. The test was made on a cohesionless soil having an Overburden (C) and Tunnel Diameter (D) relationship of C/D = 1 (D = 100 mm). The figure also presents the fitting of the proposed model with the experimental data, and the value of P_0 is of 130 kPa. As is possible to see, a good agreement between the result presented by Chambon & Corté (1994) and the proposed model is observed.

Figures 7.8 to 7.10 show the results of centrifuge test modeling performed by Osman et al. (2006). The test consisted in reduction of the supported by compressed air that at small steps until tunnel collapse. The type of soil used for this analysis was a soft clay. Different configuration analyses were considered in relation to C/D relationship, which was of 1.80 (Figure 7.8), 1.67 (Figure 7.9) and 1.67 (Figure 7.10) being the centrifuge model tunnel diameter of 60 mm, 60 mm and 36 mm, respectively. The proposed curve is also presented in the figure where a value of P_0 of 130 kPa was considered for each test result. Therefore, as it is possible to see in each respective figure, a good agreement between the proposed curve with the experimental data is observed.

Moreover, Figure 7.11 shows the centrifuge test result performed by Janin & Dias (2014). Again, the test was made on a cohesionless soil having a model geometry C/D = 2 (D = 200 mm). The fitting curve is also presented in the figure where the value of P_0 is of 390 kPa. As is it possible to see, the elastic behavior of the model agrees well with the data. However, when reducing the support pressure from 75 kPa, a difference between model and data is observed. A fair agreement regarding the plastic behavior is noticed. Nonetheless, the model provides values
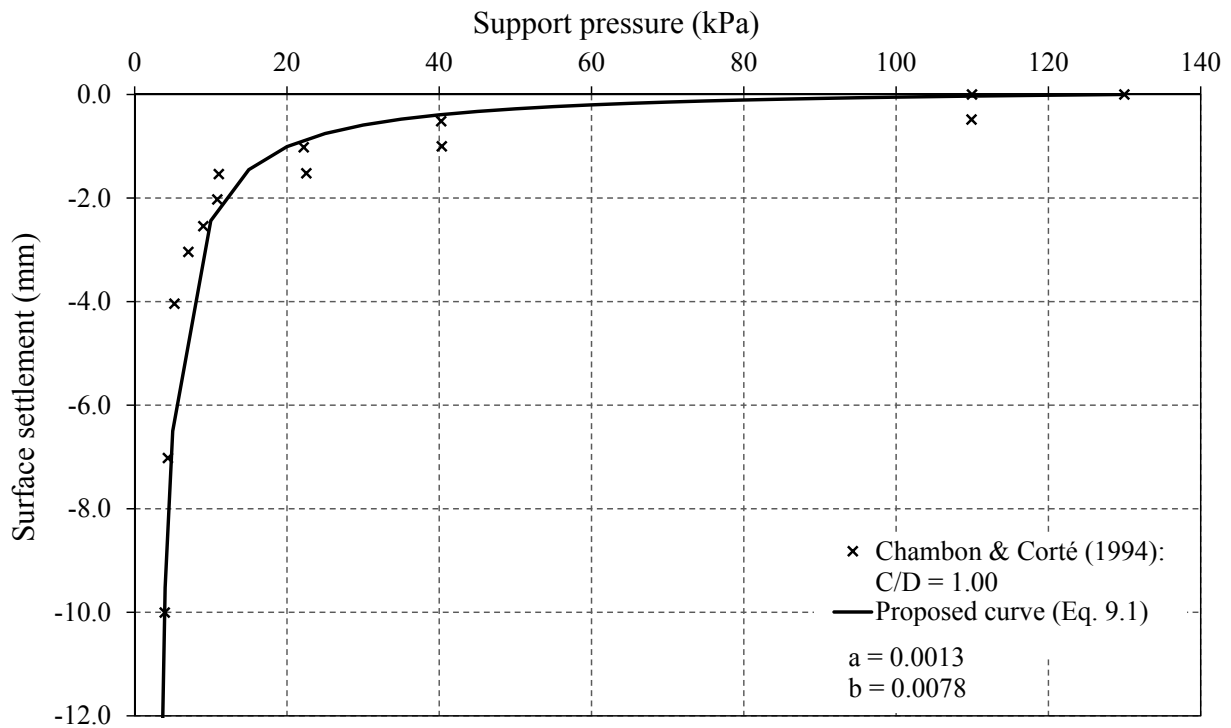
Figure 7.7 – Proposed curve and evolution of surface settlement above tunnel face (after Chambon & Corté, 1994).

that could be considered in the safety condition respect to the experimental data.

Lastly, Figure 7.12 shows a series of eight two-dimensional plane strain centrifuge model tests performed by Divall et al. (2016) to investigate how the installation of the ground supports, consti-
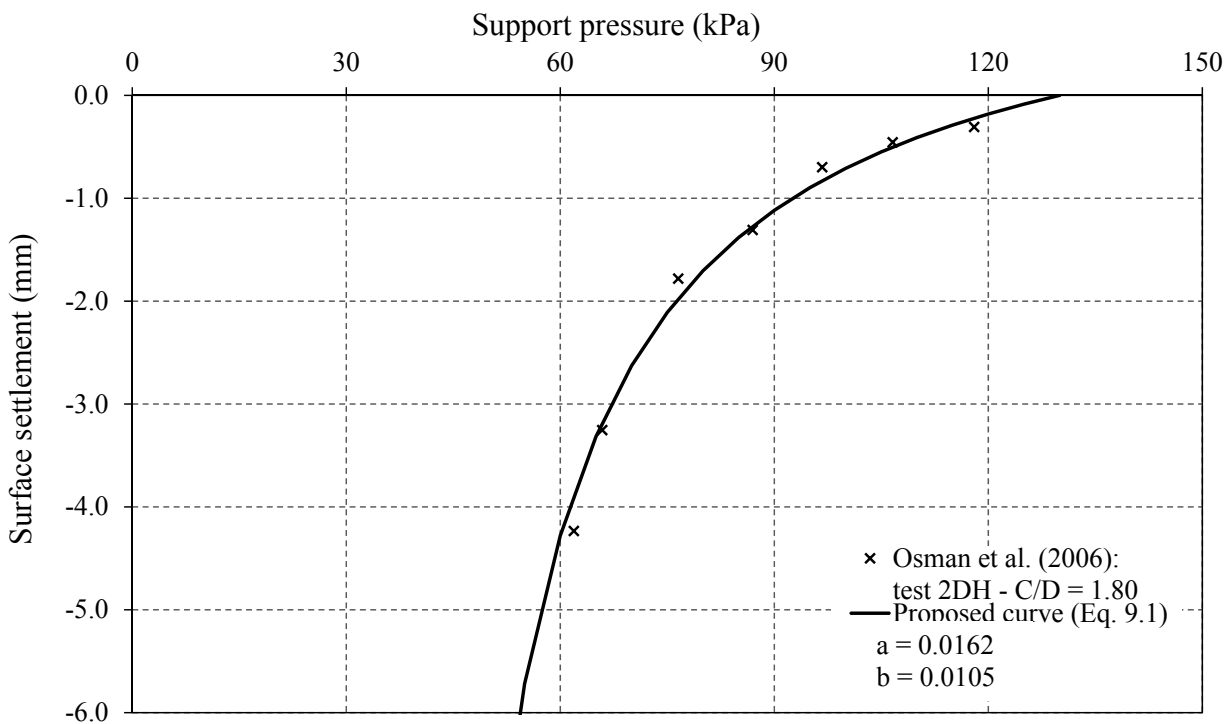
Figure 7.8 – Proposed curve and evolution of surface settlement above tunnel face (after Osman et al., 2006).
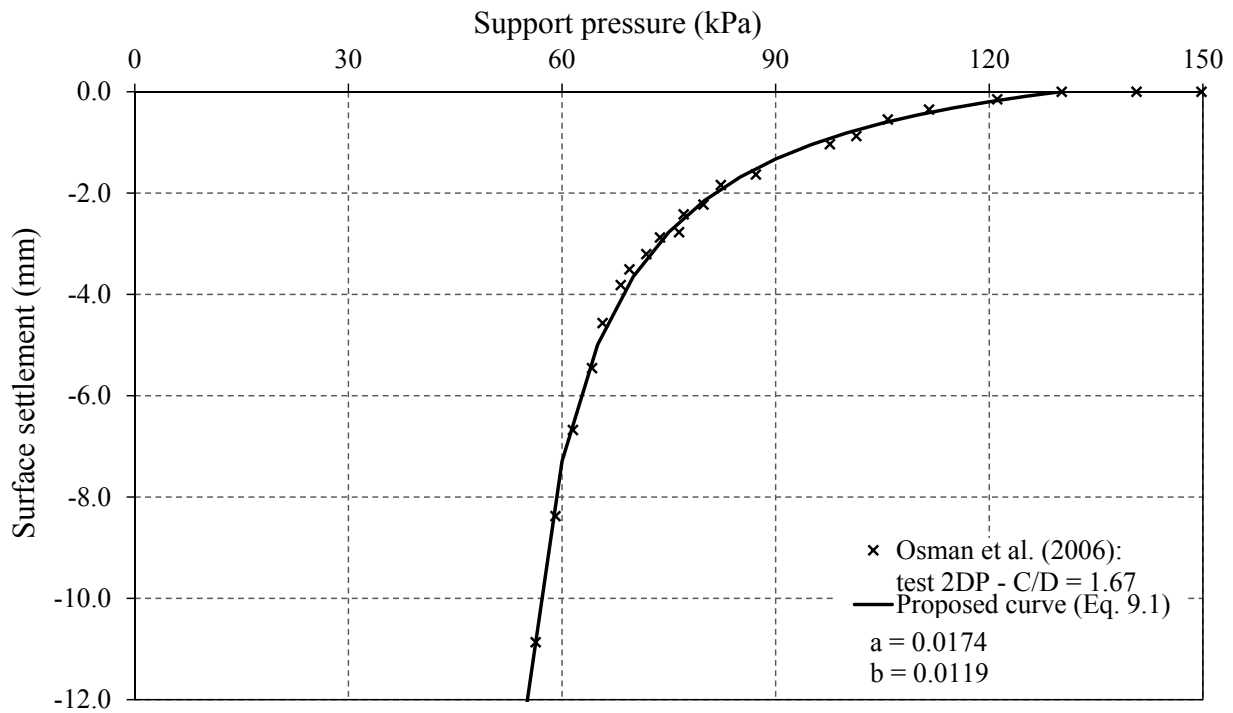
Figure 7.9 – Proposed curve and evolution of surface settlement above tunnel face (after Osman et al., 2006).
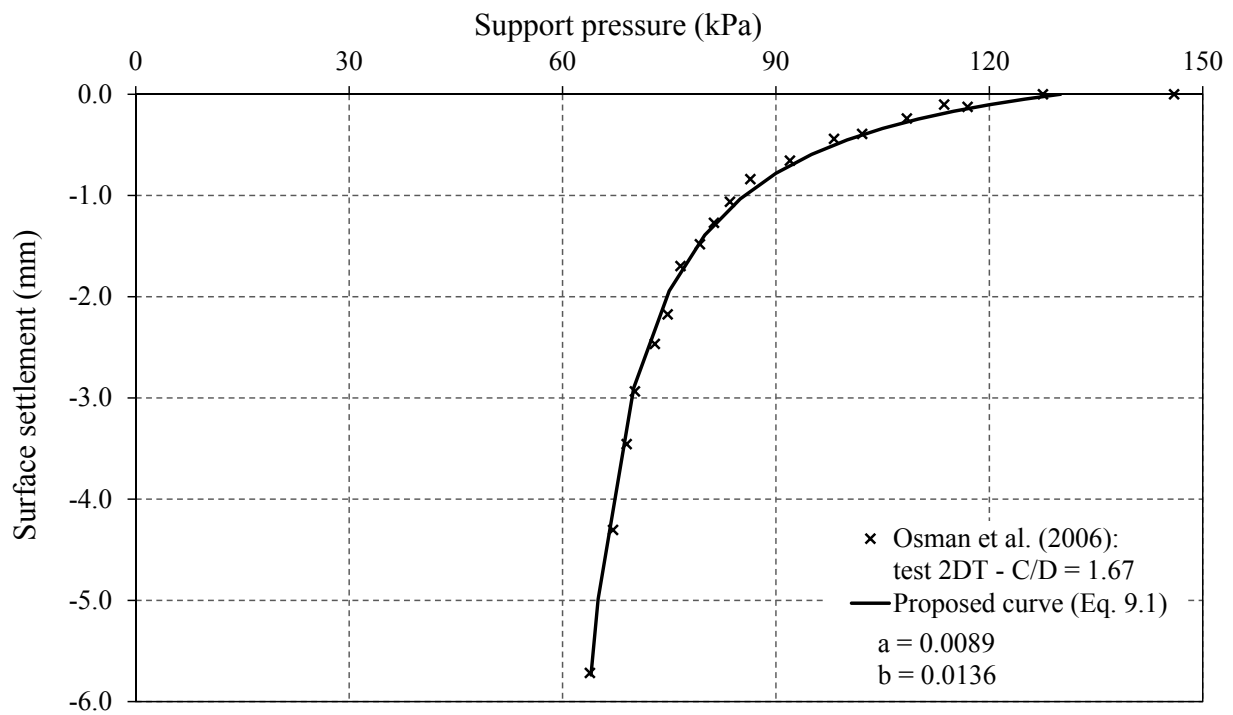
Figure 7.10 – Proposed curve and evolution of surface settlement above tunnel face (after Osman et al., 2006).

tuted by forepoling umbrella system, affects the plastic collapse mechanism surrounding a tunnel excavation in firm clay. The model used a compressed air-supported circular cavity to simulate the tunnel at a depth of C/D = 2 (D = 50 mm). Divall et al. (2016) indicated that the excavation was simulated by reducing the pressure from the average initial support pressure of 211 kPa. However, for this analysis, it was set the value of P_0 equals to 160 kPa. This because by applying
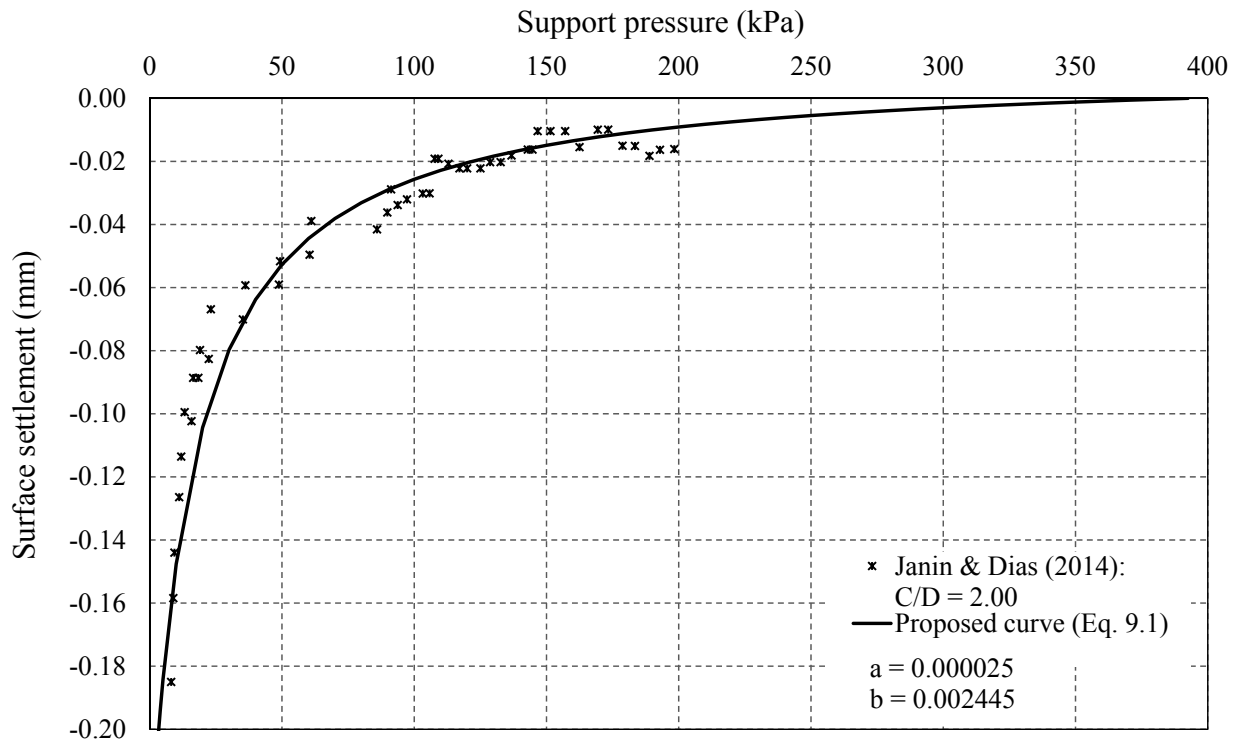
Figure 7.11 – Proposed curve and evolution of surface settlement above tunnel face (after Janin & Dias, 2014).
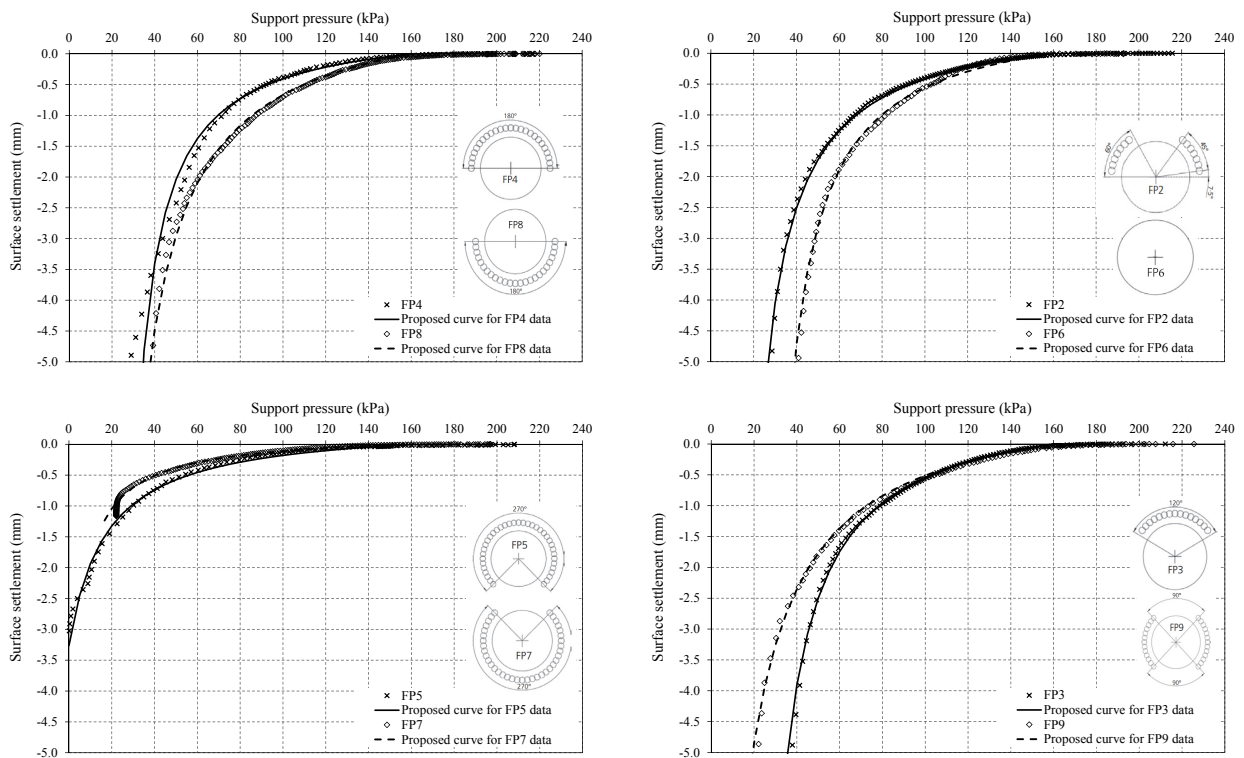
Figure 7.12 – Proposed curve for the different forepoling arrangements from centrifuges test results (after Divall et al., 2016).

support pressures between 211 and 160 kPa the ground response measured was practically null. As it is possible to see in all the arrangements centrifuge models, the proposed formulation agrees well each respective curve. In this regard, Table 7.4 shows the values of model fitting parameters

Table 7.4 – Values of model fitting parameters for each forepoling arrangement.

Forepoling arrangements	Model fitting parameters	
	a	b
FP2	0.00422	0.00665
FP3	0.00525	0.00699
FP4	0.00385	0.00720
FP5	0.00199	0.00564
FP6	0.00525	0.00722
FP7	0.00118	0.00601
FP8	0.00655	0.00687
FP9	0.00545	0.00602

obtained to each centrifuge model.

In contrast to the analysis of the case study presented in Section 7.5, the evaluation of the proposed equation by centrifuge test results neglects the consideration of variability of ground parameters. This is because the centrifuge test is a type of test where all the aspect involved in the preparation of the centrifuge model like soil, tunnel geometry, phreatic level, surcharge loads and tunnel internal support pressure can be controlled and monitored during the test. Therefore, it is unlikely to obtain an unclear behavior of groundmass due to tunneling as it is observed in the case study.

7.7 PHYSICAL MEANING DESCRIPTION OF CHOSEN EQUATION

Considering the nonlinearity and stress-strain behavior proposed by Duncan & Chang (1970), the following section presents the derivation of the parameters that express the chosen equation.

The slope of the proposed curve is obtained through the following mathematical derivation:

$$\left. \frac{dS_{\max}}{dP} \right|_{P \to P_0} = a \tag{7.12}$$

The value of the applied minimum support pressure (P_{min}) that produces the maximum surface settlement (S_{max}) is mathematically demonstrated by first transforming P (from Eq. 7.1) as a function of S_{max}, which is:

$$P = P_0 - \frac{S_{max}}{bS_{max} - a} \tag{7.13}$$

Therefore, as S_{max} approaches infinity, the value of P_{min} in which large settlements or tunnel face collapse will occur is estimated as follows:

$$\lim_{S_{\max} \to \infty} P_0 - \frac{S_{max}}{bS_{max} - a} = P_{\min} = P_0 - \frac{1}{b} \tag{7.14}$$
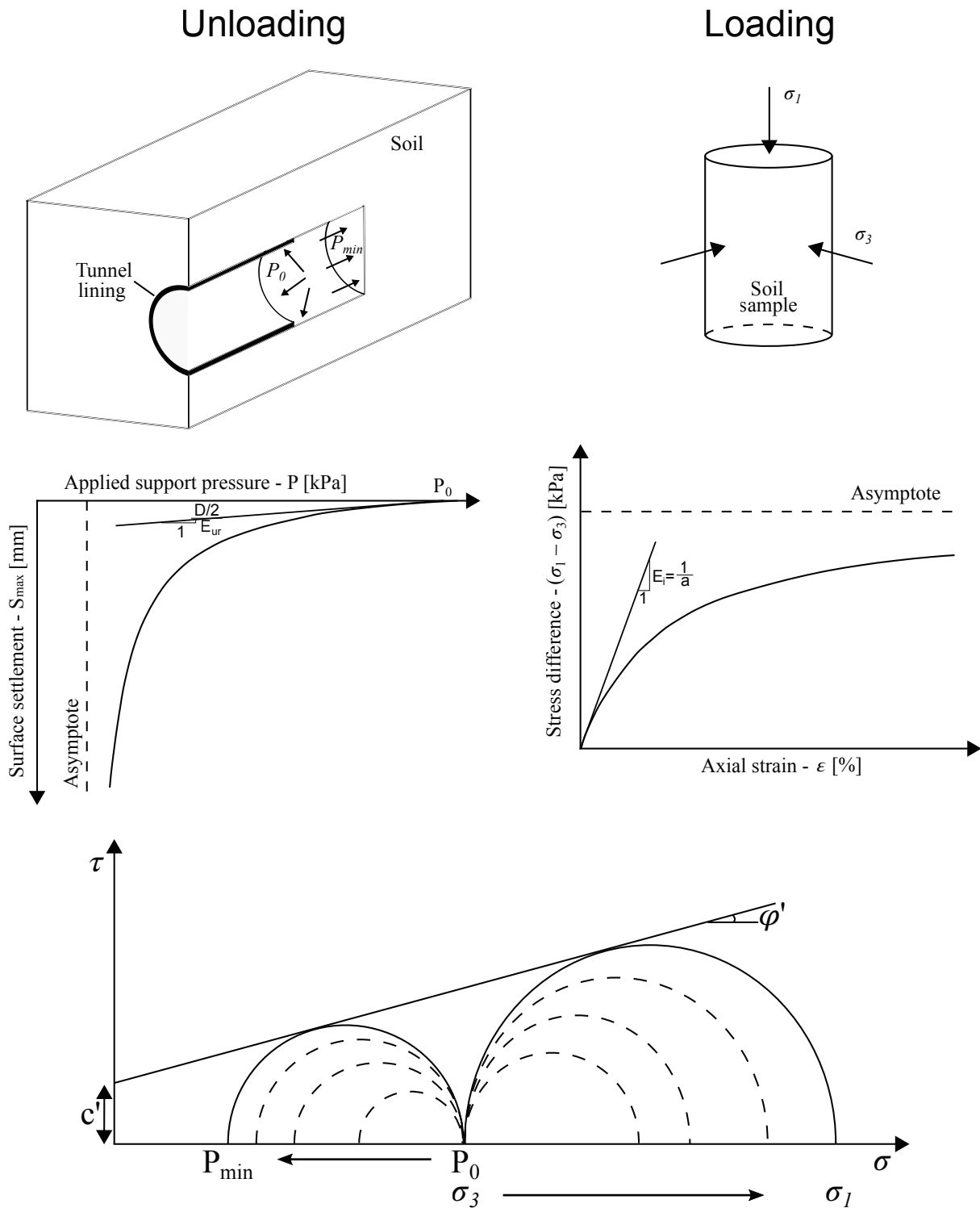
Figure 7.13 – Schematic representation of unloading and loading nonlinear stress-strain relationship.

Figure 7.13 shows the analogy adopted, from the Duncan & Chang work, for the description of the physical parameters of the chosen equation. The Duncan & Chang model is a representation of a triaxial loading test where the soil sample is subjected to an increment of differential load between the principal stress σ_1 and σ_3 and, consequently, the stress-strain relationship is registered. After a maximum increment of compressive strength, failure of the sample occurs an is expressed in terms of the Mohr-Coulomb failure criterion.

Tunnel construction with TBM may be considered as an inverse form of the loading process. The TBM face pressure constitutes the axial load, and the grout injection pressure constitutes the radial load. By keeping the grout pressure constant to a value of P_0 and decreasing the face pressure to a value of P_{min}. Then, the failure of groundmass occurs at a specific stress level of the Mohr-Coulomb failure criterion.

In this regard, the linear support pressure and surface settlement relationship obtained in Eq. 7.12 may be estimated. Then, the physical meaning of parameter a has the following expression:

$$a = \frac{D/2}{E_{ur}} \tag{7.15}$$

where D is the tunnel diameter and E_{ur} is the unloading-reloading elastic modulus. The reason for proposing to use $D/2$ instead of D is because the place of application of TBM internal support pressure is located in correspondence to the tunnel axis and should be expressed in mm. The analytical expression of the Mohr-Coulomb failure criterion (Figure 7.13) is written as:

$$\tau = c' + \sigma \tan \varphi' \tag{7.16}$$

where c' is the effective cohesion; φ' is the effective friction angle; τ and σ represent the shearing stress and normal stress on the physical plane through which material occurs. When failure takes place, the critical Mohr stress circle, derived from σ_1 and σ_3 is tangent to this line. Therefore, the values of τ and σ can be related to the principal stresses σ_1 and σ_3 by considering the following relation:

$$\begin{aligned} \tau &= \frac{1}{2}(\sigma_1 - \sigma_3)\cos\varphi' \\ \sigma &= \frac{1}{2}(\sigma_1 + \sigma_3) - \frac{1}{2}(\sigma_1 - \sigma_3)\sin\varphi' \end{aligned} \tag{7.17}$$

By relating Eqs. 7.16 and 7.17, it is found that the minimum TBM support pressure can be expressed as:

$$\begin{aligned} \sigma_3 &= k_a\sigma_1 - 2c'\sqrt{k_a} \\ P_{min} &= k_aP_0 - 2c'\sqrt{k_a} \end{aligned} \tag{7.18}$$

where $k_a = \frac{1-\sin\varphi'}{1+\sin\varphi'}$ and $\sqrt{k_a} = \frac{\cos\varphi'}{1+\sin\varphi'}$. So by relating Eqs. 7.14 and 7.18, it is obtained that:

$$P_{min} = P_0 - \frac{1}{b} = k_aP_0 - 2c'\sqrt{k_a} \tag{7.19}$$

Therefore, the physical meaning of parameter b of Eq. 7.1 can be estimated from Eq. 7.19 as:

$$b = \frac{1}{(1-k_a)P_0 + 2c'\sqrt{k_a}} \tag{7.20}$$

134

7.8   ALTERNATIVE PROPOSE OF CHOSEN EQUATION

Atkinson (2007) presented a tunnel support pressure and ground settlement relationship where the latter is represented in terms of volume loss - V_{loss} (Figure 2.37). The volume loss is a variable expressed as the ratio between the amount of over-excavated material and the theoretical volume per unit distance. This means that it has a dimensionless unit as the strain-variable. Moreover, the volume loss and strain have a certain similarity as both variables describe ground deformation.

So, as in the nonlinearity stress-strain relationship presented by Duncan & Chang (1970), the equation here analyzed can be alternatively expressed by using the volume loss variable instead of the maximum surface settlement.

$$V_{loss} = \frac{a\,(P_0 - P)}{1 - b\,(P_0 - P)} \tag{7.21}$$

In this manner, the S_{max} variable represented in the $y-axis$ in Figure 2.42 can be alternatively replaced by the V_{loss} variable. Therefore, by performing the analysis approach made in the previous section, the new form of a and b parameters of Eq. 7.21 have, respectively, the following expressions:

$$\begin{aligned} a &= \frac{1}{E_{ur}} \\ b &= \frac{1}{(1 - k_a)\,P_0 + 2c'\sqrt{k_a}} \end{aligned} \tag{7.22}$$

8 CONCLUSIONS AND RECOMMENDATIONS

8.1 CONCLUSIONS

The results of the mathematical and probabilistic approach presented in this research indicate that the primary objective of this study has been accomplished. A model for estimation of ground movement due to TBM tunneling was proposed. Therefore, the final goal will be that this model may be considered as an aid tool for practitioners during tunnel construction.

The proposed model consisted of a methodological approach divided into two main features. First, an approach that to deal with the variability of geotechnical properties and ground profile stratigraphy on the analysis of ground movement and, second, a procedure for model selection criteria for the estimation of surface settlements during TBM tunneling. In this sense, the case study of the extension of Line 5 of São Paulo Metro was used to validate this methodological approach.

Among the literature reviewed, various probabilistic methods exist and can be employed to describe these uncertainties. Even though, depending on the probabilistic approach selected the analyses may often require significant computation effort. Consequently, It was also proposed the implementation of a probabilistic and sensitivity analysis approach based on the Hybrid Point Estimate Method (HPEM). The HPEM allows the assessment of ground property variability and provides the basis for a sensitivity analysis using deterministic event tornado diagrams. Moreover, a simplified procedure for describing the variability of stratigraphy in term of random variables was also proposed.

Also, the extensive literature review presented in Chapters 2.2, 2.3 and 2.4 allowed to have an overview of the concepts, variables, and approaches for analyzing tunnel face stability, ground movement and mathematical model in tunneling, respectively. The discussion offered at the end of each respective chapter aimed to justify the selection of the path undertaken which allowed to arrive in satisfactory results in this research.

The realization of numerical analyses supported the application of the methodological approach here proposed. Therefore, in order to perform the numerical analyses, a series of geological, geotechnical, TBM performance and monitoring data were collected, from the São Paulo metro engineering department, and consequently statistically analyzed. This allowed a better proposal of the values of the input variables. Furthermore, the statistical analysis applied to those data showed that the Lognormal and Normal probability density function (PDF) fitted better to each one of the collected data respect to the other functions that were considered. This result agreed with the current geotechnical engineering practice in which Normal and Lognormal PDF can be used to describe well a geotechnical variable in probabilistic terms.

The proposed probabilistic framework, discussed in Chapter 5, allowed the assessment of which geotechnical variables had a significant impact on the development of the ground move-

ment. The selection of an optimum type of constitutive model may be made following this approach, thus, allowing a more efficient computation of 3D numerical analyses.

The deterministic event tornado diagrams provided essential and complementary information about the sensitivity of the input variables. Furthermore, the procedure for describing the variability of stratigraphy showed that could be successfully employed in those geological profiles with a recurrent persistence of every soil layer along with the profile. The junction of geotechnical parameters and stratigraphy profile as input variables in the probabilistic analyses of tunneling problems lead to a robust analysis of the induced ground movement.

The sensitivity analysis performed and presented in Chapter 6, by means of 3D numerical analyses, put in evidence the significant impact that the coefficient of earth pressure at rest (k_0) has on the Maximum surface settlement (S_{max}), Trough width parameter (i) and volume loss (V_{loss}) for the case study analyzed.

The variables k_0, E, γ and the depth of 1st layer is valid for the tunnel stretch between Hospital São Paulo and Santa Cruz Stations of the extension of São Paulo Metro Line 5. Influence of these input variables on the other tunnel stretches of the extension of Line 5 here studied need to be verified by reproducing the proposed probabilistic approach. In general, it is intended that this proposal can be employed in diverse tunneling projects. In this way, the proposed probabilistic framework will serve as a tool to better analyze tunneling-induced ground movements.

In regards with the mathematical approach, the procedure, exemplified in Chapter 7, for model selection criteria proposed in this thesis allowed to choose the best Immediate Surface Settlement Curve and fitting parameters to describe the ground movements due to TBM tunneling. The selected model, an adaptation of the nonlinear stress-strain curve proposed by Duncan & Chang (1970), may provide a good representation of ground movement for centrifuges test analysis. Additionally, in tunneling practice, the proposed curve may provide a reasonable representation of the variability of ground movements (S_{max} or V_{loss}) by incorporation of the two curves that will express the lower and upper confidence limits of the model.

8.2 RECOMMENDATIONS FOR FUTURE RESEARCH

As recommendations for future research, it is suggested the analysis of the formulation here encountered by the investigation of the impact of ground movements due to TBM tunneling when changing tunnel cover-to-diameter C/D ratio. In order to perform these analyses, it is praised to perform a series of centrifuge tests, either on cohesive and non-cohesive soils, as well as with or without the presence of water level above tunnel crown. The tunnel cover, tunnel diameter, and water level height if any are already considered in the formulation when P_0 is estimated. Even though, could be of interest to compare the variation these variables on the formulation with the respective results of centrifuge tests.

The extension of Line 5 of São Paulo metro here studied represent a perfect case of tunneling project in urban area. With all the information provided, it was possible to propose a probabilistic

approach that considers the uncertainty analysis of input geotechnical variables for a practical representation of ground movement variability. So, in order to understand the extension of applicability the probabilistic framework proposed in this work. It is also recommended to apply this approach in other TBM tunneling projects elsewhere where the geological and geotechnical conditions will be different from the one here studied, to finally make a comparison of ground movement variability between the real case and predicted by the formulation.

The face stability analysis presented in Chapter 6 was made by considering a deterministic analysis for the estimation of the internal support pressure in both analytical methods. For a better consideration of soil property uncertainties, it is recommended to perform non-deterministic analysis in the proposed methodological approach and evaluate the probability of failure, P_f, of tunnel face stability on the original formulation here found.

Finally, the formulation here proposed was derived by considering the groundmass to be fully in saturated soil condition. Therefore, it could be interesting to improve the formulation to consider the unsaturated condition of groundmass and foresee how this effect may alter the groundmass response due to TBM tunneling. The best option to realize this analysis is by carrying out centrifuge tests in undrained condition coupled with 3D numerical analyses.

REFERENCES

ABAQUS (2016). Abaqus Theory Manual. Abaqus 6.16 Edition.

ABMS (2013). TWIN CITIES – Solos das regiões metropolitanas de São Paulo e Curitiba. Editado pela ABMS.

AHMED, M. (2011). Investigation of tunnel face stability and ground movements using transparent soil models. Ph.D. thesis, Polytechnic Institute of New York University.

AKAGI, H. & KOMIYA, K. (1996). Finite element simulation of shield tunnelling processes in soft ground. Proceedings International Symposium on Geotechnical Aspects of Underground Construction in Soft Ground, : 447–452.

AKAIKE, H. (1974). A new look at the statistical model identification. IEEE transactions on automatic control, 19 (6): 716–723.

AL-HOMOUD, A. S. & TAHTAMONI, W. W. (2001). Modeling Uncertainty in Seismic Stability and Earthquake Induced Displacement of Earth Slopes Under Short Term Conditions. Internatioal Conferences on Recent Advances in Geotechnical Earthquake Engineering and Soil Dynamics, .

ALARCÓN, J. (2014). Gestão dos Riscos Geomecânicos Devidos à Escavação de Túneis Urbanos: Aplicação ao Metrô de Bogotá. Ph.D. thesis, Departamento de Engenharia Civil e Ambiental, Universidade de Brasília, Brasília, DF.

ALONSO, E. E., GENS, A. & JOSA, A. (1990). A constitutive model for partially saturated soils. Géotechnique, 40 (3): 405–430.

ANAGNOSTOU, G. & KOVÁRI, K. (1994). The face stability of slurry-shield-driven tunnels. Tunnelling and Underground Space Technology, 9 (2): 165 – 174.

ANAGNOSTOU, G. & KOVÁRI, K. (1996). Face stability conditions with earth-pressure-balanced shields. Tunnelling and Underground Space Technology, 11 (2): 165 – 173.

ANG, H.-S. A. & TANG, H. W. (1975). Probability Concepts in Engineering Planning and Design. Vol. 1, Basic Principles. John Wiley & Sons.

ASSIS, A. (2002). Métodos estatísticos e probabilísticos em geotecnia. Apostilla. Universidade de Brasília, Brasília, Brasil.

ATKINSON, J. (2007). The mechanics of soils and foundations. CRC Press.

ATKINSON, J. H. & POTTS, D. M. (1977). Stability of a shallow circular tunnel in cohesionless soil. Géotechnique, 27 (2): 203–215.

ATTEWELL, B. & WOODMAN, P. (1982). Predicting the dynamics of ground settlement and its derivatives caused by tunneling in soil, 15 (8): 13–22.

ATTEWELL, P. B., YEATES, J. & SELBY, A. R. (1986). Soil movements induced by tunnelling and their effects on pipelines and structures, .

AUGARDE, C., BURD, H. & HOULSBY, G. (1995). A three-dimensional finite element model of tunnelling. In: Proceedings of NUMOG V, Davos, Switzerland. pp. 457–462.

AVGERINOS, V., POTTS, D. M., STANDING, J. R. & WAN, M. S. P. (2018). Predicting tunnelling-induced ground movements and interpreting field measurements using numerical analysis: Crossrail case study at Hyde Park. Géotechnique, 68 (1): 31–49.

AYDIN, A. (2004). Fuzzy set approaches to classification of rock masses. Engineering Geology, 74 (3): 227 – 245.

BAECHER, G. & CHRISTIAN, J. (2005). Reliability and Statistics in Geotechnical Engineering. John Wiley & Sons.

BARI, M. W. & SHAHIN, M. A. (2014). Probabilistic design of ground improvement by vertical drains for soil of spatially variable coefficient of consolidation. Geotextiles and Geomembranes, 42 (1): 1 – 14.

BENJAMIN, J. R. & CORNELL, C. A. (1970). Probability, statistics, and decision for civil engineers. McGraw-Hill Books.

BHATTACHARYA, G., ISLAM, M. A. & GUHA, S. (2009). Probabilistic slope analysis considering various distributions for factor of safety. In: Indian Geotechnical Conference, Guntur, India. pp. 787–791.

BLIGHT, G. E. & LEONG, E. C. (2012). Mechanics of residual soils. CRC Press.

BOX, G. E. P. & WILSON, K. B. (1951). On the Experimental Attainment of Optimum Conditions. Journal of the Royal Statistical Society. Series B (Methodological), 13 (1): 1–45.

BROERE, W. (2001). Tunnel face stability & new CPT applications. Ph.D. thesis, TU Delft, Delft University of Technology.

BROERE, W. & BRINKGREVE, R. (2002). Phased simulation of a tunnel boring process in soft soil. In: Numerical Methods in Geotechnical Engineering. pp. 529–536.

BROMS, B. B. & BENNERMARK, H. (1967). Stability of clay at vertical openings. Journal of Soil Mechanics & Foundations Div, .

BUCHER, C. (2009). Computational Analysis of Randomness in Structural Mechanics: Structures and Infrastructures Book Series. Structures and Infrastructures. CRC Press.

BURNHAM, K. & ANDERSON, D. (2002). Model Selection and Multimodel Inference: A Practical Information-theoretic Approach. Intelligence, SS. of Lncs; 1501. Springer.

BURY, K. (1999). Statistical distributions in engineering. Cambridge University Press.

CAMARGO, J. B. & ALMEIDA, J. R. (1999). The Safety Analysis Case in the São Paulo Metro. In: Towards System Safety. Springer, pp. 99–110.

CAQUOT, A. & KÉRISEL, J. (1956). Traité de mécanique des sols. Gauthier-Villars.

CARRANZA-TORRES, C. (2004). Computation of Factor of Safety for Shallow Tunnels using Caquot's Lower Bound Solution. Tech. rep., Technical Report for Geodata.

CECÍLIO JR, M., VALENZUELA, L., VILLOUTA, A. & NEGRO, A. (2014). Reliability analysis for the excavation of University of Chile Station, Line 3 of Santiago Metro. In: Proceedings of the World Tunnel Congress.

CELESTINO, T., GOMES, R. & BORTOLUCCI, A. (2000). Errors in ground distortions due to settlement trough adjustment. Tunnelling and Underground Space Technology, 15 (1): 97 – 100.

CHAMBON, P. & CORTé, J. (1994). Shallow Tunnels in Cohesionless Soil: Stability of Tunnel Face. Journal of Geotechnical Engineering, 120 (7): 1148–1165.

CHAPMAN, D. N., METJE, N. & STARK, A. (2017). Introduction to tunnel construction. Vol. 3. Crc Press.

CHARBEL, P. A. (2015). Gerenciamento de risco aplicado à diluição de minério. Ph.D. thesis, Departamento de Engenharia Civil e Ambiental, Universidade de Brasília, Brasília, DF.

CHEN, M., JIANG, Y., LU, Y. & XU, C. (2016). On the Calculation Method Based on the Exponential Model for Rainfall Infiltration. Electronic Journal of Geotechnical Engineering, 21: 10587–10598.

CHI, S.-Y., CHERN, J.-C. & LIN, C.-C. (2001). Optimized back-analysis for tunneling-induced ground movement using equivalent ground loss model. Tunnelling and Underground Space Technology, 16 (3): 159 – 165.

CLAESKENS, G. & HJORT, N. (2008). Model Selection and Model Averaging. Cambridge Series in Statistical and Probabilistic Mathematics. Cambridge University Press.

CLEMEN, R. (1996). Making Hard Decisions: An Introduction to Decision Analysis. Business Statistics Series. Duxbury Press.

DAVIS, E. H., GUNN, M. J., MAIR, R. J. & SENEVIRATINE, H. N. (1980). The stability of shallow tunnels and underground openings in cohesive material. Géotechnique, 30 (4): 397–416.

DIVALL, S., TAYLOR, R. N. & XU, M. (2016). Centrifuge modelling of tunnelling with forepoling. International Journal of Physical Modelling in Geotechnics, 16 (2): 83–95.

DNV (2012). Statistical representation of soil data. Tech. rep., DET NORSKE VERITAS AS, Paper No. DNV-RP-C207.

DUNCAN, J. M. & CHANG, C.-Y. (1970). Nonlinear analysis of stress and strain in soils. Journal of Soil Mechanics & Foundations Div, .

DYM, C. (2004). Principles of Mathematical Modeling. Principles of Mathematical Modeling. Elsevier Science.

EL GONNOUNI, M., RIOU, Y. & HICHER, P. Y. (2005). Geostatistical method for analysing soil displacement from underground urban construction. Géotechnique, 55 (2): 171–182.

FABER, M. (2012). Statistics and Probability Theory: In Pursuit of Engineering Decision Support. Topics in Safety, Risk, Reliability and Quality. Springer Netherlands.

FARGNOLI, V., BOLDINI, D. & AMOROSI, A. (2013). TBM tunnelling-induced settlements in coarse-grained soils: The case of the new Milan underground line 5. Tunnelling and Underground Space Technology, 38: 336 – 347.

FARGNOLI, V., GRAGNANO, C., BOLDINI, D. & AMOROSI, A. (2015). 3D numerical modelling of soil–structure interaction during EPB tunnelling. Géotechnique, 65 (1): 23–37.

FENTON, G. & GRIFFITHS, D. (2008). Risk Assessment in Geotechnical Engineering. Wiley.

FIB (2013). Fib Model Code for Concrete Structures 2010. Ernst & Sohn, a Wiley brand.

FRANZIUS, J. N. & POTTS, D. M. (2005). Influence of Mesh Geometry on Three-Dimensional Finite-Element Analysis of Tunnel Excavation. International Journal of Geomechanics, 5 (3): 256–266.

FRANZIUS, J. N., POTTS, D. M. & BURLAND, J. B. (2005). The influence of soil anisotropy and K0 on ground surface movements resulting from tunnel excavation. Géotechnique, 55 (3): 189–199.

FUENTES, R. (2015). Internal forces of underground structures from observed displacements. Tunnelling and Underground Space Technology, 49: 50 – 66.

GELDER, P. (2000). Statistical methods for the risk-based design of civil structures. Ph.D. thesis, Delft University of Technology.

GERSHENFELD, N. & GERSHENFELD, N. (1999). The Nature of Mathematical Modeling. Cambridge University Press.

GHANEM, R. & SPANOS, P. (1991). Stochastic Finite Elements: A Spectral Approach. Civil, Mechanical and Other Engineering Series. Dover Publications.

GITIRANA JR., G. F. N. (1999). Modelagem Numérica do Comportamento de Solos Não Saturados Considerando Modelos Elásticos e de Estados Críticos. Master's thesis, Publication G.DM - 63A/99, Department of Civil and Environmental Engineering, University of Brasilia, Brasília, DF, 126p.

GITIRANA JR., G. F. N. (2005). Weather-related geo-hazard assessment model for railway embankment stability. Ph.D. thesis, University of Saskatchewan, SK, Canada, 403p.

GOUTSIAS, J., MAHLER, R. & NGUYEN, H. (1997). Random Sets: Theory and Applications. The IMA Volumes in Mathematics and its Applications. Springer New York.

GPE (2013). Empreendimentos do Metrô. Tech. rep., GERÊNCIA DE PLANEJAMENTO EM-PRESARIAL, Editado pela Companhia do Metropolitano de São Paulo.

GREENWOOD, J. A., LANDWEHR, J. M., MATALAS, N. C. & WALLIS, J. R. (1979). Probability weighted moments: definition and relation to parameters of several distributions expressable in inverse form. Water resources research, 15 (5): 1049–1054.

GRIFFITHS, D. & FENTON, G. (2007). Probabilistic Methods in Geotechnical Engineering. CISM International Centre for Mechanical Sciences. Springer Vienna.

GUGLIELMETTI, V., GRASSO, P., MAHTAB, A. & XU, S. (2008). Mechanized Tunnelling in Urban Areas: Design methodology and construction control. Taylor & Francis.

HALDAR, A. & MAHADEVAN, S. (2000). Probability, reliability, and statistical methods in engineering design. John Wiley.

HERRERA, I. & PINDER, G. (2012). Mathematical Modeling in Science and Engineering: An Axiomatic Approach. John Wiley & Sons.

HORN, N. (1961). Horizontaler Erddruck auf senkrechte Anschlussflächen von Tunnelröhren. Landerskonferenz der ungarischen Tiefbauindustrie, .

HOSKING, J. R. M. (1990). L-Moments: Analysis and Estimation of Distributions Using Linear Combinations of Order Statistics. Journal of the Royal Statistical Society. Series B (Methodological), 52 (1): 105–124.

HOSSEINI, S. A., MOHAMMADNEJAD, M., HOSEINI, S., MIKAEIL, R. & TOLOOIYAN, A. (2012). Numerical and analytical investigation of ground surface settlement due to subway excavation. Geosciences, 2 (6): 185–191.

HUAT, B. B., TOLL, D. G. & PRASAD, A. (2012). Handbook of tropical residual soils engineering. CRC Press.

HUBER, M. (2013). Soil variability and its consequences in geotechnical engineering. Ph.D. thesis, Institut für Geotechnik der Universität Stuttgart.

HUBER, M., HICKS, M. A., VERMEER, P. A. & MOORMANN, C. (2010). Probabilistic calculation of differential settlement due to tunneling. In: Proceedings of the 8th International Probabilistic Workshop, Szczecin, Poland. Akademia Morska, Szczecin, Poland, pp. 1–13.

HURVICH, C. M. & TSAI, C.-L. (1989). Regression and time series model selection in small samples. Biometrika, 76 (2): 297–307.

IBGE. (2016). Nota Técnica – Estimativas da população dos municípios brasileiros com data de referência em 1º de Julho de 2016. Tech. rep.

ICE (1996). Sprayed Concrete Linings (NATM) for Tunnels in Soft Ground. Engineering Management. Thomas Telford.

ISAAKS, E. & SRIVASTAVA, R. (1989). Applied Geostatistics. Oxford University Press.

JACOBSZ, S. W., STANDING, J. R., MAIR, R. J., HAGIWARA, T. & SUGIYAMA, T. (2004). Centrifuge Modelling of Tunnelling near Driven Piles. SOILS AND FOUNDATIONS, 44 (1): 49–56.

JANCSECZ, S. & STEINER, W. (1994). Face support for a large Mix-Shield in heterogeneous ground conditions. Springer US, Boston, MA, pp. 531–550.

JANIN, J. & DIAS, D. (2014). Tunnel face reinforcement by bolting, Numerical modelling of centrifuge tests. Soil and Rocks, 37 (1).

JANSSEN, H. A. (1895). Versuche über Getreidedruck in Silozellen. Zeitschrift des Vereins deutscher Ingenieure XXXIX, 35: 1045–1049.

KASPER, T. & MESCHKE, G. (2004). A 3D finite element simulation model for TBM tunnelling in soft ground. International Journal for Numerical and Analytical Methods in Geomechanics, 28 (14): 1441–1460.

KASPER, T. & MESCHKE, G. (2006a). A numerical study of the effect of soil and grout material properties and cover depth in shield tunnelling. Computers and Geotechnics, 33 (4): 234 – 247.

KASPER, T. & MESCHKE, G. (2006b). On the influence of face pressure, grouting pressure and TBM design in soft ground tunnelling. Tunnelling and Underground Space Technology, 21 (2): 160 – 171.

KAVVADAS, M., LITSAS, D., VAZAIOS, I. & FORTSAKIS, P. (2017). Development of a 3D finite element model for shield EPB tunnelling. Tunnelling and Underground Space Technology, 65: 22 – 34.

KENDALL, D. (1974). Foundations of a theory of random sets. In: In stochastic Geometry. Harding & Kendall (eds.), New York, Wiley, pp. 322–376.

KIMURA, T. & MAIR, R. J. (1981). Centrifugal testing of model tunnels in soft clay. In: Proc. 10th Int. Conf. Soil Mech. and Found. Engg. Vol. 1. pp. 319–322.

KOLYMBAS, D. (2005). Tunnelling and Tunnel Mechanics: A Rational Approach to Tunnelling. Springer Berlin Heidelberg.

KOMIYA, K., SOGA, K., AKAGI, H., HAGIWARA, T. & BOLTON, M. D. (1999). Finite element modelling of excavation advancement process of a shield tunnelling machine. SOILS AND FOUNDATIONS, 39 (3): 37–52.

KONDNER, R. L. (1963). Hyperbolic stress-strain response: cohesive soils. Journal of the Soil Mechanics and Foundations Division, 89 (1): 115–144.

KOOL, J., PARKER, J. & VAN GENUCHTEN, M. (1987). Parameter estimation for unsaturated flow and transport models — A review. Journal of Hydrology, 91 (3): 255 – 293.

KOOREVAAR, P., MENELIK, G. & DIRKSEN, C. (1983). Elements of soil physics. Developments in soil science. Elsevier.

KRAUSE, T. (1987). Schildvortieb mit flüssigkeits-und erdgestützer Ortsbrust. Ph.D. thesis, Technischen Universität Carolo – Wilhelmina, Braunschweig.

KULATILAKE, P., WATHUGALA, D. & STEPHANSSON, O. (1993). Stochastic three-dimensional joint size, intensity and system modelling and a validation to an area in stripa mine, Sweden. SOILS AND FOUNDATIONS, 33 (1): 55–70.

KULHAWY, F. H. (1992). On the evaluation of static soil properties. In: Stability and performance of slopes and embankments II. ASCE, pp. 95–115.

LAMBE, T. W. (1973). Predictions in soil engineering. Géotechnique, 23 (2): 151–202.

LAMBRUGHI, A., RODRíGUEZ, L. M. & CASTELLANZA, R. (2012). Development and validation of a 3D numerical model for TBM–EPB mechanised excavations. Computers and Geotechnics, 40: 97 – 113.

LANDWEHR, J. M., MATALAS, N. C. & WALLIS, J. R. (1979). Probability weighted moments compared with some traditional techniques in estimating Gumbel Parameters and quantiles. Water Resources Research, 15 (5): 1055–1064.

LECA, E. & DORMIEUX, L. (1990). Upper and lower bound solutions for the face stability of shallow circular tunnels in frictional material. Géotechnique, 40 (4): 581–606.

LECA, E. & NEW, B. (2007). Settlements induced by tunneling in Soft Ground. Tunnelling and Underground Space Technology, 22 (2): 119 – 149.

LEE, K.-H., BANG, J.-H., LEE, I.-M. & SHIN, Y.-J. (2013). Use of fuzzy probability theory to assess spalling occurrence in underground openings. International Journal of Rock Mechanics and Mining Sciences, 64: 60 – 67.

LEE, K. M. & ROWE, R. K. (1989). Deformations caused by surface loading and tunnelling: the role of elastic anisotropy. Géotechnique, 39 (1): 125–140.

LEE, K. M. & ROWE, R. K. (1991). An analysis of three-dimensional ground movements: the Thunder Bay tunnel. Canadian Geotechnical Journal, 28 (1): 25–41.

LEE, K. M., ROWE, R. K. & LO, K. Y. (1992). Subsidence owing to tunnelling. I. Estimating the gap parameter. Canadian Geotechnical Journal, 29 (6): 929–940.

LI, C., WANG, W. & WANG, S. (2012). Maximum-entropy method for evaluating the slope stability of earth dams. Entropy, 14 (10): 1864–1876.

LI, K. S. (1992). Point-Estimate Method for Calculating Statistical Moments. Journal of Engineering Mechanics, 118 (7): 1506–1511.

LIN, B.-H., YU, Y., BATHURST, R. J. & LIU, C.-N. (2016). Deterministic and probabilistic prediction of facing deformations of geosynthetic-reinforced MSE walls using a response surface approach. Geotextiles and Geomembranes, 44 (6): 813 – 823.

LITWISZYN, J. (1957). The theories and model research of movements of ground masses. In: Proceedings of European Congress Ground Movement, Leeds, Uk. pp. 203–209.

LIU, W., WU, X., ZHANG, L. & WANG, Y. (2017). Probabilistic analysis of tunneling-induced building safety assessment using a hybrid FE-copula model. Structure and Infrastructure Engineering, 14 (8): 1065–1081.

LOGANATHAN, N. & POULOS, H. G. (1998). Analytical Prediction for Tunneling-Induced Ground Movements in Clays. Journal of Geotechnical and Geoenvironmental Engineering, 124 (9): 846–856.

LOW, B. (2014). FORM, SORM, and spatial modeling in geotechnical engineering. Structural Safety, 49: 56 – 64.

LOW, B. & PHOON, K. (2002). Practical first-order reliability computations using spreadsheet. In: Proc., Probabilistics in Geotechnics: Technical and Economic Risk Estimation. Verlag Gluckauf GmbH. Essen, pp. 39–46.

LUNARDI, P. (2008). Design and Construction of Tunnels: Analysis of Controlled Deformations in Rock and Soils (ADECO-RS). Springer Berlin Heidelberg.

MACKLIN, S. (1999). The prediction of volume loss due to tunnelling in overconsolidated clay based on heading geometry and stability number. Ground engineering, 32 (4): 30–33.

MAIDL, B., HERRENKNECHT, M., MAIDL, U., WEHRMEYER, G. & STURGE, D. (2012). Mechanised Shield Tunnelling. John Wiley & Sons.

MAIDL, B., THEWES, M., MAIDL, U. & STURGE, D. (2013). Handbook of Tunnel Engineering I: Structures and Methods. Wiley.

MARQUES, S. H., BEER, M., GOMES, A. T. & HENRIQUES, A. A. (2015). Limit state imprecise interval analysis in geotechnical engineering. In: Geotechnical Safety and Risk V. IOS Press, pp. 383–388.

MARSHALL, A., FARRELL, R., KLAR, A. & MAIR, R. (2012). Tunnels in sands: the effect of size, depth and volume loss on greenfield displacements. Géotechnique, 62 (5): 385–399.

MASSAD, F. (2013). TWIN CITIES – Solos das regiões metropolitanas de São Paulo e Curitiba. Editado pela ABMS, Ch. Resistência ao Cisalhamento e Deformabilidade dos Solos Sedimentares de São Paulo, pp. 107–133.

MATHERON, G. (1975). Random sets and integral geometry. Wiley series in probability and mathematical statistics: Probability and mathematical statistics. Wiley.

MEGUID, M., SAADA, O., NUNES, M. & MATTAR, J. (2008). Physical modeling of tunnels in soft ground: A review. Tunnelling and Underground Space Technology, 23 (2): 185 – 198.

MIRANDA, T. (2007). Geomechanical parameters evaluation in underground structures : artificial intelligence, bayesian probabilities and inverse methods. Ph.D. thesis, Universidade de Minho, Escola de Engenharia.

MIRO, S., KöNIG, M., HARTMANN, D. & SCHANZ, T. (2015). A probabilistic analysis of subsoil parameters uncertainty impacts on tunnel-induced ground movements with a back-analysis study. Computers and Geotechnics, 68: 38 – 53.

MOHKAM, M. & BOUYAT, C. (1984). Le soutènement liquide–dispositif de simulation d'un bouclier à pression de boue. In: International Congress AFTES. pp. 85–95.

MOHKAM, M. & BOUYAT, C. (1985). Research studies for slurry shield tunneling. In: 4th International Conference of the Institution of Mining and Metallurgy. pp. 235–241.

MOHKAM, M. & WONG, Y. (1989). Three dimensional stability analysis of the tunnel face under fluid pressure. Numerical Methods in Geomechanics, : 2271–2287.

MOLLON, G. (2010). Etude déterministe et probabiliste du comportement des tunnels. Ph.D. thesis, L'institut national des sciences appliquées de Lyon.

MOLLON, G., DIAS, D. & SOUBRA, A.-H. (2013). Probabilistic analyses of tunneling-induced ground movements. Acta Geotechnica, 8 (2): 181–199.

MONNET, J. (2015). In Situ Tests in Geotechnical Engineering. Civil engineering and geomechanics series. Wiley.

MONTEIRO, F., GURGUEIRA, M. D. & ROCHA, H. C. (2013). TWIN CITIES – Solos das regiões metropolitanas de São Paulo e Curitiba. Editado pela ABMS, Ch. Geologia da Região Metropolitana de São Paulo, pp. 17–46.

MOORE, R. E. (1969). Interval analysis. Prince-Hall, Englewood Cliffs, NJ, .

MURAYAMA, S., ENDO, M., HASHIBA, T., YAMAMOTO, K. & SASAKI, H. (1966). Geotechnical aspects for the excavating performance of the shield machines. In: The 21st annual lecture in meeting of Japan Society of Civil Engineers. p. 265.

NAPA-GARCÍA, G., BECK, A. & CELESTINO, T. (2014). Reliability of face stability in shallow tunnel using the Caquots lower bound solution. Iguaçu: Tunnels for a better Life—Proceedings of the World Tunnel Congress.

NAPA-GARCíA, G. F., BECK, A. T. & CELESTINO, T. B. (2017). Reliability analyses of underground openings with the point estimate method. Tunnelling and Underground Space Technology, 64: 154 – 163.

NASEKHIAN, A. (2011). Application of non-probabilistic and probabilistic concepts in finite elemento analysis for tunneling. Ph.D. thesis, TU Graz, Institute of Soil Mechanics.

NBR 6118:2003 (2003). Projeto de estruturas de concreto – Procedimento. Tech. rep., ABNT NBR, Rio de Janeiro.

NEW, B. M. & BOWERS, K. H. (1994). Ground movement model validation at the Heathrow Express trial tunnel. Springer US, Boston, MA, pp. 301–329.

NG, C. W. & LEE, G. T. (2005). Three-dimensional ground settlements and stress-transfer mechanisms due to open-face tunnelling. Canadian Geotechnical Journal, 42 (4): 1015–1029.

NISHII, R., EI, S.-I., KOISO, M., OCHI AI, H., OK AD A, K., SAITO, S. & SHIRAI, T. (2014). A Mathematical Approach to Research Problems of Science and Technology. Springer.

O'CARROLL, J. B. (2005). A Guide to Planning, Constructing, and Supervising Earth Pressure Balance TBM Tunneling. Parsons Brinckerhoff.

OSMAN, A. S., BOLTON, M. D. & MAIR, R. J. (2006). Predicting 2D ground movements around tunnels in undrained clay. Géotechnique, 56 (9): 597–604.

PBA (2010). Linha 5 – Lilás: Trecho Largo Treze – Chácara Klabin com Pátio Guido Caloi. Tech. rep., PLANO BÁSICO AMBIENTAL RT 5.00.00.00/8N4-004-Rev C, Sistran Engenharia, São Paulo.

PECK, R. B. (1969). Deep excavations and tunneling in soft ground. In: Proc. 7th International Conference on Soil Mechanics and Foundation Engineering, Mexico City, State of the Art Volume, : 225–290.

PESCHL, G. (2004). Reliability analyses in geotechnics with the random set finite element method. Ph.D. thesis, Graz University of Technology.

PHOON, K. (2008). Reliability-Based Design in Geotechnical Engineering: Computations and Applications. Taylor & Francis.

PHOON, K.-K. & KULHAWY, F. H. (1999a). Characterization of geotechnical variability. Canadian Geotechnical Journal, 36 (4): 612–624.

PHOON, K.-K. & KULHAWY, F. H. (1999b). Evaluation of geotechnical property variability. Canadian Geotechnical Journal, 36 (4): 625–639.

REPETTO, L., TUNINETTI, A., GUGLIELMETTI, V. & RUSSO, G. (2006). Shield tunneling in sensitive areas: A new design approach for the optimization of the construction-phase management. Tunnelling and Underground Space Technology, 21 (3): 270, safety in the Underground Space - Proceedings of the ITA-AITES 2006 World Tunnel Congress and 32nd ITA General Assembly.

RISI, R., JALAYER, F., DE PAOLA, F., IERVOLINO, I., GIUGNI, M., TOPA, M. E., MBUYA, E., KYESSI, A., MANFREDI, G. & GASPARINI, P. (2013). Flood risk assessment for informal settlements. Natural Hazards, 69 (1): 1003–1032.

RISSANEN, J. (1978). Modeling by shortest data description. Automatica, 14 (5): 465 – 471.

ROWE, R. K. & KACK, G. J. (1983). A theoretical examination of the settlements induced by tunnelling: four case histories. Canadian Geotechnical Journal, 20 (2): 299–314.

ROWE, R. K. & LEE, K. (1992). Subsidence owing to tunnelling. II. Evaluation of a prediction technique. Canadian Geotechnical Journal, 29 (6): 941–954.

ROWE, R. K., LO, K. Y. & KACK, G. J. (1983). A method of estimating surface settlement above tunnels constructed in soft ground. Canadian Geotechnical Journal, 20 (1): 11–22.

SAGASETA, C. (1987). Analysis of undraind soil deformation due to ground loss. Géotechnique, 37 (3): 301–320.

SCHEFFER, M., MATTERN, H., KÖNIG, M., CONRADS, A. & THEWES, M. (2016). Simulation of maintenance strategies in mechanized tunneling. In: Winter Simulation Conference (WSC), 2016. IEEE, pp. 3345–3356.

SCHNAID, F. (2009). In Situ Testing in Geomechanics: The Main Tests. Taylor & Francis.

SILVA, M.A.A.P.; TAKEUCHI, M. R. H. (2011). A expansão da Linha 5 – Lilás e seus desafios. Revista Engenharia, .

SPIESS, A.-N. & NEUMEYER, N. (2010). An evaluation of R^2 as an inadequate measure for nonlinear models in pharmacological and biochemical research: a Monte Carlo approach. BMC Pharmacology, 10 (1): 6.

STANDING, J. & SELEMETAS, D. (2013). Greenfield ground response to EPBM tunnelling in London Clay. Géotechnique, 63 (12): 989–1007.

STONE, M. (1979). Comments on Model Selection Criteria of Akaike and Schwarz. Journal of the Royal Statistical Society. Series B (Methodological), 41 (2): 276–278.

SUDRET, B. & DER KIUREGHIAN, A. (2000). Stochastic finite element methods and reliability: a state-of-the-art report. Department of Civil and Environmental Engineering, University of California Berkeley.

SUWANSAWAT, S. & EINSTEIN, H. H. (2006). Artificial neural networks for predicting the maximum surface settlement caused by EPB shield tunneling. Tunnelling and Underground Space Technology, 21 (2): 133 – 150.

SWEI, O., GREGORY, J. & KIRCHAIN, R. (2013). Probabilistic Characterization of Uncertain Inputs in the Life-Cycle Cost Analysis of Pavements. Transportation Research Record: Journal of the Transportation Research Board, 2366 (1): 71–77.

SWOBODA, G. (1979). Finite element analysis of the New Autrian Tunnelling Method (NATM). In: Proc. 3rd Int. Conf. on Numerical Methods in Geomechanics, Aachen. Vol. 2. pp. 581–586.

TAMAGNINI, C., MIRIANO, C., SELLARI, E. & CIPOLLONE, N. (2005). Two-dimensional FE analysis of ground movements induced by shield tunnelling: the role of tunnel ovalization. Riv Ital Geotech, 1: 11–33.

TEENA, N., KUMAR, V. S., SUDHEESH, K. & SAJEEV, R. (2012). Statistical analysis on extreme wave height. Natural hazards, 64 (1): 223–236.

UZIELLI, M., LACASSE, S., NADIM, F. & PHOON, K. (2007). Soil variability analysis for geotechnical practice. Characterization and engineering properties of natural soils, 3: 1653–1752.

VELTEN, K. (2009). Mathematical modeling and simulation: introduction for scientists and engineers. John Wiley & Sons.

VERMEER, P., BONNIER, P. & MÖLLER, S. (2002). On a smart use of 3D-FEM in tunnelling. In: Proceeding of eighth international symposium on numerical models in geomechanics. pp. 361–6.

VERRUIJT, A. & BOOKER, J. R. (1996). Surface settlements due to deformation of a tunnel in an elastic half plane. Géotechnique, 46 (4): 753–756.

VIVEKANANDAN, N. (2015). Flood frequency analysis using method of moments and L-moments of probability distributions. Cogent engineering, 2 (1): 1018704.

VORSTER, T. E., KLAR, A., SOGA, K. & MAIR, R. J. (2005). Estimating the Effects of Tunneling on Existing Pipelines. Journal of Geotechnical and Geoenvironmental Engineering, 131 (11): 1399–1410.

WALLEY, P. (1991). Statistical Reasoning with Imprecise Probabilities. Chapman & Hall/CRC Monographs on Statistics & Applied Probability. Taylor & Francis.

WANG, X., LI, Z., WANG, H., RONG, Q. & LIANG, R. Y. (2016). Probabilistic analysis of shield-driven tunnel in multiple strata considering stratigraphic uncertainty. Structural Safety, 62: 88 – 100.

WEDEKIN, V. M., KASTNER, R., GUILLOUX, A., BEZUIJEN, A., STANDING, J. & NEGRO JR., A. (2012). Urban tunnels in soft ground: Review of current design practice. In: Proceedings of the International Symposium on Geotechnical Aspects of Underground Construction in Soft Ground. pp. 1047–1064.

WHITMAN, R. V. (1984). Evaluating calculated risk in geotechnical engineering. Journal of Geotechnical Engineering, 110 (2): 143–188.

WILLIAMSON, R. C. & DOWNS, T. (1990). Probabilistic arithmetic. I. Numerical methods for calculating convolutions and dependency bounds. International Journal of Approximate Reasoning, 4 (2): 89 – 158.

WONG, R. & KAISER, P. (1987). Prediction of ground movements above shallow tunnels. In: Conference on Prediction and Performance in Geotechnical Engineering, Calgary.

XIE, Y., LI, X., LIU, X., DU, X., LI, F. & CAO, Y. (2016). Performance Evaluation of Remediation Scenarios for DNAPL Contaminated Groundwater Using Analytical Models and Probabilistic Methods. Procedia Environmental Sciences, 31: 264 – 273, selected Proceedings of the Tenth International Conference on Waste Management and Technology.

YANG, J., LIU, B. & WANG, M. (2004). Modeling of tunneling-induced ground surface movements using stochastic medium theory. Tunnelling and Underground Space Technology, 19 (2): 113 – 123.

ZADEH, L. (1965). Fuzzy sets. Information and Control, 8 (3): 338 – 353.

ZENG, B. & HUANG, D. (2016). Soil deformation induced by Double-O-Tube shield tunneling with rolling based on stochastic medium theory. Tunnelling and Underground Space Technology, 60: 165 – 177.

ZHAI, Q. & RAHARDJO, H. (2013). Quantification of uncertainties in soil–water characteristic curve associated with fitting parameters. Engineering Geology, 163: 144 – 152.

ZHANG, H., MULLEN, R. & MUHANNA, R. (2010a). Finite element structural analysis using imprecise probabilities based on p-box representation. In: 4th International Workshop on Reliable Engineering Computing, Professional Activities Centre, National University of Singapore. pp. 211–225.

ZHANG, H., MULLEN, R. L. & MUHANNA, R. L. (2010b). Interval Monte Carlo methods for structural reliability. Structural Safety, 32 (3): 183 – 190.

ZHANG, J. (2009). Characterizing geotechnical model uncertainty. Ph.D. thesis, The Hong Kong University of Science and Technology.